The Role of Endoplasmic Reticulum Stress Responses in Contact Dermatitis

Inaugural-Dissertation
zur Erlangung der Doktorwürde
der Fakultät für Biologie
der Albert-Ludwigs-Universität Freiburg im Breisgau

vorgelegt von

Fabian Gendrisch

Freiburg im Breisgau
Oktober 2018

Angefertigt in der Forschergruppe Allergologie,
Klinik für Dermatologie und Venerologie, Universitätsklinikum Freiburg im Breisgau

Dekan der Fakultät für Biologie: Prof. Dr. Wolfgang Driever
Promotionsvorsitzender: Prof. Dr. Andreas Hiltbrunner

Betreuer der Arbeit: Dr. Philipp R. Esser, Prof. Dr. Stefan F. Martin

Referent: Prof. Dr. Stefan F. Martin
Ko-Referent: Prof. Dr. Georg Häcker
Drittprüferin: Prof. Dr. Dr. h.c. Leena Bruckner-Tuderman

Datum der mündlichen Prüfung: 12.12.2018

Table of contents

1 Index of abbreviations

Abbreviation	Full form
4-PBA	4-phenylbutyric acid
ACD	Allergic contact dermatitis
APC	Antigen-presenting cell
ATG	Autophagy-related gene
ATP	Adenosine triphosphate
BCR	B cell receptor
BSA	Bovine serum albumin
CA	Cinnamaldehyde
CD	Cluster of differentiation
CHOP	C/EBP-homologous protein
CHS	Contact hypersensitivity
COCAHS	Co-culture after HaCaT stimulation
COCAT	Co-culture activation test
CTL	Cytotoxic T lymphocyte
DAMP	Damage-associated molecular patterns
DAPI	4′,6-diamidino-2-phenylindole
DC	Dendritic cell
DMEM	Dulbecco modified eagle medium
DMSO	Dimethyl sulfoxide
DNBS	Dinitrobenzene sulfonic acid
DNFB	1-fluoro-2,4-dinitrobenzene
DNTB	Dinitrothiocyanobenzene
ECM	Extrcacellular matrix
EDTA	Ethylenediaminetetraacetic acid
ER	Endoplasmic reticulum
ERAD	ER-associated degradation
FACS	fluorescence-activated cell scanning/sorting
FBS	Fetal bovine serum
HA	Hyaluronic acid
HEPES	4-(2-hydroxyethyl)-1-piperazineethanesulfonic acid
HMGB1	High-mobility group box 1
HRP	Horseradish peroxidase
IL	Interleukin
IRE-1	Inositol-requiring enzyme 1
LC	Langerhans cell
LC3	Microtubule-associated protein 1 light chain 3
LDH	Lactate dehydrogenase
LPS	Lipopolysaccharide
MDC	Monodansylcadaverine
MHC	Major histocompatibility complex
MTT	3-(4,5-dimethylthiazol-2-yl)-2,5-diphenyltetrazolium bromide
NBR1	Neighbor of BRCA1 gene 1
NF-κB	Nuclear factor kappa-light-chain-enhancer of activated B-cells

NK	Natural killer cell
NLRP3	NLR family pyrin domain containing 3
PBS	Phosphate Buffered Saline
PERK	Protein kinase R-like endoplasmic reticulum kinase
PRR	Pattern recognition receptor
ROS	Reactive oxygen species
SDS	Sodium dodecyl sulfate
TCR	T cell receptor
TLR	Toll-like receptor
TNBS	2,4,6-Trinitrobenzenesulfonic acid solution
TNCB	1-chloro-2,4,6-trinitrobenzene
TNF	Tumor necrosis factor
TUDCA	Tauroursodeoxycholic acid
UPR	Unfolded protein response
XBP-1	X-box binding protein 1

2 Summary

The major aim of this thesis was to deepen the knowledge gained from our earlier work regarding the role of the unfolded protein response (UPR) in ACD development. The experiments conducted here were able to uncover pro-inflammatory downstream events of sensitizer-mediated UPR activation. Strong sensitizers led to an UPR-dependent activation of the NF-κB pathway. This resulted in an increased release of pro-inflammatory cytokines by keratinocytes and a subsequent activation of immature dendritic cells by those. All these inflammatory processes were blocked when specific inhibitors of the UPR (IRE-1 or PERK inhibitors) were used. In addition, the potency amplification of weak sensitizers as observed when these were used in combination with other weak sensitizers or an irritant was shown to be linked to an increased UPR activation causing the activation of the NF-κB pathway. This effect was not seen by treatment of cells with just one weak sensitizer alone. Weak sensitizers used in combination therefore show a synergistic effect mimicking strong sensitizers.

To simplify the initial analysis of chemicals for their ability to induce ER stress and the UPR, a UPR reporter strain of the model organism *Caenorhabditis elegans* was used to perform a proof of concept experiment showing the increased expression of the reporter after sensitizer treatment.

Finally, as the UPR has been shown to be connected to autophagy, another cellular stress response playing a role in the immune system, the induction of autophagy after sensitizer treatment and a potential interaction with the UPR was analyzed and could not show a clear activation of autophagy or a link between these to stress responses in this setting.

The results of the experiments in this thesis were able to confirm the importance of the UPR in the setting of the ACD and uncover further effects of the UPR in the development of the disease. In addition, the use of specific UPR inhibitors was able to decrease all effects caused by sensitizers in the experiments. Topical application of these inhibitors might therefore pose as a potential treatment option for patients suffering from ACD. Differences in their ability to induce pro-inflammatory responses might be useful for the differentiation of weak and strong sensitizers in potential new *in vitro* assays.

3 Zusammenfassung

Ziel dieser Arbeit war es, das Wissen über die Rolle der ungefalteten Proteinantwort (UPR) in der allergischen Kontaktdermatitis (ACD) zu vertiefen. Die durchgeführten Experimente konnten eine Aktivierung des entzündlichen NF-κB-Signalwegs durch die allergeninduzierte UPR nachweisen, was eine Produktion von proinflammatorischen Zytokinen zur Folge hatte. Außerdem konnte gezeigt werden, dass diese entzündlichen Vorgänge in Keratinozyten dazu in der Lage sind dendritische Zellen zu aktivieren. Mittels spezifischer Inhibitoren für sowohl den IRE-1 als auch den PERK-Arm der UPR konnte die Beteiligung der UPR an diesen Prozessen nachgewiesen werden.

Weiterhin konnte die Rolle der UPR in der Erhöhung der Allergenstärke von Kombinationen schwacher Allergene mit entweder anderen schwachen Allergenen oder einem Irritans aufgezeigt werden. Dies geschieht durch eine erhöhte Aktvierung eben jener Signalwege, die bei starken Kontaktallergenen aktiviert werden, bei schwachen Allergenen alleine jedoch nicht. Eine Kombination von schwachen Allergenen scheint also den Wirkmechanismus von starken Allergenen nachzuahmen.

Um die zeit- und materialaufwändige anfängliche Analyse von Chemikalien auf ihre ER-Stress erzeugende Wirkung zu vereinfachen wurde ein Reporterstamm des Modellorganismus *Caenorhabditis elegans* in einem Testexperiment untersucht. Dieses konnte zeigen, dass die Behandlung der Tiere mit verschiedenen Allergenen tatsächlich zu einer Induktion der Reporterexpression führt und daher als Testsystem geeignet sein könnte.

Zum Schluss wurde noch eine eventuelle Aktivierung einer weiteren Zellstressantwort, der Autophagie, im Rahmen der ACD untersucht. Obwohl eine Verbindung von UPR und Autophagie schon bekannt ist und sie eine Rolle im Immunsystem spielen kann, konnte keine klare Modulation der Autophagie durch Allergene und die UPR gezeigt werden.

Die Ergebnisse dieser Arbeit bestätigten die Rolle der UPR in der ACD. Da eine Modulation der UPR mittels spezifischer Inhibitoren die beobachteten Effekte reduzieren konnte wäre eine topische Behandlung der ACD-vorstellbar. Außerdem könnten die beobachteten Unterschiede von starken und schwachen Allergenen der Entwicklung von *in vitro*-Testsystemen zu deren Unterscheidung dienen.

4 Introduction

4.1 The skin

The outermost of the cellular barriers of our body is the skin. It constitutes the first defensive measure against invading pathogens. Besides its barrier function, it is also very important in maintaining body temperature, acts via a diversity of many receptors as our largest sensory organ and protects us from chemical and physical insults like ultraviolet radiation. This shows, that the skin is “an organ that is more than a covering for the innards” (Goldsmith 2014).

Because of this plethora of functions of the skin, one can easily imagine that it is not just a homogeneous layer of cells. It rather consists of three parts – the dermis, the basement membrane and the epidermis, which itself is subdivided in four layers. Starting from the bottom, Figure 1 shows the first layer of the skin, the dermis.

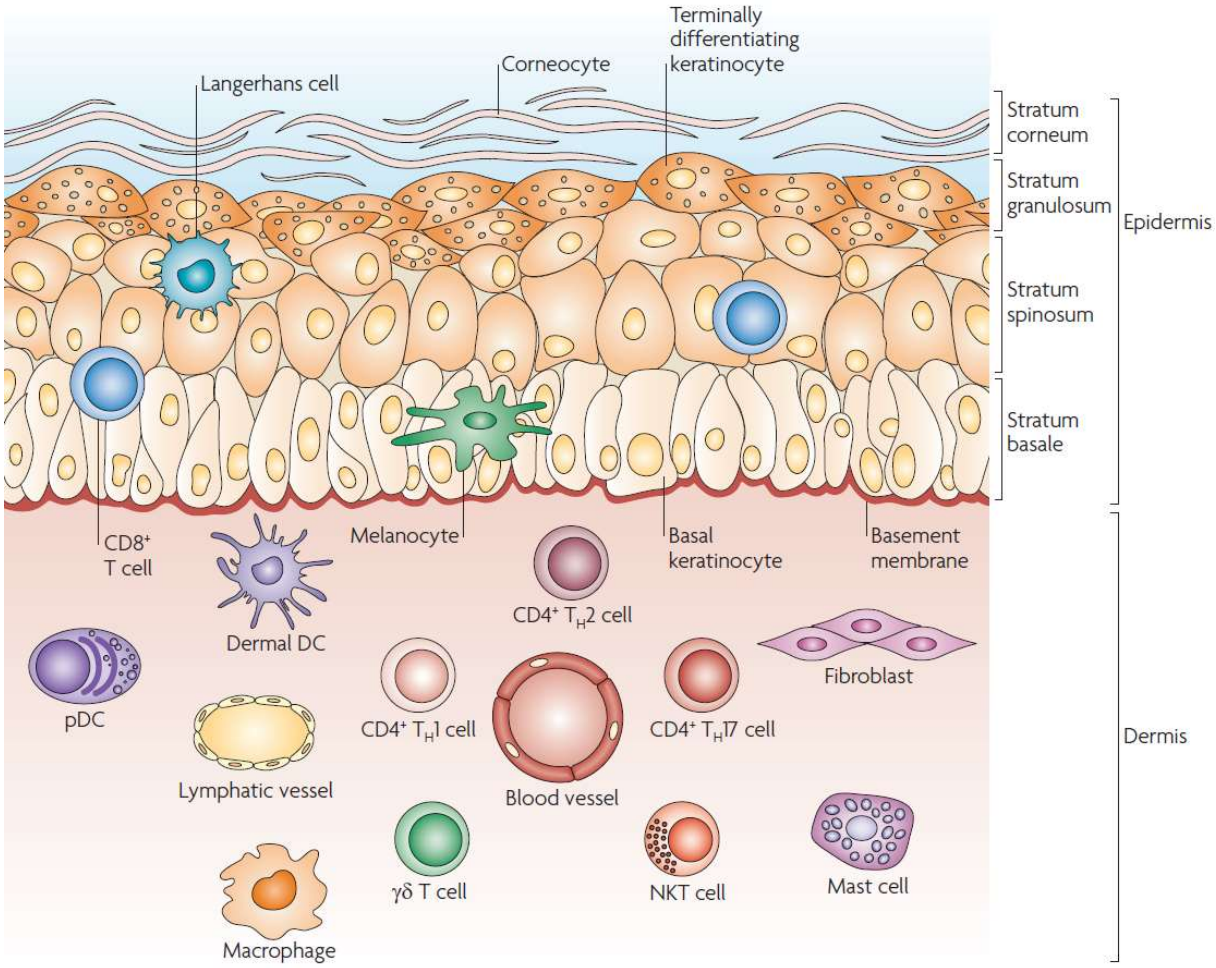

Figure 1: Schematic composition of the skin and the cells it inherits (Nestle et al. 2009). The figure shows the layers of the epidermis, the dermis and the different types of cells they inherit.

It is mostly made up of fibroblasts, which provide the structural framework and are a significant part of the connective tissue. But immune cells like macrophages, mast cells and dendritic cells (DCs) can also be found there (Matejuk 2018). Blood vessels running through the dermis are essential for the supply of nutrients to all cells within the skin, while lymphatic vessels are a transport way for immune cells that migrate to the skin or leave the skin homing to skin draining lymph nodes. The dermis is also the area where the roots of our hair and the sweat glands are residing. Between the dermis and the epidermis lies the basement membrane, a thin connective tissue that anchors the epidermis to the dermis via adhesion molecules. As mentioned before, the third major layer of the skin, the epidermis, is subdivided into four layers. The *stratum basale* lies right next to the basement membrane and is the place where the structural skin cells of the epidermis, the keratinocytes, regenerate. It consists of only one to three layers of basal keratinocyte stem cells that proliferate there. The daughter cells from there on begin to move up through the different layers. In the *stratum spinosum* on top of it, keratinocytes start to connect to each other via desmosomes, change their shape from columnar to polygonal and begin the production of keratins distinct from basal keratinocytes. The *stratum basale* and the *stratum spinosum* are also the layers where melanocytes, Langerhans cells (LC) and some $CD8^+$ T cells can be found (Matejuk 2018). LCs are a special type of immune cells residing in the skin. For a long time, they were considered to be a subtype of DCs, but more and more evidence is found that they are more of a macrophage in DC clothing (Thorbecke, Silberberg-Sinakin, and Flotte 1980; Doebel, Voisin, and Nagao 2017; Kaplan 2017). After activation, they migrate to the next skin draining lymph node (Itano et al. 2003). In the *stratum granulosum* keratinocytes start to show granula in their cytoplasm and produce lipids to create a lipid layer in the skin as another protective layer. The *stratum corneum* is the outermost layer of the skin and consists of corneocytes. In a process called cornification, these dead cells are derived from keratinocytes. They provide an important barrier function to exclude pathogens, toxic substances and prevent a loss of water to avoid dehydration. Because of the high encroachment, the *stratum corneum* is renewed about every 10 to 14 days.

4.2 The immune system

Despite its complex structure, the skin alone is not sufficient to defend our body against pathogens like bacteria, viruses, fungi or parasites. Over the course of time, a system evolved to counteract these noxes, the immune system. After entering the organism different immune cell types either eradicate invading pathogens or act as supporters to help other cells in the execution of their protective actions. To coordinate the activities of all these cells a large variety of molecules and substances are produced that aid communication, mediate assistance and activate other cells or even have protective capabilities themselves.

If a pathogen manages to invade our body, the first line of defense is the innate immune system. The concept of a rather unspecific acting system to defend an organism against pathogens can already be found in plants, fungi, insects and some simple multicellular organisms. However, their innate immune system is much more primitive than the ones in vertebrates. One important part of innate immunity is the complement system, a variety of plasma proteins able to either destroy microorganisms or to act as a connection between innate and adaptive immunity by opsonizing pathogens. The cellular part of the innate immune system includes macrophages, dendritic cells, three types of granulocytes (basophil, eosinophil and neutrophil), natural killer (NK) cells and mast cells. Cells of the innate immune system are unable to recognize a specific pathogen, but are only able to discriminate between general groups of pathogens. They achieve this by the employment of pattern recognition receptors (PRRs), a group of receptors that recognize specific groups of molecules found on pathogens (Akira, Uematsu, and Takeuchi 2006). These molecules, including well-known representatives like lipopolysaccharide (LPS), which is found on the surface of many Gram-negative bacteria and is recognized by a PRR called Toll-like receptor 4 (TLR4) (Poltorak 1998), one of the 13 known members of the Toll-like-receptor (TLR) family (Hua and Hou 2013), are called pathogen-associated molecular patterns (PAMPs). Besides PAMPs, the PRRs are also able to recognize molecules released upon cell damage or destruction (Gallucci, Lolkema, and Matzinger 1999). Examples for these damage-associated molecular patterns (DAMPs) are high-mobility group box 1 (HMGB1) and different heat shock proteins (Álvarez and Vasquez 2017) as well as components of the extracellular matrix (ECM) like hyaluronic acid (HA) (Rock et al. 2005). Together with danger signals like reactive oxygen species (ROS) or adenosine triphosphate (ATP) all of

those are able to initiate an immune response by activating innate immune cells (Rock et al. 2005). Upon recognition of a pathogen via a PRR several measures can be taken. Phagocytic cells like macrophages or neutrophils might take up a pathogen and destroy it using specialized enzymes such as lysozyme (Fleming 1922) and myeloperoxidase (Klebanoff 1999) stored in vesicles. Similar enzymes can be utilized by eosinophils to damage pathogens such as parasites simply by releasing them to the extracellular space in a process called exocytosis. After the phagocytosis of pathogens, several actions can be taken by the phagocytes. Macrophages for example activate other cells by secreting pro-inflammatory cytokines like interleukin 6 (IL-6) and attract them to the site of infection. Besides pro-inflammatory cytokines like tumor necrosis factor α (TNF-α) (Arango Duque and Descoteaux 2014), a pro-apoptotic cytokine, macrophages can also secrete anti-inflammatory cytokines like IL-10 (Galdiero et al. 2013) to dampen certain defense mechanisms that would cause harm to the organism. A typical pathway important for the expression of pro-inflammatory cytokines is the nuclear factor kappa-light-chain-enhancer of activated B-cells (NF-κB). There are two pathways for the activation of NF-κB, a canonical and a noncanonical (Shih et al. 2011). They differ in the signals resulting in their activation and in the members of the NF-κB protein family used, but in general have a similar mode of activation. In the resting state, NF-κB dimers are retained in the cytoplasm in an inactive form. Upon a stimulus, the inhibitory protein is phosphorylated, ubiquitinated and then degraded by the proteasome. The now active NF-κB dimers can translocate into the nucleus and initiate their transcriptional activity.

Activation of other cells is also a property of DCs. They are very efficient in priming T cells by presenting antigens. While memory T cells can be activated by any APC, only mature DCs can activate and prime naïve T cells. This is the reason why DCs are seen as a link between the innate and adaptive immune system (Hammad and Lambrecht 2008). Another cell type that plays an important role in innate immunity against for example parasitic infections is the mast cells. They are probably best-known for the production of histamine, a very important signaling mediator also playing a role in allergy. But not only cells of the immune system play a role in innate immunity. Other cells like keratinocytes have been shown to be a potent promotor of innate immunity, as well (Sugita et al. 2007).

Over time, a new part of the immune system only found in vertebrates evolved. It is

able to mount a highly specific immune response to pathogens. Furthermore, this part of the immune system is capable of establishing an immunological memory to quickly react to a recurring infection. Because of these mechanisms, this part of the immune systems is called the adaptive immune system. Adaptive immunity is a very effective process, but comes with the drawback of time it needs to act because of the necessity of several types of helper and effector cells to proliferate and differentiate. Therefore, it takes about five days for an adaptive immune response to begin its actions (Charles A Janeway et al. 2001). Two families of cells are the main actors of the adaptive immune system - T and B cells. Their names arise from the location of their maturation. T cells develop and mature in the thymus (T), while B cells develop in the bone marrow (B) (Alberts et al. 2002). One reason for the high specificity of the adaptive immune system is the presence of B and T cell receptors (BCRs and TCRs) on the surface of these cells. These receptors are used for the detection of antigens and are highly specific for a single epitope of an antigen. BCRs and TCRs both belong to the immunoglobulin superfamily. The BCR is a membrane-bound version of a complete immunoglobulin, while the TCR resembles structurally the membrane-bound Fab (fragment antigen binding) fragment of an immunoglobulin. In contrast to these membrane-bound receptors, Immunoglobulins can also be found as antibodies secreted by B cells. A process called V(D)J recombination is responsible for the high variability of the immunoglobulins (Jackson et al. 2013). The antigen binding region of the BCR and TCR genes are built up of different gene segments called variable (V), diversity (D) or joining (J) elements that are randomly recombined in the bone marrow and thymus, respectively, during the maturation process of T and B cells. This recombination enables an enormous diversity of antigen specificities that can theoretically deal with any antigen encountered for example on pathogens. But there is a difference in the recognition of antigens by BCR and TCR. TCRs are only able to recognize short peptides derived from proteins that have been processed by antigen presenting cells (APCs), while BCRs can recognize whole protein antigens. Cells that process antigens and present them to B- and T cells include so called professional APCs like DCs or macrophages. They take up and process pathogens and present short peptide fragments to T cells on MHC molecules because the TCR recognizes antigens only in a complex of the peptide and a major histocompatibility complex (MHC) molecule (Blum, Wearsch, and Cresswell 2013). There are two classes of MHC molecules, MHC I and MHC II. On MHC I molecules 8 – 10 amino acid long

peptides derived from intracellular proteins are presented to CD8+ T cells. These so-called cytotoxic T cells (CTL) are specifically designed to remove infected or somehow abnormal cells using cytotoxins like granzymes or perforin. These molecules in a series of events cause the induction of apoptosis in target cells. Basically, all somatic cells with the exception of anuclear erythrocytes express MHC I molecules on their cell surface. This is important for the immune system and allows the recognition of infected cells. On MHC II molecules 15 – 24 amino acids long peptides derived from extracellular proteins, e.g. from phagocytosed pathogens, are presented to T cells. MHC II is mostly present on the surface of professional APCs and peptides presented on it can be recognized by CD4+ T helper cells (T_h). One of their functions is to activate other immune cells like B cells by producing and secreting cytokines and other messenger molecules (Zhu and Paul 2008). After the activation by T_h cells, B cells differentiate into antibody-producing plasma cells. These proteins recognize and opsonize or neutralize antigens.

Since an ongoing immune response without regulation could cause harm to the organism, there are special cells to slow down the immune system. Regulatory T cells (T_{reg}) are very important for control, regulation and shut down of immune responses after the clearance of an infection and to prevent autoimmunity. Using cytokines like IL-10, or IL-4, or similar mechanisms as CTLs, these cells downregulate or destroy active immune cells (Corthay 2009). This is necessary to stop the immune system after the clearance of an infection or to prevent autoimmune diseases caused by an overshooting immune system.

One of the great advantages of the adaptive immune system is the formation of an immunological memory. B and T cells are able to differentiate into memory cells that circulate in the body for months to years, even after the shutdown of an immune response. For example, there are still living humans that have B cells producing antibodies against the virus of the 1918 influenza pandemic (Yu et al. 2008). These are also the cells that are important for successful vaccination.

However, besides its beneficial activities, our immune system sometimes causes damage to the organism. Autoreactive immune cells can cause severe autoimmune diseases that lead to severe damage to the organism or even be lethal (L. Wang, Wang, and Gershwin 2015). Another type of harmful response of the immune system is an allergic reaction. Allergies are caused by a hypersensitivity response to

innocuous molecules, which under normal conditions have no negative effect on the body.

4.2.1 The allergic contact dermatitis (ACD)

There are four types of immunological hypersensitivity reactions. Types I to III are all mediated by different classes of antibodies and are categorized by the type of antigen they recognize. Type IV hypersensitivities are mediated by T cells and include the allergic contact dermatitis (ACD) as one the of the most frequent ones (Peiser et al. 2012). The ACD is one of the most prevalent occupational diseases and affects about 20% of the European population (Thomas L. Diepgen et al. 2016). Examples for affected occupations are hairdressers (Lind et al. 2017), professions that come in close contact with preservatives (Deza and Giménez-arnau 2017) and fragrances (Cheng and Zug 2014), as well as health care employees (Kadivar and Belsito 2015). A study monitoring occupational skin diseases showed that in Bavaria 24 out of 1000 hairdressers are sensitized to a contact sensitizer (Thomas L. Diepgen 2003). The major issue for affected people is the lack of a causative treatment for ACD. Using immunosuppressive drugs to treat symptoms would work but comes with the downside of massive side effects. Therefore, currently the only solution to their problem is avoiding allergens by switching the occupation, leading to a major economic and personal challenge. Due to the high appearance of contact sensitizers many industries are confronted with challenging tasks. The cosmetics industry has a high need for assays to test new substances for their sensitizing properties due to the ban of animal testing (Merenyi 2014). Manufacturers of metal osteosynthesis implants also face new challenges, since it has been shown that the release of metal from these implants can lead to the sensitization of patients (Cobb et al. 2017).

Mechanistically, the ACD is a T cell mediated immune response to an innocuous molecule leading to erythema and eczema formation as seen in Figure 2. In total, there are more than 4350 known contact allergens (Parish 2010) with nickel being the leading molecule (Mahler, Geier, and Schnuch 2014). Sensitizers include metal ions and a wide variety of low molecular weight (MW) organic chemicals. For a long time, sensitizers were thought to have a molecular weight of 500 Da or lower. Recent studies could show that molecules up to 2.2 kDa can be classified as potential sensitizers (Fitzpatrick, Roberts, and Patlewicz 2017) and, therefore, refute the 500 Da theory. Maybe partially due to their size , a crucial ability of sensitizers is to enter

the skin by penetration of the *stratum corneum* and to enter the epidermis (Malmberg et al. 2017). Genetic pre-dispositions like mutations in the filaggrin (Thyssen et al. 2013) or claudin-1 gene (Ross-Hansen et al. 2013), causing barrier defects of the skin, might contribute to an eased penetration of sensitizers (De Benedetto, Kubo, and Beck 2012; D. Kim et al. 2017).

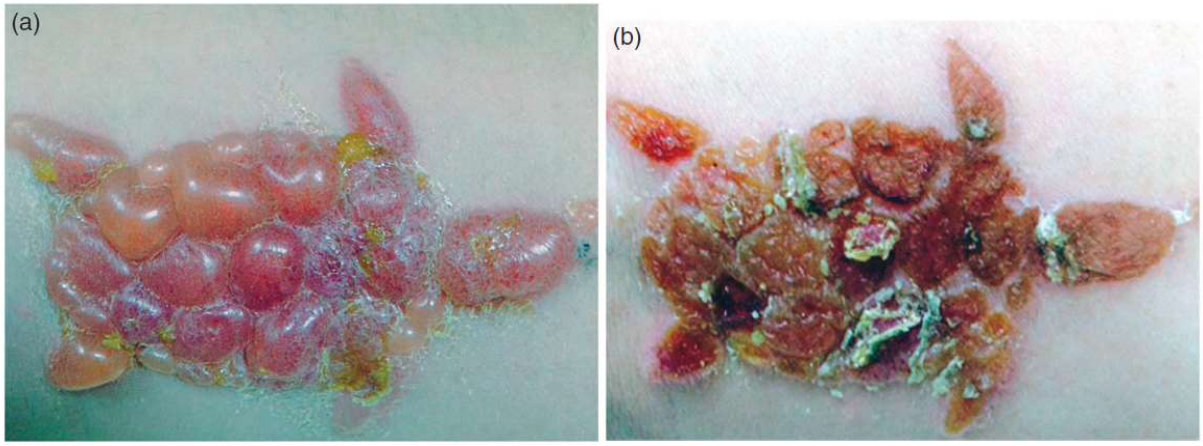

Figure 2: Clinical manifestation of allergic contact dermatitis (Choovichian, Chatapat, and Piyaphanee 2015). Shown is a strong allergic reaction to the hapten p-Phenylenediamine (PPD) (a) 13 days after application of a PPD containing henna tattoo and (b) three days after treatment with topical steroids.

Contact sensitizers, also called haptens, are non-immunogenic due to their low MW. However, due to their electrophilic nature, haptens bind covalently to endogenous proteins to form hapten-carrier conjugates or, in the case of metal ions, form complexes and thus become recognizable by the immune system (Parker, Long, and Turk 1983; Divkovic et al. 2005) in a process called haptenization. Only then can T cells recognize the hapten-modified peptides presented by MHC molecules on antigen-presenting cells and start an immune response (S. F. Martin et al. 2011). There are studies pointing towards weak sensitizers modifying less sites of human serum albumin than stronger sensitizers (Aleksic et al. 2007; Jenkinson et al. 2010; Parkinson et al. 2014). This indicates that potency assessment of chemicals by looking at the number of protein sites being modified might be conceivable, however, since these studies were performed with only a few substances, more work has to be done on that issue. Besides haptens, there are so called *pre*-haptens and *pro*-haptens. *Pre*-haptens like geraniol (Hagvall, Karlberg, and Bråred Christensson 2012) are activated physically or chemically outside of the skin for example by oxidation while *pro*-haptens like diphenylthiourea (Samuelsson et al. 2011) undergo enzymatic activation inside the skin changed by the body to be reactive. This

processing leads to an increase of the potency of the sensitizers and is therefore an important factor that has to be considered when testing for sensitization either in patients or hazard assessment in *in vitro* assays used for example in the cosmetics industry.

Generally, the ACD proceeds in two phases (Figure 3). The first contact of the immune system with a new allergen happens in the sensitization phase, without causing any clinical signs. After penetrating the skin, sensitizers form the above mentioned hapten-protein complexes with endogenous proteins.

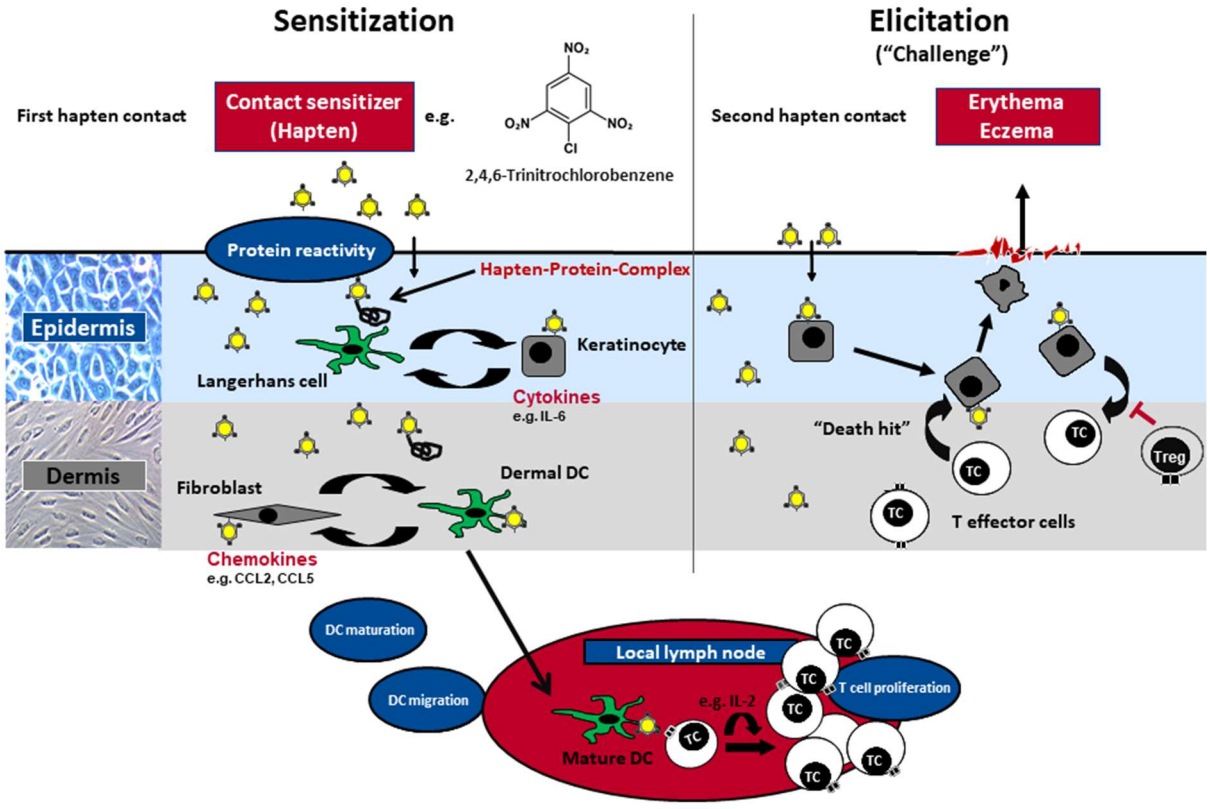

Figure 3: Schematic course of an allergic reaction to a contact sensitizer from sensitization to elicitation (modified from (S. F. Martin et al. 2011)). The first contact with a sensitizer leads to the formation of hapten-protein complexes, the generation of a pro-inflammatory micromilieu and subsequently activation and maturation of immature DCs. These cells migrate to the next local lymph node where they prime antigen-specific T cells. The second contact with the sensitizing chemical triggers the elicitation phase. Antigen-specific T cells are recruited to the skin and their cytotoxic activities lead to the formation of the clinical signs of ACD which include erythema and eczema.

Hapten-protein complexes are then taken up by innate immune cells. It is still under debate whether or not DCs alone are the only cells taking up the antigens and priming naïve T cells after antigen processing on presentation of MHC after migrating to the next local lymph node, or if other cells like the Langerhans cells of the epidermis play a role in sensitization. Concerning Langerhans cells, contradicting

results on their role in ACD have been found in studies using different types of mouse models lacking LCs pointing towards a pro-inflammatory (Bennett et al. 2005) as well as a suppressive function (Gomez de Agüero et al. 2012) in contact hypersensitivity (CHS), the mouse model for ACD. Either way, after naïve antigen-specific T cells are activated they start to proliferate and differentiate into effector and memory T cells that circulate in the blood.

A crucial requirement for an efficient sensitization is the existence of a pro-inflammatory micromilieu caused by the local release of cytokines from cells (McFadden and Basketter 2000). The importance of the cytokine release has been proven for example in an experiment where the potency of the weak sensitizer DNTB provoking a CHS reaction was enhanced after the addition of the pro-inflammatory cytokine Interleukin 12 (IL-12) (Riemann et al. 2005), a cytokine that together with TLR 2 and 4 plays an important role in CHS (S. F. Martin et al. 2008). Sensitizers themselves are able to induce a pro-inflammatory milieu via a variety of mechanisms, leading to a sterile inflammatory response (Kaplan, Igyártó, and Gaspari 2012). Inducing the production of reactive oxygen species (ROS) production (Migdal et al. 2010; Esser et al. 2012) as shown in Figure 4 would be one example.

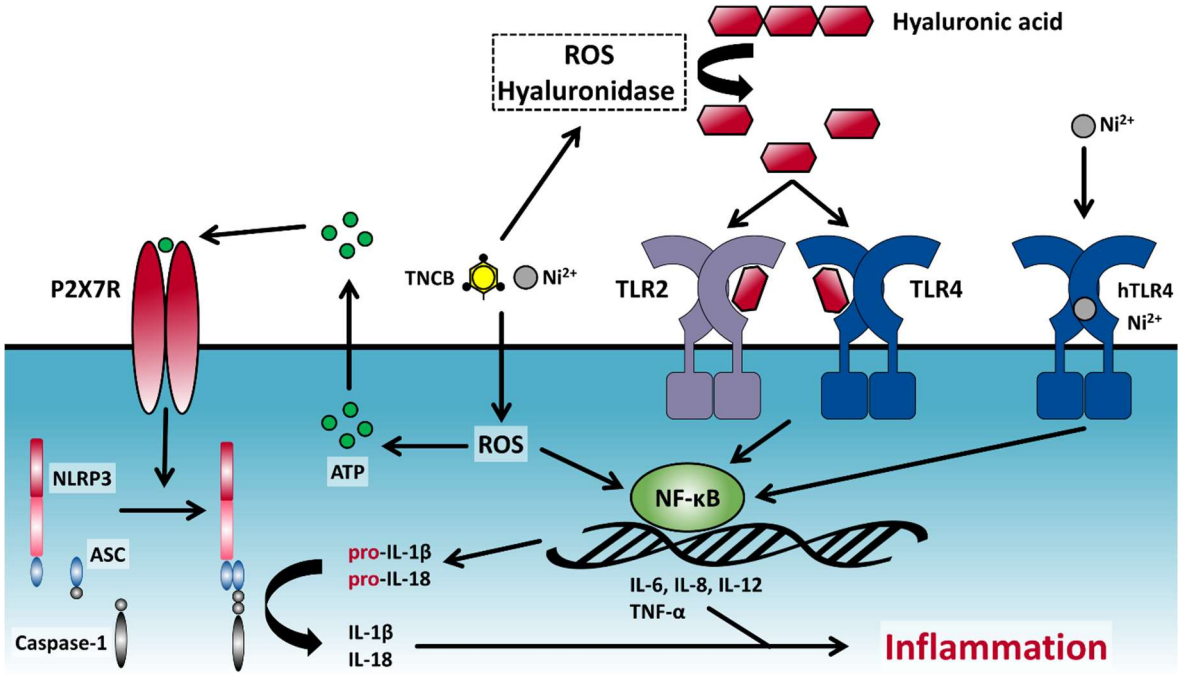

Figure 4: The role of DAMPs in the contact sensitizer mediated activation of the innate immune system. The contact sensitizer-induced ROS production is one of the key events in the production and release of DAMPs. The breakdown of hyaluronic acid into small fragments, the release of intracellular ATP and the activation of the NF-κB pathway are all directly linked to ROS. Metal allergens constitute a special group of sensitizers as they can directly bind and activate human TLR4.

ROS themselves have been shown to cause pro-inflammatory cytokine production (Naik and Dixit 2011) but also their role in the breakdown of hyaluronic acid (HA) (Esser et al. 2012) and the subsequent activation of TLRs 2 and 4 by these HA fragments contribute to the formation of a pro-inflammatory milieu. In an experimental setting where $Nrf2^{-/-}$ mice lacking a fully functional ROS detoxification are sensitized to a weak sensitizer, the resulting allergic reaction looks more like the reaction to a strong sensitizer, further highlighting the key role of ROS in the CHS response (El Ali et al. 2013). Another danger signal important in ACD development is ATP. Intracellular ATP is released and once in the extracellular space can bind to the P2X7 receptor. P2X7R is crucial for the activation of the NLRP3 inflammasome, resulting in an active caspase-1 that then cleaves pro-IL-1β and pro-IL-18 into their active forms, further contributing to the ACD (Weber et al. 2010). A contrast to this indirect activation of the innate immune system is the response triggered by metal allergens like nickel and cobalt. They are able to directly bind to human TLR4 and thereby cause the expression of pro-inflammatory cytokines (Schmidt et al. 2010; Raghavan et al. 2012). Palladium seems to engage the same way of action, directly targeting human TLR4 (Rachmawati et al. 2013). Another mechanism for increasing levels of pro-inflammatory cytokines might be mediated by antimicrobial peptides typically needed to fight bacterial infections. There are hints in the literature that point to a role of beta-defensins in the reaction to sensitizers in rats (Hartmann et al. 2006) as well as in human patients (Kamsteeg et al. 2010).

Upon a subsequent encounter with the same sensitizer the second phase of ACD begins. In the elicitation phase, antigen-specific effector/memory T cells facilitate a rapid immune response. Circulating T effector cells that developed during the sensitization phase migrate to the site of sensitizer contact in a process mediated by the release of inflammatory cytokines and chemokines from local skin cells. CD8+ CTLs are the major effector cells in ACD (S. Martin et al. 2000), although recent studies could show a potential involvement of CD4+ T helper cells (Purath et al. 2016). Since sensitizers not only form hapten-carrier complexes with soluble free proteins but might also bind to cellular surface proteins, immune reactions which are targeted against these complexes found on the surface of cells might lead to the destruction of the modified skin cells causing the typical clinical signs of ACD, reaching from mild rashes up to massive eczema formation.

Protein modification is an essential part of many cellular pathways enabling the

activation of different signaling pathways (Theillet et al. 2012). However, these modifications can also lead to changes of the protein conformation (Groban, Narayanan, and Jacobson 2006; Xin and Radivojac 2012) that not always have a positive outcome for the protein and the cells. Modifications might lead to the misfolding or unfolding of proteins disturbing its proper function (Stefani 2004) and cause the accumulation of these defective proteins in the ER leading to cell stress (Araki and Nagata 2011). This might also be the case during ACD when the hapten-protein complexes are formed or by protein oxidation caused by the sensitizer-induced ROS production. To resolve ER stress, cells have a stress response pathway to try and restore protein homeostasis leading to the survival of stressed cells. The so-called unfolded protein response (UPR) is an essential pathway not only deciding between cellular survival or removal of a stressed cell but has also been shown to play important roles in the immune system (Schmitz et al. 2018).

4.3 The unfolded protein response (UPR)

As stated above, the initial activation of the innate immune system in the sensitization phase of ACD is only sparsely understood. However, it is known that a pro-inflammatory cytokine milieu in the skin caused by contact sensitizers is a crucial prerequisite for the full activation of DCs. In our recent work, tissue stress has been highlighted as a promising target for further analysis to uncover its potential role in the early sensitization process (Gendrisch et al. submitted). Typical causes of cellular stress can be physical stressors like temperature or also infections by bacteria or viruses. Besides these external noxes, several intracellular processes offer the potential to generate stress. Pathways like the protein biosynthesis are fine-tuned procedures and little disturbances can have severe effects. Complications during protein synthesis can include errors of translation, protein misfolding or posttranslational modification caused by hypoxia, nutrient deprivation or mutations in secreted proteins (Scheper, van der Knaap, and Proud 2007). The endoplasmic reticulum (ER) is regulating the synthesis, folding and the processing of about a third of all cellular proteins including most secreted proteins, therefore these types of errors can lead to the accumulation of un- or misfolded proteins in the ER and finally to a stressed ER. In a process called ER-associated degradation (ERAD) incompletely folded proteins are transported back to the cytosol and after ubiquitylation get degraded by the proteasome (M. H. Smith, Ploegh, and Weissman

2011). Despite its potent regulatory mechanisms highly secretory cell types like β cells of the pancreas or plasma cells producing antibodies are often operating their ER at its limit. In this case ERAD alone is not capable to maintain homeostasis of the ER. To ensure a proper protein-folding capacity cells are monitoring unfolded proteins in the ER, activating the UPR when stress reaches a certain level. The main goal of the UPR is to restore protein-folding homeostasis of the ER by reducing translation and activating expression of target genes including chaperones (A.-H. Lee, Iwakoshi, and Glimcher 2003), assisting proper protein folding. If this fails, terminal UPR is activated leading to apoptosis to remove the stressed cell (Shore, Papa, and Oakes 2011).

With the UPR, vertebrates have established a network of three interacting signaling pathways which are shown in Figure 5. Each branch is named after the sensor molecule located in the membrane of the ER detecting unfolded proteins.

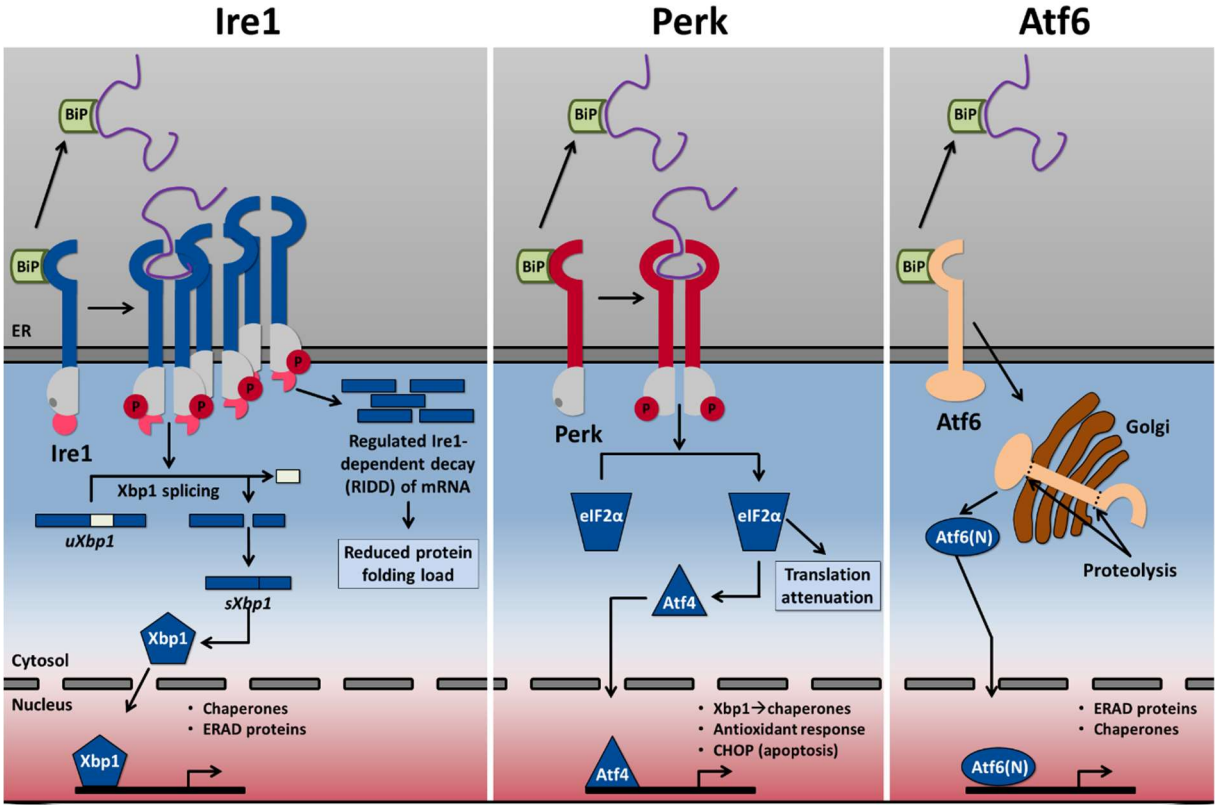

Figure 5: Scheme of the three branches of the UPR. The UPR consists of three branches that are all activated upon ER stress. All pathways lead to the production of a transcription with the goal to restore ER homeostasis or remove the stressed cell by apoptosis. While the IRE-1 branch achieves this goal with an unconventional splicing of the Xbp1 mRNA, the PERK branch uses eIF2α as an intermediate step resulting in the production of Atf4. The last branch of the UPR has no need for the synthesis of a transcription factor as the proteolytic cleavage of the stress sensor results in the needed protein.

They inherit different modes of action all resulting in UPR target gene expression. The first and also evolutionary most conserved branch is the inositol-requiring enzyme 1α (IRE-1α) branch. It can already be found in yeast in a homologous form (Morl et al. 1993, 2). Upon ER stress, IRE-1α dimerizes leading to trans-autophosphorylation activating the RNase domain. The following binding of unfolded proteins then leads to oligomerization of IRE-1α. There are three possible ways of IRE-1αs next action: IRE-1α is able to cleave multiple RNAs endonucleolytically in a process called regulated IRE-1α-dependent decay (RIDD) (Hollien and Weissman 2006). Long thought to degrade RNAs at random, RIDD has been ascribed a role in glucose metabolism, inflammation and apoptosis (Maurel et al. 2014). IRE-1αs main function is the sequence-specific unconventional splicing of X-box binding protein 1 (*XBP1*) mRNA. Using its RNase domain 26 nucleotides of the unspliced *XBP1* (*XBP1u*) are excised, resulting in the spliced form of *XBP1* (*XBP1s*) (Yoshida et al. 2001). This splicing event causes a shift of the reading frame generating the stable transcription factor XBP1s responsible for the expression of genes that control protein folding, secretion and translocation as well as ERAD (A.-H. Lee, Iwakoshi, and Glimcher 2003; Acosta-Alvear et al. 2007), all contributing to the attempt to restore ER homeostasis. Last but not least, IRE-1α has been shown to interact with TNF receptor-associated factor 2 (TRAF2) and to activate the apoptosis signal-regulating kinase 1 (ASK1) (Nishitoh et al. 2002) as well as JUN N-terminal kinase (JNK) (Urano et al. 2000), driving the cell towards apoptosis. For a long time IRE-1α was thought to be only responsible for pro-survival activities (Lin et al. 2007), while more recent studies highlight IRE-1α as an important switch between life and death, regulating cell fate decisions (Upton et al. 2012; Y. Chen and Brandizzi 2013).

The second branch of the UPR is the protein kinase R-like endoplasmic reticulum kinase (PERK) branch. Upon the binding of unfolded proteins, PERK dimerizes and *trans*-autophosphorylates (Bertolotti et al. 2000) in a similar way as IRE-1α, but without the subsequent oligomerization. The phosphorylation activates PERK which afterwards phosphorylates the eukaryotic translation initiation factor 2α (eIF2α) at serine 51 (P. Walter and Ron 2011). eIF2α then on the one hand reduces general protein synthesis (Harding et al. 2000), cutting down the protein overload of a stressed ER, and on the other hand enables the selective expression of activating transcription factor 4 (ATF4), resulting in UPR target gene expression. This includes genes for an antioxidant responses as well as chaperones aiding protein folding

(Harding et al. 2000, 2003). Under chronic ER stress accompanied by continuous ATF4 expression, the PERK branch can drive the cell towards apoptosis by increasing the expression of C/EBP-homologous protein (CHOP). For a long time, IRE-1α was thought to be the anti-apoptotic branch of the UPR, while PERK was seen as rather pro-apoptotic. However, recent studies could show that apoptosis initiated by the UPR is not dependent on the activation of a specific branch or the switch from one branch to the other, but rather related to the relative timing of IRE-1α and PERK signaling (F. Walter et al. 2015). The last branch of the UPR is the activating transcription factor 6 (ATF6) branch. The ATF6 branch is functionally clearly different from the other two branches of the UPR. Upon the accumulation of unfolded proteins in the ER, ATF6 leaves the ER membrane and translocates to the Golgi apparatus. Two proteases cleave ATF6, releasing its cytosolic domain ATF6f which acts as a transcription factor activating UPR target gene expression (Haze et al. 1999). These target genes include ERAD pathway components (Yamamoto et al. 2007). Interestingly, the three branches of the UPR do not operate totally separated from one another but several groups have shown connections between the different pathways. Majumder and colleagues have uncovered an important role of eIF2α in *XBP1* splicing induction (Majumder et al. 2012), while other studies showed a connection of ATF6 and IRE-1α branch in driving specific gene expression programs (Shoulders et al. 2013).

The exact mechanism of the detection of unfolded proteins and the activation of the UPR remains poorly understood. A common feature of all three sensor molecules is that the chaperone binding immunoglobulin protein (BiP) is bound to them under steady state conditions, keeping them in a monomeric conformation (Bertolotti et al. 2000; Shen et al. 2002, 6). There are two opinions on the activation of the UPR: Some think that the UPR is triggered by the release of BiP from the luminal domains of the sensor molecules without the need for the sensors to actually bind unfolded proteins (Shen et al. 2002; Oikawa et al. 2009). The binding of unfolded proteins to the sensors has been debated because *in vitro* studies failed to show a binding and there were concerns about the binding abilities because of space restraints (Kimata and Kohno 2011). The other opinion on UPR activation is that a direct binding of unfolded proteins to the sensors in crucial for signaling activation. First demonstrated in yeast (Gardner and Walter 2011), a recent study could show that direct binding of unfolded proteins to a MHC-like binding groove on human IRE-1α is essential for a

conformational change to allow oligomerization and therefore pathway activation (Karagöz et al. 2017).

4.4 The UPR in the immune system and diseases

While its main function lies in the maintenance of the protein folding homeostasis of the ER, new functions and involvements of the UPR in many different types of cells and pathways have been uncovered. Since many cellular processes include the translation of proteins and are therefore error-prone, the UPR emerged as an important part in basic cellular activities starting with their development and viability. This has been shown for a variety of cell types like chondrocytes, osteoclasts and pancreatic cells which are heavily dependent on eIF2α (Zhang et al. 2002). Interesting for this work is that the UPR has also been linked to the immune system. DCs (N. N. Iwakoshi, Pypaert, and Glimcher 2007) as well as other highly secretory cells like plasma cells (Neal N. Iwakoshi et al. 2003) depend on a system to cope with the load of unfolded proteins originating from the high rate of protein synthesis and mistakes that naturally come with it. Furthermore, antigen presentation has been linked to be partially dependent on the UPR as reviewed by Janssens, Pulendran and Lambrecht (Janssens, Pulendran, and Lambrecht 2014). The importance of the UPR for a functional organism can be seen in cases of defective protein folding, either from external causes or through genetic mutations of a UPR component, resulting in inflammatory phenotypes. A well-known example for this is the inflammatory bowel disease. A loss of XBP1 in intestinal epithelial or Paneth cells causes a hyperactive IRE-1α, leading to an increased activation of the pro-inflammatory NF-κB (Adolph et al. 2013). But not only dysregulation of the UPR can trigger inflammation. As shown in Figure 6, the UPR itself is also able to induce inflammation via the intersection with several pro-inflammatory pathways. Activation of the PERK branch and subsequent inhibition of the protein translation leads to an activation of NF-κB due to an altered ratio of NF-κB and its shorter-lived inhibitor IκB (Jiang et al. 2003). Another mechanism of the PERK branch triggering inflammation has been shown by Lerner and colleagues. Their work highlighted an induction of thioredoxin-interacting protein (TXNIP) via IRE-1α and PERK, ultimately leading to the activation of the NLRP3 inflammasome (Lerner et al. 2012).

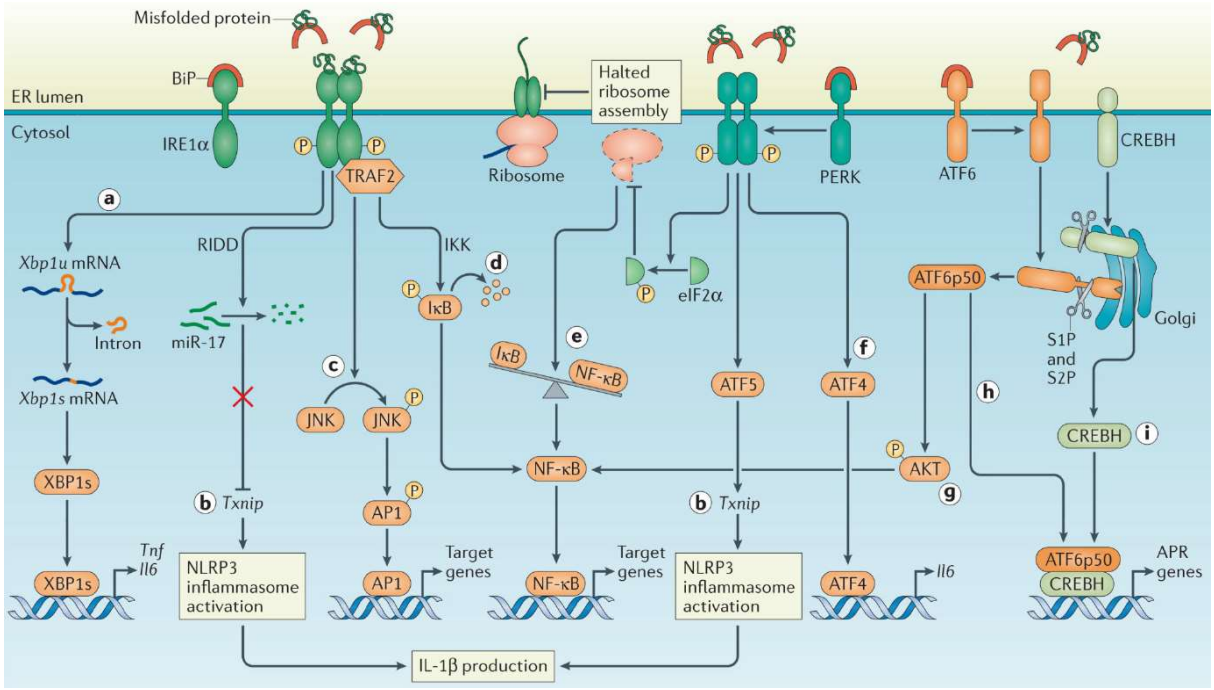

Figure 6: The role of the UPR in inflammation (Grootjans et al. 2016). All three branches of the UPR are able to interfere with inflammatory pathways. The IRE-1α pathway can lead to an activation of AP1. The activation of NF-κB is a common feature of all three UPR branches while only the transcription factors of the IRE-1α and the PERK pathway are able to induce pro-inflammatory cytokine expression and activate the NLRP3 inflammasome.

Just like PERK, IRE-1α is also able to induce NF-κB activation. This happens by the interaction of IRE-1α with TNF receptor-associated factor 2 (TRAF2) as a response to increased ER stress (Urano et al. 2000). This results in an recruitment, phosphorylation and following degradation of IκB, releasing NF-κB to the nucleus (Hu et al. 2006). Furthermore, triggering RIDD leads to a subsequent retinoic acid inducible gene I (RIG-I)-dependent immune response including the NF-κB pathway (Cho et al. 2013). Interestingly, the third branch of the UPR acting via ATF6 is also able to activate NF-κB by phosphorylating Akt (Yamazaki et al. 2009), IRE-1α achieves NF-κB activation via TRAF2 (Hu et al. 2006). Therefore, all three UPR branches can result in NF-κB activation. Pro-inflammatory actions by the UPR are not only triggered by different types of stress but can also occur as a reaction to pathogens and support the immune system. TLR engagement by PAMPs has been shown to affect certain UPR branches. For example, TLR2 and TLR4-mediated activation of IRE-1α and its downstream target XBP-1 in macrophages has been demonstrated to play a critical role in the cytokine response to *Francisella tularensis* in an ER stress-independent way (Martinon et al. 2010).

As mentioned above, the far-reaching functions and effects of the UPR can especially be seen in cases of its malfunction. Studies have shown a role in a multitude of neurodegenerative diseases including Alzheimer´s disease. These patients show an increased expression of UPR components in their brain (O'Connor et al. 2008; Nijholt et al. 2011). Alterations in ER homeostasis and the UPR can also be found in different types of cancer, leading to a number of promising clinical trials including BiP inhibitors for the treatment of melanoma (Sykes, Mactier, and Christopherson 2016). But not only an increased activation of UPR branches can cause problems, a loss or defect in protein folding caused by problems with the UPR can be just as severe and trigger several diseases. Induction of inflammation has been linked to a non-functioning UPR caused by a mutation in the *XBP-1* gene in illnesses like the inflammatory bowel disease (Adolph et al. 2013). Other diseases associated with the UPR are the amyotrophic lateral sclerosis, Parkinson´s disease, diabetes or glaucoma (Hetz, Chevet, and Harding 2013).

Taking all the actions of the UPR and its important role in the immune system into consideration, it is not far-fetched to think about a potential involvement of the UPR in the development of ACD. As seen in Figure 7, several outcomes of sensitizer actions in the skin have the potential to cause ER stress.

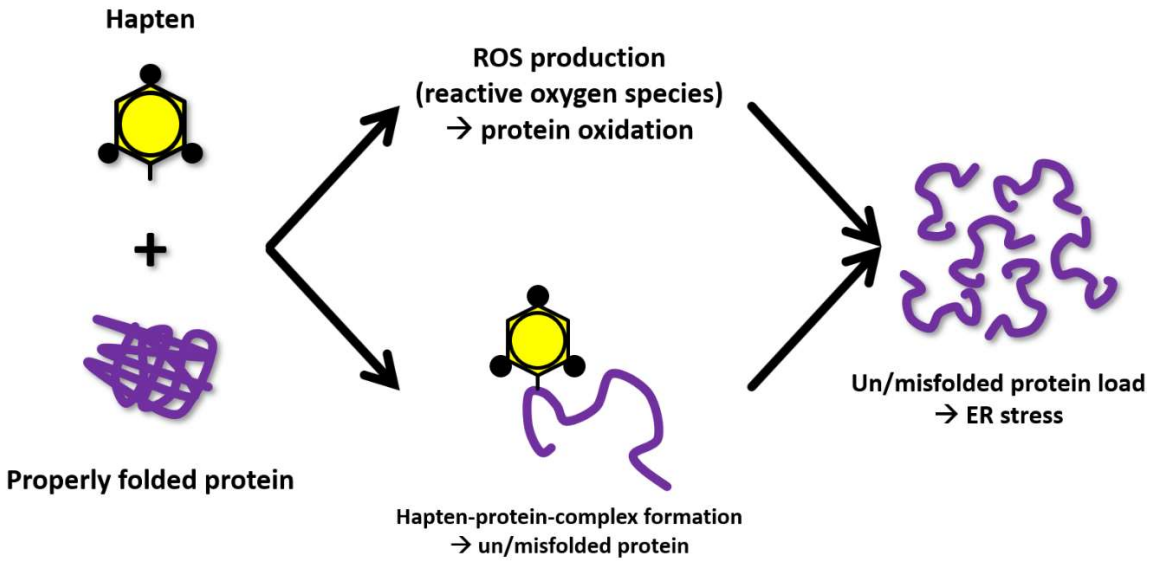

Figure 7: Possible ways of ER stress induction by haptens. Un- or misfolding of proteins could be the result of two actions of contact sensitizers. While the ROS production induced by sensitizers could result in protein oxidation causing a conformational change, the hapten-protein complex formation also offers the possibility of changing the conformation of proteins. An accumulation of un- or misfolded protein could then result in ER stress.

As mentioned above, contact sensitizers need to form hapten-protein complexes to be recognized by the immune system. This complex formation could lead to an alteration of the protein structure. Furthermore, contact with sensitizers has been shown to induce the production of ROS in skin cells *in vitro* and *in vivo* (Esser et al. 2012). These ROS are able to oxidize proteins (A. J. Swallow 1960), posing a second, more indirect mechanism of sensitizers to alter protein folding. The change of folding in a lot of proteins could then lead to an accumulation of un- or misfolded proteins, causing ER stress and a subsequent activation of the UPR. It has also been shown that ROS are able to directly activate the unfolded protein response (Malhotra and Kaufman 2007) with Ca+ depletion from the ER being a possible cause (Görlach et al. 2015). The above described pro-inflammatory actions of the UPR that could be caused by contact sensitizers might play an important role in the development of the ACD. This could be mediated by an enhancement of the initial innate immune response against allergens in an adjuvant manner, leading to a full activation of the immune system enabling the establishment of an allergy.

Besides the UPR, cells have many other conserved processes needed for the maintenance of cellular homeostasis. One of them is autophagy, a highly sensitive process that reacts to a variety of stress types including physical or metabolic stress through nutrient factor deprivation.

4.5 Autophagy

Autophagy is a common term that includes selective and non-selective autophagy in which a cell disassembles its either defect or non-essential components by engulfing it in a membrane (Figure 8). This so called autophagosome fuses with a lysosome, creating the autolysosome containing the enzymes needed for the degradation of its cargo. The difference between the two types of autophagy lies in the eponymous target selection (Reggiori et al. 2012). While the non-selective autophagy degrades anything that is captured within a forming autophagosome, the target cargo for the selective autophagy is chosen by the binding of autophagy receptors to the target. The main components of the autophagy pathway are the so-called autophagy-related (ATG) proteins. Figure 8a shows the main phases of autophagy and the most important components. In the initiation step, the ULK1/2 protein complex is forming the phagosome assembly site (PAS), the very beginning of phagophore formation (Hurley and Young 2017).

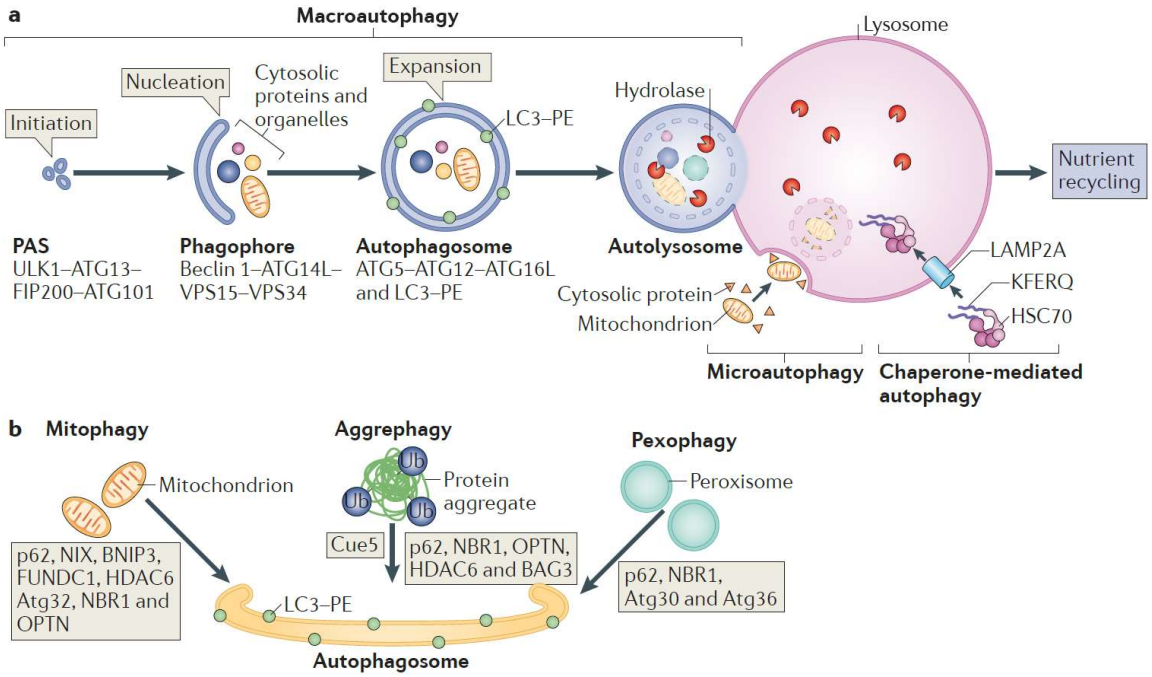

Figure 8: Scheme of the process of autophagy (Kaur and Debnath 2015). There are several forms of autophagy. Macroautophagy is a non-selective type of autophagy degrading anything that is engulfed during autophagosome formation. In contrast, in pathways like mitophagy or pexophagy the specific target is directed towards the autophagosome using adaptor proteins.

During nucleation, a phosphatidylinositide 3-kinase (PI3K) complex consisting of Beclin 1 among other components leads to an increased production of phosphatidyl-inositol 3-phosphate forming a cup-like structure. The expansion of this membrane cup to the closed autophagosome is mediated by a complex of different ATGs including ATG3, 5 and 12 that supports the lipidation of microtubule-associated protein 1 light chain 3 (LC3) (Mizushima, Ohsumi, and Yoshimori 2002). This is essential for the elongation of the phagophore membrane, the targeting of the cargo into the phagophore and the final step of the fusion of the now finished autophagosome with a lysosome creating the autolysosome. There, the cargo is degraded by the hydrolytic enzymes of the lysosome (Klionsky, Eskelinen, and Deretic 2014). The selective autophagy can be divided into several subgroups, depending on the target. These targets include cell organelles like mitochondria (mitophagy) and the ER (ERphagy), protein aggregates (aggrephagy) and peroxisomes (pexophagy) as well as invading microbes (xenophagy) (Anding and Baehrecke 2017). These types of selective autophagy are mediated by the binding of autophagy cargo receptors like sequestome 1 (SQSTM1/p62) or neighbor of BRCA1 gene 1 (NBR1). These receptors bind to the target and transport it to the phagophore using their LC3-interacting region. Another type of selective autophagy is the

chaperone-mediated autophagy. Instead of cargo receptors the chaperone heat shock cognate 70 kDa protein (HSC70) recognizes a specific peptide motif on substrates, binds to it and translocates to the lysosome in a LAMP2A-dependent manner (Cuervo and Wong 2014). Non-selective autophagy has basically the same mode of action, just without the autophagy cargo receptors. The degraded components are simply captured in the phagosome during its formation.
A main function of the autophagy is to react to different kinds of stress. Metabolic stress caused by nutrient deprivation of hypoxia is counteracted by the recycling of cellular contents, creating new metabolites and energy for the cell to restore homeostasis. But the role of autophagy in the immune system should not be underrated. As mentioned above, killing of pathogens by xenophagy poses an important mechanism in a variety of phagocytic and non-phagocytic cells. Phagocytic cells can recognize bacteria with their PRRs, leading to the internalization of the microbe and its elimination in the autolysosome in addition to the PRR-triggered activation of an immune response (Flannagan, Cosío, and Grinstein 2009). But also non-phagocytic cells can use autophagy to remove bacteria which has been first demonstrated in study showing that group A *Streptococcus* are efficiently removed by autophagy (Nakagawa et al. 2004). When it comes to viruses, there are two modes of action for autophagy. Some viruses have evolved functions that not only secure them from autophagy but use it for their replication. An example for this strategy is the Dengue virus (Y.-R. Lee et al. 2008). Exemplary for viruses that can be eliminated by the autophagy machinery are Sindbis viruses (Liang et al. 1998). But also, direct actions of autophagy on the immune system have been described. There, autophagy can have an anti-inflammatory effect by reducing inflammasome activation. Mice lacking ATG16L in hematopoietic cells are highly susceptible to colitis induced by pathogenic bacteria or dextran sodium sulfate (Murthy et al. 2014). Also the removal of damaged mitochondria releasing ROS acts immunosuppressive, because these damaged mitochondria and the ROS they release are potent activators of the NLRP3 inflammasome (Zhou et al. 2011). Interestingly, under other conditions autophagy can also support the immune system. The development of T is highly dependent on autophagy, since clearance of defect mitochondria is essential for these cells (Pua et al. 2007). Not only their development but also the education of T cells in the thymus needs autophagy. Thymic epithelial cells present self-antigens on MHC II, a process that is essential for tolerance (Nedjic et al. 2008). An interesting fact is the

relationship of autophagy with the UPR. A study could show a UPR-dependent activation of autophagy after ER stress induction which could be reduced with the use of UPR inhibitors (Deegan et al. 2015). Since aggrephagy is a described phenomenon it is conceivable that autophagy could play a role in the reaction to ER stress induced by the effect of contact sensitizers on endogenous proteins.
In summary, our skin is more than just the outer layer of the body. It consists of a variety of cell types including cells of the immune system. Unfortunately, these cells not only ward pathogens but can also react to harmless molecules in ACD resulting erythema and eczema of different severities. One of the processes taking part in the development of the ACD might be the UPR, a cell stress response caused by the accumulation of misfolded proteins in the ER. Together with other cell stress responses that can cause sterile inflammation, the UPR poses an interesting target for the analysis of their exact involvement of the ACD and the possibilities that modifications of their actions pose.

5 Aims

We have previously shown a direct involvement of the unfolded protein response (UPR) activation in the murine model for ACD, the contact hypersensitivity model (Gendrisch 2012, 2015). However, the mechanisms by which the UPR is able to control the ACD remained elusive.

Therefore, the major aim of this thesis was to gain a more detailed insight into the mode of action of the sensitizer-induced UPR modulation. To address this question, the activation of pro-inflammatory pathways in keratinocytes after sensitizer treatment was to be analyzed using qPCR, immunofluorescence and ELISA. Since an involvement of keratinocytes in the provision of a pro-inflammatory skin micromilieu might aid the initial activation of dendritic cells, another aim was to analyze the capability of keratinocytes to activate antigen-presenting cells (APCs) using a HaCaT/THP-1 co-culture assay and flow cytometry.

Since most patients suffering from ACD are sensitized to chemicals with a weak potency (Diepgen et al. 2016) and combinations of weak sensitizers with other sensitizers or irritants are often found in cosmetics or cleaning products, another aim was to analyze the ability of weak sensitizers either alone or in combination with other sensitizers or irritants to activate the UPR and pro-inflammatory pathways using qPCR and immunofluorescence. Ideally, these results were supposed to uncover potential differences in the modes of action of weak and strong sensitizers which would be useful for the development of a much-needed *in vitro* assay to test new chemicals for their ability to sensitize and their potency.

Finally, the potential involvement of a second cell stress response called autophagy was to be analyzed as autophagy and the UPR are tightly connected (Deegan et al. 2015). Analyzing all these factors was also needed to look for a potential mechanism to distinguish between sensitizers of different potencies.

In summary, the aim of this thesis was to deepen the insight into the mechanistic basics of the ACD and the role of the UPR in this process aiding the development of treatment options for ACD patients.

6 Material

6.1 Chemicals

Chemicals	Manufacturer	Order number
1-Fluoro-2,4-dinitrobenzene (DNFB)	Sigma-Aldrich Chemie GmbH, Stein, Germany	D1529
2,4,6-Trinitrobenzenesulfonic acid (TNBS)	Sigma-Aldrich Chemie GmbH, Stein, Germany	37075
2,4-Dinitrochlorobenzene (DNCB)	Sigma-Aldrich Chemie GmbH, Stein, Germany	C6396
2,4-Dinitrothiocyanobenzene (DNTB)	Alfa Aesar GmbH & Co KG, Karlsruhe, Germany	B24147
2-Chlor-1,3,5-trinitrobenzol (TNCB)	Sigma-Aldrich Chemie GmbH, Stein, Germany	79874
2-Propanol	Sigma-Aldrich Chemie GmbH, Stein, Germany	59300
3-(4,5-dimethylthiazol-2-yl)-2,5-diphenyltetrazolium bromide (MTT)	Sigma-Aldrich Chemie GmbH, Stein, Germany	M2128
4-(2-hydroxyethyl)-1-piperazineethanesulfonic acid (HEPES)	Life Technologies GmbH, Darmstadt, Germany	15630-056
4',6-diamidino-2-phenylindole (DAPI)	Sigma-Aldrich Chemie GmbH, Stein, Germany	D9542
4-Ethoxymethylene-2-phenyl-2-oxazolin-5-one (Oxazolone)	Sigma-Aldrich Chemie GmbH, Stein, Germany	E0753
4-Phenylbutyric acid (4-PBA)	Sigma-Aldrich Chemie GmbH, Stein, Germany	P21005-259
Acetone	Sigma-Aldrich Chemie GmbH, Stein, Germany	32201
Agarose, UltraPure™	Invitrogen GmbH, Karlsruhe, Germany	16500-500
Ammonium persulfate	Sigma-Aldrich Chemie GmbH, Stein, Germany	A3678
Aqua ad injectabilia	B. Braun AG, Melsungen, Germany	
Bovine serum albumin (BSA)	Carl Roth GmbH & Co. KG, Karlsruhe, Germany	8076.3
Bromphenol blue	SERVA Electrophoresis GmbH, Heidelberg, Germany	15375
Chloroform	Carl Roth GmbH & Co. KG, Karlsruhe, Germany	3313.1
Cinnamaldehyde	Sigma-Aldrich Chemie GmbH, Stein, Germany	239968
Dimethyl sulfoxide (DMSO)	Sigma-Aldrich Chemie GmbH, Stein, Germany	D5879
DMEM	Biochrom AG, Berlin, Germany	FG0445
Ethanol	Sigma-Aldrich Chemie GmbH, Stein, Germany	32205
Ethidium bromide	Merck KGaA, Darmstadt, Germany	111608
Ethylenediaminetetraacetic acid (EDTA)	Sigma-Aldrich Chemie GmbH, Stein, Germany	E5134
Eugenol	Sigma-Aldrich Chemie GmbH, Stein, Germany	E51791
Fat-free dry milk	AppliChem GmbH, Darmstadt, Germany	A0830
Fetal bovine serum (FBS)	PAA Laboratories GmbH, Pasching, Austria	A04305-08.98
Fixable Viability Dye eFluor® 780	eBioscience, Frankfurt am Main, Germany	65-0865-14
Fluorescence Mounting Medium	Dako Deutschland GmbH, Hamburg, Germany	S3023
Fluorescent Mounting Medium	Dako Deutschland GmbH, Hamburg, Germany	S3023
Formaldehyde 37%	Th Geyer GmbH Co KG, Renningen, Germany	21.371.011
Glacial acetic acid	AppliChem GmbH, Darmstadt, Germany	A3686
Glycerol	Sigma-Aldrich Chemie GmbH, Stein, Germany	G8773
HRP-conjugated Streptavidin	Jackson Immunoresearch, West Grove, USA	016-030-084
IRE-1 inhibitor II	Merck KGaA, Darmstadt, Germany	412511
L-Glutamine	Thermio Fisher Scientific, Dreieich, Germany	25030-081
Methanol	Sigma-Aldrich Chemie GmbH, Stein, Germany	32213
Nonident P40	Sigma-Aldrich Chemie GmbH, Stein, Germany	56741
PBS	PAA Laboratories GmbH, Pasching, Austria	H15-002
peqGOLD DNA ladder mix 100 - 10000 bp	Peqlab Biotechnologie GmbH, Erlangen, Germany	25-2040
Phosphate buffered saline (PBS) powder	Merck KGaA, Darmstadt, Germany	182-50

Precision Plus Protein™ Dual Color Standards	Bio-Rad Laboratories GmbH, Munich, Germany	161-0374
Resorcinol	Sigma-Aldrich Chemie GmbH, Stein, Germany	398047
Rotiphorese gel 30 (37.5:1)	Carl Roth GmbH & Co. KG, Karlsruhe, Germany	3029.2
RPMI 1640	Thermio Fisher Scientific, Dreieich, Germany	21875-091
Salubrinal	Calbiochem GmbH, Bad Soden, Germany	324895
Sodium azide	Merck KGaA, Darmstadt, Germany	S2002
Sodium deoxycholate	Sigma-Aldrich Chemie GmbH, Stein, Germany	D6750
Sodium dodecyl sulfate (SDS)	Carl Roth GmbH & Co. KG, Karlsruhe, Germany	2326.1
Tauroursodeoxycholic acid (TUDCA)	Calbiochem GmbH, Bad Soden, Germany	580549
Tris base	AppliChem GmbH, Darmstadt, Germany	A1379
Triton X-100	Sigma-Aldrich Chemie GmbH, Stein, Germany	T8787
TRIZOL	Thermio Fisher Scientific, Dreieich, Germany	15596018
Trypsin	Life Technologies GmbH, Darmstadt, Germany	A12177-01
Tunicamycin	Thermio Fisher Scientific, Dreieich, Germany	T7765
Tween-20	Sigma-Aldrich Chemie GmbH, Stein, Germany	P7949
Versene	Thermio Fisher Scientific, Dreieich, Germany	15040-066
Xylene cyanol	Sigma-Aldrich Chemie GmbH, Stein, Germany	X4002
β-Mercapthoethanol	Sigma-Aldrich Chemie GmbH, Stein, Germany	M7522

6.2 ELISA Sets

ELISA sets	Manufacturer	Order number
BD OptEIA™ Human IL-1β ELISA Set II	BD Bioscience, Heidelberg, Germany	557953
BD OptEIA™ Human IL-6 ELISA Set	BD Bioscience, Heidelberg, Germany	555220
BD OptEIA™ Human IL-8 ELISA Set	BD Bioscience, Heidelberg, Germany	555244
BD OptEIA™ Human TNF ELISA Set	BD Bioscience, Heidelberg, Germany	555212
BD OptEIA™ Mouse GM-CSF ELISA Set	BD Bioscience, Heidelberg, Germany	555167
BD OptEIA™ Mouse IFN-γ ELISA Set	BD Bioscience, Heidelberg, Germany	555138
BD OptEIA™ Mouse IL-12 (p40) ELISA Set	BD Bioscience, Heidelberg, Germany	555165
BD OptEIA™ Mouse IL-6 ELISA Set	BD Bioscience, Heidelberg, Germany	555240
BD OptEIA™ Mouse TNF (Mono/Mono) ELISA Set	BD Bioscience, Heidelberg, Germany	555268

6.3 Kits

Kit	Manufacturer	Order number
iScript™ cDNA Synthesis Kit	Bio-Rad Laboratories GmbH, Munich, Germany	170-8891
Hot Start Taq 2X Master Mix	New England BioLabs GmbH, Frankfurt, Germany	M0496
Maxima SYBR Green qPCR Master Mix 2x	Thermo Fisher Scientific, Dreieich, Germany	K0253

6.4 Antibodies

Antibody	Manufacturer	Order number
Mouse anti-mouse NF-κB (p65), clone F-6	Santa Cruz Biotechnology Inc.	sc-8008
Goat anti-mouse IgG Alexa Fluor 555	Thermo Fisher Scientific, Dreieich, Germany	A-21422
Mouse anti-human CD86 FITC, clone 2331 (FUN-1)	BD Bioscience, Heidelberg, Germany	555657
Mouse anti-human CD54, clone HA58	BD Bioscience, Heidelberg, Germany	559771
Rat anti-mouse IL-1α, clone 40508	R & D Systems GmbH, Wiesbaden, Germany	MAB400
Goat anti-mouse IL-1α Biotinylated	R & D Systems GmbH, Wiesbaden, Germany	BAF400

Rabbit anti-mouse LC3B	Cell Signaling Technology, Frankfurt, Germany	2755
Donkey anti-rabbit IgG Alexa Fluor 555	Thermo Fisher Scientific, Dreieich, Germany	A-31572

6.5 Consumable materials

Consumable Material	Manufacturer
0.2 ml Thermostrips	Thermo Scientific GmbH, Schwerte, Germany
24-Well plate	Greiner Bio-One International AG, Frickenhausen, Germany
6-Well plate	Greiner Bio-One International AG, Frickenhausen, Germany
96-well plates (flat bottom)	Greiner Bio-One International AG, Frickenhausen, Germany
96-well plates (round bottom)	Corning GmbH, Kaiserslautern, Germany
Bluecaps 15 ml	Corning GmbH, Kaiserslautern, Germany
Bluecaps 50 ml	Greiner Bio-One International AG, Frickenhausen, Germany
Cell culture flasks (T25)	Greiner Bio-One International AG, Frickenhausen, Germany
Cell culture flasks (T75, T175)	Greiner Bio-One International AG, Frickenhausen, Germany
Cell strainer (100 µm)	BD Bioscience, Heidelberg, Germany
Chamber slides 8-Well	Nunc, Inc. Naperville, USA
Cover slips 25x55 mm	R.Langenbrinck, Teningen, Germany
Cryotubes 1.5 ml	Corning GmbH, Kaiserslautern, Germany
FACS tubes	Greiner Bio-One International AG, Frickenhausen, Germany
Filter tips, 10 µl, 20 µl, 100 µl, 200 µl, 1000 µl	Nerbe plus GmbH, Winsen, Germany
Gloves (latex)	Meditrade GmbH, Kiefersfelden, Germany
Gloves (nitrile)	Ansell Occupational Healthcare, Munich, Germany
Light cycler capillaries	GeneOn GmbH, Ludwigshafen, Germany
Micro reaction container 0.5 ml - 5 ml	Eppendorf GmbH, Hamburg, Germany
Needles 20Gx2 4/5 0.9 x 70 mm	Brand GmbH + Co KG, Wertheim, Germany
Parafilm®	Greiner Bio-One International AG, Frickenhausen, Germany
Petri-dishes (10 cm)	Eppendorf GmbH, Hamburg, Germany
Pipette tips 10 µl	Eppendorf GmbH, Hamburg, Germany
Pipette tips 1000 µl	Eppendorf GmbH, Hamburg, Germany
Pipette tips 20 µl, 100 µl, 200 µl	VWR Lab Services GmbH, Darmstadt, Germany
Pipette tips multi-channel pipette	Corning GmbH, Kaiserslautern, Germany
Stripettes® 5 ml, 10 ml, 25 ml, 50 ml	B. Braun AG, Melsungen, Germany
Syringes (U 100 insulin) 1 ml	Carl Roth GmbH & Co. KG, Karlsruhe, Germany
Weighing dish	Macherey-Nagel GmbH & Co. KG, Düren, Germany
Weighing paper	Roche Deutschland Holding GmbH, Grenzach-Wyhlen, Germany

6.6 Equipment

Equipment	Manufacturer
Centrifuge 5417 R	Eppendorf GmbH, Hamburg, Germany
Centrifuge 5417R	Eppendorf GmbH, Hamburg, Germany
Centrifuge Megafuge 11 R	Heraeus Sepatech GmbH, Osterode, Germany
Centrifuge Megafuge 3.0 R	Heraeus Sepatech GmbH, Osterode, Germany
Centrifuge Megafuge 40 R	Heraeus Sepatech GmbH, Osterode, Germany
Coulter counter	Coulter Electronics Limited, Krefeld, Germany
Cryo freezing container	Sigma-Aldrich Chemie GmbH, Stein, Germany
Electrophoresis chamber (SDS-PAGE)	Biometra GmbH, Göttingen, Germany

Electrophoresis power supply	Pharmacia Biotech GmbH, Freiburg, Germany
Electrophoresis tank (SUB-CELL GT)	Bio-Rad Laboratories GmbH, München, Germany
ELISA reader (Sirius HT-TRF)	BioTek Instruments GmbH, Bad Friedrichshall, Germany
FACSCanto II	BD Bioscience, Heidelberg, Germany
Incubator Heraeus 6000	Heraeus Sepatech GmbH, Osterode, Germany
Laminar flow cabinet (Safe 2020)	Thermo Scientific GmbH, Schwerte, Germany
Light Cycler	Roche Deutschland Holding GmbH, Grenzach-Wyhlen, Germany
Microscope Axiovert 135	Carl Zeiss Microscopy GmbH, Jena, Germany
Nanodrop 1000	Thermo Scientific GmbH, Schwerte, Germany
Pipetboy	INTEGRA Biosciences GmbH, Fernwald, Germany
Pipettes	Eppendorf GmbH, Hamburg, Germany
Power supply Consort E861	Sigma-Aldrich Chemie GmbH, Stein, Germany
Scanner (ViewPix 700)	EPSON Deutschland GmbH, Meerbusch. Germany
Thermocycler	Bio-Rad Laboratories GmbH, München, Germany
Thermomixer	Eppendorf GmbH, Hamburg, Germany
Trans-Blot SD transfer cell	Bio-Rad Laboratories GmbH, München, Germany
Ultraviolet (UV) transilluminator	Peqlab Biotechnologie GmbH, Erlangen, Germany
Vortex	VWR Lab Services GmbH, Darmstadt, Germany

6.7 Murine Primers

Gene	Sequence (5´- 3´)	MT (in °C)	Product size (in bp)	Reference
β-Actin	CACTGTCGAGTCGCGTCC	60,50	89	
	TCATCCATGGCGAACTGGTG	60,39		
beta defensin 3 (BD3)	CGGGATCTTGGTCTTCTCTA	55,76	85	
	GCATTGGCAACACTCGTCAGA	61,47		
Atg12	TGGCCTCGGAACAGTTGTTTA	59,86	138	
	ATCCCCATGCCTGGGATTTG	60,11		
Atg5	ACCTCGGTTTGGCTTTGGTT	60,40	440	
	AAAGTGAGCCTCAACCGCAT	60,25		
Atg3	GCTATGATGAGCAACGGCAG	59,41	604	
	AGGCTGGCATGGAACACTTT	60,18		
Nbr1	GATTCACCCCGCAGGGATAG	59,96	538	
	CCCTTCGTGGACTTGCATCT	60,04		
Chop	ACCTGAGGAGAGAGTGTTCCA	59,85	112	
	CAAGGTGAAAGGCAGGGACT	59,89		
Il-23 (alpha subunit p19)	GCACCAGCGGGACATATGAA	60,46	129	
	CAAGCAGAACTGGCTGTTGTC	60,00		
Tnf-alpha	CCACATCTCCCTCCAGAAAAGA	59,43	719	
	GCTGGGTAGAGAATGGATGAAC	58,53		
Il-6	GCCTTCTTGGGACTGATGCT	60,03	181	
	TGCCATTGCACAACTCTTTTC	57,90		
Ifn-gamma	CGGCACAGTCATTGAAAGCC	60,11	119	
	TGTCACCATCCTTTTGCCAGT	60,13		
Il-1beta	TGCCACCTTTTGACAGTGATG	59,04	220	
	AAGGTCCACGGGAAAGACAC	59,89		

Tnfaip3 (=A20)	GATCGGGTGTCCATGGGG	59,49	143	
	CGACAAGGCCTCTTGGGG	60,05		
Cxcl-16	AGCGCAAAGAGTGTGGAACT	60,18	193	
	GGTTGGGTGTGCTCTTTGTT	58,89		
Il-1 alpha	CGCTTGAGTCGGCAAAGAAAT	59,80	115	
	CAGAGAGAGATGGTCAATGGCA	59,83		
β-Actin	CCTCTATGCCAACACAGTGC	58,91	206	Lenna et al. 2013
	CCTGCTTGCTGATCCACATC	58,98		Lenna et al. 2013
Xbp-1	CCATGGGAAGATGTTCTGGG	57,94	145 + 171	Iwakoshi et al. 2007
	ACACGCTTGGGAATGGACAC	60,89		Iwakoshi et al. 2007

6.8 Human primers

Gene	Sequence (5´- 3´)	MT (in °C)	Product size (in bp)	Reference
β-Actin	GACCCCGTCACCGGAGTCCA	65.83	537	
	CGAGCACAGAGCCTCGCCTTT	65.28		
XBP-1	TTACGAGAGAAAACTCATGGC	56.00	257 + 289	Lin et al. 2007
	GGGTCCAAGTTGTCCAGAATGC	61.72		Lin et al. 2007

6.9 Cell culture media

PAM212 medium

	Component	Final concentration	Amount
1	RPMI 1640		443.75 ml
2	FBS	10%	50 ml
3	HEPES	5 mM	2.5 ml of 1 M
4	L-Glutamine	1.5 mM	3.75 ml of 200 mM
5	β-Mercaptoethanol	12.5 µM	0.4375 µl

THP-1 medium

	Component	Final concentration	Amount
1	RPMI 1640		427.5 ml
2	FBS	10%	50 ml
3	HEPES	25 mM	12.5 ml of 1 M
4	L-Glutamine	4 mM	10 ml of 200 mM
5	β-Mercaptoethanol	50 µM	1.75 µl of 14.3 M

HaCaT medium

	Component	Final concentration	Amount
1	DMEM		445 ml
2	FBS	10%	50 ml
3	L-Glutamine	2 mM	5 ml of 200 mM

6.10 Solutions for DNA gel electrophoresis

50x TAE buffer

	Component	Final concentration	Amount
1	Tris	2 M	242 g
2	EDTA	0.05 M	18.61 g
3	Glacial acetic acid	5.7%	57 ml
4	ddH_20		ad 1000 ml

6x DNA loading dye

	Component	Final concentration	Amount
1	Tris-HCl (pH 7.6)	10 mM	1 ml of 0.1 M
2	EDTA (disodium salt)	60 mM	0.223 g
3	Glycerol	60%	6 ml
4	Xylene cyanol	0.03%	0.003g
5	Bromphenol blue	0.03%	0.003 g
6	dH_2O		ad 10 ml

6.11 FACS buffer

	Component	Final concentration	Amount
1	PBS		45 ml
2	FBS	10%	5 ml

6.12 ELISA solutions

Assay diluent

	Component	Final concentration	Amount
1	PBS		45 ml
2	FBS	10%	5 ml

Coating buffer 0.1 M sodium carbonate pH 9.5

	Component	Final concentration	Amount
1	$NaHCO_3$		7.13 g
2	Na_2CO_3		1.59 g
3	ddH_2O		ad 1000 ml
4	NaOH		pH to 9.5

ELISA washing buffer

	Component	Final concentration	Amount
1	PBS		2000 ml
2	Tween-20	0.05%	1 ml

6.13 NF-κB assay buffer

NF-kB assay fix solution

	Component	Final concentration	Amount
1	PBS		8.91 ml
2	Paraformaldehyde	4%	1.08 ml of 37%

NF-kB assay perm solution

	Component	Final concentration	Amount
1	PBS		10 ml
2	Triton X-100	0.25%	25 µl

7 Methods

7.1 Cell culture

7.1.1 Cultivation of cells

All cells were handled under sterile conditions and grown at 37°C and 5 % CO_2 in a humidified incubator. The murine keratinocyte cell line PAM212 (Yuspa et al. 1980) shown in Figure 9 was cultured in complete RP10 medium (6.9**)**. The medium volume used was adjusted to the size of the culture flask (T25 → 8 ml, T75 → 15 ml, T175 → 25 ml). Cells of the human keratinocyte cell line HaCaT (Figure 10 and Boukamp et al. 1988) were kindly provided by Dr. Ute Wölfle and kept in DMEM supplemented with 10% FBS. The human monocytoid cell line THP-1 (Figure 11 and (Tsuchiya et al. 1980)), a cell line that can be used as a surrogate for DCs (Berges et al. 2005; Bocchietto et al. 2007), was cultured in THP-1 medium (6.9) and provided by the BIOSS toolbox of the University of Freiburg. Immortalized normal human keratinocytes (NHKi) (Figure 12) were kindly provided by PD Dr. Yinghong He and Juna Leppert. These cells were cultured in Keratinocyte-SFM medium from Gibco.

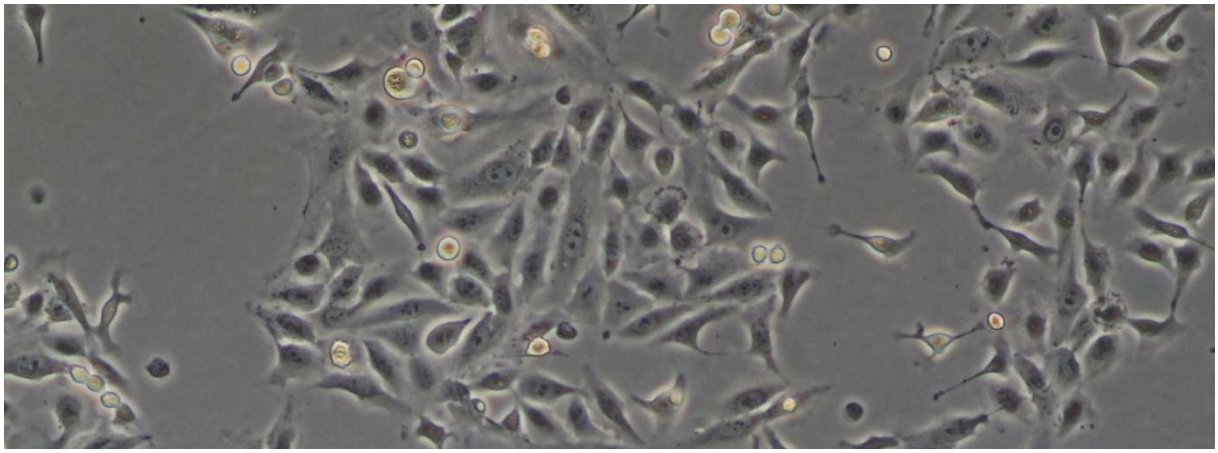

Figure 9: PAM212 cells grown in a T175 culture flask at 100x magnification. Picture shows cells after 24 h of culture with a starting density of $6x10^3$ cells/ cm^2.

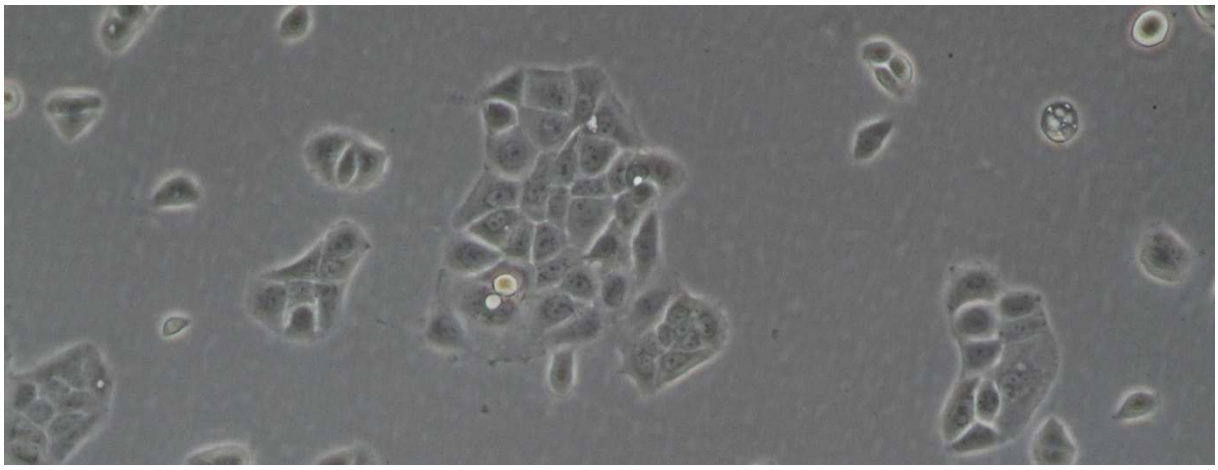

Figure 10: Cultured HaCaT cells at 100x magnification. Picture shows cells after 24 h of culture with a starting density of $1.3x10^4$ cells/ cm^2.

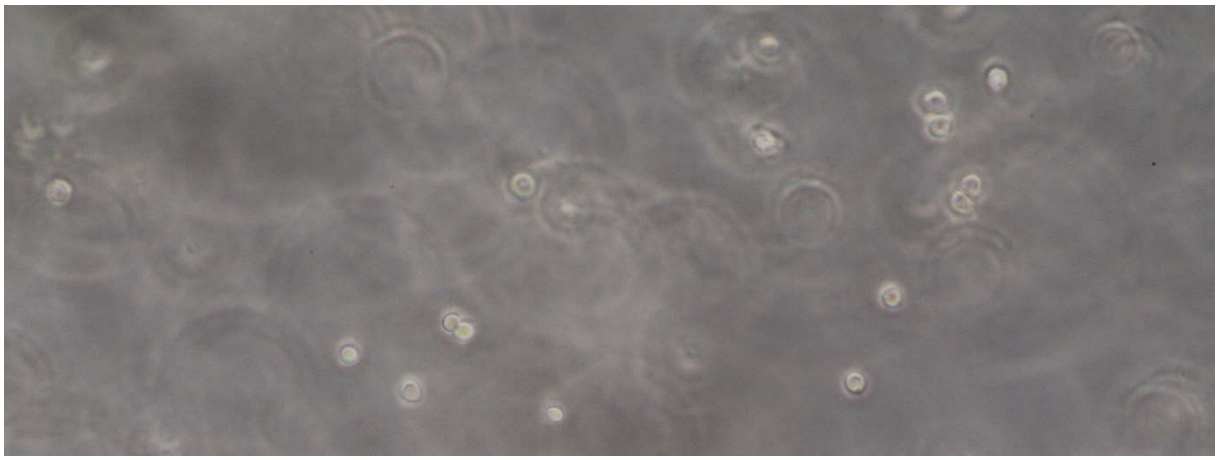

Figure 11: Cultured THP-1 cells at 100x magnification. Picture shows cells after 24 h of culture with a starting density of 1x105 cells / ml.

Figure 12: Cultured NHKi (immortalized NHKs) at 100x magnification. Picture shows cells after 24 h of culture with a starting density of $1x10^4$ cells/ cm^2.

7.1.2 Passaging of cultured cells

For passaging or to prepare them for an experiment, cells had to be removed from the culture flask. First the culture medium was removed and the cells were washed with 10 ml PBS to remove any remains of the FCS-containing medium. For HaCaT cells this was followed by a 10 min incubation with 0.05% EDTA. Afterwards trypsin (0.05% in 0.02% EDTA) was added to the cells (T25 → 1 ml, T75 → 2 ml, T175 → 3 ml) and the flask was placed in the incubator for 5 – 10 min at 37°C, 5 % CO_2 to detach the adherent cells from the bottom of the flask. After microscopic control for cell detachment, 10 ml medium was added to the cells to inhibit the trypsin. The cell suspension was transferred to a 50 ml blue cap and centrifuged for 5 min at 230 xg at 4°C. After removal of the supernatant the cell pellet was resuspended in fresh medium, counted and seeded either in a new culture flask or a multiwell plate and placed in the incubator. In the case of non-adherent cells like the THP-1 cells the trypsination step was omitted and they were simply removed from the culture flask and directly centrifuged.

7.1.3 Cryopreservation of cells

For stock keeping and long-term storage cells were held in liquid nitrogen. First the cells were removed from the culture flask as described in 7.1.2. After counting the cells, they were centrifuged at 230 xg for 5 min at 4°C and resuspended in FCS at a concentration of $1.1x10^7$ cells/ ml. The cell suspension was distributed in cryotubes (900 µl per tube) and 100 µl of the cryoprotectant DMSO were added to get a final concentration of 10 % DMSO in each tube. Because DMSO is cytotoxic at RT the tubes were rapidly placed in special freezing boxes that allow for an even freezing process and stored at -80°C for 3 days prior to storage in liquid nitrogen.

7.1.4 Thawing of cells

Since DMSO is cytotoxic at RT, the thawing process has to be performed as fast as possible to remove the cells from the DMSO. The cryotube containing the cells of interest was removed from liquid nitrogen storage and placed in a water bath at 37°C for 2 min. Afterwards the cells were transferred into a blue cap containing 14 ml of prewarmed culture medium to dilute the DMSO in the freezing medium. The cell suspension was centrifuged for 5 min at 280 xg at RT, the supernatant was removed and the pellet was resuspended in fresh culture medium. After placing the cells in a culture flask, they were cultured as described in 7.1.1.

7.2 Cytotoxicity assays

7.2.1 3-(4,5-dimethylthiazol-2-yl)-2,5-diphenyltetrazolium bromide (MTT) assay

The MTT assay is a colorimetric assay that assesses the viability of cells by correlating it to their metabolic activity. In this assay the activity of NAD(P)H-dependent cellular oxidoreductase enzymes is taken as an indicator for the number of viable cells. The enzyme activity is assessed by their ability to reduce MTT to formazan, its purple water-insoluble form. To detect cellular viability the chemical-treated cells were washed with PBS and incubated in a 0.5 mg/ml MTT solution in culture medium using the same volume as was used for the experiment. The incubation lasted 2 h and the culture medium was removed afterwards. After discarding the MTT solution, the water-insoluble formazan crystals were dissolved in a 1:49 mixture of hydrochloric acid and 2-propanol using the same volume as for the experiment. The absorption of this solution was measured at 595 nm using an ELISA reader. An untreated (100% viable cells) as well as a maximal cell death control (0% viable cells) were included and the cellular viability was calculated using the following formula:

$$\%\ \text{viable cells} = \frac{\text{Compound treated value} - \text{untreated value}}{\text{Maximum value} - \text{untreated value}} * 100$$

Since the assay correlates metabolic activity with viability, one has to be sure that the treatment of cells is not just inhibiting the cellular metabolism leading to the false assumption of decreased viability. To exclude this possibility, cells were also monitored microscopically, looking for signs of cell death like detachment from the culture vessel, blebbing or rupture of cells (Tinari et al. 2008).

7.2.2 Lactate dehydrogenase (LDH) release assay

The LDH assay was used as an alternative assay to determine the cytotoxicity of the used chemicals. This assay uses the fact that LDH, a cytosolic enzyme, is released into the culture medium when the plasma membrane is damaged. To quantify this extracellular LDH the LDH Cytotoxicity Assay Kit (Thermo Scientific) was used. In a coupled reaction, lactate is converted to pyruvate. This process is catalyzed by LDH via the reduction of the oxidized form of nicotinamide adenine dinucleotide (NAD^+ to NADH). The NADH is then used by diaphorase to reduce a tetrazolium salt to a red formazan product. This product can then be measured at 490 nm. The whole assay

was performed according to the manufacturer's instruction. For this, 50 µl of medium from the chemical-treated cells were transferred to a 96-well plate. For later calculation one well of cultured cells was left untreated to determine the amount of spontaneous LDH release and another well was used as reference for the maximal amount of LDH that could be released. For this, the cells were lysed by adding the lysis buffer supplied by the kit 45 min before the end of the incubation time. After pipetting all the media samples (triplicates of each) into their respective wells, 50 µl of reaction mix were added and the plate was incubated for 30 min at RT protected from light. After the 30 min 50 µl of stop solution was added to each well to stop the reaction described above. The absorbance was measured at 490 nm and 680 nm. The 680 nm value is the background and was subtracted from the 490 nm absorbance value. To calculate the cytotoxicity the following formula was used:

$$\%\ Cytotoxicity = \frac{Compound - treated\ LDH\ activity - Spontaneous\ LDH\ activity}{Maximum\ LDH\ activity - Spontaneous\ LDH\ activity} * 100$$

7.3 Molecular biological methods

7.3.1 Isolation of RNA

To analyze the expression of a certain gene within cells the first step is to isolate the RNA from the cells using TRIzol reagent (which is an improved form of the single-step RNA isolation method developed by Chomcynski and Sacchi (Chomczynski and Sacchi, 1987)). For this the culture medium was removed from cells and they were washed once with 1x PBS. After adding TRIzol (300 µl per well in 24-well plates, 600 µl per well in 6-well plates) and incubation for 5 min at RT the cells were scraped of the well using the tip of a pipette and transferred to a 1.5 ml Eppendorf tube. Subsequently, the cells were homogenized by passing them through a syringe (20 G) 10 times. After a second incubation of the cell lysate for 5 min, chloroform was added (100 µl per 300 µl TRIzol) and the tube was shaken vigorously by hand for 15 sec. Incubation for 3 min was followed by centrifugation for 15 min at 12000 xg at 4°C to get a phase separation of organic and aqueous phase. The clear top layer containing the RNA was removed and transferred to a new 1.5 ml Eppendorf tube. To precipitate the RNA from the aqueous layer 250 µl isopropanol per 300 µl TRIzol were added and after incubation for 10 min at RT the tube was centrifuged for 10 min at 12000 xg, 4°C. The supernatant was removed, 500 µl 75% ethanol per 300 µl

TRIzol were added to the RNA pellet and the tube was vortexed briefly before centrifugation for 5 min at 7500 xg at 4°C to wash out any impurities from the RNA. The supernatant was removed as much as possible and any remaining ethanol was evaporated by incubating the pellet with an open lid for 5 min. The RNA pellet was then resuspended in 20 µl RNase-free water and the RNA concentration was determined spectrophotometrically using a Nanodrop. The RNA was then ready to use for downstream applications and was either used immediately or was frozen at -20°C afterwards for later use.

7.3.2 cDNA synthesis

The next step in the analysis of gene expression is to transcribe the RNA into cDNA using reverse transcription. This was done using the iScript cDNA synthesis kit following the manufacturer's instructions. If RNA was frozen prior to use it was thawed slowly on ice. For each reaction 1 µg of RNA in 15 µl nuclease-free water was used. To obtain this concentration from higher RNA stocks they were diluted to the final volume of 15 µl. The total reaction mix comprised the ingredients as listed in Table 1.

	Component	Amount
1	5x Reaction mix	4 µl
2	Reverse transcriptase	1 µl
3	RNA	x µl (=1 µg)
4	Nuclease-free water	ad 25 µl

Table 1: Components for one reverse transcription of RNA into cDNA.

The following thermal cycler protocol was used for the reaction:

	Temperature	Duration
1	25°C	5 min
2	42°C	30 min
3	85°C	5 min
4	4°C	□

Table 2: Thermal cycler protocol for reverse transcription.

7.3.3 Conventional polymerase chain reaction (PCR)

After transcribing RNA into cDNA, the next step of analyzing gene expression is amplifying the sequence of the gene of interest using PCR. With this method one can easily get a large amount of a certain DNA fragment by using oligonucleotide primers specific for the gene one is interested in. To make sure that the primers only bind to

DNA that was transcribed from the isolated mRNA and not to genomic DNA carried on from the RNA isolation, they were designed to span an exon-exon junction. The total reaction mix (Table 3) was composed of the following ingredients:

	Component	Amount
1	2x HotStart master mix	12 µl
2	Primer forward	1 µl (=0.4 µM)
3	Primer reverse	1 µl (=0.4 µM)
4	cDNA	x µl (=100 ng)
5	Nuclease-free water	ad 25 µl

Table 3: Components for one PCR reaction.

Just like cDNA synthesis, this reaction was also done using a thermal cycler. The following protocol was used:

	Temperature	Duration	
1	95°C	30 sec	
2	95°C	30 sec	**35x**
3	58°C	30 sec	
4	68°C	30 sec	
5	68°C	5 min	
6	4°C	□	

Table 4: Thermal cycler protocol for murine XBP-1 and beta-actin PCR.

7.3.4 Agarose gel electrophoresis

To separate the DNA fragments received from the PCR by their size, a gel electrophoresis was performed. By connecting voltage to an agarose gel loaded with the PCR products, DNA fragments are transported through the gel at different speeds according to their size. Agarose gels were made by heating agarose in 0.5x TAE buffer. The concentration of the gel was chosen according to the size of the expected PCR products to ensure the best possible separation. 5 µl ethidium bromide per 100 ml of gel volume were added to visualize the DNA fragments afterwards. Gels were run at 11 V/cm, 300 W and 400 mA for 105 min with constant voltage. DNA visualization was done using a gel documentation system with UV lamps.

7.3.5 Analysis of *XBP-1* splicing

XBP-1 splicing was analyzed using ImageJ (NIH). The gel pictures are loaded into the program (Figure 13a) and each lane is selected using the rectangular selection tool (Figure 13b). The intensity of each lane is plotted (Figure 13c) and the spliced and the unspliced *XBP-1* measured using the wand tool (Figure 13d). Using the

straight line tool, spliced and unspliced *XBP-1* are separated (Figure 13e) and the intensity of the spliced XBP-1 alone is measured (Figure 13f).

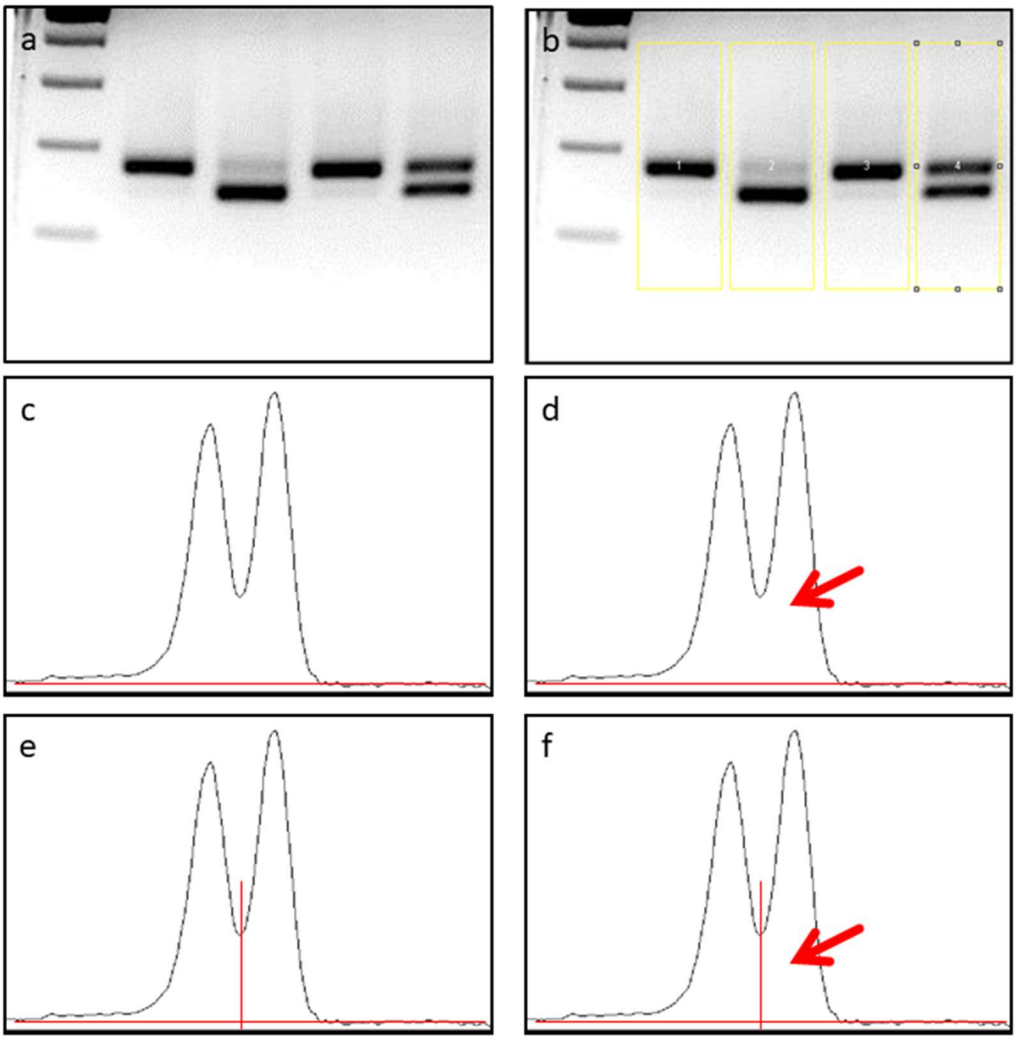

Figure 13: Schematic process of the quantification of XBP-1 splicing within a sample. The image of the gel is loaded into ImageJ (a) and the PCR products are selected using the rectangular selection tool (b). The intensity levels of the gel are then shown as plots (c), background intensity is removed (c) and the total intensity of the XBP-1 band is measured. Afterwards, the two peaks are separated using the line tool (c) and the intensity of the spliced band is measured.

The ratio of spliced *XBP-1* is calculated using the following formula:

$$\%\ \text{of spliced}\ XBP-1\alpha = \frac{\text{intensity of spliced XBP}-1\alpha}{\text{intensity of total}\ XBP-1\alpha} * 100$$

7.3.6 Real-time polymerase chain reaction (qPCR)

In contrast to the regular PCR, also called end-point PCR, the qPCR measures the amplification of the DNA in real time. This is done by using a fluorescent dye that intercalates with all double-stranded DNA. At the end of each replication cycle the

fluorescent intensity of each sample is measured. The course of the fluorescence for each sample is depicted as a curve (left side of Figure 14) and the exact point where the fluorescence is crossing a set threshold point is calculated and noted as a C_T values (threshold cycle), which indicate the number of cycles that were necessary to get a signal that is above the background level. Using the C_T values from the gene of interest and a housekeeping gene makes it possible to get a relative quantification of the gene expression by using the comparative C_T method (Schmittgen and Livak 2008). To make sure that there are no unwanted byproducts amplified during the PCR reaction, a melting curve (top and bottom right of Figure 14) is performed to make sure that the primers are indeed specific. An optimal result is characterized by a single drop of fluorescence for each sample without the appearance of a plateau and a second drop which would show the presence of another PCR product.

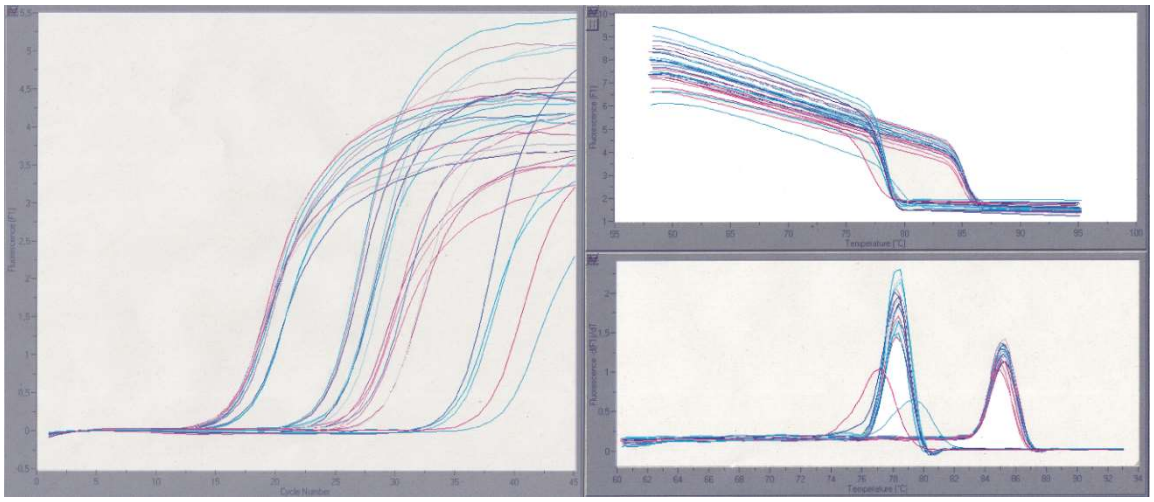

Figure 14: Example of the results of a qPCR run. Left side: Course of the fluorescence of each sample over time. Right side top: Melting curve for each sample (course of fluorescence over increasing temperature). Right side bottom: Melting curve for each sample (course of the change of fluorescence over increasing temperature).

The total reaction mix (Table 5) was composed of the following ingredients:

	Component	Amount
1	2x SybrGreen Master mix	10 µl
2	Primer forward (10 µM)	0.6 µl (=0.3 µM)
3	Primer reverse (10 µM)	0.6 µl (=0.3 µM)
4	Nuclease-free-water	Ad 20 µl
5	cDNA	X µl (=25 ng)

Table 5: Components for one qPCR reaction.

The following protocol was used:

Spalte1	Temperature	Duration		
1	95°C	10 min		Pre-incubation
2	95°C	30 sec		
3	55°C	35 sec	**45x**	Quantification
4	72°C	35 sec		
5	95°C	20 sec		
6	58°C	20 sec		
7	58°C --> 95°C	0,05°C / sec		Melting curve
8	95°C --> 40 °C			Cooling

Table 6: Light cycler protocol for qPCR.

The results received from the qPCR reaction are shown as curves comparable to Figure 14. The relative gene expression was calculated using the comparative C_T method (Schmittgen et al. 2008).

7.4 Protein biological methods

7.4.1 Immunocytochemistry

To analyze the amount and location of a specific protein within cells immunocytochemistry is a good method of choice. The protein of interest on or within a cell is labeled with a specific antibody against it which is made visible using a secondary antibody against the primary antibody. The secondary antibody is labeled with a fluorophore. Using a microscope, a mercury vapor lamp and filters for specific wave lengths the fluorophore can be excited and fluoresces.

At the beginning, the cells to be analyzed were seeded in 24-well plates containing glass slides that were covered with rat collagen I for optimal adhesion of the cells. After culturing the cells for 24 h they were ready for the experiment. When the treatment of the cells for the experiment was finished, the culture medium was removed and the cells were washed with 200 µl PBS for 5 min once. By adding 200 µl of 4% formaldehyde (FA) in PBS for 10 min the cells were fixed. The FA solution was aspirated and the cells were washed three times with PBS for 5 min. Permeabilization of the cells was achieved by incubating them in 0.25 % Triton X-100 in PBS for 10 min at RT. This is necessary to enable the antibodies to enter the cell to stain intracellular proteins or structures. The cells were washed three times and 200 µl of the primary antibody diluted in AB diluent was added to the cells and they were incubated overnight at 4°C in a humid chamber protected from light. After

aspirating the antibody solution, the cells were washed three times with PBS and 200 µl of the secondary antibody labeled with the fluorophore and diluted in AB diluent was added and incubated for 2 h at RT. The cells were rinsed three times with PBS after incubation and nucleus staining with DAPI was performed by adding 200 µl of 100 ng/ml DAPI in PBS. The staining solution was removed and the glass slides were mounted using Mowiol mounting medium.

7.4.2 Quantification of NF-κB nuclear translocation

To determine the activation of the NF-κB pathway the translocation of the p65 subunit from the cytoplasm to the nucleus was used as this is an essential step in the activation of this proinflammatory pathway. The nuclear translocation of p65 was assessed using the method described by Guzman et al. (Guzman et al. 2013). Pictures of three random fields per sample were taken and the total cell numbers as well as the number of cells with increased nuclear translocation of p65 were counted. Increased translocation was defined as the lack of a shadow in the place of the nucleus as seen in Figure 15. Finally, the ratio of cells with increased nuclear translocation was calculated.

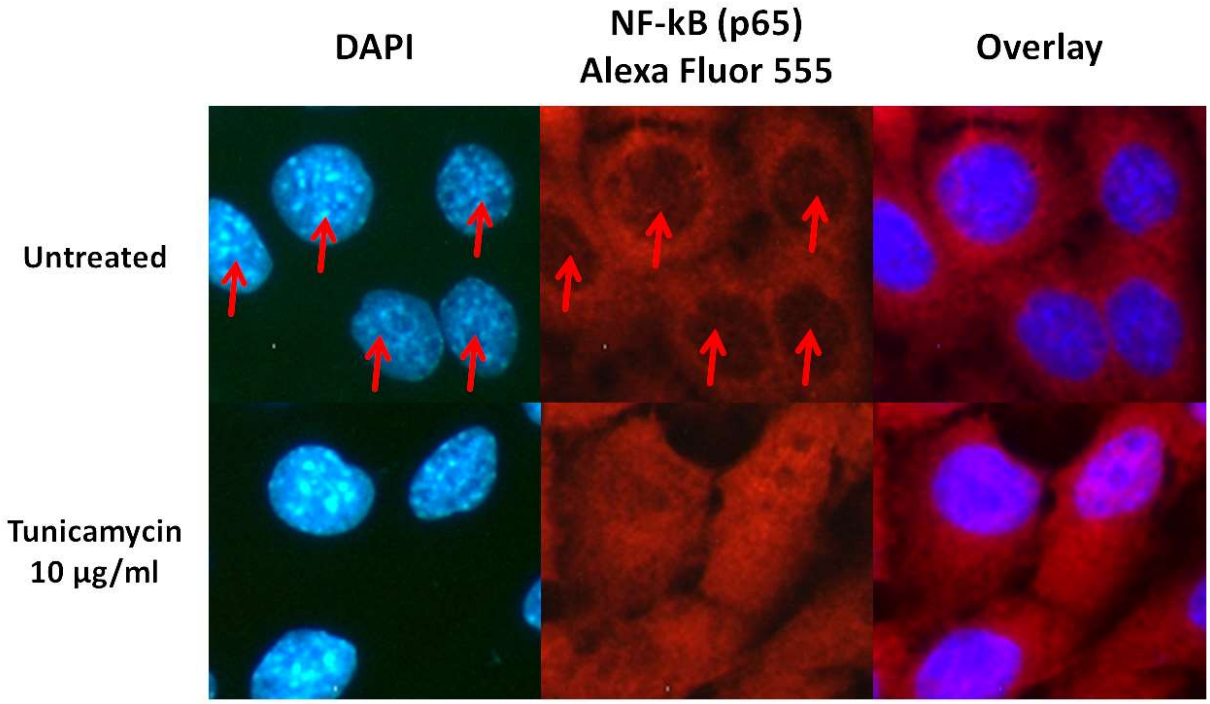

Figure 15: Examples for NF-κB p65 localization in PAM212 cells. In the steady state there is a shadow in the p65 staining in the place of the nucleus (red arrows). After stimulation with 10 µg/ml Tunicamycin for 1 h this shadow is gone indicating an increased nuclear translocation of the p65 subunit of NF-κB.

7.4.3 Enzyme-linked immunosorbent Assay (ELISA)

The ELISA is a test based on antibody binding used to identify and quantify a substance or protein. The ELISA variant used in this thesis is the so-called sandwich ELISA. A 96-Well plate is coated with a capture antibody specific for the protein of interest. The supernatant of cultured cells is added to the wells and the antibodies bind the protein they are specific for. After removing the supernatant and washing off any residuals a second antibody specific for the protein of interest is added. This antibody has to detect a different epitope on the antigen than the capture antibody. The detection antibody is conjugated to biotin. To detect the protein of interest an enzyme called horseradish peroxidase (HRP) was used. HRP conjugated to streptavidin was added to the detection antibody and biotin bound to streptavidin. Adding the substrate of this enzyme to the well creates a change of color of the substrate that can be detected with a microplate reader.

In detail, the wells of the 96-Well plate were coated with 100 µl of capture antibody diluted in coating buffer according to the manufacturer's specification. The plate was sealed and incubated at 4°C over night. Then the buffer was removed and the wells were washed with washing buffer three times. Following this, the plates were blocked by adding 200 µl of assay diluent to the wells and incubating them for 1 h at RT. After the assay diluent was removed the wells were washed three times and 50 µl of standard prepared according to the manufacturer's instructions as well as 50 µl of the samples were added to the plate. After 2 h of incubation the wells were washed five times. 50 µl of working detector containing the detection antibody as well as the streptavidin-conjugated HRP were added to the wells and incubated for 1 h at RT. After aspirating and washing seven times 50 µl of substrate solution were added to the wells. Incubation in the dark for 30 min allowed the HRP to degrade its substrate and cause the change of color. This reaction was stopped by adding 50 µl of 2 N H_2SO_4. Absorbance was read at 450 nm and 570 nm for wavelength correction and the protein concentration of the samples were calculated using the software of the microplate reader.

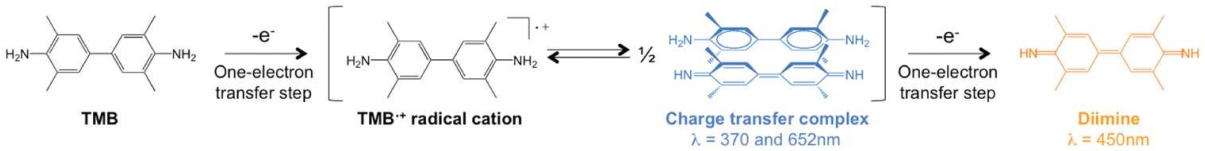

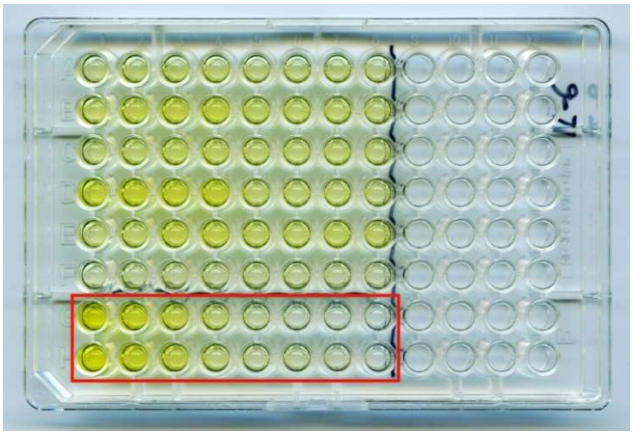

Figure 16: Detailed oxidation pathway of TMB used for the quantification of proteins in an ELISA (modified from Stefan, Denat, and Monchaud 2012) and an example of an ELISA plate with a standard serial dilution (red box).

7.5 Coculture after HaCaT stimulation (COCAHS)

To test the ability of keratinocytes to activate innate immune cells, especially DCs, a modified version of the COCAT assay (Jenny Hennen et al. 2011; Jennifer Hennen and Blömeke 2017) was used. Hennen and colleagues developed the COCAT assay to predict the sensitizing potential and the potency of chemicals. In the COCAT assay HaCaT keratinocytes and THP-1 cells, a surrogate cell line for DCs, were cocultured and treated with different sensitizers. They could show that in comparison to THP-1 cells in monoculture the cocultured cells were more activated (based on CD54 and CD86 expression) and offered an improved prediction of the sensitizing potency of chemicals. The goal of the modified assay was to evaluate the exact role of keratinocytes in this process and to learn more about a potential role of the UPR in keratinocyte-mediated DC activation. To analyze if keratinocytes alone are able to activated DCs in the absence of a sensitizer the COCAT assay was modified.

To prepare the assay, HaCaT cells were seeded in 96-well flat bottom plates in 200 µl HaCaT medium per well with a concentration of $1{,}25 \times 10^5$ cells/ml and were cultured for 48 h. At this point, the COCAT assay would start by co-culturing the HaCaT cells with THP-1 cells. Instead of that, the HaCaT cells were pre-treated with an IRE-1 inhibitor, a PERK inhibitor or DMSO as the solvent control in fresh HaCaT medium for 1 h in the absence of THP-1 cells. Afterwards, oxazolone or DMSO as

the solvent control was added to the HaCaT cells and they were stimulated for 6 h, still without THP-1 cells. Subsequently, the culture medium was removed and the HaCaT cells were rinsed twice with THP-1 medium to remove any residues of the inhibitor and stimulant before adding 180 µl of a THP-1 cell solution with a concentration of $4{,}44 \times 10^5$ cells/ml and beginning the co-culture for 18 h. Finally, the activation status of the THP-1 cells was determined by analyzing the expression of CD54 and CD86 using flow cytometry as described in 7.6. This type of experiment will from here on be called COCAHS (**co-c**ultured **a**fter **H**aCaT **s**timulation). Since initial experiments shown in Figure 17 could show that the solvent control had no significant effect on CD54 and CD86 expression when comparing it with completely untreated cells, the untreated samples were omitted from the further experiments carrying on with the solvent control as a reference point.

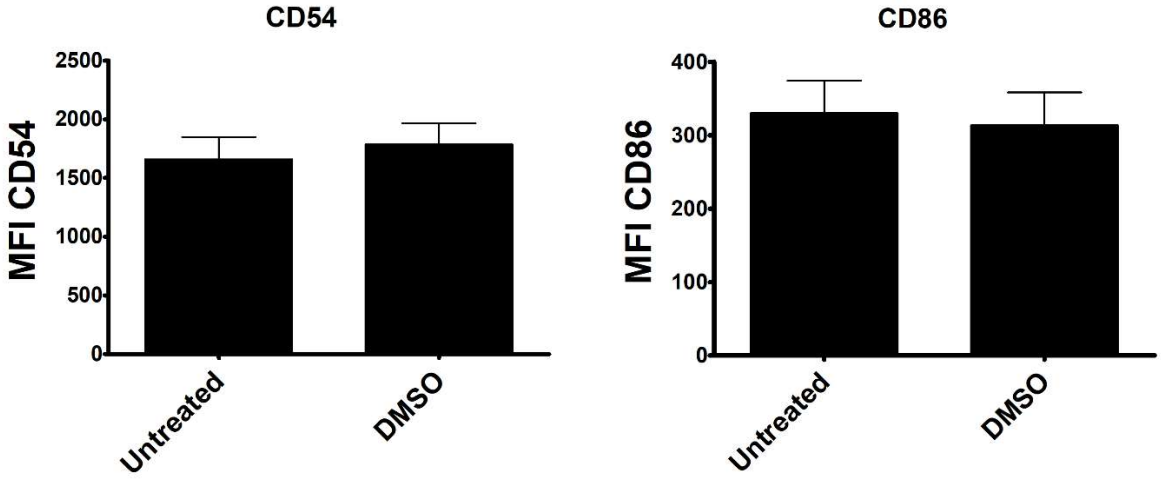

Figure 17: Effect of DMSO on the expression of CD54 and CD86 in comparison to untreated cells in the COCAHS assay. The COCAHS assay was performed with HaCaT cells that were left completely untreated and cells that received DMSO treatment as solvent control for the UPR inhibitors and oxazolone. CD54 and CD86 levels were analyzed by flow cytometry and show that the DMSO has no significant effect on the cells. Results are shown as mean MFI +/- SEM of five independent experiments.

7.6 Flow cytometry

Flow cytometry is a laser-based technique to analyze large amounts of cells in a very short period of time. With the use of fluorophore-labeled antibodies the presence and amount of any targetable structure on or within cells can be detected. In this thesis, flow cytometry is used to analyze the expression of the activation markers CD54 and CD86 on the surface of THP-1 cells after co-culturing them with sensitizer-treated HaCaT cells.

The first step was to carefully remove the THP-1 cells from the co-culture plate and

transfer them into a new 96 well plate. 40 µl of each sample were taken and pooled together to create four compensation controls (unstained, DAPI, APC(CD54), FITC (CD86)) to account for a potential spectral overlap of the used fluorophores. The cells then were centrifuged at 4°C, 250 xg for 5 min to remove them from the culture medium. They were washed by adding 200 µl FACS buffer to each well, resuspending the cells and centrifuging again. To stain the cells, they were resuspended in 50 µl staining solution that contains 2 µl of each antibody in 50 µl FACS buffer per sample. The compensation controls were resuspended in 50 µl FACS buffer and the CD54 and CD86 controls were stained by addition of 2 µl of the respective antibody. The other two controls were left unstained. After resuspension the cells were incubated for 30 min at 4°C in a dark place. The incubation step was followed by the addition of 150 µl FACS buffer and centrifugation as described above. The supernatant was removed and the cells were resuspended in 200 µl FACS buffer and transferred to a tube suitable for flow cytometric analysis. The DAPI for the exclusion of dead cells was added right before analysis to a final concentration of 500 ng/ml. DAPI can be used for the analysis of cell viability because of its ability to bind double-stranded DNA. Because of the short incubation time of the cells with DAPI a staining is only possible in dead cells were the cell membrane is already defect, living cells stay unstained. The raw data was collected using a FACSCanto II from BD. The data was then analyzed using FlowJo. The following gating strategy was used to analyze only single THP-1 cells (SSC/FSC gate) that are alive (DAPI-):

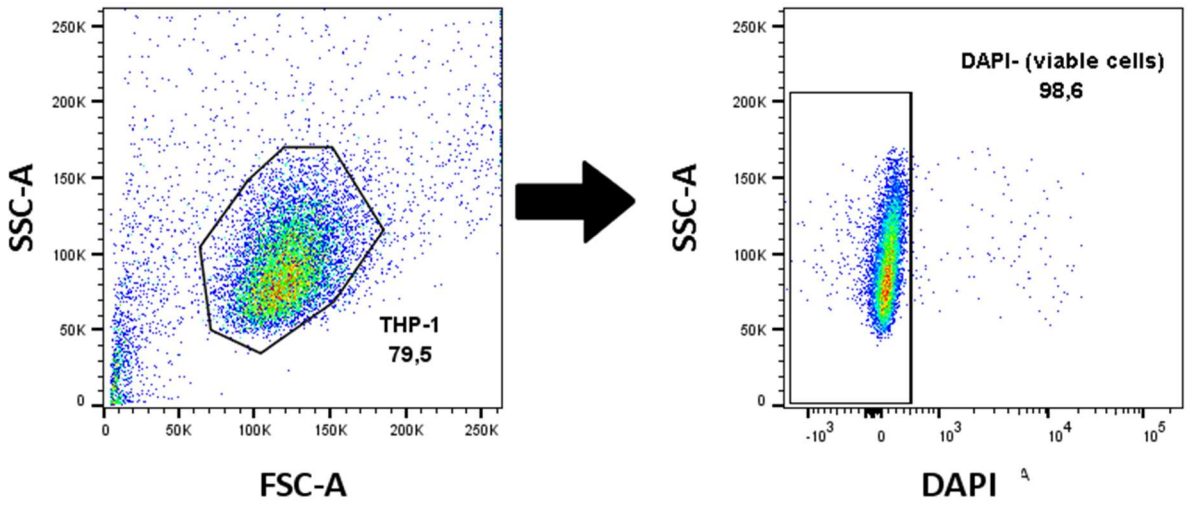

Figure 18: Gating strategy for the flow cytometry analysis of THP-1 activation: Using the first gate, dead cells and cell clumps were excluded from the further analysis. To remove dead cells, the second gate excluded DAPI+ cells.

7.7 Labeling of autophagosomes using monodansylcadaveridine (MDC)

To visualize autophagy in cells usually immunocytochemistry is used. However, stainings of autophagosome-specific proteins like LC3 can be difficult to evaluate as the protein might already be present in the cytoplasm although the autophagic process has not started yet. Some time ago an autofluorescent drug called monodansylcadaveridine (MDC) was discovered to specifically stain autophagosomes (Biederbick, Kern, and Elsässer 1995). The advantage of this staining is the very rapid protocol.

Similar to the ICC protocol, the cells to be analyzed were seeded in 24-well plates containing glass slides that were covered with rat collagen I for optimal adhesion of the cells. After culturing the cells for 24 h they were ready for the experiment. When the treatment of the cells for the experiment was finished, the culture medium was removed and the cells were washed with 200 µl PBS for 5 min once. The autophagosomes were stained by incubating the cells in 200 µl of a 0.05 mM MDC solution for 10 min at 37°C. Afterwards, the cells are washed four times with PBS and mounted on glass slides using Mowiol. The cells then were ready to be analyzed under the microscope using an excitation wavelength of 380 nm and an emission filter of 525 nm. Autophagosomes are visualized as bright dots within the cells.

8 Results

8.1 Sensitizers and irritants activate the PERK branch of the UPR

Sensitizers as well as irritants are able to activate the UPR as shown by the induction of *Xbp-1* splicing in PAM212 cells (Gendrisch 2015). Our preliminary data also suggested a potential activation of the PERK branch of the UPR. This has been shown for the sensitizer DNFB in THP-1 cells (Luís et al. 2014). To address the question whether or not other contact sensitizers and/or irritants can activate the PERK branch of the UPR in keratinocytes, we analyzed the phosphorylation of PERK, a key event in this branch. Therefore, the phosphorylated form of PERK (pPERK) was stained using a specific monoclonal primary anti-phospho-PERK antibody and a secondary antibody conjugated to the fluorescent dye Alexa555 after stimulation of Pam212 cells with different chemicals for 6 h.

As shown in Figure 19 (Gendrisch et al. submitted), the untreated cells as well as the solvent controls show only a minor PERK phosphorylation (red = phospho-PERK staining, blue = DAPI staining visualizing nuclei), while treatment with the positive controls tunicamycin and thapsigargin as well as the sensitizers TNCB and oxazolone or the irritant SDS show an increased phosphorylation of PERK.

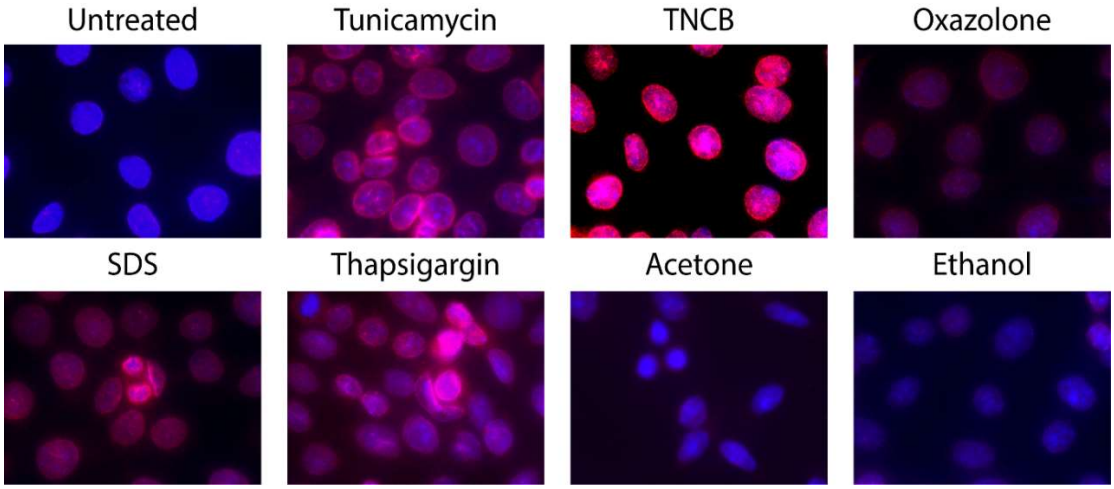

Figure 19: Chemicals induce the phosphorylation of PERK. PAM212 cells were cultured in chamber slides and treated for 6 h with either 10 µg/ml tunicamycin, 30 µM TNCB, 625 µM oxazolone, 260 µM SDS, 300 nm thapsigargin or the solvent controls acetone (for TNCB) or ethanol (for oxazolone). PERK phosphorylation was analyzed with an α-pPERK antibody and Alexa555 secondary antibody (red staining). DAPI (blue staining) was used for visualization of nuclei. Each picture shows an overlay of DAPI and the Alexa 555-conjugated pPERK antibody. Magnification = 100x. Figure shows results from one representative experiment out of four.

A quantification of the activation of the PERK branch by determining the integrated density (ID) of the pPERK using ImageJ shows that treatment with all chemicals except the solvent controls lead to an increase of PERK phosphorylation (Figure 20) (Gendrisch et al. submitted). TNCB showed the strongest activation of the PERK branch with an over three-fold increase to an ID over 7000. Tunicamycin, SDS and thapsigargin had similar levels of pPERK with an ID of about 5500. Interestingly, oxazolone was the weakest of the chemicals in pPERK induction with an ID of little over 4000. The solvent controls acetone and ethanol showed a minor increase of pPERK ID without being significantly increased in comparison to the untreated control. These results are in contrast to former work on the IRE-1 branch of the UPR where TNCB has been lacking any major effect and oxazolone was presenting as a potent activator (Gendrisch 2015).

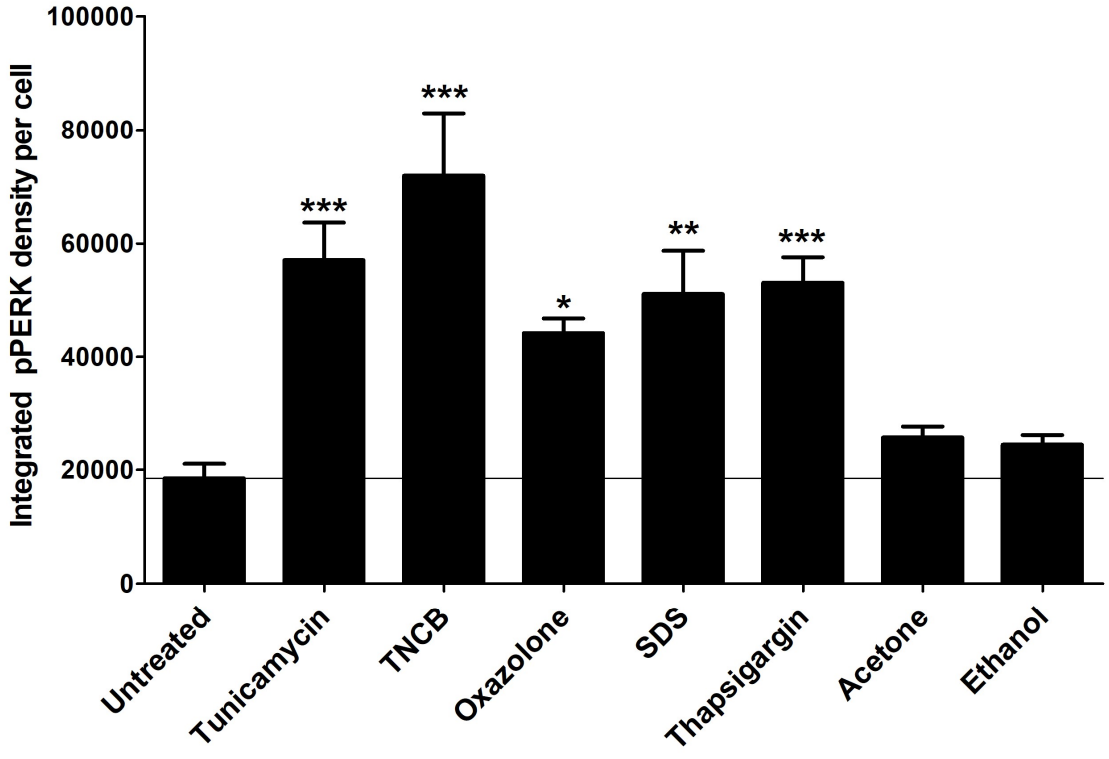

Figure 20: Quantification of PERK phosphorylation from Figure 19. The integrated density of pPERK staining per chemical treated PAM212 cell was measured using ImageJ. Data shown as mean +/- SEM from four independent experiments. Statistics: 1way ANOVA with Dunnet´s posttest, * P ≤ 0.05, ** P ≤ 0.01, *** P ≤ 0.001. Line = untreated control value.

In conclusion, this experiment confirms the activation of the PERK branch by both contact sensitizers as well as irritants and indicates that different sensitizers might be able to differentially activate the three branches of the UPR, as shown by the strong

activation of the IRE-1 branch and a weak activation of the PERK branch by Oxazolone while TNCB showed the opposite effect.

8.2 NF-κB pathway activation by contact sensitizers and irritants

Since we were able to confirm that contact sensitizers and irritants activate the UPR, we wanted to address the relevance of this pathway activation on a potential downstream modulation of inflammation. The UPR has been shown to play a role in the activation of several pro-inflammatory pathways, with NF-κB being one of the most well-known (Kitamura 2011). Therefore, the goal of the next experiments was to look for a possible activation of this pathway by different chemicals and for a potential role of the UPR opening a potential point to interfere with the sensitizer-induced inflammation. Under steady-state conditions, NF-κB is mainly found in the cytosol and translocates to the nucleus after the activation of the pathway to induce the expression of pro-inflammatory genes. To examine the activation of NF-κB, the nuclear translocation was analyzed by immunocytochemistry (Guzman et al. 2013).

8.2.1 Tunicamycin leads to a time-dependent nuclear translocation of the p65 subunit of NF-κB

The goal of this initial experiment was to confirm that activation of the UPR itself results in a translocation of NF-κB to the nucleus and to determine the time kinetics of this process.

Here, PAM212 cells were stimulated with tunicamycin, a positive control for the UPR activation. The p65 subunit of NF-κB was stained at different time points using a specific primary anti-p65 antibody and a secondary antibody conjugated to the fluorescent dye Alexa Fluor 488.

Figure 21 shows that p65 (green staining) was evenly distributed in untreated cells throughout the cytoplasm while the nuclear area showed a shadow-like darker color. The disappearance of this lack of nuclear staining (shadow) indicates the translocation of NF-κB to the nucleus. The number of cells with this nuclear shadow was reduced with increasing time of tunicamycin stimulation. The highest number of cells with a lack of the nuclear shadow was found after 1 h of stimulation.

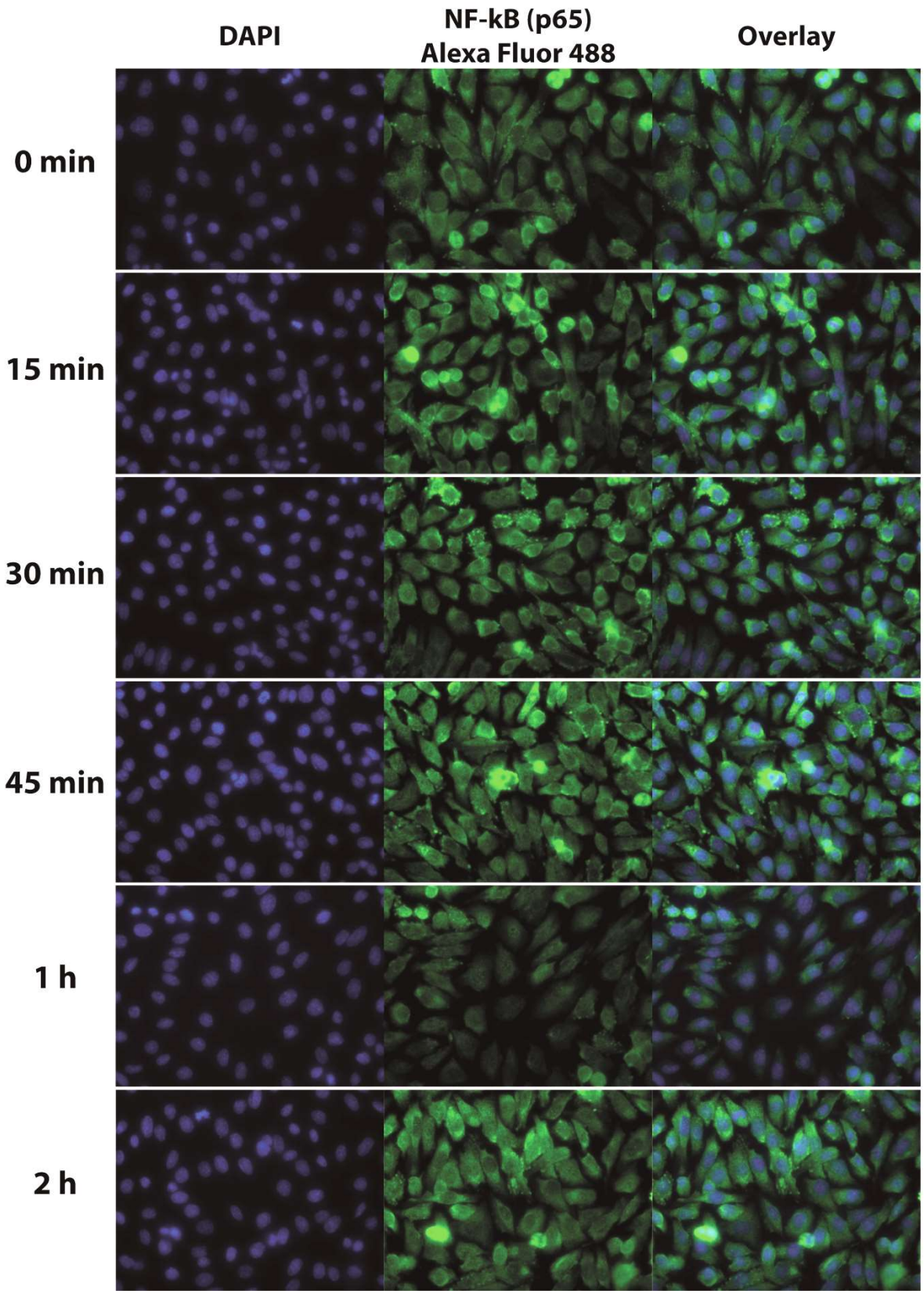
DAPI
NF-kB (p65)
Alexa Fluor 488
Overlay
0 min
15 min
30 min
45 min
1 h
2 h

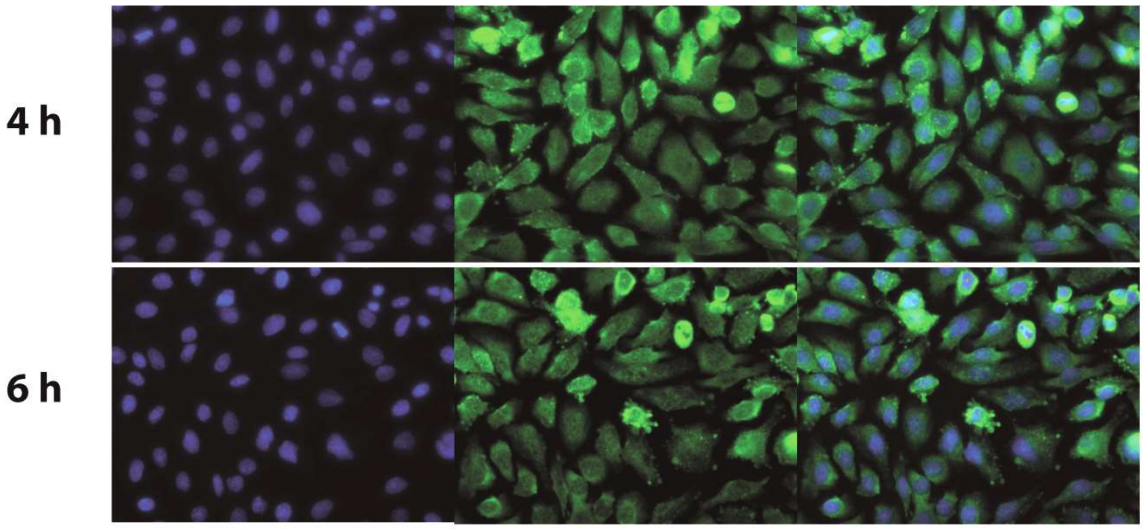

Figure 21: Tunicamycin leads to time-dependent nuclear translocation of p65 in PAM212 cells. PAM212 cells grown on collagen-coated cover slips were treated with 10 µg/ml tunicamycin for the indicated time points. Cells were then fixed, permeabilized and the p65 subunit of NF-κB was detected using an anti-mouse p65 primary anti- NF-κB antibody and visualized using a goat anti-mouse antibody coupled to Alexa Fluor 488 while DAPI was used for nuclear staining. Magnification = 400x.

This experiment showed the feasibility to detect NF-κB translocation in PAM212 cells after activation of the UPR and provided us with a starting time point for treatments in subsequent experiments as the time kinetics of tunicamycin and the other chemicals to be tested were comparable in other experiments (Gendrisch 2015).

8.2.2 UPR-dependent nuclear translocation of p65 after chemical stimulation of PAM212 cells

To analyze the chemical-induced activation of the NF-κB pathway, PAM212 cells were stimulated with different chemicals for 1 h. To address the potential role of the UPR in this process, sets of samples were stimulated after a 1 h pre-incubation with either an IRE-1 or a PERK inhibitor. Afterwards, the p65 subunit of NF-κB was detected using a specific primary anti-p65 antibody and a secondary antibody conjugated to the fluorescent dye Alexa Fluor 555 due to its increased fluorescence intensity in comparison to the Alexa Fluor 488 used in the initial experiment (Figure 2).

Just like in the initial experiment, untreated cells in Figure 22 showed an even distribution of p65 staining throughout the entire cytoplasm, yet leaving a darker shadow in the area of the nucleus. Treatment of the cells with tunicamycin, TNCB, oxazolone and SDS led to a reduction of the number of cells showing a nuclear shadow. A pre-treatment of the cells with either an IRE-1 or a PERK inhibitor was able to reduce this effect.

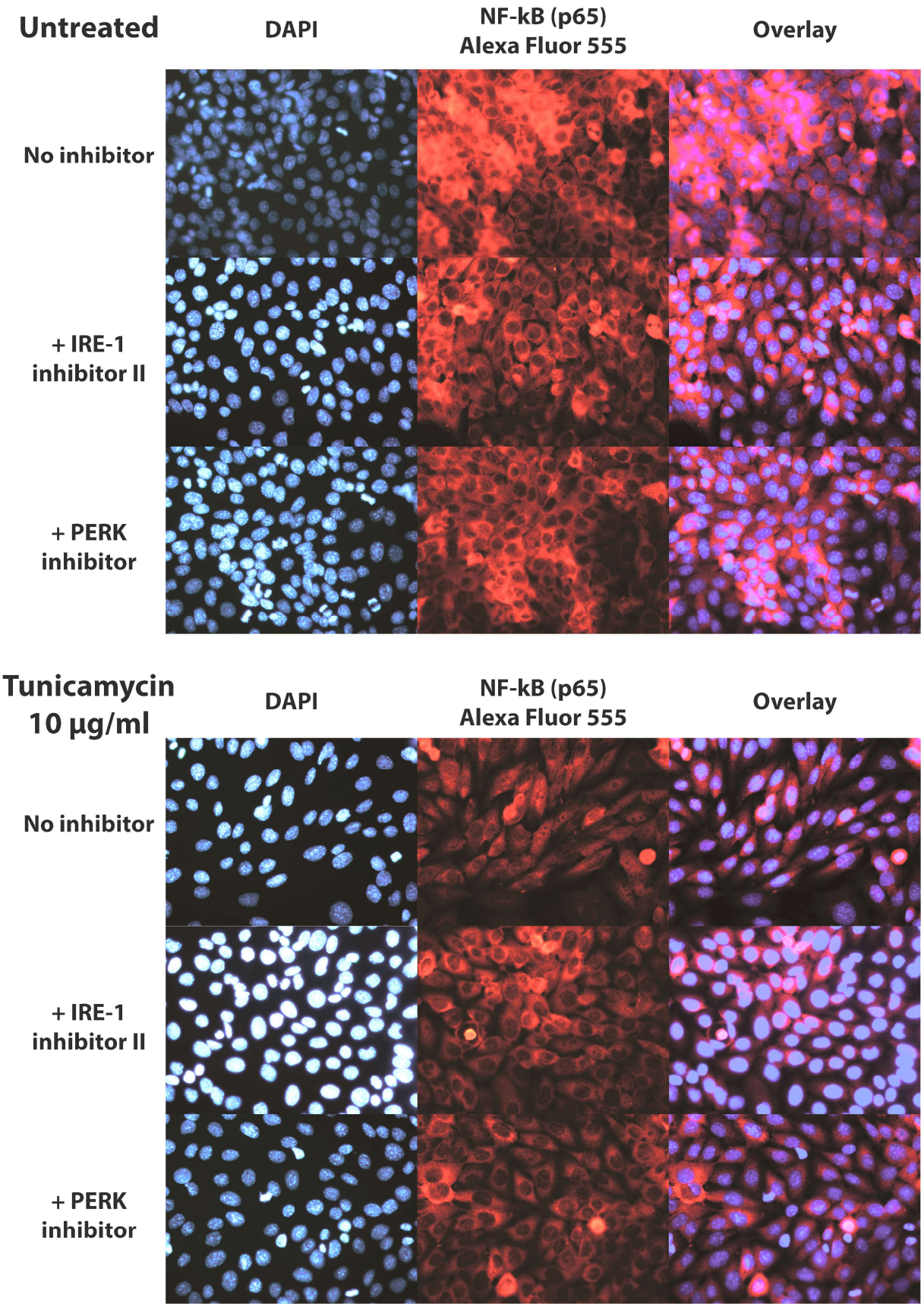
Untreated
DAPI
NF-kB (p65)
Alexa Fluor 555
Overlay
No inhibitor
+ IRE-1
inhibitor II
+ PERK
inhibitor
Tunicamycin
10 µg/ml
DAPI
NF-kB (p65)
Alexa Fluor 555
Overlay
No inhibitor
+ IRE-1
inhibitor II
+ PERK
inhibitor

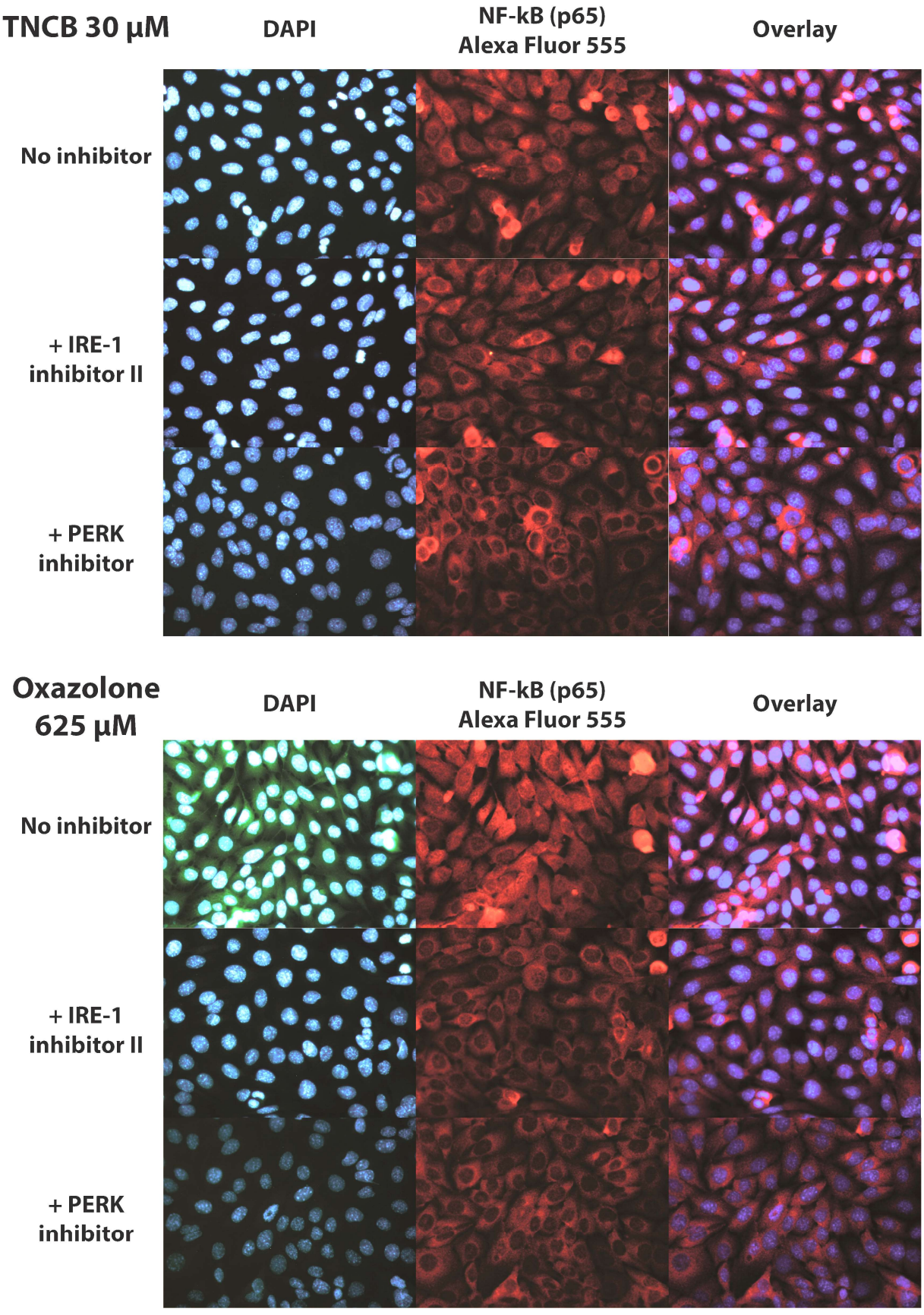
TNCB 30 µM
DAPI
NF-kB (p65)
Alexa Fluor 555
Overlay
No inhibitor
+ IRE-1
inhibitor II
+ PERK
inhibitor
Oxazolone
625 µM
DAPI
NF-kB (p65)
Alexa Fluor 555
Overlay
No inhibitor
+ IRE-1
inhibitor II
+ PERK
inhibitor

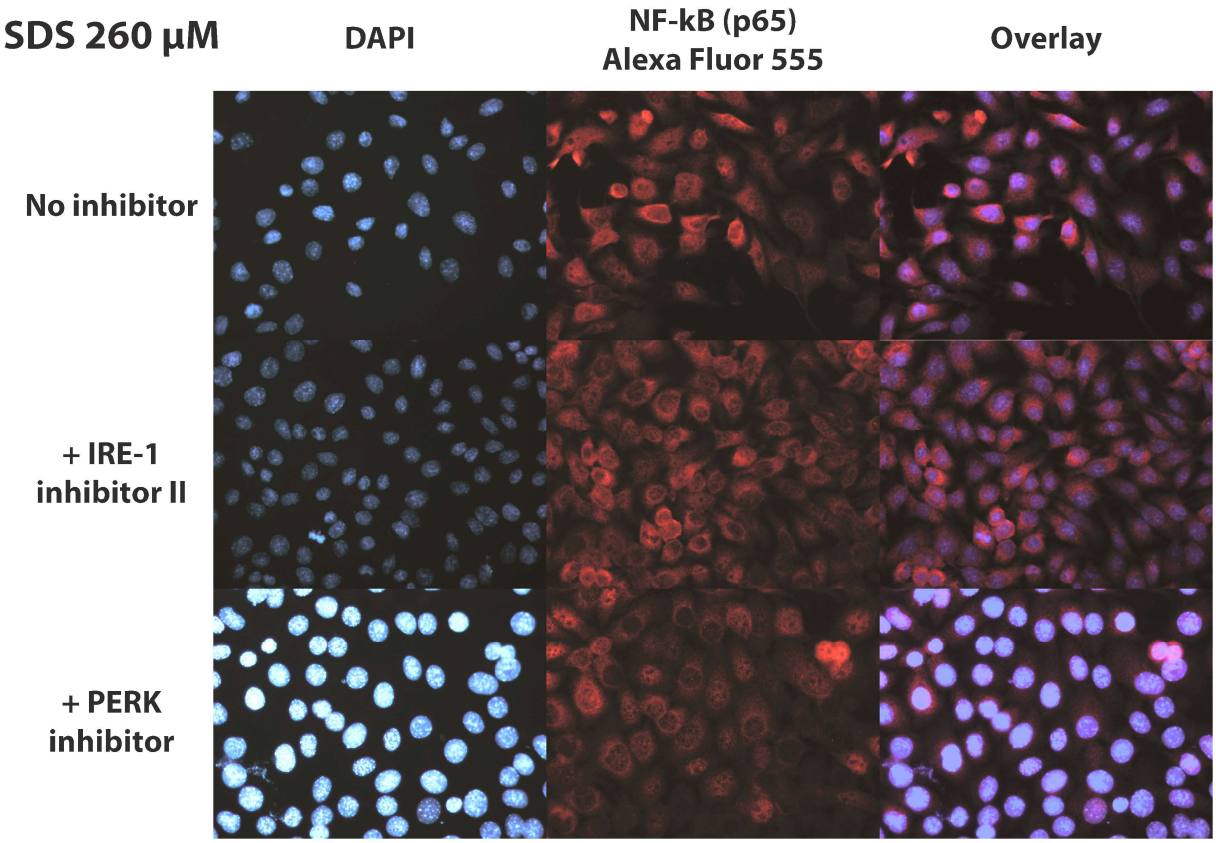

Figure 22: Chemicals induce the UPR-dependent NF-κB (p65) nuclear translocation in PAM212 cells. PAM212 cells were pre-treated with either 25 µM IRE-1 inhibitor II or 10 µM PERK inhibitor for 1 h before adding tunicamycin (10 µg/ml), TNCB (30 µM), oxazolone (625 µM) or SDS (260 µM) for 1 h. Cells were fixed, permeabilized and the p65 subunit of NF-κB was detected using an anti-mouse p65 primary antibody and visualized using a goat anti-mouse antibody coupled to Alexa Fluor 555 while DAPI was used for nuclear staining. One representative experiment out of four is shown. 400x magnification.

A quantification of these results is shown in Figure 23 (Gendrisch et al. submitted). It can be seen, that the treatment of PAM212 cells with different chemicals resulted in a significant increase of nuclear p65+ cells, with tunicamycin and oxazolone showing the strongest effect. SDS was also able to induce a prominent increase of nuclear p65 while the effect of TNCB was much lower. Interestingly, these changes could be inhibited by a pre-treatment of the cells with either the IRE-1 or the PERK inhibitor. Both inhibitors were able to reduce the amount of nuclear p65+ cells in all conditions down to a level where they were not significantly different from the completely untreated control samples.

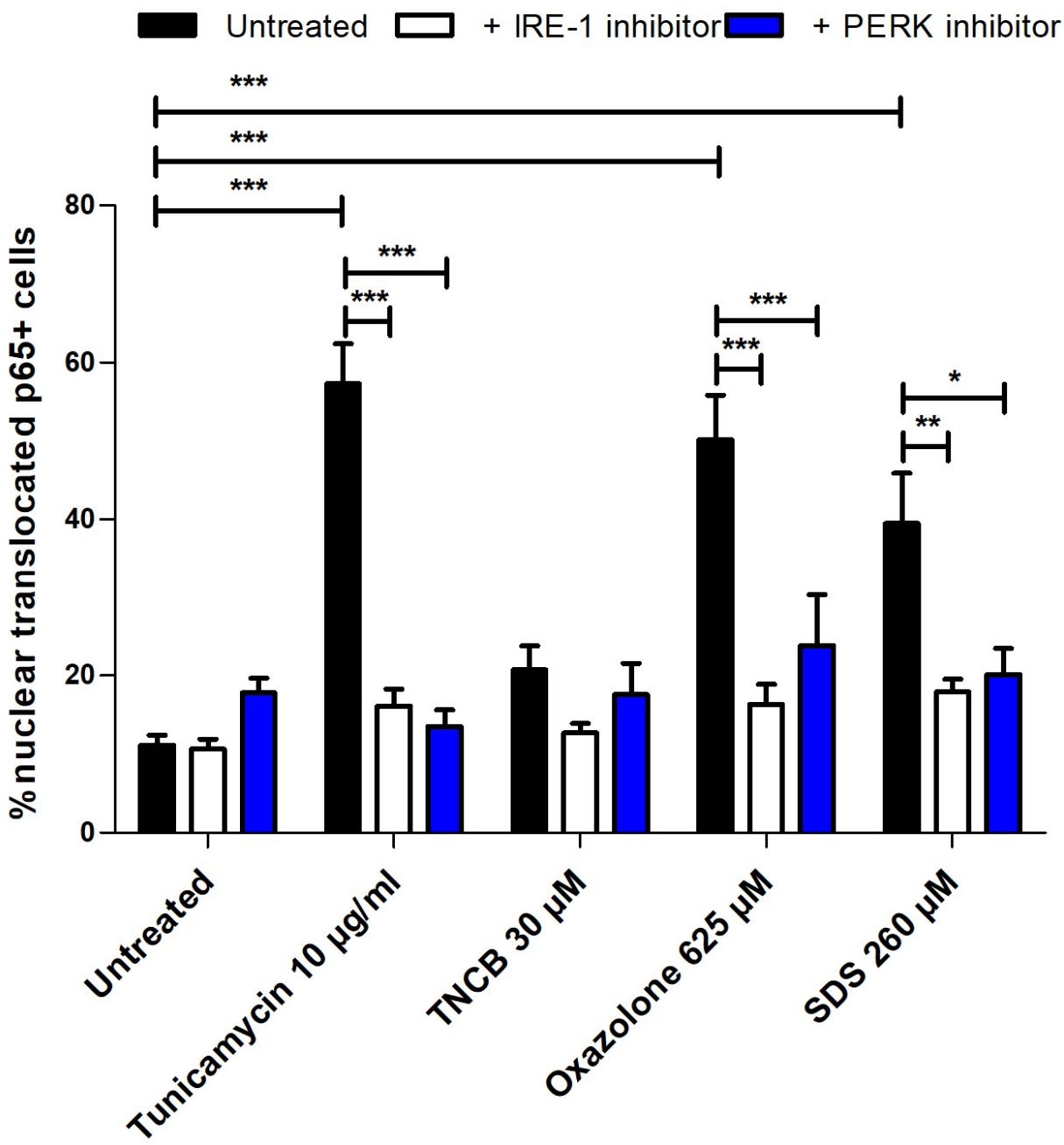

Figure 23: Quantification of NF-κB (p65) nuclear translocation in chemical-treated PAM212 cells after UPR inhibition. Images were analyzed as described in 7.4.2. Data shown as mean +/- SEM of four independent experiments with three pictures per experiment. Statistics: 1way ANOVA with Bonferroni posttest, * P ≤ 0.05, ** P ≤ 0.01, *** P ≤ 0.001, all in comparison to untreated control cells.

In summary, this experiment proves that contact sensitizers and irritants activate the NF-κB signaling pathway and that this process is depending on the activation of the IRE-1 and PERK branch of the UPR.

8.2.3 Chemical-treated PAM212 cells fail to regulate gene expression levels of pro-inflammatory cytokines

After the nuclear translocation of NF-κB, the next step is the activation of target gene expression. These target genes include genes for several pro-inflammatory cytokines, important mediators in the immune system that have been shown to be crucial for the development of ACD. Therefore, the next aim was to analyze a possible induction of pro-inflammatory cytokine gene expression levels in treated PAM212 cells, again including the IRE-1 and PERK inhibitor for the determination of a potential participation of the UPR in this process.

The analysis shown in Figure 24 included known target genes of NF-κB like *Il-1α* and *β*, *Ifn-γ* and *Tnf-α* as well as *Cxcl-16* (Pahl 1999). With the exception of SDS treatment on *Tnf*, no chemical was able to induce a significant upregulation of the expression of pro-inflammatory cytokine genes after 6 h (Nouri-Aria et al. 2000; Linard et al. 2004). The only cytokine gene that showed a trend matching the observations of the NF-κB translocation was *Il-1α*. This cytokine gene expression level was slightly upregulated by all chemicals in similar proportions as seen with the p65 nuclear translocation. In addition, the inhibitors showed the same reduction as seen with p65.

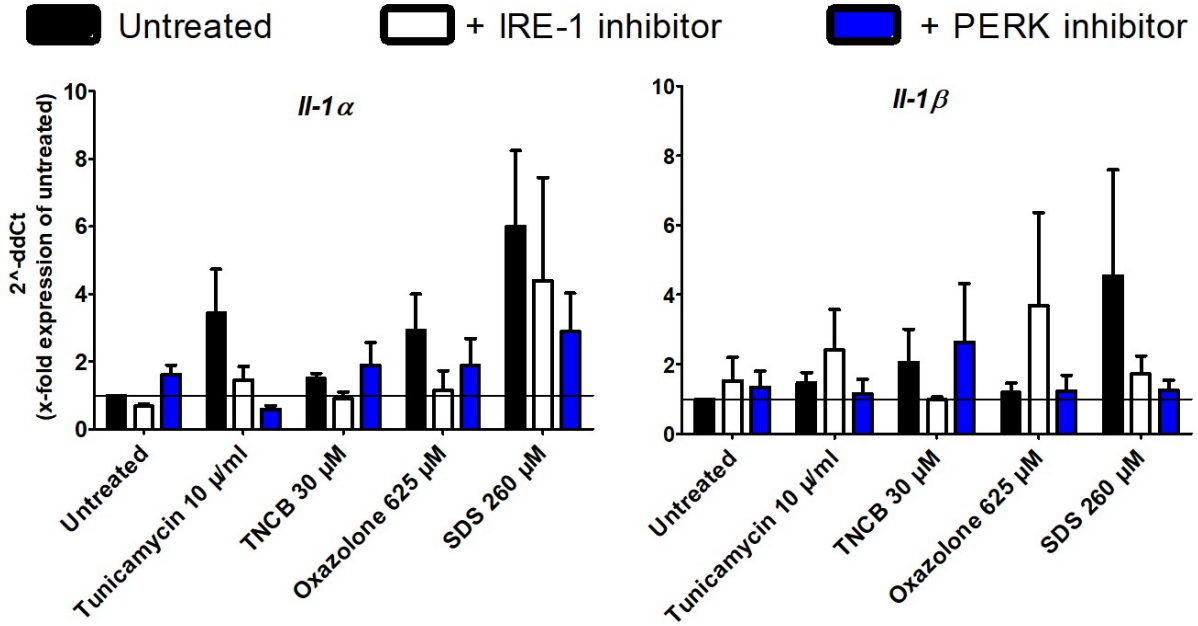

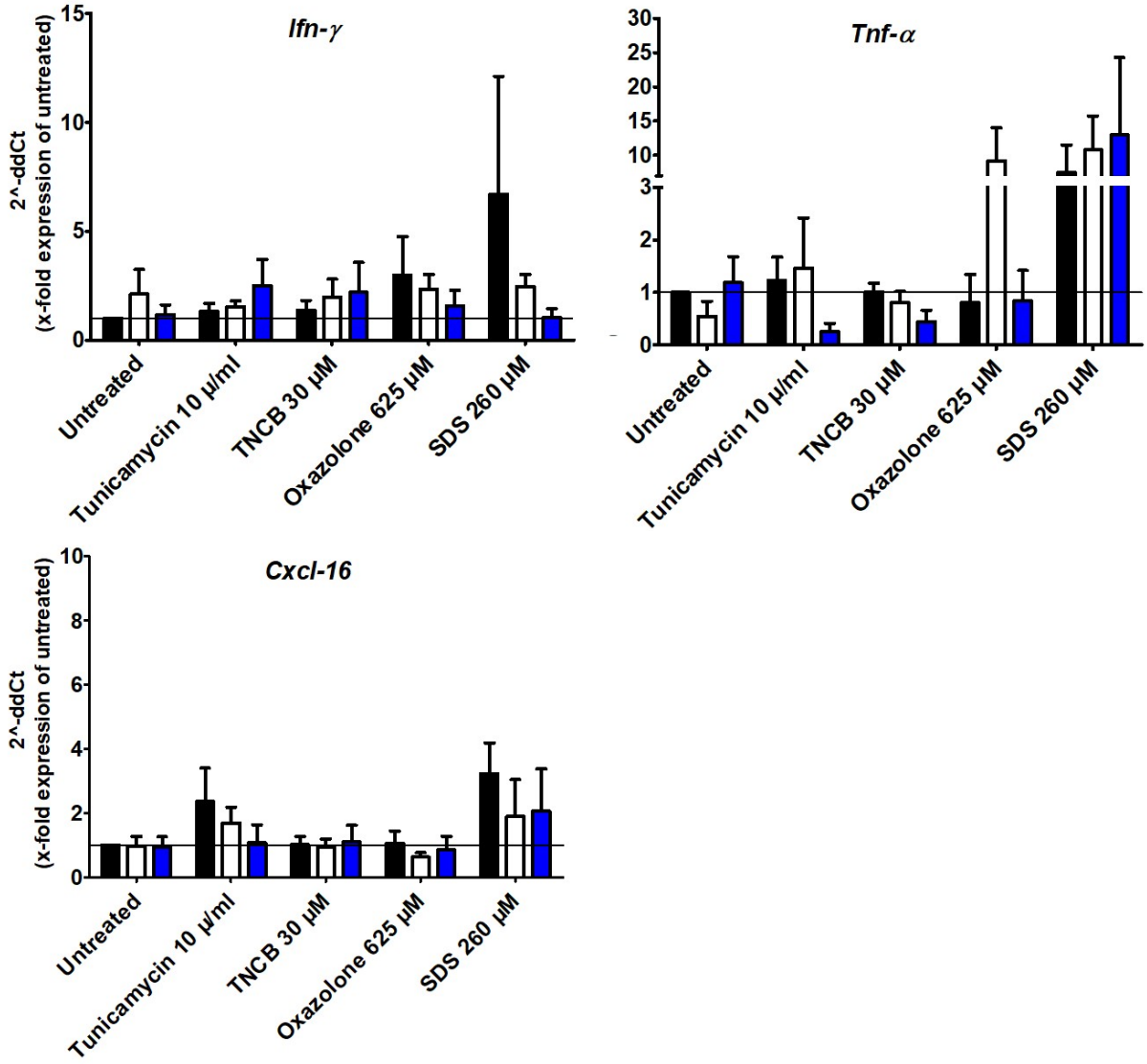

Figure 24: Chemicals fail to induce an UPR-dependent regulation of pro-inflammatory gene expression after 6 h. PAM212 cells were pre-treated with either 25 µM IRE-1 inhibitor II or 10 µM PERK inhibitor for 1 h before adding tunicamycin (10 µg/ml), TNCB (30 µM), oxazolone (625 µM) or SDS (260 µM) for 6 h. RNA was isolated, reversely transcribed into cDNA and real-time PCR analysis was performed. Gene expression in relation to the untreated control was assessed using the $2^{-\Delta\Delta CT}$ method (Schmittgen and Livak 2008). Data is shown as mean +/- SEM of three to four independent experiments. Statistics: 1way ANOVA with Bonferroni posttest, * P ≤ 0.05, ** P ≤ 0.01, *** P ≤ 0.001.

To address the question if the weak effect of sensitizers and irritants on the mRNA expression levels would be different for other cytokines, an additional panel of cytokines was analyzed. Figure 25 shows the results for cytokines that were tested once for their expression after stimulation. Of the analyzed cytokine genes, *Il-6* was the one that showed the highest response after the treatment of the cells with the chemicals.

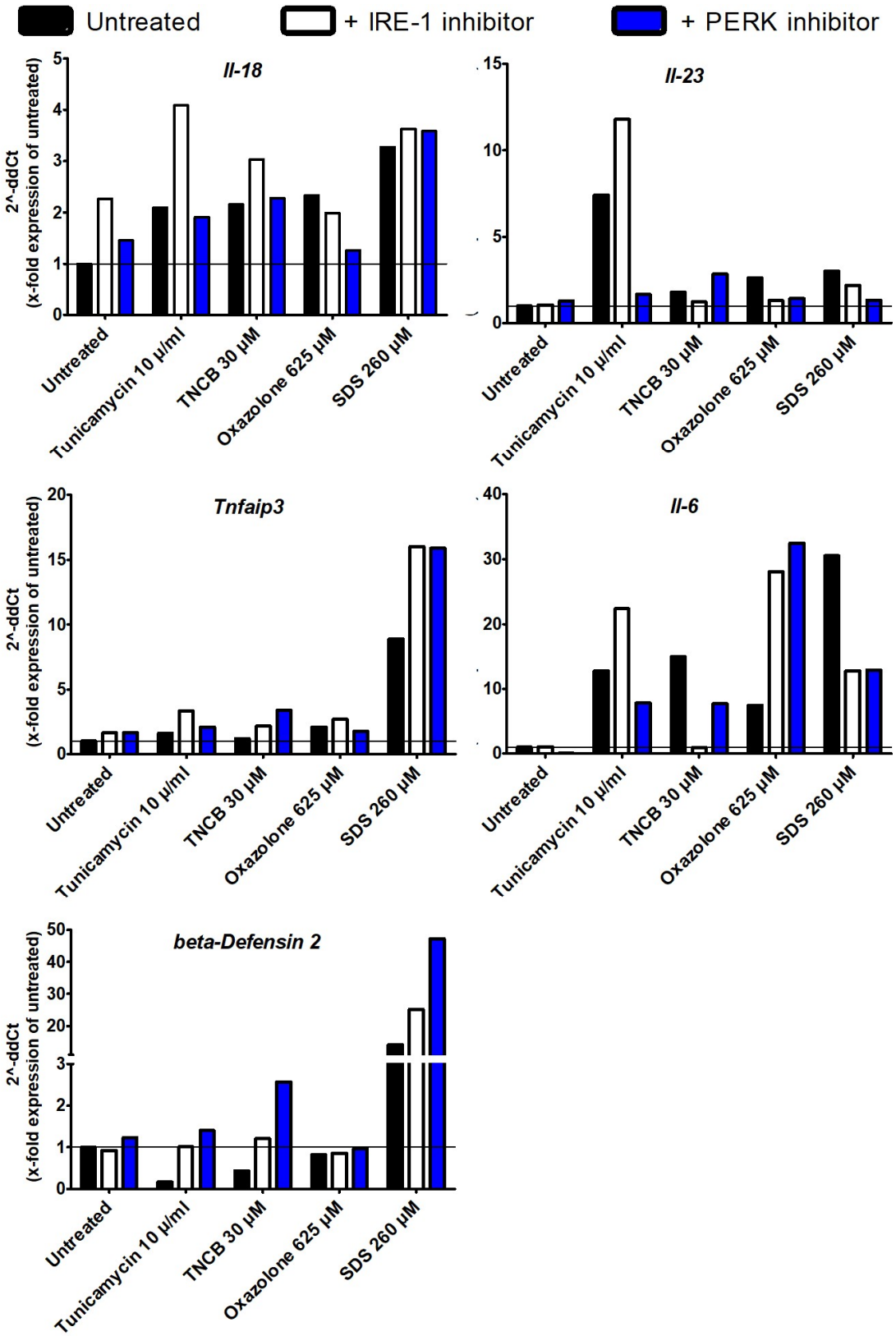

Figure 25: Chemicals fail to induce an UPR-dependent regulation of pro-inflammatory gene expression after 24 h. PAM212 cells were pre-treated with either 25 µM IRE-1 inhibitor II or 10 µM PERK inhibitor for 1 h before adding tunicamycin (10 µg/ml), TNCB (30 µM), oxazolone (625 µM) or SDS (260 µM) for 6 h. RNA was isolated, reversely transcribed into cDNA and real-time PCR analysis was performed. Gene expression in relation to the untreated control was assessed using the $2^{-\Delta\Delta CT}$ method (Schmittgen and Livak 2008). Data of one test experiment is shown.

These results indicate that interestingly PAM212 cells are unable to translate the increase in NF-κB activation observed in Figure 22 and Figure 23 to an increase in pro-inflammatory cytokine expression at the mRNA level.

8.2.4 PAM212 cells are not able to release pro-inflammatory cytokines in response to chemical treatment

Since an increased protein synthesis is not necessarily linked to an increased transcription but could be a result of increased translation, the next step was to analyze the protein levels of pro-inflammatory cytokines in the supernatant after the treatment of PAM212 cells.

As shown in Figure 26, apart from IL-1α there was no significant cytokine production by PAM212 cells detectable. Most cytokines were not even produced at a detectable level. The ones where a result can be seen are comprised of a non-detectable value and a value slightly above the detection limit as the experiments were carried out in duplicates. The IL-1α production was increased about two-fold after tunicamycin and SDS treatment. In tunicamycin-treated cells the IRE-1 and the PERK inhibitor were able to slightly reduce this effect while the cytokine production in SDS-treated cells was unchanged after inhibitor application.

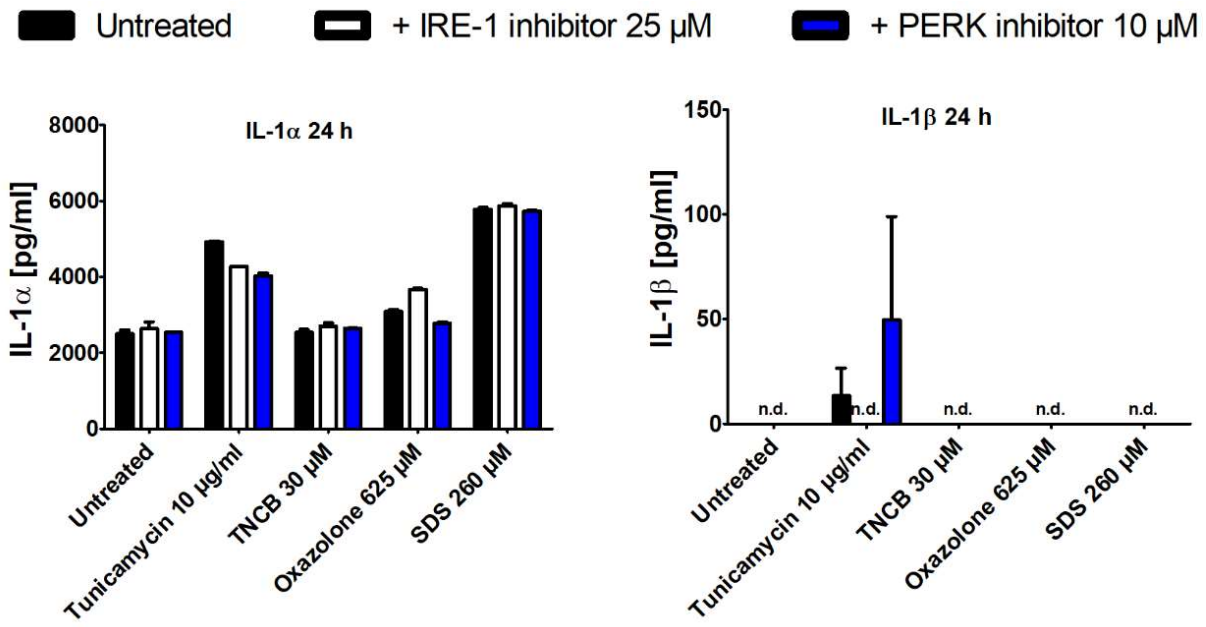

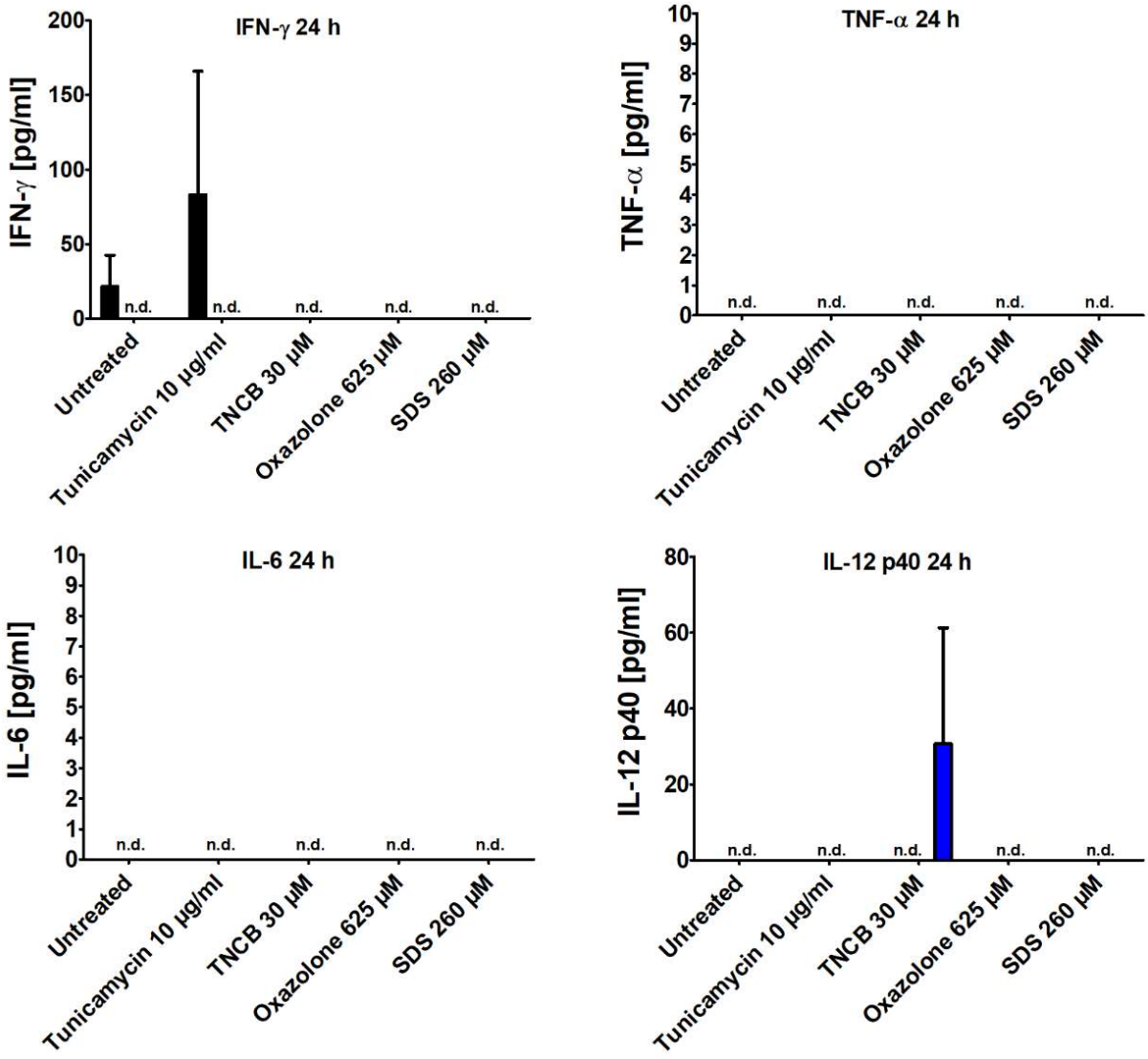

Figure 26: Chemicals fail to induce a pro-inflammatory cytokine production in PAM212 cells. PAM212 cells were pretreated with either 25 µM IRE-1 inhibitor II or 10 µM PERK inhibitor for 1 h before adding tunicamycin (10 µg/ml), TNCB (30 µM), oxazolone (625 µM) or SDS (260 µM) for 24 h. Cytokine production was analyzed using the supernatant of the cultures performing ELISAs. Data of one representative experiment out of two is shown as mean +/- SEM. "n.d." = not detectable.

To exclude the possibility that 24 h was the wrong time point to analyze cytokine production in PAM212 cells as they might have a slower protein biosynthesis, the next step was to repeat the experiment with a prolonged stimulation of 48 h. Just like in the experiment before, Figure 27 shows that PAM212 cells were not producing any pro-inflammatory cytokines with the exception of IL-1α. The amounts of IL-1α produced were comparable to results after stimulating the cells for 24 h (Figure 8).

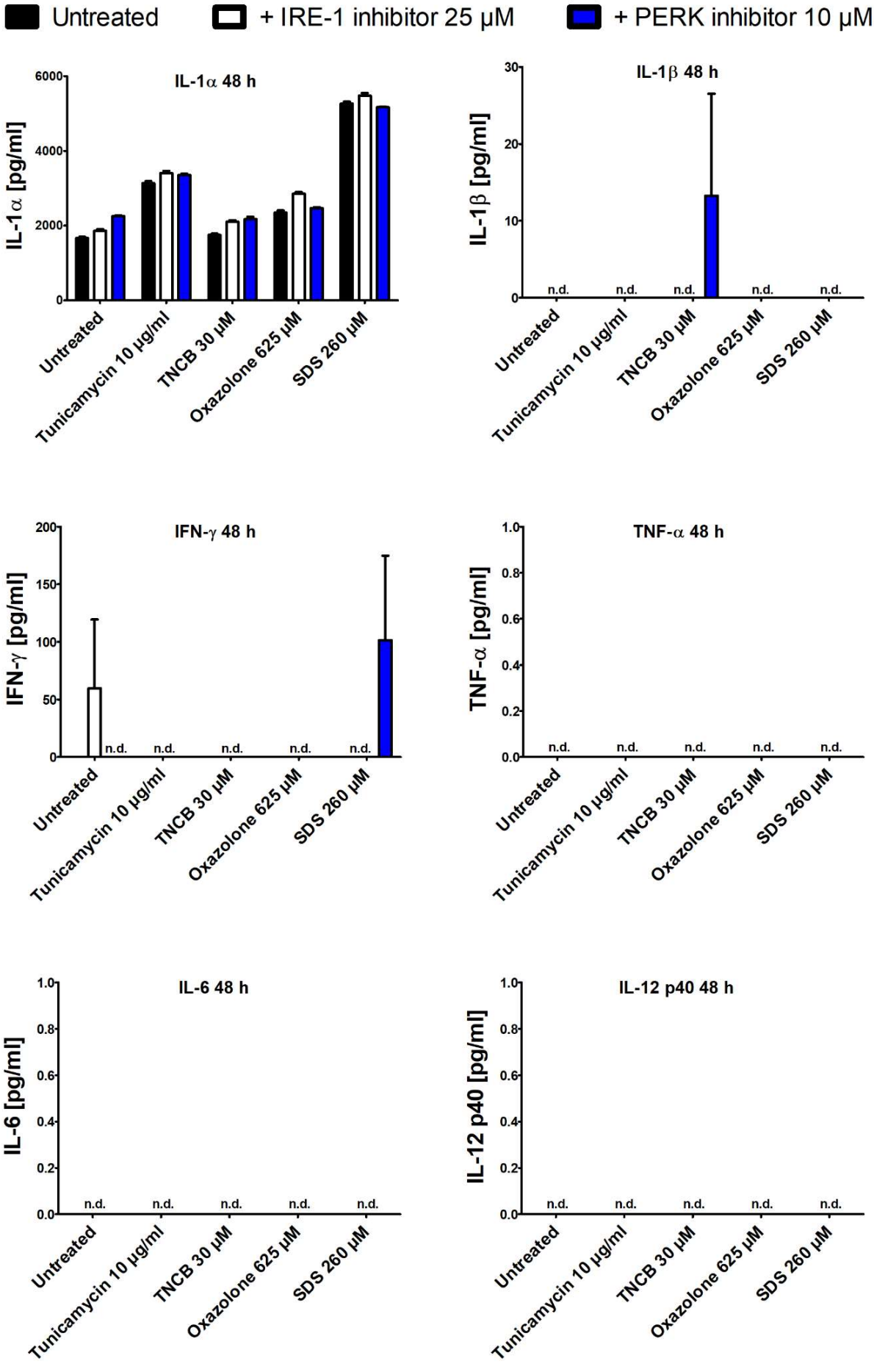
Untreated
+ IRE-1 inhibitor 25 µM
+ PERK inhibitor 10 µM
IL-1α 48 h
IL-1α [pg/ml]
IL-1β 48 h
IL-1β [pg/ml]
IFN-γ 48 h
IFN-γ [pg/ml]
TNF-α 48 h
TNF-α [pg/ml]
IL-6 48 h
IL-6 [pg/ml]
IL-12 p40 48 h
IL-12 p40 [pg/ml]
n.d.
Untreated
Tunicamycin 10 µg/ml
TNCB 30 µM
Oxazolone 625 µM
SDS 260 µM

Figure 27: Chemicals fail to induce a pro-inflammatory cytokine production in PAM212 cells after 48 h of stimulation. PAM212 cells were pretreated with either 25 µM IRE-1 inhibitor II or 10 µM PERK inhibitor for 1 h before adding Tunicamycin (10 µg/ml), TNCB (30 µM), Oxazolone (625 µM) or SDS (260 µM) for 48 h. Cytokine production was analyzed using the supernatant of the cultures performing ELISAs. Data of one representative experiment is shown as mean +/- SEM. “n.d.” = not detectable.

These results confirm the inability of Pam212 cells to produce cytokines in response to different stimuli upregulating NF-κB activation (Figure 22 and Figure 23) as already observed in the experiments analyzing cytokine mRNA expression levels (Figure 24 and Figure 25).

8.3 Influence of sensitizer/irritant-induced UPR modulation on immortalized normal human keratinocytes

Since the PAM212 cell line presented itself as unsuitable for further experiments concerning inflammation due to the lack of cytokine production, the next task was to find an alternative cell line. Leaving behind murine cells and switching to the human system, the next cells to be tested were immortalized normal human keratinocytes (NHKi). These are primary cells isolated from healthy skin tissue of patients undergoing surgery. Following the isolation, the cells were immortalized by transfection with the *E6* and *E7* genes of the human papillomavirus types (HPVs) and could then be handled like cells of a cell line with an indefinite life-span (Hawley-Nelson u. a. 1989).

8.3.1 Chemicals activate the IRE-1 branch in NHKi

To make sure that the new cells were suitable for further analysis they had to undergo a series of test experiments. To test for the activation of the UPR in NHKi after chemical treatment, the standard protocol with 6 h stimulation was used treating the cells with the concentrations used for PAM212 cells. Afterwards, RNA was isolated, reversely transcribed into cDNA and a PCR with primers specific for *XBP-1* was performed and the amount of spliced *XBP-1* calculated.

Figure 28 shows that NHKi cells increased the splicing of *XBP-1* after chemical treatment with tunicamycin, TNCB or oxazolone. Oxazolone showed the biggest effect with an increase of splicing about 4.5-fold to over 70% in comparison to the untreated control. Oxazolone treatment resulted in a two-fold increase while TNCB only had a minor effect. In contrast to the PAM212 cells, SDS at the used concentration did not induce *XBP-1* splicing in NHKi cells.

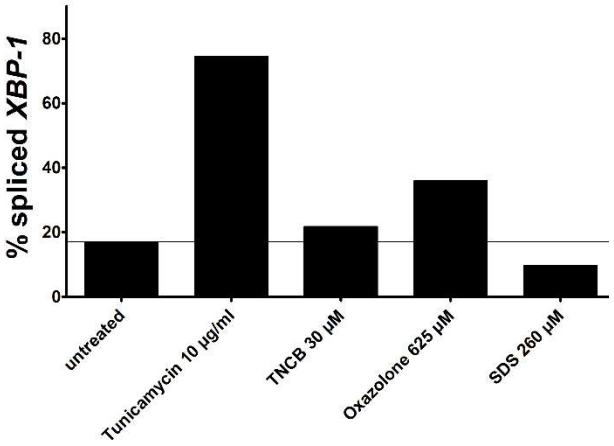

Figure 28: Activation of the IRE-1 branch of the UPR in immortalized NHKs by contact sensitizers and irritants. NHK cells were treated with the stated concentrations of chemicals for 6. IRE-1 activation was assessed by analyzing the splicing of *XBP-1*. Data is shown as the x-fold splicing in comparison to the untreated control (line). Data of one experiment is shown.

8.3.2 Chemicals activate the PERK branch in NHKi

To include the PERK branch in the analysis of NHKi, the RNA of the cells from 8.3.1 was used to analyze its activation by looking at the expression of *CHOP*, the transcription factor that is expressed as a result of the PERK branch activation.

As seen in Figure 29, treatment of NHKi cells with the concentrations used with PAM212 cells led to an increased expression of *CHOP*. While tunicamycin and oxazolone led to a robust induction of expression to about the three-fold level of untreated cells, TNCB and SDS had only a minor effect on the expression of *CHOP* that caused only a slight increase in comparison to the untreated cells.

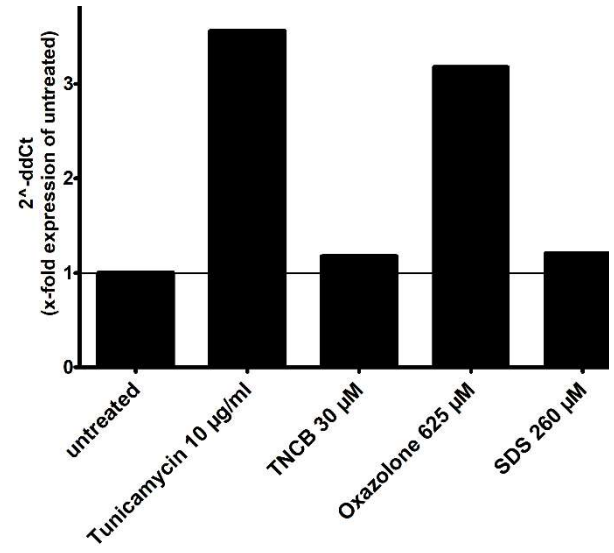

Figure 29: Activation of the PERK branch of the UPR by chemical treatment. NHKi cells were treated with the stated concentrations of chemicals for 6 h. PERK activation was assessed after RNA isolation and cDNA synthesis by analyzing the expression of *CHOP* using qPCR and the $2^{-\Delta\Delta CT}$ method (Schmittgen and Livak 2008). Data is shown as the x-fold splicing in comparison to the untreated control (line). Data of one representative experiment out of two is shown.

8.3.3 Assessment of NHKi viability

To make sure that the effects observed after the chemical treatment are not caused by their toxicity, viability of the NHKi cells was measured using the MTT assay. The target range was a maximal toxicity of 20%, leaving 80% viable cells as some slight

decrease in viability is needed for contact sensitizers to act properly and was used as a basis for all former work (Dr. Philipp R. Esser, unpublished data).

As seen in Figure 30, the TNCB concentration used for PAM212 cells is well in the target range and even showed an increased viability in comparison to the untreated cells. In contrast, tunicamycin and oxazolone showed a decrease of viability to about 70% undercutting the set minimal viability of 80%. SDS treatment had the highest effect in the cellular viability lowering the viability to below 10%.

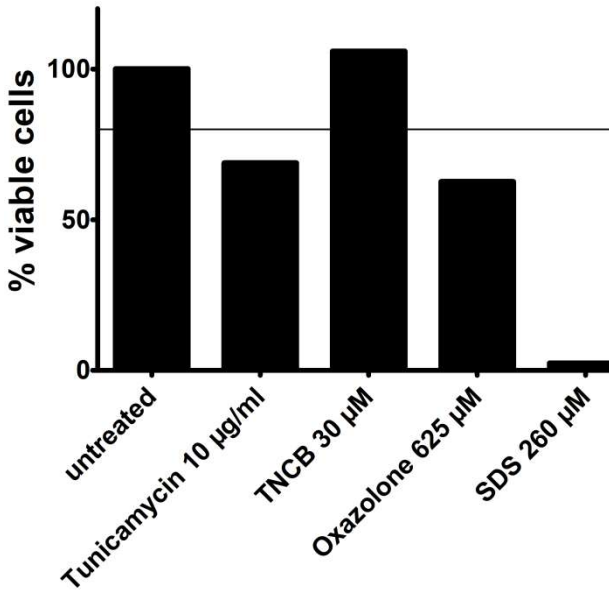

Figure 30: Viability assessment of NHKi cells after chemical treatment using MTT assay. NHK cells were treated with the stated concentrations of chemicals for 6. Afterwards, the culture medium containing the stimulants was removed, cells were rinsed and then incubated in medium containing 0.75 mg/ml MTT for 30 min. Cells were rinsed with PBS and the formed formazan crystals were dissolved in a 1:49 mixture of HCl and isopropanol. Finally, the absorption was measured at 570 nm. The targeted minimal viability of 80% is shown with a line. Data of one experiment is shown.

8.3.4 Chemical-treatment induces pro-inflammatory cytokine production by immortalized NHKs

As the NHKi cells showed an active UPR after chemical treatment, the next aim was to look for the production of pro-inflammatory cytokines. Cells were treated with increasing concentrations of different chemicals for 24 h and the IL-6 levels of the cell culture supernatant were analyzed using ELISA.

All tested concentrations of tunicamycin had no major effect on the IL-6 levels. TNCB-treated cells with the exception of 30 µM showed no detectable IL-6 production. Treatment of NHKi cells with increasing concentrations of oxazolone resulted in a minimal yet not significant increase of IL-6 production. SDS-treated cells showed the biggest response with a dose-dependent increase of IL-6 levels up to 0.0015% (52 µM). In contrast, the two highest concentrations showed no effect on IL-6 levels.

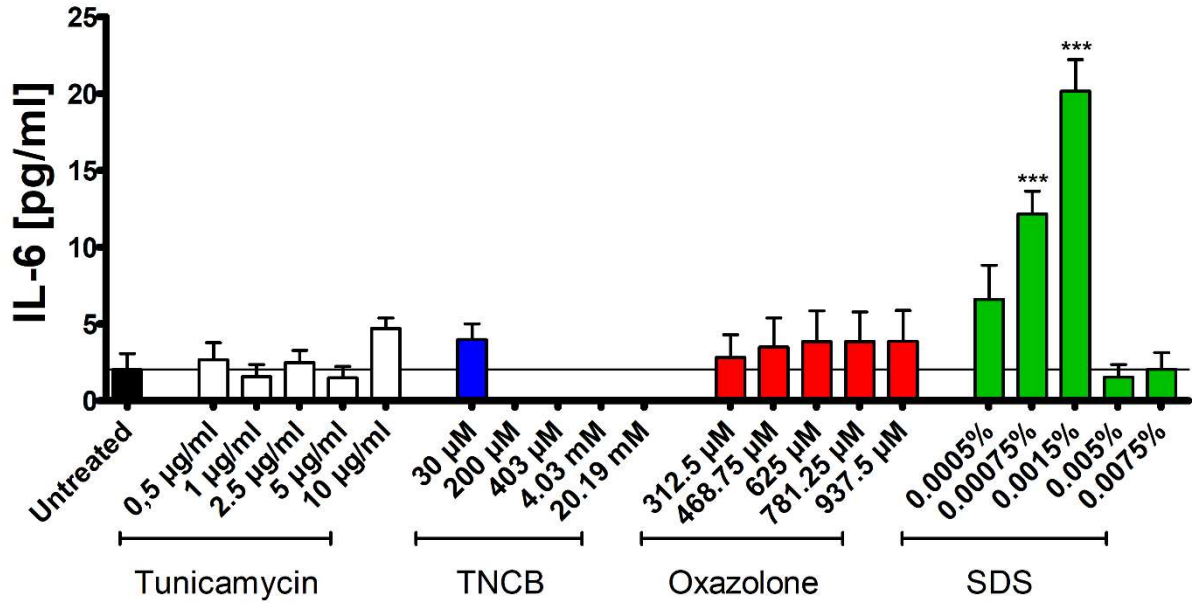

Figure 31: Chemicals induce pro-inflammatory cytokine release in immortalized NHKs. NHKs were incubated with the stated concentration of chemicals for 24 h and ELISAs detecting IL-6 were performed using the cell culture supernatants. Data is shown as mean +/- SEM of three independent experiments. Statistics: 1way ANOVA with Dunnett's posttest, * P ≤ 0.05, ** P ≤ 0.01, *** P ≤ 0.001.

To check for potential toxic effects of the treatment conditions an LDH assay was used as problems with the MTT assay in combination with these cells arose. The treatment of the cells was performed with the same conditions as for the ELISA. The results of the assay show that the used concentrations of tunicamycin have no effect on the viability of the NHKi cells. In contrast, treatment with TNCB even at the lowest concentration used was already around the set mark of 20% toxicity. With increasing concentrations, the toxicity rose up to 100% at 20.19 mM. Just like tunicamycin, oxazolone was not very toxic for the cells as only one concentration resulted in a slight increase of toxicity but still well below the 20% mark. The same holds true for the first three concentrations of SDS that cause no toxicity. In contrast, 0.005% and 0.0075% results in complete death of all cells.

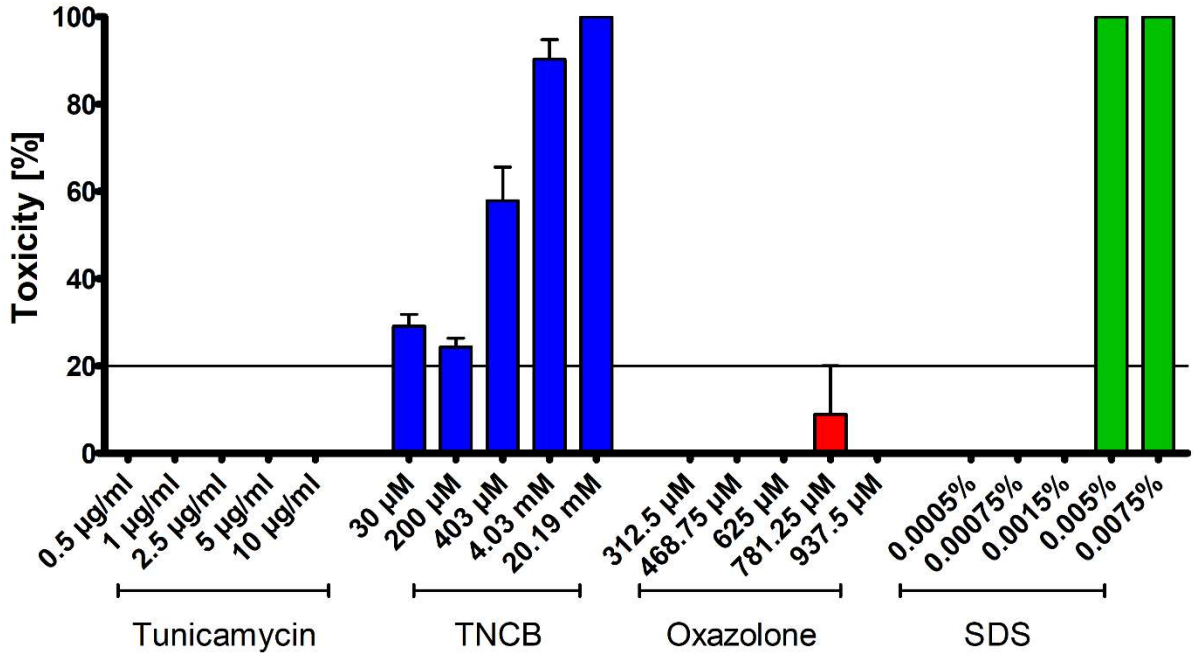

Figure 32: Cytotoxicity assay for the NHKi 24 h stimulation. NHKi cells were stimulated for 24 h with the indicated concentrations of different chemicals. After the stimulation, the supernatant was collected and an LDH release assay was performed. Results are shown as mean +/- SEM of three independent experiments. Line = 20% toxicity.

Influence of sensitizer/irritant-induced UPR modulation on HaCaT cells

To examine another cell line as an alternative for the formerly used PAM212 cells, HaCaT cells were analyzed for UPR activation and cytokine production to test if they pose an alternative.

8.3.5 Chemicals induce increased *XBP-1* splicing in HaCaT cells

The initial experiment was to test the effect of our chemicals on the UPR in HaCaT cells after 6 h of stimulation. As seen in Figure 33 (Gendrisch et al. submitted), HaCaT cells showed an upregulation of the UPR visualized by the increase of *XBP-1* splicing after treatment with tunicamycin, TNCB, oxazolone and SDS. The basal level of splicing in untreated cells was about 1.5%. While TNCB resulted in a splicing of about 8%, oxazolone and tunicamycin treatment caused about 11% and 18% respectively. 80% splicing of total *XBP-1* was achieved in SDS-treated HaCaT cells.

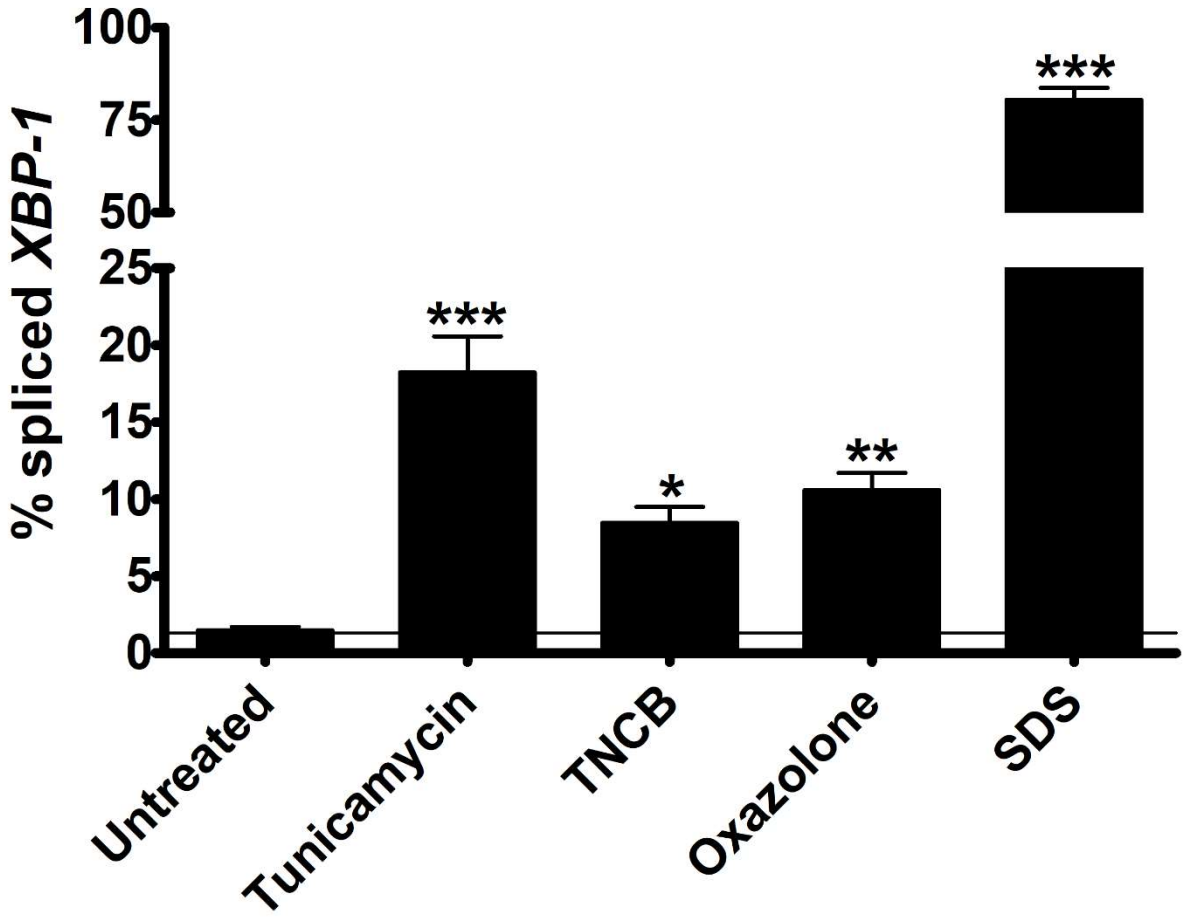

Figure 33: Sensitizers and irritants induce *XBP-1* splicing in HaCaT cells. HaCaT cells were treated with either 10 µg/ml tunicamycin, 170 µM TNCB, 4 mM oxazolone or 0.01% SDS for 6 h. UPR activation was analyzed by looking at the splicing of *XBP-1* using PCR after RNA isolation and cDNA synthesis. Data is shown as mean +/- SEM of four independent experiments with triplicates in each. Statistics: 1way ANOVA with Dunnett's posttest, * P ≤ 0.05, ** P ≤ 0.01, *** P ≤ 0.001. Line = untreated control.

8.3.6 Chemicals induce the release of pro-inflammatory cytokines in HaCaT cells

In addition to the UPR activation, the production of pro-inflammatory cytokines by HaCaT cells after stimulation was assessed. For this, HaCaT cells were stimulated for 24 h with either tunicamycin, TNCB, oxazolone or SDS. The supernatant was collected after the stimulation and the IL-6 levels were measured using ELISA.

Figure 34 shows the results of these experiments. It can be seen that all tested chemicals increased the levels of IL-6 after 24 h. Tunicamycin and oxazolone treatment led to an about six-fold increase of IL-6 to about 90 pg/ml while SDS increased the production of IL-6 to over 150 pg/ml. TNCB treatment resulted in an IL-6 release of about 50 pg/ml in comparison to untreated cells releasing 15 pg/ml.

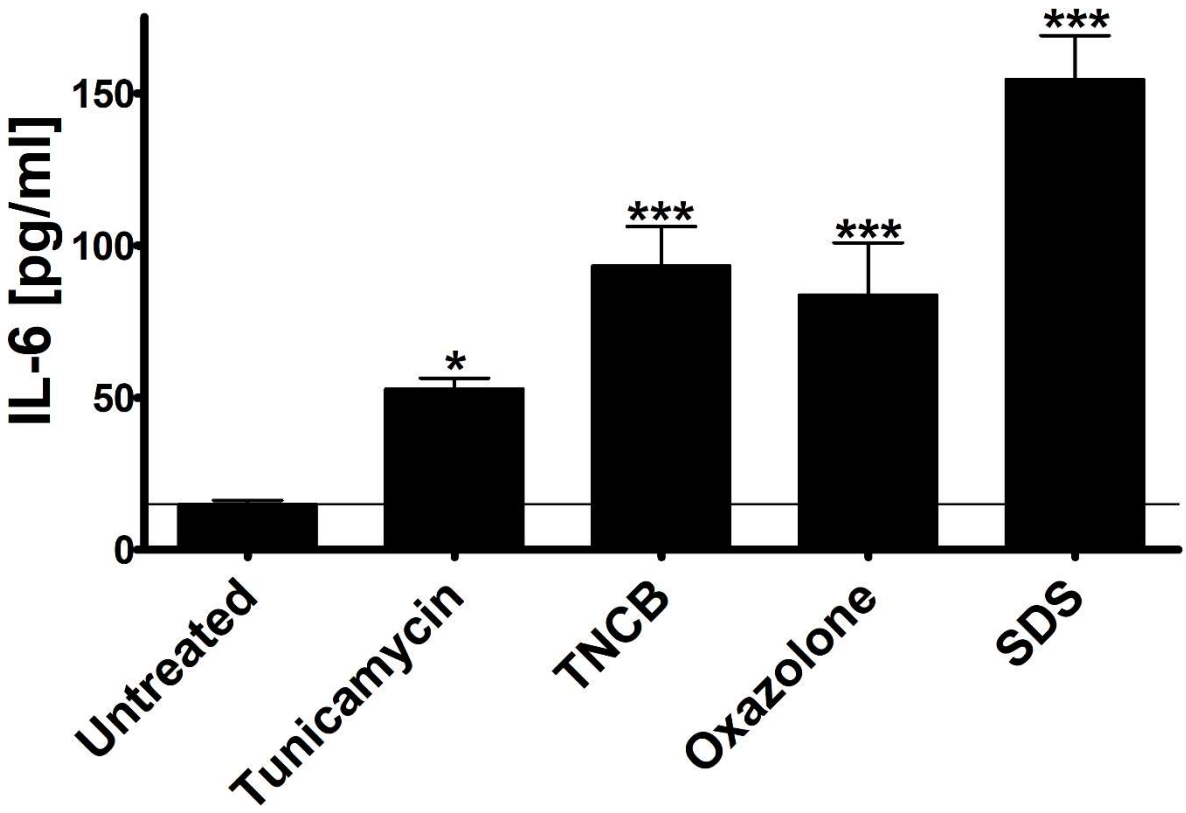

Figure 34: Chemicals lead to an increased release of pro-inflammatory cytokines by HaCaT cells. HaCaT cells were incubated with either 10 µg/ml tunicamycin, 170 µM TNCB, 4 mM oxazolone or 0.01% SDS for 24 h and cytokine production was analyzed using an IL-6 ELISA kit. Data is shown as mean +/- SEM of five independent experiments. Statistics: 1way ANOVA with Dunnett's posttest, * P ≤ 0.05, ** P ≤ 0.01, *** P ≤ 0.001. Line = untreated control. Line = untreated control value.

8.4 Keratinocytes are able to activate DCs in an UPR-dependent manner

As mentioned in the introduction, keratinocytes are the first cells to come into contact with a sensitizer and react to it. Since a recent study hints towards reactive sensitizers not penetrating the skin deeper than the epidermis (Malmberg et al. 2017) the question remains how the immune system is activated. To test the ability of keratinocytes to activate DCs after contact to a sensitizer and the role of the UPR in this process, a modified version of the COCAT assay (Hennen and Blömeke 2017) was used. In the COCAHS (Co-culture after HaCaT stimulation) assay HaCaT cells are stimulated with a sensitizer for 6 h in the absence of THP-1 cells. After the stimulation, the sensitizer is washed of and the THP-1 cells are added to the HaCaT cells for 18 h of co-culture.

8.4.1 Comparison of THP-1 monoculture, COCAT and HaCaT stimulation

A comparison of monocultured THP-1 cells, the COCAT and the COCAHS assay was performed to determine if HaCaT cells alone are able to activate THP-1 cells and their efficiency in doing that in comparison to assays where the THP-1 cells have direct contact with the allergen.

As seen in Figure 35, all of the three different types of experiments led to an increased ΔMFI (MFI of treated sample – MFI of solvent control) after oxazolone stimulation. In both CD54 and CD86, the monocultured THP-1 cells had the lowest ΔMFI in comparison to the other two assay types that had ΔMFIs of a similar range.

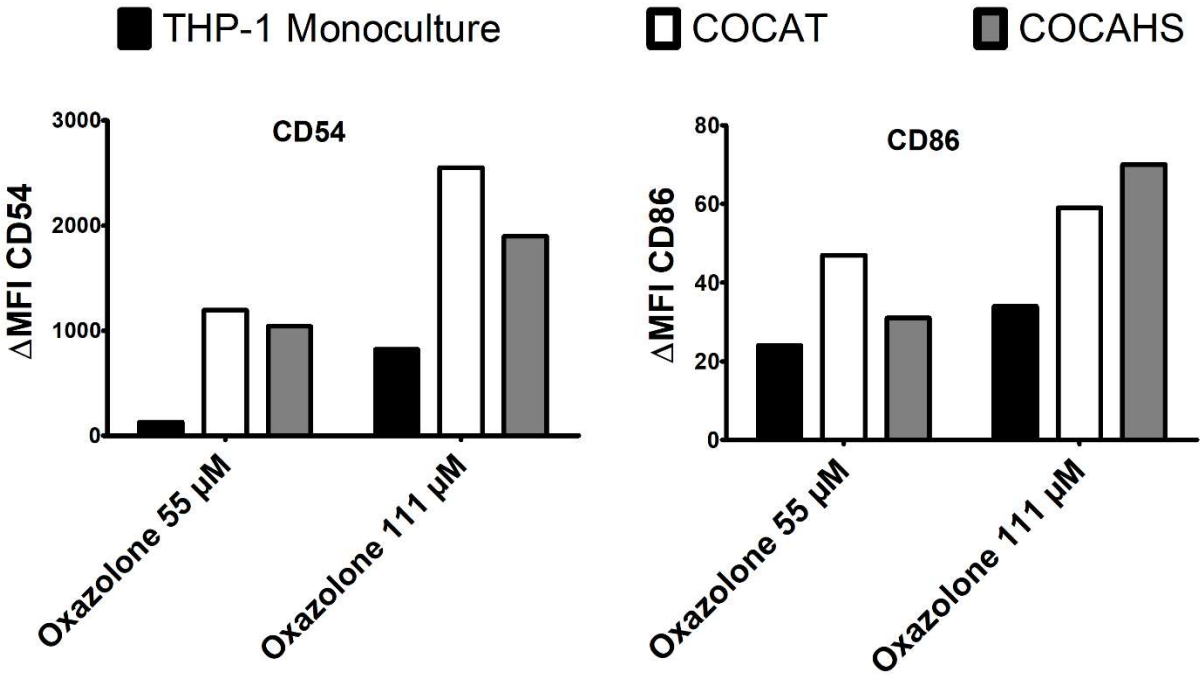

Figure 35: Comparison of different types of HaCaT and THP-1 co-culture. Bars show results from THP-1 cells that were treated with two different concentrations of oxazolone: alone as a control (THP-1 monoculture), together with HaCaT cells (COCAT) or added to HaCaT cells that were stimulated for 6 h (COCAHS). Results are shown as the ΔMFI (difference between stimulated sample and solvent control) of each method from one experiment.

8.4.2 Oxazolone-treated HaCaT cells are able to activate THP-1 cells in the absence of an antigen

To test the ability of keratinocytes to activate DCs and to address the role of the UPR, the COCAHS assay was performed as described in 7.5.

As shown in Figure 36 (Gendrisch et al. submitted), the oxazolone treatment resulted in an increase in MFIs of both CD54 and CD86 in comparison to the solvent control and untreated cells. As there was no difference between untreated and DMSO-treated samples (seen in 7.5) those are not included in the further graphs. The MFI

for CD54 showed an increase of about 1400 while the CD86 had an increase of about 70.

To assess the role of the UPR in this process, an IRE-1 and a PERK inhibitor were used to pretreat HaCaT cells before the stimulation. The inhibitors alone without the following stimulation led to an increase of the MFI of CD54 while they reduced the MFI of CD86 clearly below the DMSO control level. The pre-treatment of the cells with UPR inhibitors before oxazolone stimulation had no significant effect on the MFI of CD54 showing only a minor reduction in comparison to the oxazolone-treated samples. In contrast, the MFI of CD86 was reduced nearly back to the level of the DMSO control using the IRE-1 inhibitor while the PERK inhibitor pre-treatment was able to reduce the MFI of CD86 even below the DMSO control value.

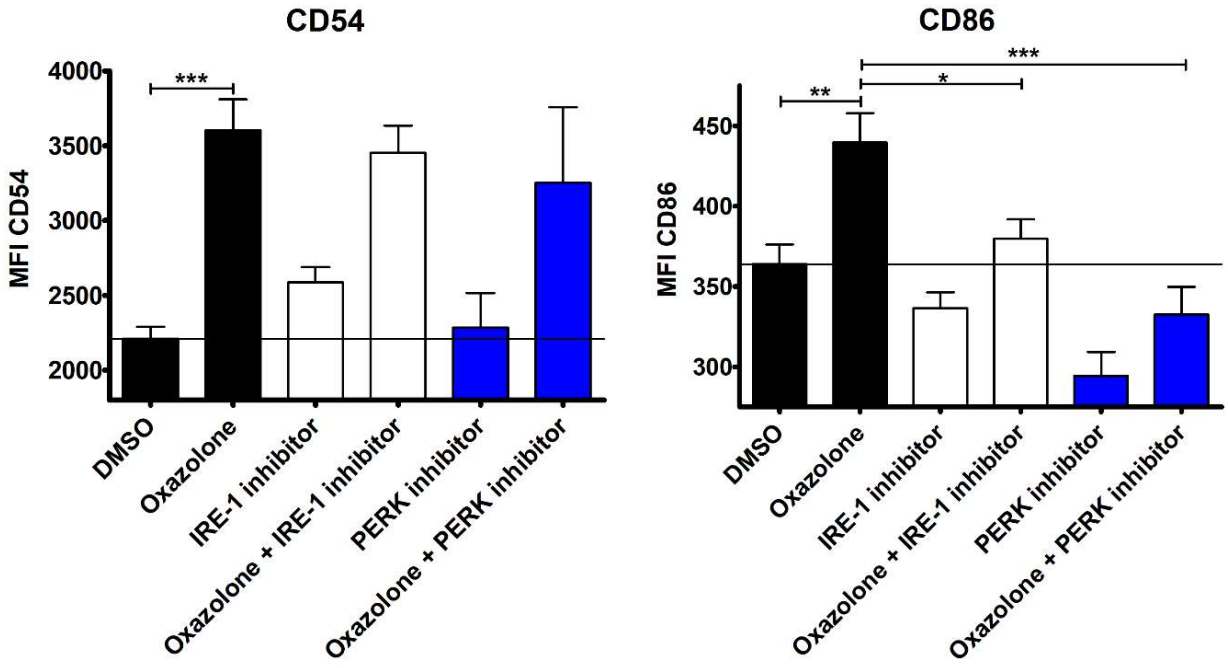

Figure 36: Oxazolone-treated HaCaT cells are able to activate THP-1 cells in the absence of an antigen in an UPR-dependent manner. HaCaT cells were stimulated with 625 µM oxazolone for 6 h with or without pre-incubation with either 20 µM IRE-1 inhibitor or 10 µM PERK inhibitor. Subsequently, cells were washed and THP-1 cells were added and co-cultured for 18 h. The activation of the THP-1 cells was analyzed by looking at the expression of CD54 and CD86 using flow cytometry. Data is shown as MFI mean +/- SEM of five to seven independent experiments. Statistics: 1way ANOVA with Bonferroni posttest, * $P \leq 0.05$, ** $P \leq 0.01$, *** $P \leq 0.001$. Line = solvent control value.

8.5 Effects of combining weak allergens

Up until here all experiments were carried out using sensitizers with a very high potency. This is not the real-life situation for most patients as the contact to a very strong sensitizer is far less common than the contact to a combination of several weak sensitizers found in products like fragrances (T. L. Diepgen et al. 2016).

Therefore, it was to be tested if a combination of weak sensitizers would react the same way as a strong sensitizer regarding the activation of the UPR and the pro-inflammatory NF-κB pathway. The tested chemicals included eugenol, a compound of the essential oil of clove important for its odor, cinnamaldehyde, a compound responsible for the flavor and odor of cinnamon, and DNTB, a weak sensitizer that can induce tolerance to the much stronger sensitizer DNFB. Furthermore, other chemicals tested were DNBS, a sensitizer often used for the induction of experimental colitis models, glyoxal, a component of some disinfectants, and resorcinol, an antiseptic substance that is a main natural phenol of argan oil. In addition, citral, a main part of lemongrass essential oil and penicillin G, an antibiotic.

8.5.1 Weak sensitizers fail to induce a significant induction of the IRE-1 branch of the UPR

To get an idea of the capability of weak sensitizers to activate the UPR, PAM212 cells were stimulated with different concentrations of weak sensitizers for 6 h and the activation of the UPR, visualized by the splicing of *Xbp-1*, was analyzed. Interestingly, none of the sensitizers used in Figure 37 was able to induce a substantial increase of *Xbp-1* splicing in comparison to the untreated control. Eugenol led to a general downregulation of the splicing with only the highest concentration showing a comparably weak increase in spliced *Xbp-1* beyond the control. Cinnamaldehyde always stayed below the level of the untreated control while DNTB-treated cells showed a splicing minimally higher than the control (Figure 37a). DNBS-treated cells showed no real difference to the control in contrast to glyoxal-treated cells whose *Xbp-1* splicing was reduced with increasing concentrations (Figure 37b). Resorcinol was the only sensitizer with a constant but still minor increase of the splicing. Finally, both citral and penicillin showed a decrease of splicing with increasing concentrations (Figure 37c).

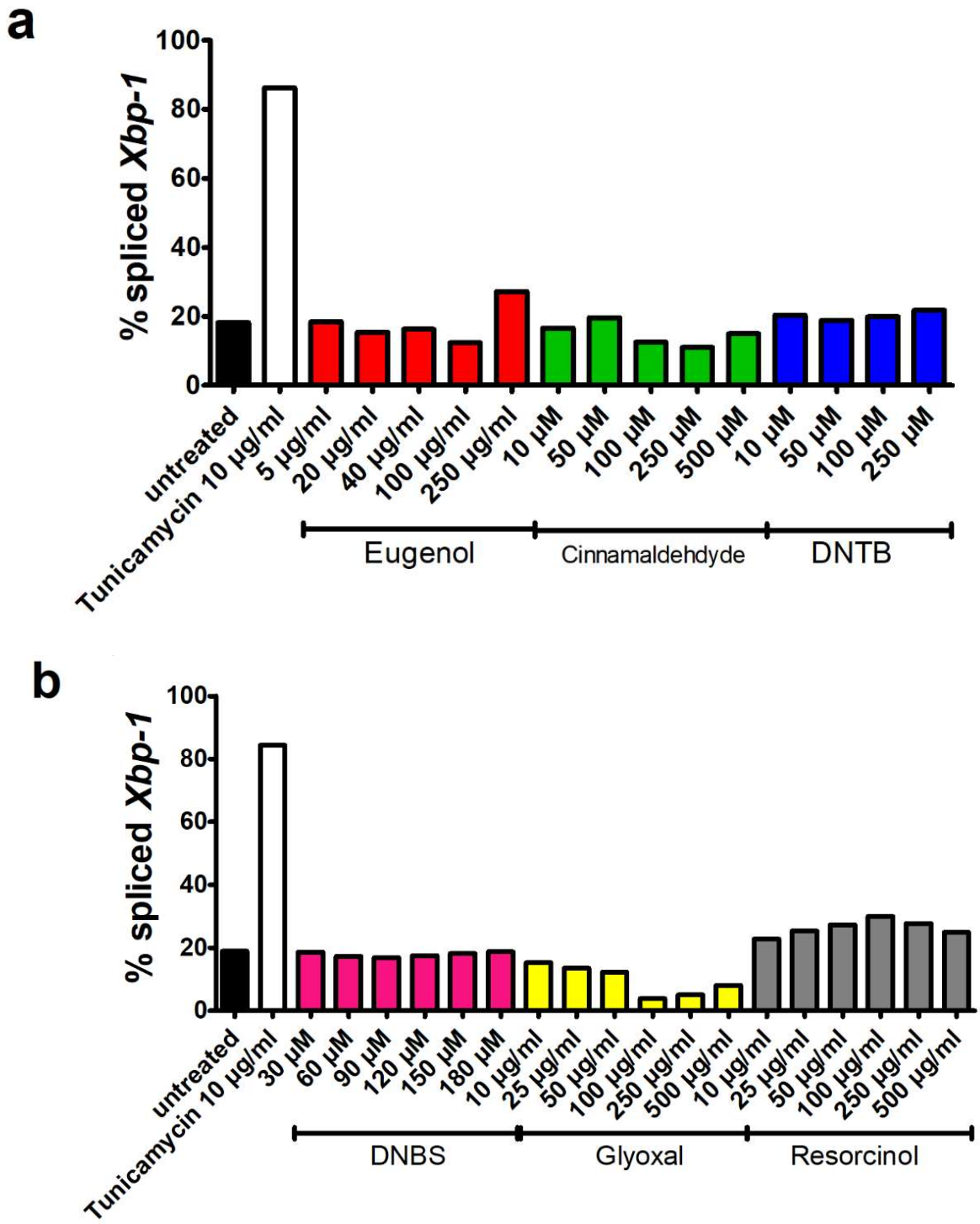
a
% spliced Xbp-1
100
80
60
40
20
0
untreated
Tunicamycin 10 µg/ml
5 µg/ml
20 µg/ml
40 µg/ml
100 µg/ml
250 µg/ml
10 µM
50 µM
100 µM
250 µM
500 µM
10 µM
50 µM
100 µM
250 µM
Eugenol
Cinnamaldehdyde
DNTB
b
% spliced Xbp-1
100
80
60
40
20
0
untreated
Tunicamycin 10 µg/ml
30 µM
60 µM
90 µM
120 µM
150 µM
180 µM
10 µg/ml
25 µg/ml
50 µg/ml
100 µg/ml
250 µg/ml
500 µg/ml
10 µg/ml
25 µg/ml
50 µg/ml
100 µg/ml
250 µg/ml
500 µg/ml
DNBS
Glyoxal
Resorcinol

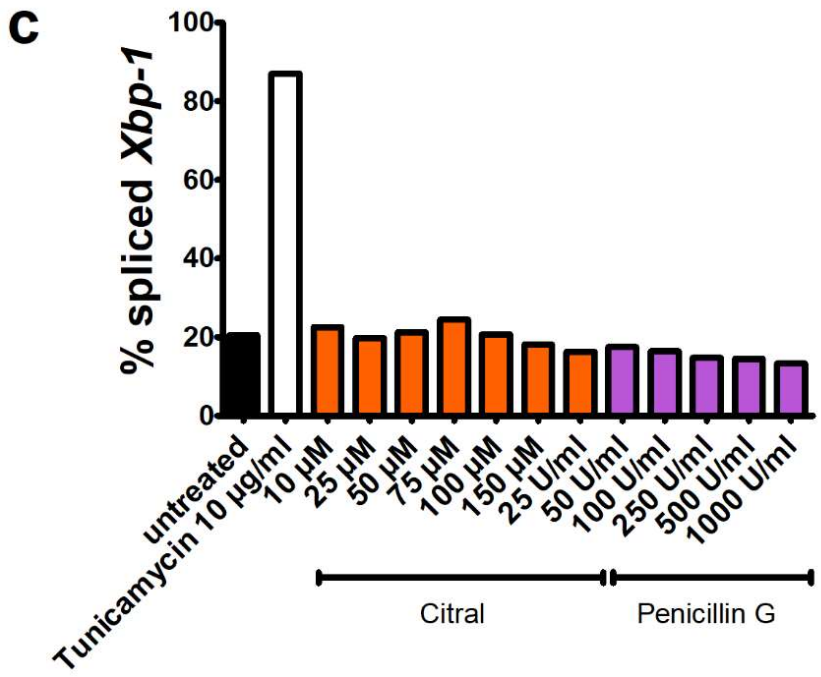

Figure 37: Weak sensitizers fail to induce an increase of *Xbp-1* splicing in PAM212 cells. PAM212 cells were treated with increasing concentrations of different weak sensitizers for 6 h. The UPR activation was analyzed by measuring the *Xbp-1* splicing by PCR after RNA isolation and cDNA synthesis. Results are shown as % spliced *Xbp-1* of one test experiment.

8.5.2 Combinations of weak sensitizers activate the IRE-1 branch of the UPR

As a single weak sensitizer was not able to induce *Xbp-1* splicing (Figure 37), PAM212 cells were treated with combinations of two weak sensitizers. Cinnamaldehyde, resorcinol and eugenol were chosen for this experiment. Cells were treated for 6 h before the RNA was isolated, reversely transcribed into cDNA and a PCR with primers specific for *Xbp-1* was performed. The PCR products were separated on an agarose gel and the splicing of *Xbp-1* was evaluated.

As Figure 38 (Gendrisch et al. submitted) shows, the weak allergens alone did not increase the splicing of *Xbp-1*. In contrast, cinnamaldehyde treatment resulted in a reduction of splicing activity. Resorcinol and eugenol had only minor effects. Interestingly, a combination of either cinnamaldehyde or resorcinol with eugenol resulted in a significant upregulation of *Xbp-1* splicing. While the combination of cinnamaldehyde with eugenol lead to a splicing of about 55% equaling a nearly 2.5-fold increase, resorcinol and eugenol reached a splicing rate of about 40% nearly doubling the control value.

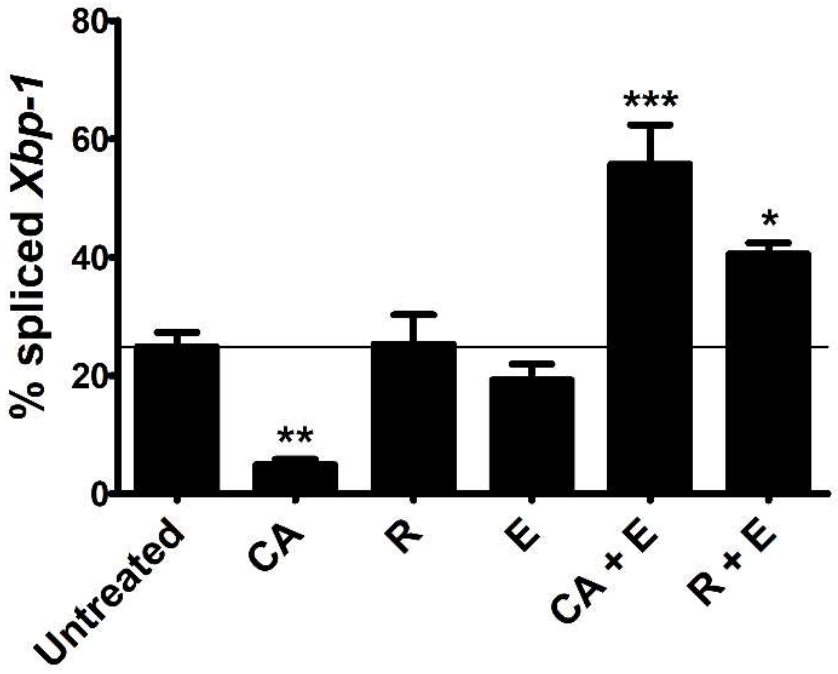

Figure 38: Combining two weak allergens induces the splicing of *Xbp-1* in PAM212 cell. Pam212 cells were stimulated for 6 h with either 75 µM cinnamaldehyde (CA), 100 µg/ml resorcinol (R), 200 µg/ml eugenol (E) or a combination of cinnamaldehyde and eugenol (CA + E) or resorcinol and eugenol (R + E). Afterwards, UPR activation was analyzed by looking at the % of *Xbp-1* splicing. Data shown as mean +/- SEM of three independent experiments. Statistics: 1way ANOVA with Dunnett's posttest, * P ≤ 0.05, ** P ≤ 0.01, *** P ≤ 0.001, all in comparison to untreated control cells (line).

These results indicate that the combination of two weak sensitizers - at doses that if used alone do not induce Xbp-1 splicing - results in a synergistic effect on the activation of the IRE-1 branch of the UPR.

8.5.3 Viability of PAM212 cells treated with weak sensitizers

To exclude potential effects of the cytotoxicity of the allergens, an MTT assay was performed to analyze the viability of the sensitizer-treated cells.

Figure 39 shows that cinnamaldehyde (CA) led to a decrease of viability in Pam212 cells in comparison to the untreated control and slightly crossed the set minimal viability of 80% while not being significantly lower. Besides CA, resorcinol (R) also decreased the viability of the cells with both reductions not being significant. In contrast, eugenol (E) and the combinations of CA+E and R+E led to a significant increase of viability in comparison to the untreated control.

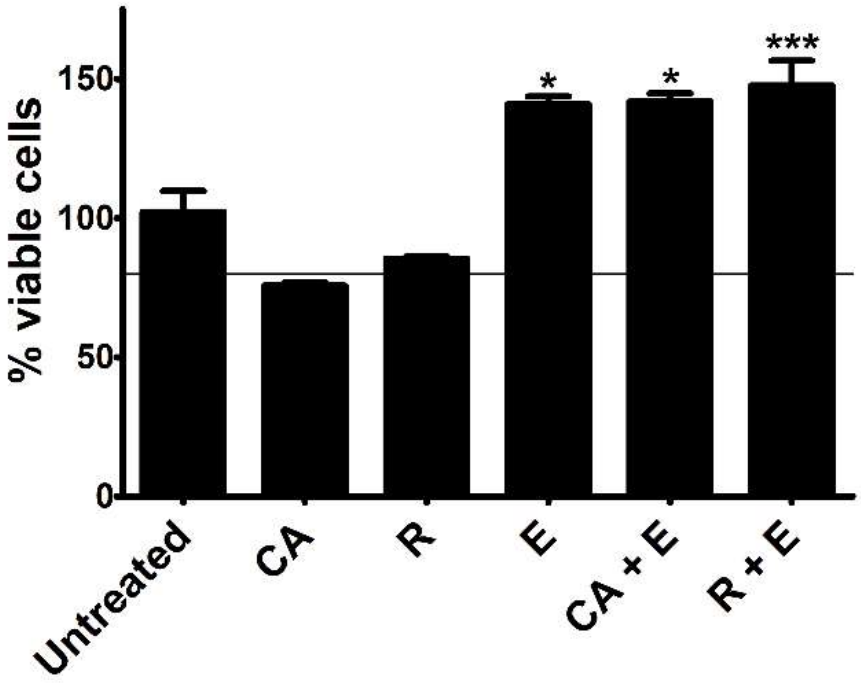

Figure 39: Combining two weak allergens increases the viability of PAM212 cells. Pam212 cells were treated for 6 h with either 75 µM cinnamaldehyde (CA), 100 µg/ml resorcinol (R), 200 µg/ml eugenol (E) or a combination of cinnamaldehyde and eugenol (CA + E) or resorcinol and eugenol (R + E). Afterwards, cell viability was analyzed using an MTT assay. Results are shown as mean +/- SEM of three experiments. Statistics: 1way ANOVA with Dunnett's posttest, * P ≤ 0.05, ** P ≤ 0.01, *** P ≤ 0.001, all in comparison to the untreated control. The line indicates 80% cell viability.

These results show that the observed synergistic effects on UPR activation observed after the combination of weak sensitizers is not mediated by an increase in cytotoxicity in these samples.

8.5.4 Combinations of weak sensitizers activate the NF-κB pathway

As combination of weak sensitizers showed the same activation of the UPR that was seen with more potent sensitizers, the question was if they also activate pro-inflammatory pathways. Just like with the strong sensitizers, the nuclear translocation of the p65 subunit of NF-κB was used to address this question. Figure 40 shows example pictures of the experiments and the result are quantified in Figure 41 (Gendrisch et al. submitted). Untreated cells showed about 8% cells with increased nuclear p65 levels. Treatment of the cells with CA, resorcinol or eugenol resulted in no significant increase in NF-κB activation. In addition, the combination of eugenol with either CA or resorcinol led to an increased nuclear translocation of p65. The combination of CA with resorcinol had a weaker effect on the p65 translocation, showing a trend towards an increased p65 translocation. However, the results were not statistically significant.

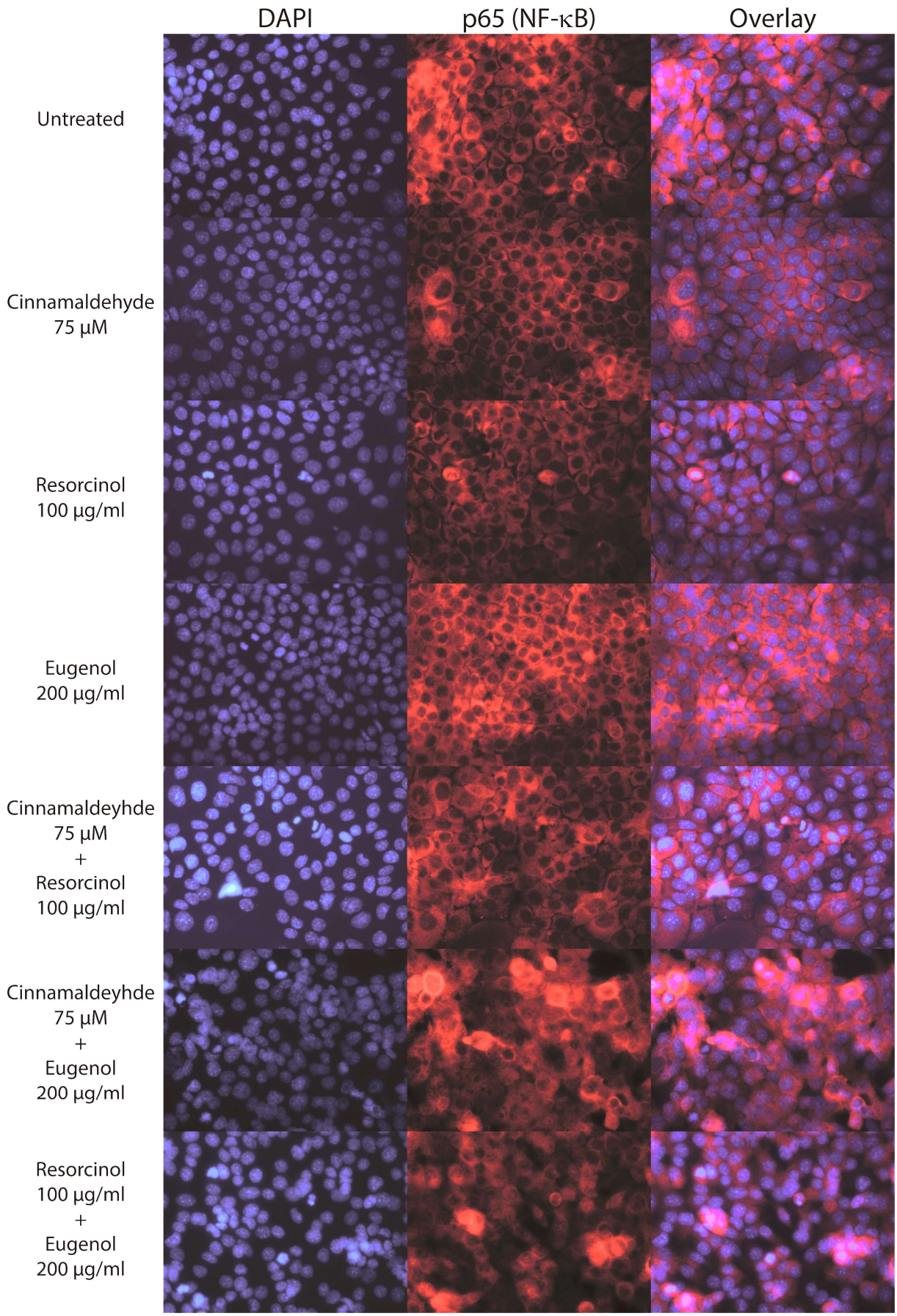
DAPI
p65 (NF-κB)
Overlay
Untreated
Cinnamaldehyde
75 µM
Resorcinol
100 µg/ml
Eugenol
200 µg/ml
Cinnamaldeyhde
75 µM
+
Resorcinol
100 µg/ml
Cinnamaldeyhde
75 µM
+
Eugenol
200 µg/ml
Resorcinol
100 µg/ml
+
Eugenol
200 µg/ml

Figure 40: Combinations of weak allergens induce the nuclear translocation of the p65 subunit of NF-κB. PAM212 cells were treated with either 100 µg/ml resorcinol, 75 µM cinnamaldehyde (CA), or 200 µg/ml eugenol alone or in combination for 1 h. Afterwards cells were fixed, permeabilized and the p65 subunit of NF-κB was detected using an anti-mouse p65 primary antibody and visualized using a goat anti-mouse antibody coupled to Alexa Fluor 555 while DAPI was used for nuclear staining. One representative experiment out of three is shown. 400x magnification.

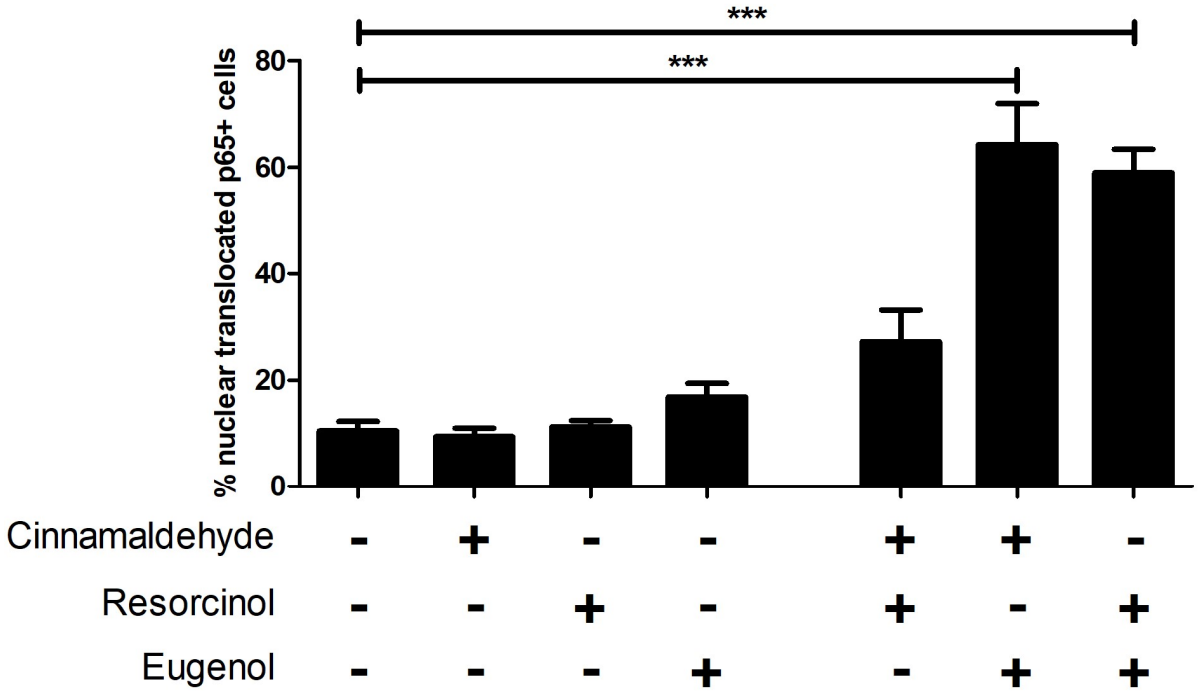

Figure 41: The nuclear translocation of the p65 subunit of NF-κB in PAM212 cells is induced by the combination of two weak sensitizers. Pam212 cells were treated for 1 h with either 75 µM cinnamaldehyde (CA), 100 µg/ml resorcinol (R), 200 µg/ml eugenol (E) or a combination of cinnamaldehyde and resorcinol, cinnamaldehyde and eugenol or resorcinol and eugenol. Afterwards, the p65 subunit of NF-κB was detected using ICC as described in 7.4.1 and 7.4.2. Results are shown as mean +/- SEM of three independent experiments with analyzing three different fields per sample. Statistics: 1way ANOVA with Bonferroni posttest, * P ≤ 0.05, ** P ≤ 0.01, *** P ≤ 0.001, all in comparison to the untreated control.

8.6 Effects of combinations of weak sensitizers with the irritant SDS

In addition to a combination of different weak sensitizers, everyday products often contain irritants. An example are shampoos where the irritant SDS is used for its washing active properties and to increase foam formation. As SDS was shown to activate the UPR, the goal of the following experiments was to find a potential effect of the combination of the irritant SDS with weak sensitizers that enables them to act in a fashion comparable to stronger sensitizers.

8.6.1 SDS leads to a dose-dependent decrease of cellular viability in combination with weak sensitizers

Different weak sensitizers with concentrations that showed no negative effect on cell viability in PAM212 cells were combined with different concentrations of SDS. This was done to find a combination for each sensitizer and SDS that does not reduce the viability below the 80% mark.

Figure 42 shows that the combination of the sensitizers with all four concentrations of SDS did not decrease cellular viability below 80% with the exception of DNTB + 200 µM SDS. This combination crossed the line by just 5%. Interestingly, the viability of the PAM212 cells was enhanced in all cases when a weak sensitizer was combined with 125 µM or 150 µM of SDS. Addition of 175 µM SDS delivered mixed results while addition of 200 µM SDS decreased the cellular viability in all settings below the level shown by each sensitizer alone.

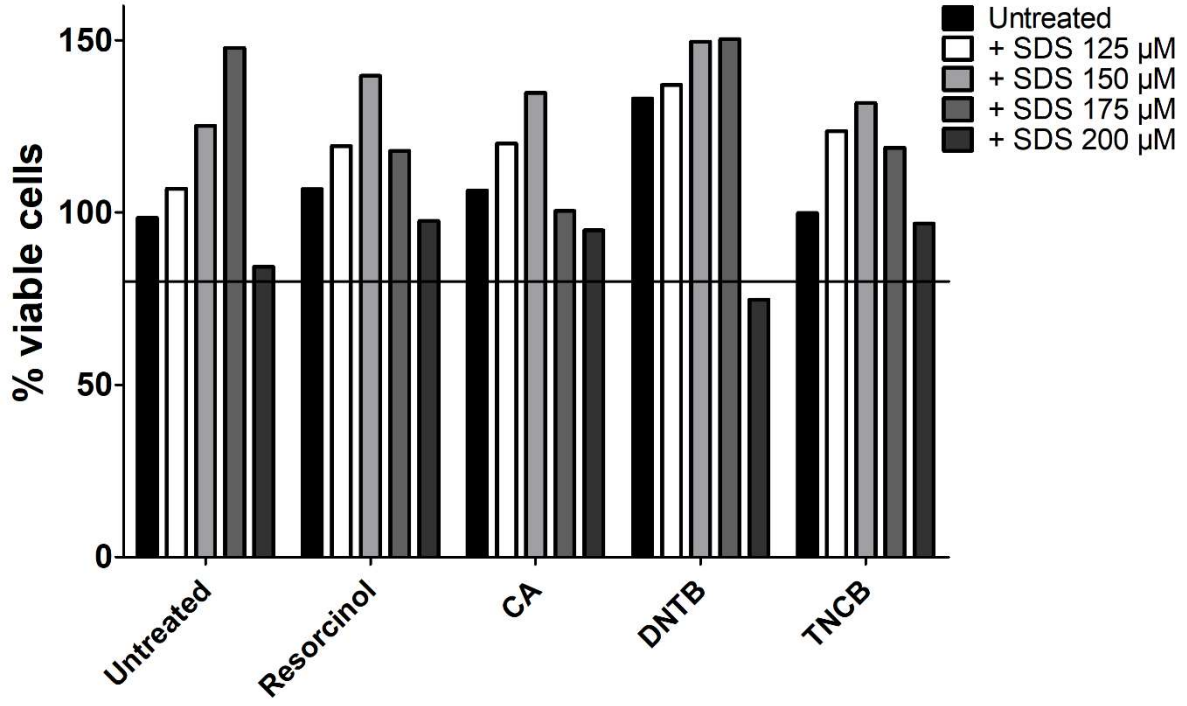

Figure 42: Increasing concentrations of SDS lead to a decreased cellular viability in combination with weak sensitizers. PAM212 cells were treated with 100 µg/ml resorcinol, 75 µM cinnamaldehyde (CA), 75 µM DNTB or 30 µM TNCB alone or in combination with different concentrations of SDS for 6 h Viability of the treated PAM212 cells was assessed using an MTT assay. Viability is shown as % viable cells in comparison to the untreated control (100%).

8.6.2 Combinations of weak sensitizers and SDS activate the UPR in a synergistic manner

To test for a potential activation of the UPR by weak sensitizers or combinations of weak sensitizers and the irritant SDS in a similar fashion to the combinations of weak sensitizers (Figure 38), the splicing of *Xbp-1* was analyzed.

Figure 43 (Gendrisch et al. submitted) shows that the weak sensitizers at the used concentrations did not induce a significant increase of *Xbp-1* splicing in comparison to the untreated control. SDS treatment led to an increase of splicing, however it was not significant. To get an idea of what the extent of an additive effect of the combinations of weak sensitizers with SDS might look like, the increase of splicing caused by SDS or sensitizer treatment over the untreated cells were added up and shown as a theoretical value (grey bars). The actual experimental data of the combination treatment is shown as white bars. The weak sensitizers alone were not able to induce a significant increase of *Xbp-1* splicing, all of them reached values between 10% and 20%. The splicing induced by SDS was around 20%. Therefore, the theoretical additive effect of SDS and weak sensitizer was set between 30% and 40%. Interestingly, the combination of SDS with either resorcinol, DNTB or TNCB did not only reach the amount of splicing calculated by assuming an additive effect but clearly went beyond that level. The *Xbp-1* splicing induction of all combinations was significantly increased in comparison to cells that were treated with SDS alone with values that ranged from 50% to over 60%. With the exception of CA, all weak sensitizers in combinations with SDS did not only reach the level of the theoretical additive effect but went well beyond them.

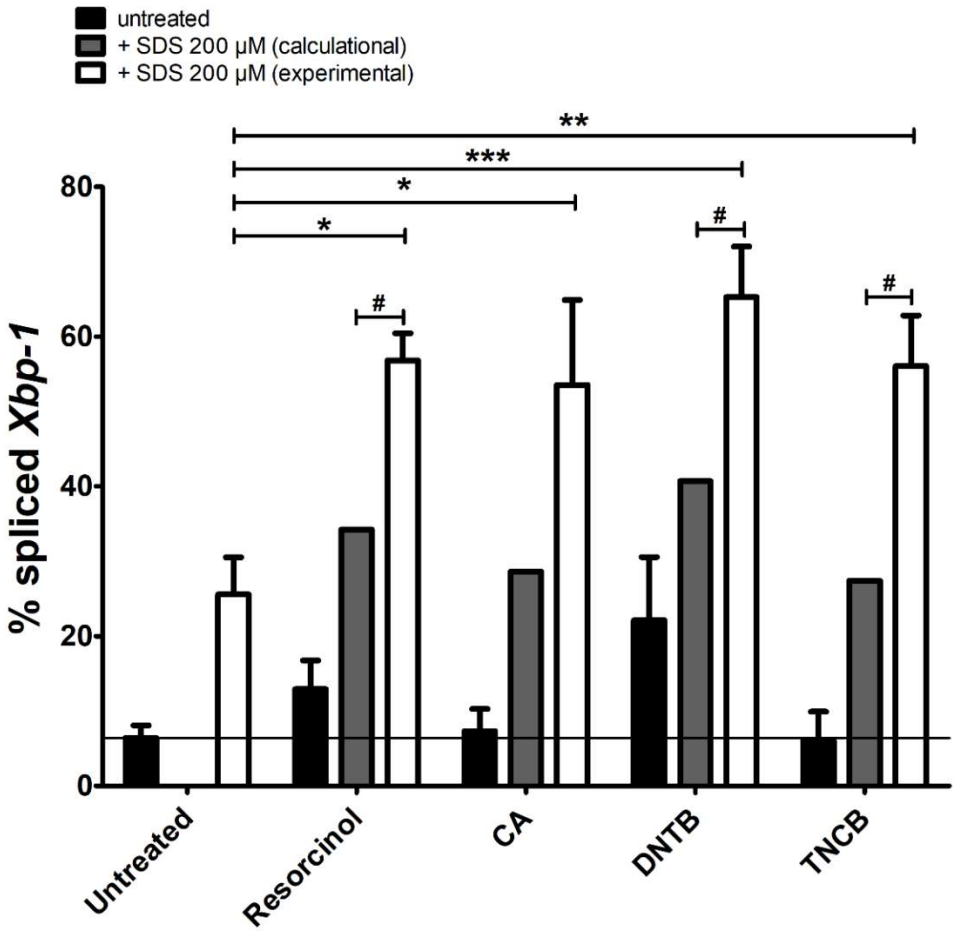

Figure 43: Analysis of the activation of the IRE-1 branch of the UPR by weak sensitizers in combination with SDS in PAM212 cells. PAM212 cells were treated with 100 µg/ml resorcinol, 75 µM cinnamaldehyde (CA), 75 µM DNTB or 30 µM TNCB alone or in combination with 200 µM SDS for 6 h. Subsequently, the RNA was isolated, reversely transcribed into cDNA and a conventional PCR with primers specific for murine *Xbp-1* was performed. *Xbp-1* splicing was analyzed as described in 7.3.5. A theoretical value for an additive effect of the combination of SDS and weak allergen was calculated (grey bars). Data shown from at least three independent experiments as mean +/- SEM. Statistics: 1way ANOVA with Bonferroni posttest, * P ≤ 0.05, ** P ≤ 0.01, *** P ≤ 0.001. To compare the theoretical combination values to the experimental combination values the column statistics function of GraphPad Prism was used, # P ≤ 0.05. Line = untreated control value.

8.6.3 Weak sensitizers in combination with the irritant SDS activate the NF-κB pathway in a synergistic manner

Since strong sensitizers were able to activate the NF-kB pathway, the same experiment was repeated with cells treated with either a weak sensitizer alone or in combination with SDS. As shown in Figure 44, PAM212 cells which were treated with a weak sensitizer showed a high ratio of cells with a nuclear shadow in the p65 staining. The same holds true for untreated and SDS only treated cells. Interestingly, when cells were treated with a weak sensitizer in combination with SDS it can be seen that the number of cells with a lacking nuclear shadow in the p65 staining is going up.

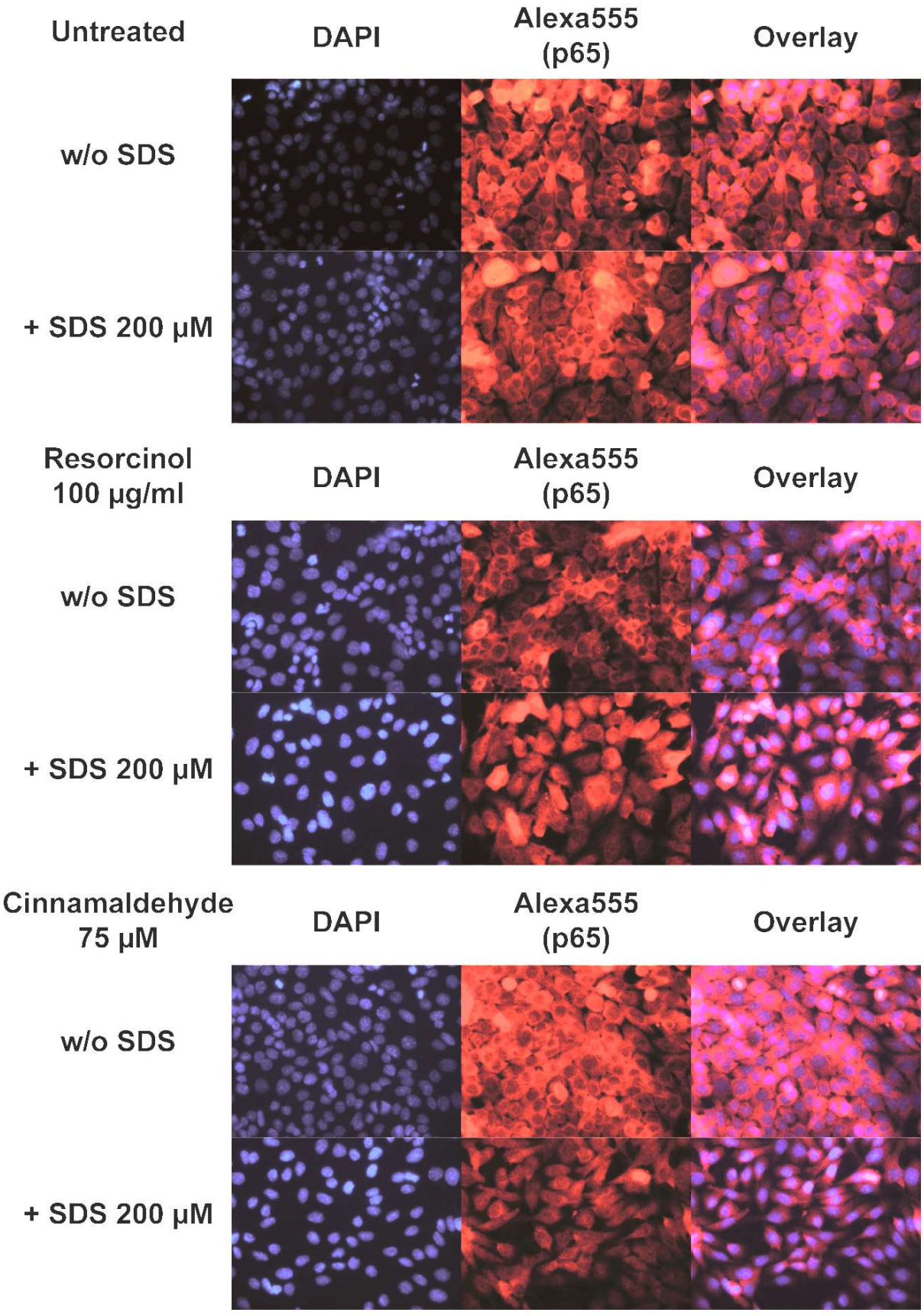
Untreated
DAPI
Alexa555 (p65)
Overlay
w/o SDS
+ SDS 200 µM
Resorcinol 100 µg/ml
DAPI
Alexa555 (p65)
Overlay
w/o SDS
+ SDS 200 µM
Cinnamaldehyde 75 µM
DAPI
Alexa555 (p65)
Overlay
w/o SDS
+ SDS 200 µM

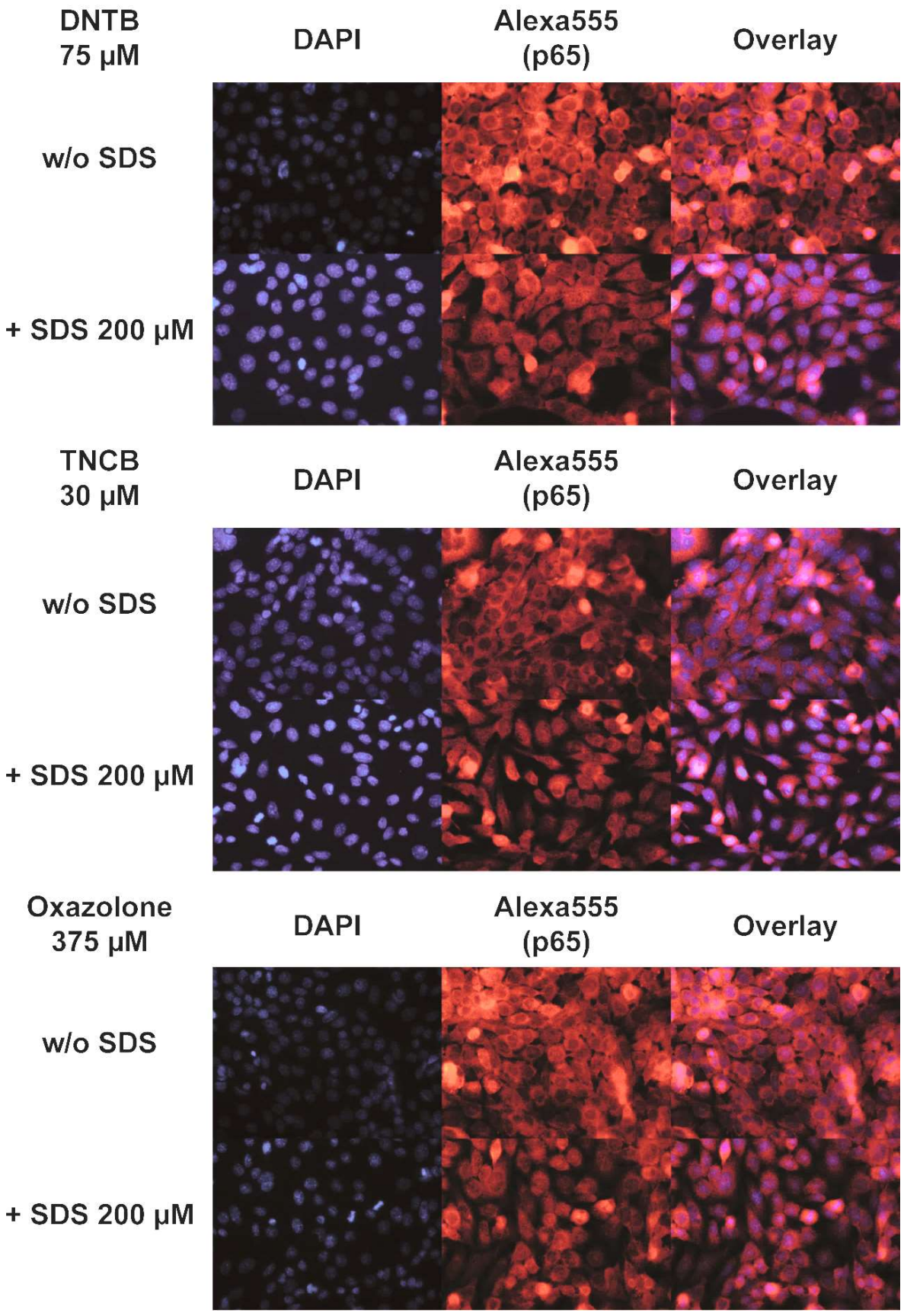
DNTB
75 µM
DAPI
Alexa555
(p65)
Overlay
w/o SDS
+ SDS 200 µM
TNCB
30 µM
DAPI
Alexa555
(p65)
Overlay
w/o SDS
+ SDS 200 µM
Oxazolone
375 µM
DAPI
Alexa555
(p65)
Overlay
w/o SDS
+ SDS 200 µM

Figure 44: Analysis of NF-κB (p65) nuclear translocation in PAM212 cells after treatment with weak sensitizers in combination with SDS. PAM212 cells were treated with either 100 µg/ml resorcinol, 75 µM cinnamaldehyde (CA), 75 µM DNTB, 30 µM TNCB or 375 µM oxazolone alone or in combination with 200 µM SDS for 1 h. Afterwards cells were fixed, permeabilized and the p65 subunit of NF-κB was detected using an anti-mouse p65 primary antibody and visualized using a goat anti-mouse antibody coupled to Alexa Fluor 555 while DAPI was used for nuclear staining. One representative experiment out of three is shown. 400x magnification.

Again, the ratio of cells showing a lack of a nuclear shadow in the p65 staining was quantified to get a better idea of the exact numbers. As it can be seen in Figure 45 (Gendrisch et al. submitted), Pam212 cells that were treated with either a weak sensitizer (black bars) or SDS (first white bar) alone showed only minor changes of the amount of nuclear p65+ cells in comparison to the untreated cells. All these conditions led to about 10% nuclear p65+ cells. Just like with the UPR experiment before, a theoretical value of the combinatory effect was calculated by adding up the changes of SDS and sensitizer treatment (grey bar). Again, only minor changes are visible in comparison to the untreated control. Interestingly, the experimental data of the combinations of a weak sensitizer with SDS showed that in contrast to the low values of around 10% nuclear p65+ cells the results ranged from little over 40% for resorcinol to just below 70% for CA. These results were of course significantly different from the theoretical calculated additive effect values.

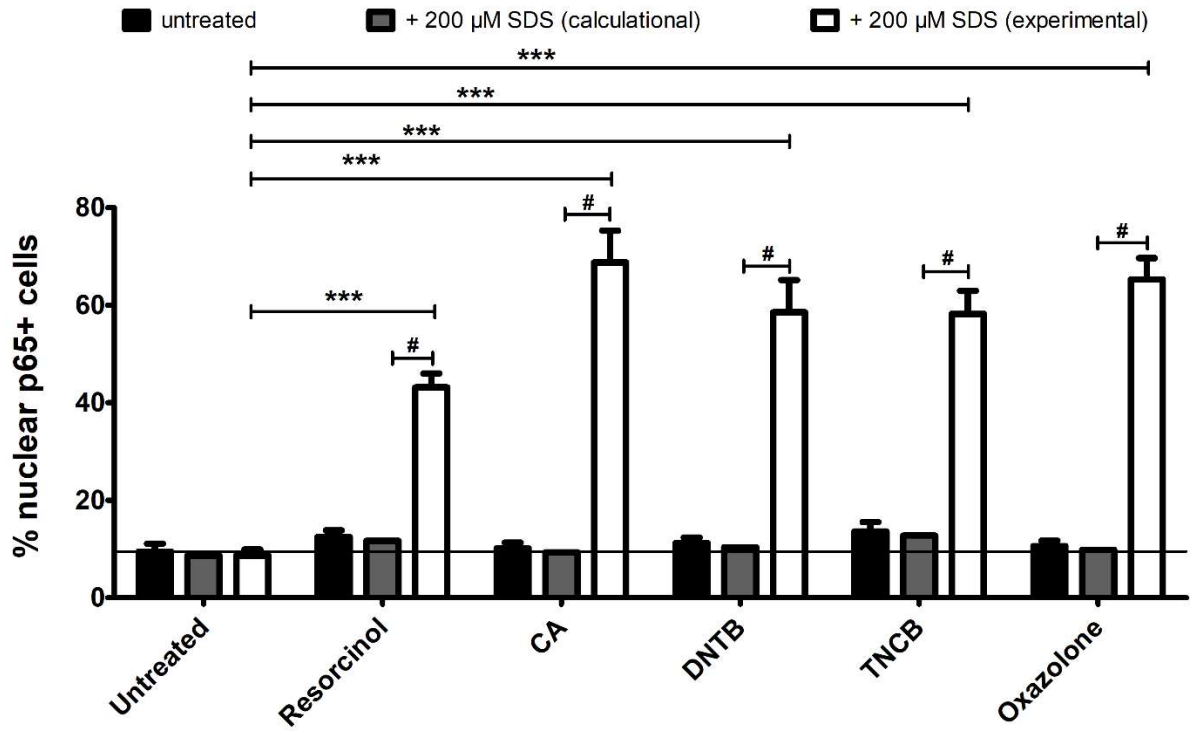

Figure 45: Quantification of NF-κB (p65) nuclear translocation in PAM212 cells after treatment with weak sensitizers with or without an irritant. PAM212 cells were treated with 100 µg/ml

resorcinol, 75 µM cinnamaldehyde (CA), 75 µM DNTB, 30 µM TNCB or 375 µM oxazolone alone or in combination with 200 µM SDS for 1 h. p65 localization was analyzed as described in 7.4.2. A theoretical value for an additive effect of SDS and weak allergens was calculated. Data shown as mean +/- SEM of three independent experiments with three pictures taken per experiment. Statistics: 1way ANOVA with Bonferroni posttest, * P ≤ 0.05, ** P ≤ 0.01, *** P ≤ 0.001. To compare the theoretical combination values to the experimental combination values the column statistics function of GraphPad Prism was used, # P ≤ 0.05. Line = untreated control value.

8.7 *Caenorhabditis elegans* (*C. elegans*) hsp-4::GFP reporter strain shows increased UPR activity after sensitizer treatment

As seen in the experiments before, analyzing the activity of the UPR is a quite cumbersome process. Large numbers of cells are needed and the stimulation is followed by a variety of processes afterwards. IRE-1 analysis is associated with time and material-consuming activities like RNA isolation while the PERK branch was analyzed using pricey antibodies. Therefore, these methods are unsuitable for the screening of large amounts of chemicals for their UPR-inducing capabilities. An interesting alternative might be the model organism *C. elegans*. It is a nematode with a total length of about 1 mm that is widely used as a model organism for a variety of research fields including immunology and neuroscience (Sengupta and Samuel 2009; Marsh and May 2012). Many different reporter strains of this nematode are commercially available and large numbers of animals are easy to grow due to their undemanding breeding and culture.

The strain used for these test experiments is called hsp-4::GFP and is characterized by an induction of GFP expression when the protein hsp-4, the homolog of the mammalian BiP, is expressed. In cooperation with Dr. Ekkehard Schulze of the Baumeister Lab, University of Freiburg, these animals were treated with increasing concentrations of different contact sensitizers as well as the irritant SDS and tunicamycin as a UPR activator. After 48 h of treatment on an agar plate, the animals were picked of the plate, placed on object slides and documented using a camera mounted on a binocular. The GFP fluorescence was excited using filtered light with a wavelength of 390 nm. Example pictures are shown in Figure 46. It can be seen that water-treated animals exhibit slight background fluorescence. This is to be expected, since there is always some background UPR activation in living cells/tissues (Iwawaki et al. 2004). Animals treated with cobalt (II) chloride hexahydrate show no increased GFP expression, nickel (II) chloride hexahydrate treatment resulted in a slight

increase. The animals treated with nickel (II) sulfate hexahydrate showed a clear response to the stimulation visualized by an increased GFP expression.

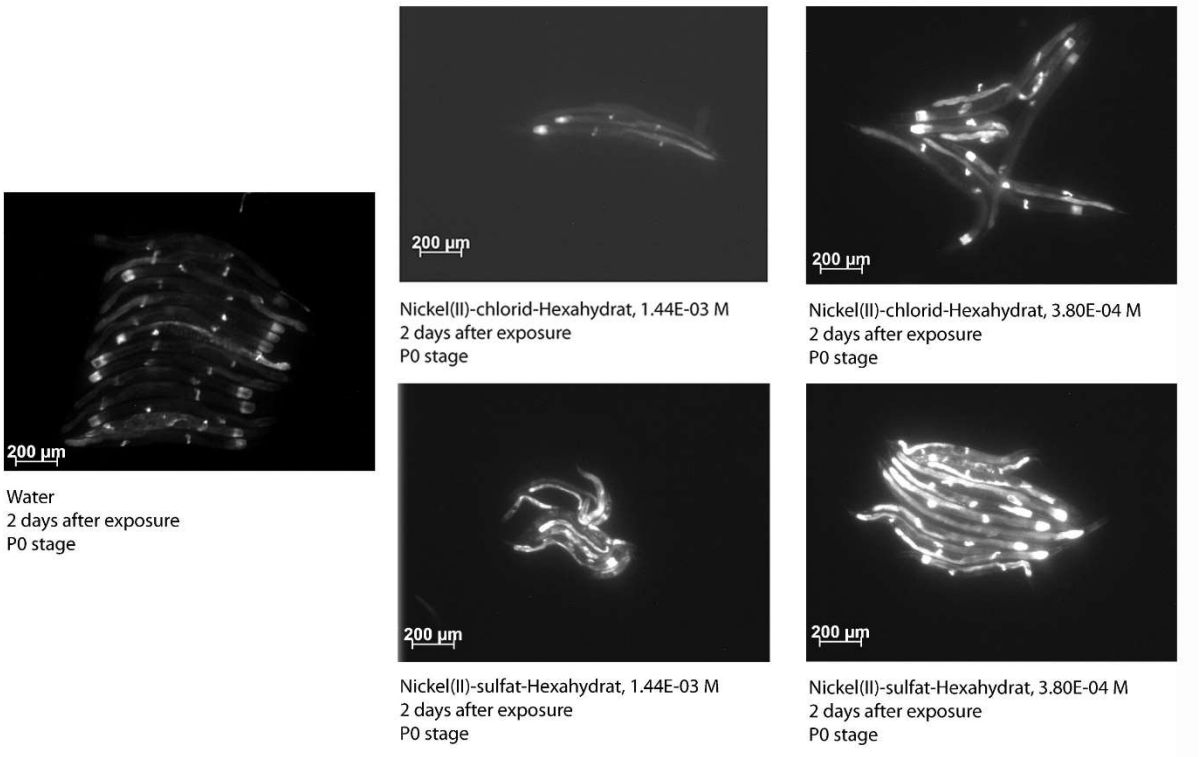

Figure 46: Examples of hsp-4::GFP reporter animals after sensitizer treatment. C. elegans in the P0 stage were treated with the described chemicals for 48 h and fluorescence of the hsp-4 reporter was analyzed. Pictures show representative examples of animals treated with nickel (II) chloride hexahydrate or nickel (II) sulfate hexahydrate.

A quantification of all treatment results in Figure 47 shows that most conditions did not lead to an increased GFP expression. Only the 380 µM and 1.44 mM of NS and NC as well as 650 µM oxazolone caused a clear increase of expression over the water-treated controls. But these still did not even closely reach the level of the positive control tunicamycin.

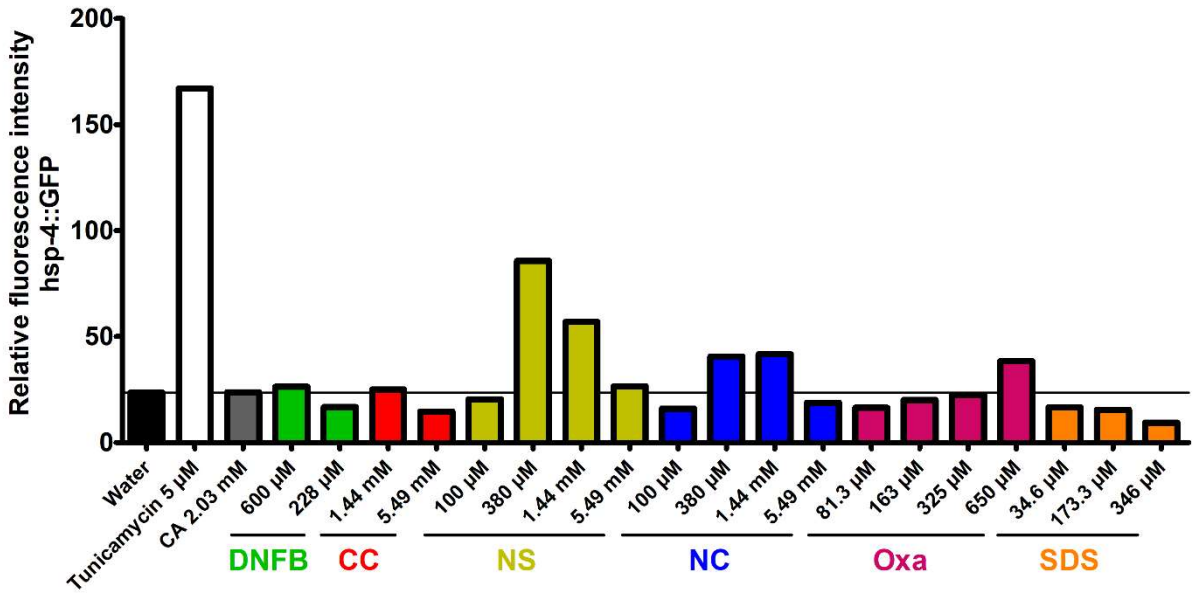

Figure 47: Quantification of fluorescence intensity of the hsp-4::GFP reporter strain of C.elegans after treatment with different chemicals. Animals were treated with Tunicamycin, cinnamaldehyde (CA), DNFB, cobalt (II) chloride hexahydrate (CC), nickel (II) sulfate hexahydrate (NS), nickel (II) chloride hexahydrate (NC), Oxazolone (Oxa) or SDS in the stated concentrations for 48 h on agar plates. After taking pictures the fluorescence was quantified using ImageJ. Data of one experiment is shown.

8.8 Autophagy in the ACD

More and more evidence of an important interplay of the UPR and other stress response pathways is found (Kupsco and Schlenk 2015; Senft and Ronai 2015a). One important stress response is autophagy, a degradation process proving to play an important role in the immune system (Shibutani et al. 2015; Kabat, Pott, and Maloy 2016). Therefore, we hypothesized, that an interplay between autophagy and UPR induction might play a role in the development of an pro-inflammatory cytokine milieu and the development of ACD as there are hints towards a role of autophagy in the ACD (X. Wang et al. 2016).

8.8.1 Sensitizers fail to consistently induce changes in autophagy gene expression in an UPR-dependent manner

To analyze a potential activation of autophagy by sensitizers and irritants, PAM212 cells were treated with different chemicals for 6 h and the expression of four autophagy genes was analyzed by qPCR. To address a potential involvement of the UPR in the activation of the autophagy a pre-treatment with UPR inhibitors 1 h before the stimulation was included.

Figure 48 shows the downregulation of *Nbr1* expression after the chemical treatment for 6 h. NBR in cells treated with tunicamycin, TNCB and oxazolone was

downregulated to about 0.05-fold expression while SDS treatment resulted in an expression of about 0.4-fold in comparison to the untreated control. The pretreatment of unstimulated cells with the UPR inhibitors resulted in a nearly complete downregulation of *Nbr1* while they had not much of an effect on the chemical-treated cells. Analyzing *Atg3*, treatment of PAM212 cells resulted in a downregulation of expression when using tunicamycin and TNCB while oxazolone and SDS were able to upregulate the expression to about two-fold. In treatments where *Atg3* was downregulated the UPR inhibitors upregulated the expression while in treatment conditions that led to an upregulation the use of inhibitors tended to dampen that effect. Looking at *Atg5*, tunicamycin led to an increase of expression to about four-fold with both UPR inhibitors downregulating the expression. The other stimulants did not lead to any significant change in gene expression and an inhibition of the UPR did not change that. When analyzing the expression of *Atg12*, tunicamycin treatment resulted in a similar picture as in *Atg5*, an upregulation that is counteracted by both UPR inhibitors. While TNCB and oxazolone resulted in a slight downregulation of *Atg12*, SDS increased the expression slightly but was once again counteracted by the use of UPR inhibitors.

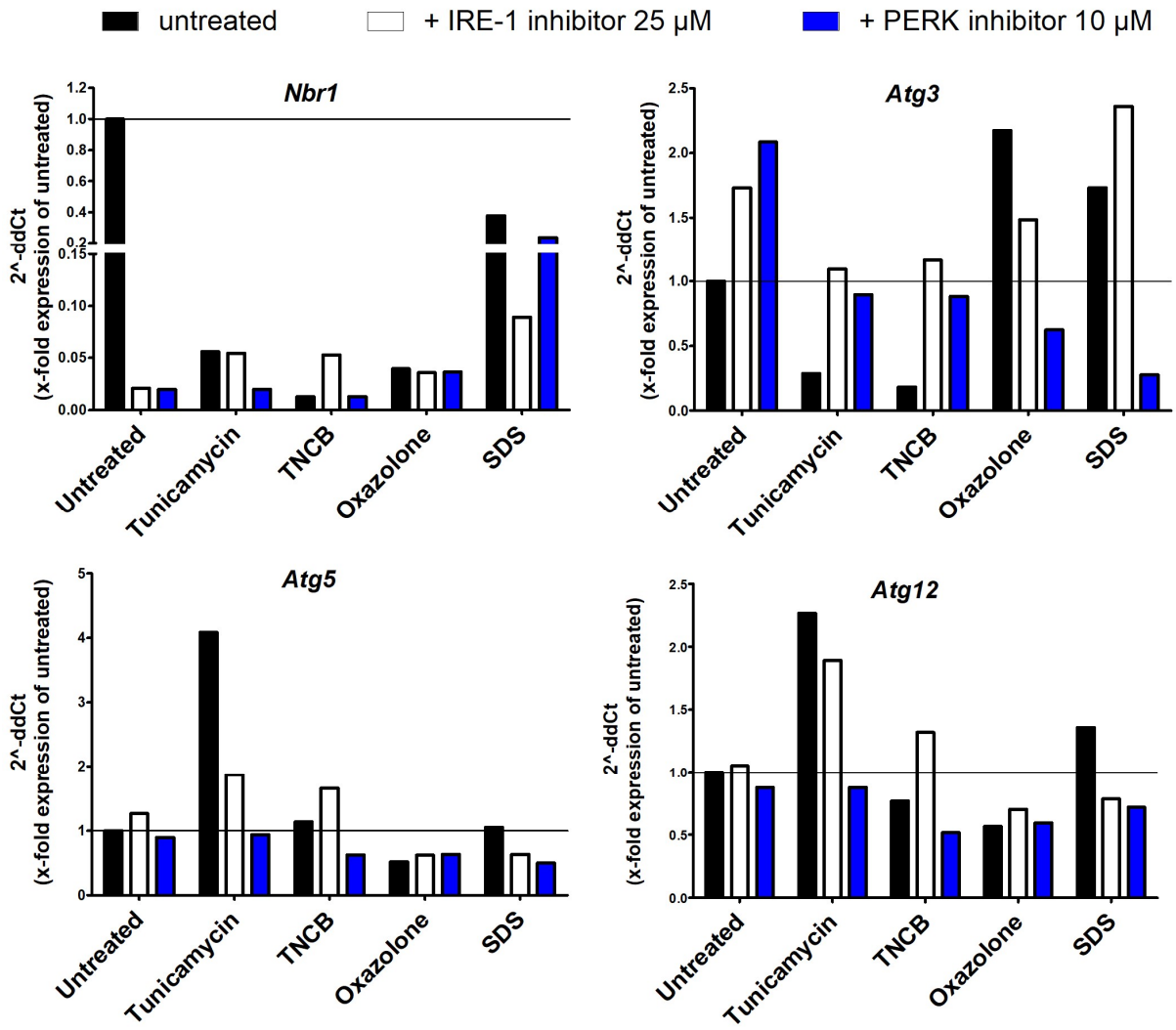

Figure 48: Analysis of chemical-induced autophagy gene expression after 6 h and the role of the UPR. PAM212 cells were pre-treated with either 25 µM IRE-1 inhibitor II or 10 µM PERK inhibitor for 1 h before adding Tunicamycin (10 µg/ml), TNCB (30 µM), Oxazolone (625 µM) or SDS (260 µM) for 6 h. RNA was isolated, reversely transcribed into cDNA and real-time PCR analysis was performed. Gene expression in relation to the untreated control was assessed using the 2-ΔΔCT method (Schmittgen and Livak 2008). Data is shown from one experiment.

The same kind of experiment was repeated with a stimulation time of 24 h before the start of the gene expression analysis. The results for the expression of *Nbr1* in Figure 49 show a different picture than after 6 h stimulation. *Nbr1* expression was increased over three-fold by tunicamycin treatment while TNCB, oxazolone and SDS had no effect. Again, UPR inhibitor pre-treatment was included to account for a possible role of the UPR in the activation of the autophagy. The IRE-1 inhibitor led to an increased expression in the tested conditions, the PERK inhibitor was able to upregulate the expression of *Nbr1* after tunicamycin, TNCB and oxazolone treatment. In untreated as well as SDS treated cells the PERK inhibitor showed no effect.

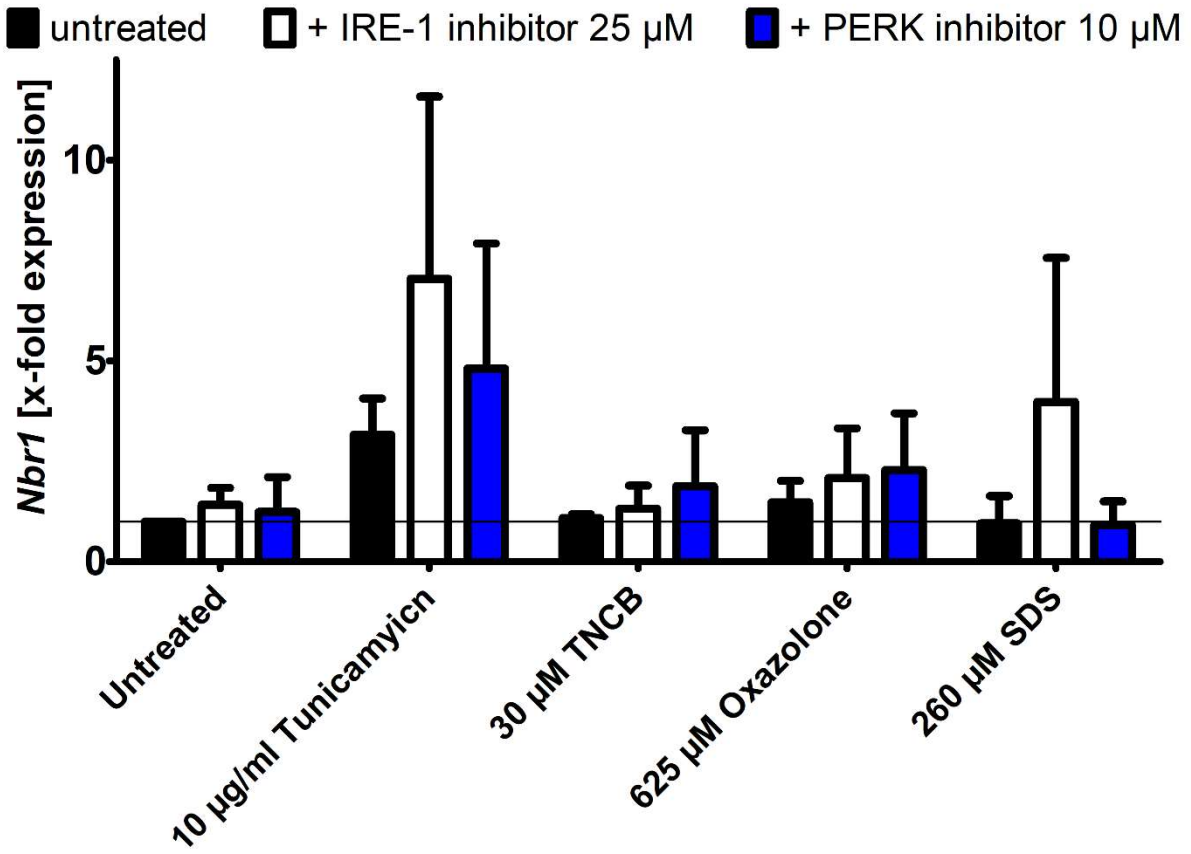

Figure 49: Analysis of chemical-induced *Nbr1* gene expression after 24 h of stimulation and the role of the UPR. PAM212 cells were pre-treated with UPR either 25 µM IRE-1 inhibitor II or 10 µM PERK inhibitor for 1 h before adding Tunicamycin (10 µg/ml), TNCB (30 µM), Oxazolone (625 µM) or SDS (260 µM) for 24 h. RNA was isolated, reversely transcribed into cDNA and real-time PCR analysis was performed. Gene expression in relation to the untreated control was assessed using the $2^{-\Delta\Delta CT}$ method (Schmittgen and Livak 2008). Data is shown as mean +/- SEM of three independent experiments. Statistics: 1way ANOVA with Bonferroni posttest, * P ≤ 0.05, ** P ≤ 0.01, *** P ≤ 0.001.

8.8.2 LC3 protein levels

One very important component of autophagy is the protein LC3 being indispensable for the formation of autophagosomes (Tanida, Ueno, and Kominami 2008). To analyze the expression of LC3, the protein was detected in cells using ICC with a fluorophore-labeled antibody. PAM212 cells were treated with the usual set of chemicals for 6 h with or without a pre-incubation with UPR inhibitors for 1 h. This was followed by the ICC protocol.

Figure 50a shows that LC3 levels were reduced in chemical-treated PAM212 cells after 6 h of stimulation. A slight downregulation was seen upon tunicamycin and oxazolone treatment while TNCB and SDS resulted in a larger reduction of LC3 protein levels. An effect of UPR inhibitors was detectable in nearly all conditions. Both the IRE-1 and the PERK inhibitor reduced the basal levels of LC3 in untreated cells. This was an effect that was repeated under all treatment conditions with the

PERK inhibitor being a little more effective in downregulating LC3 levels than the IRE-1 inhibitor. 24 h of stimulation (Figure 50b) had an opposite effect. An upregulation of LC3 levels was found in all chemicals. However, the UPR inhibitors led to varying results. While the IRE-1 inhibitor downregulated LC3 in tunicamycin and oxazolone-treated cells, it upregulated LC3 after TNCB and SDS treatment. The PERK inhibitor upregulated LC3 levels after tunicamycin and TNCB treatment. No effect was seen in oxazolone-treated cells while LC3 was downregulated after SDS treatment with a pre-incubation with the PERK inhibitor.

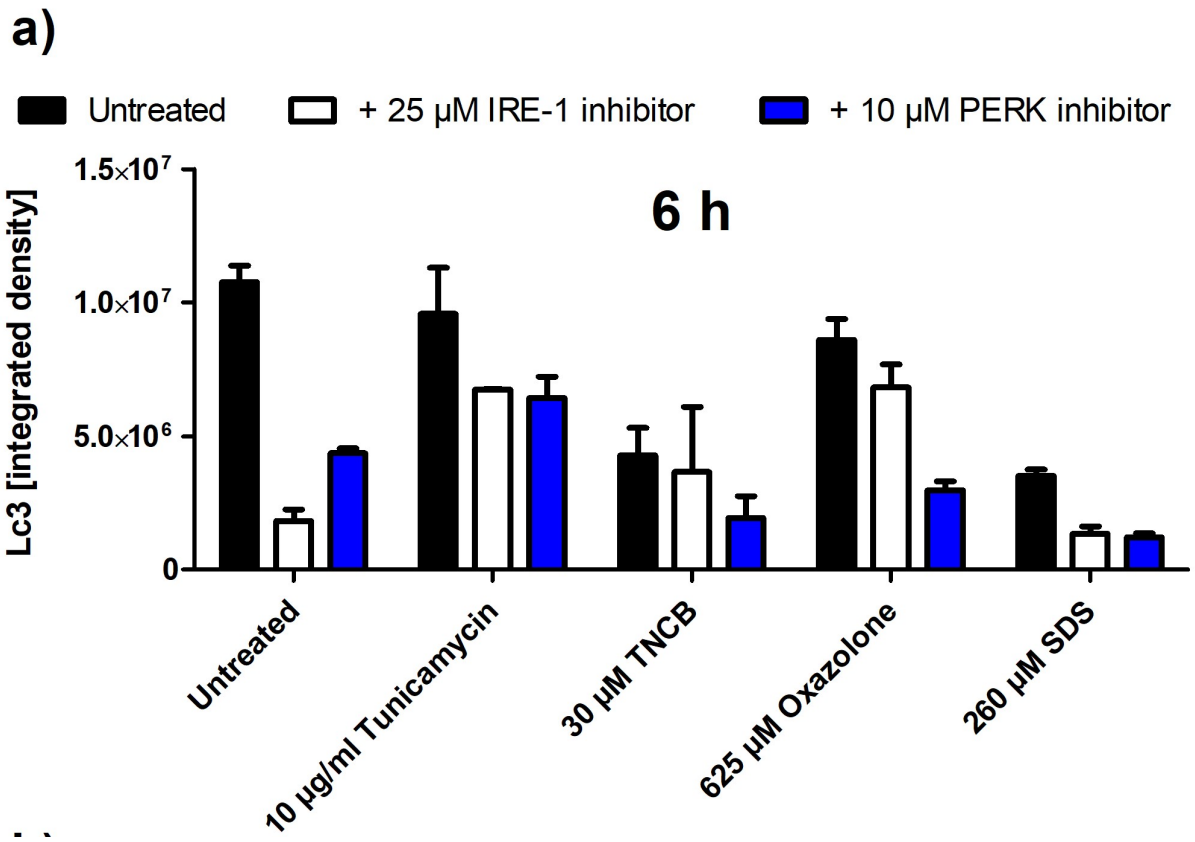

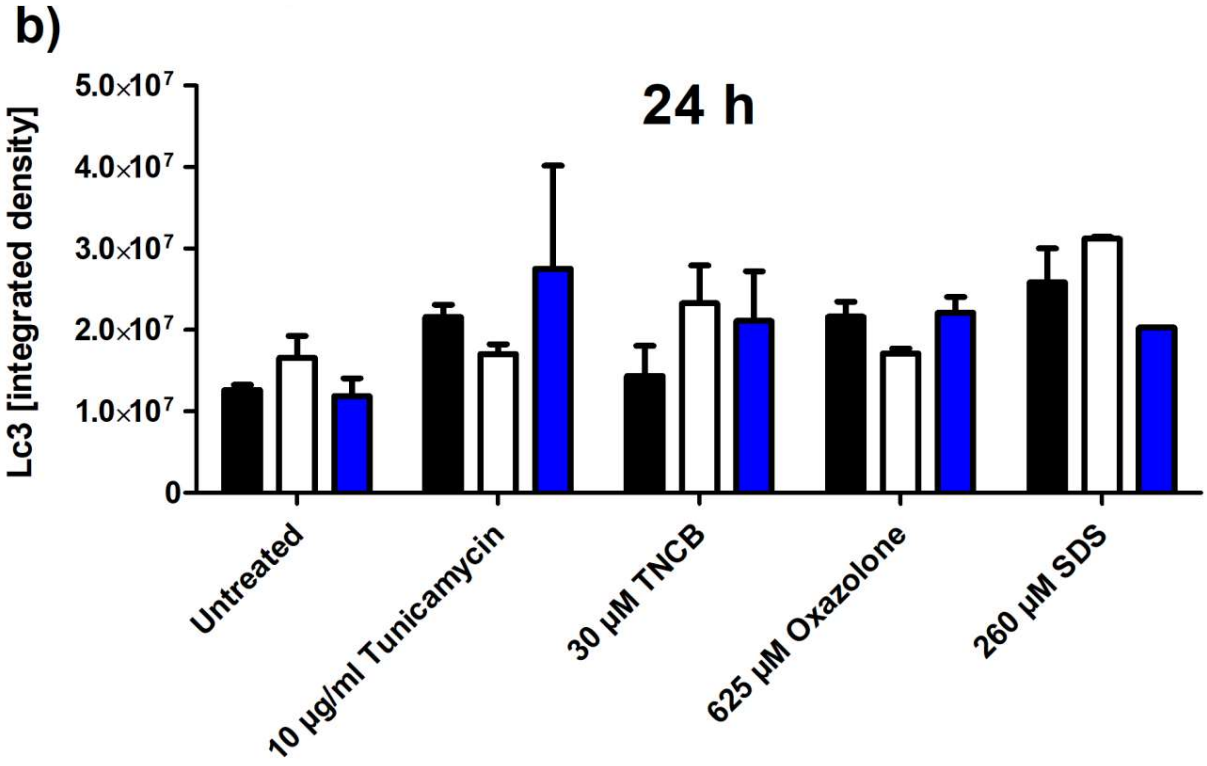

Figure 50: ICC for detection of LC3 protein in chemical-treated PAM212 cells. PAM212 cells were stimulated with tunicamycin, TNCB, oxazolone or SDS at the stated concentrations for a) 6 h or b) 24 h with or without a pre-treatment with a UPR inhibitor for 1 h. LC3 was stained as described in 7.4.1. Results are shown as mean +/- SEM of one experiment.

8.8.3 Chemicals fail to consistently induce autophagosome formation

Finally, to visualize the potential formation of autophagosomes after chemical stimulation, the MDC labeling protocol described in 7.7 was used. UPR inhibitors were once again used to analyze a potential role of the UPR in chemical-triggered autophagy.

Autophagosomes visualized as bright spots can be clearly seen in Figure 51. In comparison to the completely untreated cells the use of UPR inhibitors led to a decrease of autophagosomes in the steady state. Tunicamycin, TNCB and SDS had no effect on the number of autophagosomes. But oxazolone-treated cells showed an increased number of autophagosomes that was reduced when cells were pre-treated with either an IRE-1 or PERK inhibitor.

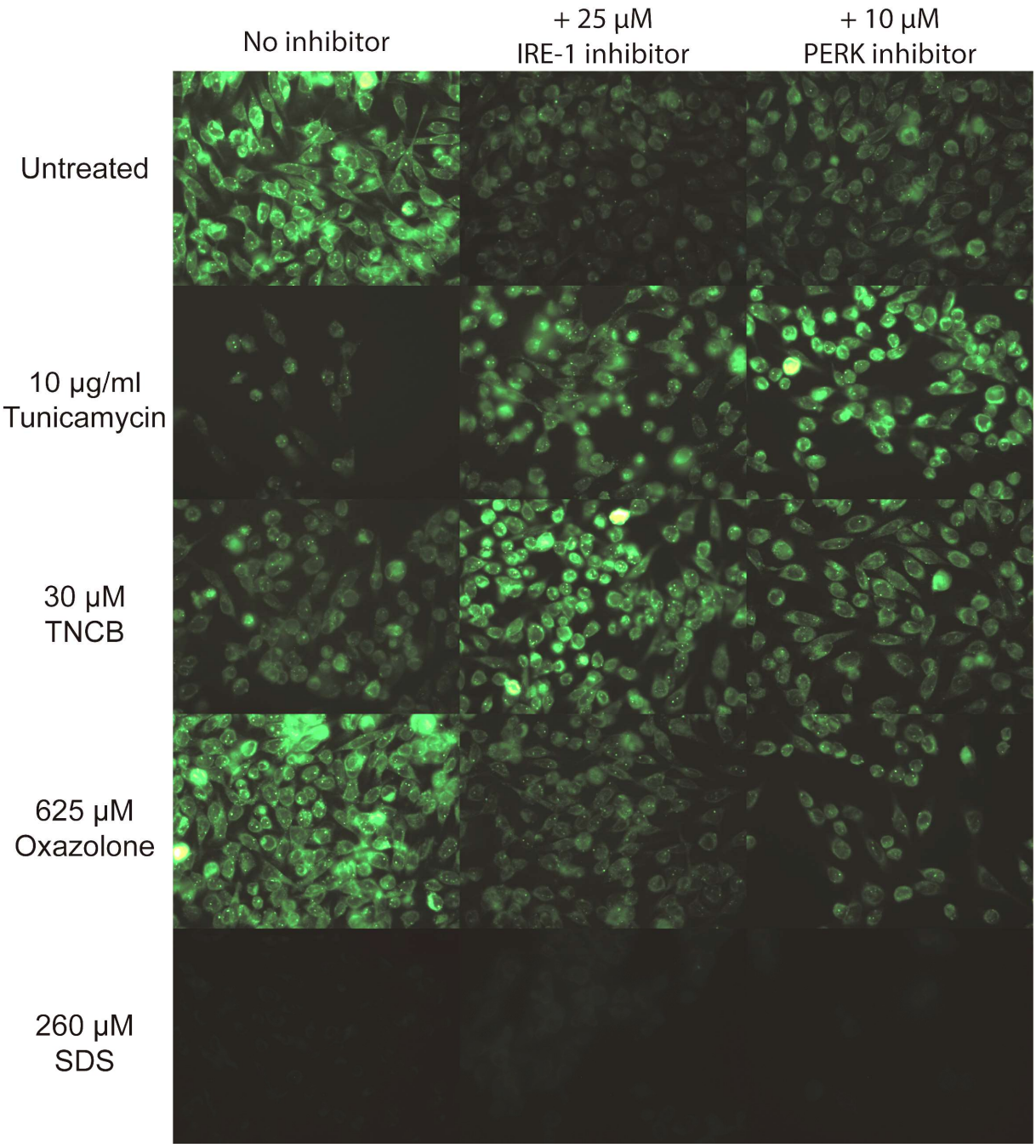

Figure 51: MDC staining of autophagosomes after chemical treatment of PAM212 cells. PAM212 cells were stimulated for 6 h with or without pre-treatment using an IRE-1 or PERK inhibitor 1 h before stimulation. Autophagosomes were stained using MDC as described in 7.7.

9 Discussion

The immune system has evolved as protection against external noxes as well as malfunctioning or mutated host cells. Although it has an elaborate selection system and is tightly regulated, unwanted reactions of the immune system can occur in different forms. These include unwanted reactions against regular host cells resulting in autoimmune diseases of different severities as well as to innocuous external molecules as seen in allergic reactions (Bartůňková, Kayserová, and Shoenfeld 2009). Almost 20% of German adults have been reported to be affected by at least one type of allergy with hay fever being at the top with a rate of 14.8% (Bergmann, Heinrich, and Niemann 2016). In this study, ACD is rated at the third place with a prevalence of 8.1%. When comparing this number with the average of different European countries, Germany has a rather low case number since a study could show that 27% of the sampled persons had a positive reaction to at least one allergen (T. L. Diepgen et al. 2016). This is not a surprising number as there are more than 4350 different sensitizers known (Parish 2010). ACD not only affects the patients but also has a major economic impact as it is the second-most common occupational skin disease. Up to this date, there is no causative treatment option for patients since the development of the disease is not fully understood. The only relief is a symptomatic treatment including corticosteroids, nonsteroidal anti-inflammatory drugs and the avoidance of the sensitizer. However, this often comes at a cost for the affected patients as an avoidance of the sensitizer is equivalent to an occupational ban if they are sensitized to a substance commonly used at their job (Qin and Lampel 2015).

Therefore, uncovering the mechanisms underlying the development of ACD is an important goal not only for the treatment of already sensitized patients but also to discover means of prevention for workers in many different fields ranging from health care professionals to food producers and metal workers. In addition, knowledge of the underlying mechanisms could aid the development of *in vitro* assays for the evaluation of potential sensitizers in the ongoing replacement of animal testing in the cosmetics industry (Esser and Martin 2017).

9.1 Contact sensitizers activate all three branches of the UPR

The working theory behind this thesis was that contact sensitizers induce an accumulation of un-/ or misfolded protein through conformational changes due to the formation of hapten-protein complexes or protein oxidation by ROS induced by sensitizers (Esser et al. 2012; Stefan F. Martin 2012). This could then lead to an activation of the UPR, a stress response responsible for the protein homeostasis of the cell. In earlier work, an activation of the IRE-1 and the Atf6 branch of the unfolded protein response after sensitizer treatment was shown in a variety of cell types including different skin cells as well as cells of the immune system (Gendrisch 2012, 2015). To conclude the analysis of all branches of the UPR, the signs of PERK branch activation were confirmed by looking at the phosphorylation of PERK after the stimulation of PAM212 keratinocytes with different chemicals. Treatment of these cells led to an increase of PERK branch activation as visualized by the increased intensity of the stained pPERK after the stimulations (Figure 19 and Figure 20, Gendrisch et al. submitted). Interestingly, TNCB was the strongest activator of the PERK branch. This stands in contrast to the results of the IRE-1 branch where oxazolone was a potent activator while TNCB was rather weak in activating the *Xbp-1* splicing (Gendrisch 2015). The activation of the UPR by a sensitizer has been shown by other groups as well (Luís et al. 2014). However, the authors of the study only showed an activation of the PERK branch in THP-1 cells after stimulation with the extreme sensitizer DNFB. In contrast, our group was able to show the activation of all three branches of the UPR in a variety of different cell types including human and murine skin and immune cells. A difference in the potential of sensitizers to activate certain branches of the UPR more than others is not surprising due to the chemical diversity of the more than 4.000 sensitizers which may not all react in the same manner. It will be interesting to see if the differential activation of the UPR branches may be a differentiator of sensitizers of different potencies. In addition, the activity might not be different at one time point but sensitizers could have different temporal dynamics in activating the UPR owing to their potency and toxicity (Walter et al. 2015). This differential activation could be a potential starting point for an *in vitro* assay to determine the sensitizing potency of a chemical. Unfortunately, a specific activation pattern of the UPR for sensitizers of a particular potency could not

be detected with the limited number of chemicals analyzed up to now. Interestingly, there have been and are still ongoing efforts by other groups trying to use a specific property of chemicals, including their protein reactivity (Wareing et al. 2017) or structure-activity relationships (Aptula, Patlewicz, and Roberts 2005), to group them in different sub-classes reflecting their potency . However, none of these approaches has been found to be the optimal solution to the problem. In addition, not only contact sensitizers are able to activate the UPR. An example often used in this thesis is SDS, an irritant found in many every-day products like shampoo or tooth paste. Solely relying on the activation of the UPR would label SDS a sensitizer which is not the case.

Since the UPR was activated by contact sensitizers it was not far-fetched to think of it as a target point for the treatment of ACD. *In vivo* studies using inhibitors for the IRE-1 and the PERK branch in the murine model for ACD, called CHS, were used to test this (Gendrisch et al. submitted). The inhibitors were applied systemically either before sensitization or elicitation of CHS. By using this approach, a role of the UPR limited to one phase of the CHS would be detectable. Interestingly, the inhibition of only one UPR branch either before sensitization or elicitation was enough to reduce the CHS response nearly back down to the level of mice receiving only a single treatment with the sensitizer showing the irritant effect of the chemical. However, one might argue that the reduced CHS response arises from the fact that the UPR plays a pivotal role in different types of immune cells including cells responsible for the development of the CHS like DCs (Iwakoshi, Pypaert, and Glimcher 2007) and inhibition of this stress response would simply have negative effects on these cells rendering them useless. This thought can be rebutted by the additional use of the chemical chaperones 4-phenylbutyric acid (4-PBA) and tauroursodeoxycholic acid (TUDCA). Both of them are able to reduce ER stress by aiding the proper re-folding of un- or misfolded proteins, therefore inhibiting the UPR without a direct effect on it (Engin and Hotamisligil 2010). As both substances were able to cause a reduction of CHS responses it becomes obvious that the effect that inhibits the CHS is not the total block of immune cell function by shutting down the UPR, because that does not happen in chaperone-treated animals. In these settings, there is no increased UPR activation as there is no ER stress due to the increased folding of proteins caused by 4-PBA and TUDCA. These substances have no direct effect on the UPR, yet the outcome remains the same. Therefore, it seems that the effect seen in the UPR

inhibitor-treated animals is caused by the reduction of the sensitizer-mediated UPR activation and not a malfunction of immune cells.

9.2 The sensitizer-induced UPR activates the NF-κB pathway

What remains unknown to this point is the mechanism by which the UPR is responsible for the activation of CHS responses and how the inhibition of said pathway leads to a reduction of the CHS. As mentioned in the introduction, the UPR has been shown to play an important role in many parts of the immune system including inflammation (Grootjans et al. 2016). A pro-inflammatory function of keratinocytes caused by the UPR would be helpful for the establishment of a pro-inflammatory micromilieu that is needed for the full activation of the innate immune system during the sensitization phase of the ACD (Esser and Martin 2017). One important pro-inflammatory pathway that comes to mind when talking about pro-inflammatory processes is NF-κB. The role of all three branches of the UPR in the activation of NF-κB have been discovered some time ago (Jiang et al. 2003; Hu et al. 2006; Yamazaki et al. 2009). Therefore, the idea was to analyze a potential activation of the NF-κB pathway after the treatment of keratinocytes with different chemicals. This was achieved by looking at the nuclear translocation of the p65 subunit of NF-κB, a crucial step in the way of NF-κB to activate target gene expression. To analyze if sensitizer treatment induces NF-κB activation in keratinocytes, PAM212 cells were treated with different chemicals for 1 h. To address the question of a potential role of the UPR in this process, an additional pre-incubation with either an IRE-1 or a PERK inhibitor was included. The results of the p65 staining showed an increase of cells lacking a nuclear shadow in the p65 staining. This effect could be reduced by the pre-treatment with a UPR inhibitor. The quantification of cells with increased nuclear p65 (Figure 22 and Figure 23, Gendrisch et al. submitted) revealed a strong induction of the NF-κB activation. With the use of the UPR inhibitors the ability of the UPR to activate NF-κB signaling after sensitizer treatment of keratinocytes was confirmed in this setting as inhibitor pre-treatment led to a reduction of nuclear p65+ cells nearly back down to the level of untreated control cells. Interestingly, Luis et al. could show that THP-1 cells did not show increased nuclear translocation of p65 after the stimulation with the sensitizer DNFB (Luís et al. 2014). The lack of increased translocation might arise from the fact that they chose the wrong time points. Their

shortest duration was 1 h of stimulation before the analysis. This works for keratinocytes as seen in this work, however other cells react much quicker with a maximum of translocation after as short as 15 min (Schichl et al. 2009). One might argue that the nuclear translocation of p65 is not a sufficient proof for the activation of the NF-κB pathway. These concerns can be invalidated by an experiment where PAM212 cells were transfected with a plasmid carrying a gene coding for luciferase under the control of a NF-κB response element (Gendrisch et al. submitted). Using this system, an actual induction of gene expression by NF-κB can be detected by adding the substrate for luciferase resulting in a luminescence signal if NF-κB is transcriptionally active leading to luciferase synthesis. The treatment of the reporter cells with our set of chemicals led to an increased luminescence signal visualizing the actual transcriptional activity of NF-κB. Interestingly, pre-treatment of these reporter cells with UPR inhibitors led to a decreased activation of NF-κB complementing the results of the p65 staining complementing the results of the p65 staining and fitting a study showing that inhibition of PERK in cancer cells was able to reduce NF-κB activity (Fan et al. 2018).

Due to these effects, targeting the activation of NF-κB signaling would also be an interesting option for the treatment of ACD. Interestingly, a study on atopic dermatitis, another inflammatory skin disease, achieved good results using NF-κB decoy oligonucleotides in a topical application on the skin (Dajee et al. 2006). However, potential effects on the defense against infections in decoy-treated skin were not discussed. Shutting down a key element of pro-inflammatory responses could lead to a decreased protection against pathogens invading the skin as NF-κB inhibition acts as a partial immunosuppression (Sha et al. 1995).

The next step following the activation of pro-inflammatory pathways like NF-κB is the induction of target gene expression. These genes include important mediators of the immune system like cytokines. Examples for well-known targets genes of NF-κB are *Il-1α, Il-1β, Ifn-γ* and *Tnf* (Pahl 1999). Since the last experiment (Figure 22 and Figure 23) could show a role of the UPR in inflammatory pathway induction it is very well conceivable that a result of the NF-κB activation might be the increased expression of genes coding for pro-inflammatory cytokines. A recent review by Judith A. Smith described different effects the UPR can have regulating cytokine production in infection or diseases (J. A. Smith 2018). To analyze a potential induction of NF-κB target gene expression, PAM212 keratinocytes were treated with the usual set of

chemicals and the expression of different known NF-κB target genes as well as additional genes coding for pro-inflammatory cytokines was examined using qPCR. However, the results could not deliver a conclusive response to the question if the sensitizer-induced UPR led to an increased pro-inflammatory gene expression. The results (Figure 24 and Figure 25) of some cytokines show a tendency towards the expected outcome after the p65 staining. None of the cytokines achieved any significance in their changes of gene expression. The logical conclusion from the p65 experiments would have been an increased cytokine expression after the stimulation and the inhibition of UPR-induced cytokine expression using UPR inhibitors as it has been shown before in the setting of pathogen-mediated UPR activation (Keestra-Gounder et al. 2016, 1).

9.3 The UPR-induced NF-κB pathway leads to the release of pro-inflammatory cytokines in immortalized NHKs and HaCaT cells

As the gene expression analysis was not successful and increased gene expression is not necessarily linked to an increased protein synthesis and cytokine release (Vogel and Marcotte 2012), we turned to the analysis of the synthesis of the actual cytokine using ELISA. The effect of the UPR-mediated inflammation might not arise from an increased gene expression but from increased pro-inflammatory cytokine synthesis of the same amount of mRNA. PAM212 cells were treated with the known chemicals for 24 h or 48 h as these are the most common treatment durations when looking for cytokine production. Cytokine levels were analyzed in the cell culture supernatant to concentrate only on the cytokines actually released by the cells, as some are already synthesized in steady-state cells.

Interestingly, besides IL-1α, no cytokine was consistently released in detectable amounts after 24 h and 48 h (Figure 26 and Figure 27). IL-1α release however was following a similar pattern as the p65 translocation and the gene expression analysis showing an increase of cytokine release after treatment with the different chemicals. Looking at the result of IL-1α levels one has to keep in mind that keratinocytes are producing large amounts of the precursor form of IL-1α in the steady-state (Mosley et al. 1987). Therefore, the cytokine found in the supernatant might not be the result of actual processing and active release of IL-1α as an inflammatory response but might be due to an increased cell death occurring after the chemical treatment since up to

20% cytotoxicity were accepted during the finding of the concentrations used for stimulation (Gendrisch 2015). This has been observed before (Hogquist et al. 1991; England et al. 2014) and might be also the case here since it cannot be ensured that the antibodies used for the ELISA reliably only detect the processed form of IL-1α. This is based on previous observations showing that even the precursor form of Il-1α possesses biological activity (B. Kim et al. 2013, 1) and might therefore contain the epitope which is recognized by the ELISA antibodies.

PAM212 cells seem to be an unsuitable cellular model for the detection of cytokine expression and release in the setting tested here. One cause of these problems might be a defect in cytokine synthesis and release. Looking in the literature, it is hard to find studies looking at cytokine levels in PAM212 cells. Interestingly, most of the studies using Pam212 cells to look at cytokines work in some context of IL-1α (Mee et al. 2005), the only cytokine detected in this work. The analysis of other cytokines is rarely seen and if there is some data the levels found are close to the detection limit of the ELISA used (Yun and Li 2010) or the assays to determine the release are prone to external influences (Matsue et al. 1992).

Therefore, the next step was to find an alternative cell line for the continuation of the experiments. NHKi cells were the next cells to be analyzed. These cells were chosen to switch from murine to human cells and in addition these cells were as close to primary cells as one can get when not using primary cells. As there was no preliminary data on these cells, initial test experiments were performed to see if NHKi cells are suitable for further use. Primarily, a functional UPR was of importance. Therefore, NHKi cells were treated with the same concentrations of chemicals used for PAM212 cells and the activation of the IRE-1 and PERK branch of the UPR were analyzed. Both pathways were activated as visualized by the splicing of *XBP-1* and the increased expression of *CHOP* (Figure 28 and Figure 29). The next step was to directly look at the cytokine expression of these cells. IL-6 was the cytokine of choice for the analysis as is has been shown to be an important pro-inflammatory cytokine of the skin (Paquet and Piérard 1996). NHKi cells were treated with increasing concentrations of the usually used chemicals for 24 h and the release of IL-6 into the cell culture supernatant was measured. As seen in Figure 31, the cytokine production induced by the tested chemicals was rather limited with the exception of SDS. Of notice, an increase of cytokine release in SDS-treated cells came with an increase in cytotoxicity over the level usually targeted with 20% (Figure 32). Therefore, an effect

of the toxicity itself on the release of cytokines cannot be excluded. Tunicamycin treatment also led to a significant increase of IL-6. However, the question remains if an increase from 3 pg/ml to 10 pg/ml has any biological relevance. Taken all together, NHKi cells have turned out to be limited in their use for the analysis of cytokine release as they are only released when using concentrations of chemicals causing cytotoxicity beyond the set limit. In addition, primary keratinocytes have been shown to lack a prominent cytokine production when the stimulation is adjusted to limited levels of cytotoxicity as they need more stress and cell death to produce cytokines (Newby et al. 2000).

The last cells to be tested were HaCaT cells, a human keratinocyte cell line widely used in dermatological research. Just like with the NHKi cells, the HaCaT cells were tested for their UPR activity after chemical treatment. HaCaT cells showed a robust induction of *XBP-1* splicing after 6 h of treatment (Figure 33, Gendrisch et al. submitted). As the cells reacted adequately to stimulation, the cytokine production was the next step to be assessed. After stimulation for 24 h HaCaT keratinocytes produced detectable amounts of IL-6 (Figure 34, Gendrisch et al. submitted). In addition, these cells also reacted with increased IL-6 levels to the stimulation with the usual chemicals. As the nuclear translocation of p65 and the transcriptional activity of NF-κB were shown to be dependent on the UPR, the same was confirmed for the release of IL-6 with the use of UPR inhibitors (Gendrisch et al. submitted).

9.4 Keratinocytes activate DCs in an UPR-dependent process

HaCaT cells were able to produce pro-inflammatory cytokines upon stimulation with different chemicals. These cytokines might contribute to the pro-inflammatory micromilieu needed in the skin to get a full activation of DCs (Esser and Martin 2017). However, it remains unclear if the cytokine production by keratinocytes alone is enough to create the micromilieu leading to an activation of DCs or if other cells take part in this process. To address this question, one has to think about the mechanisms underlying ACD and the location they take place. Contact sensitizers enter our body through the skin. The first point to address is the penetration depth of sensitizers into the skin. A recent proof-of-concept study by Malmberg and colleagues (Malmberg et al. 2017) using imaging mass spectrometry could show that nickel is hardly entering the epidermis after 24 h of incubation on human skin

samples. The results showed that nickel ions were only detectable to a depth of 25 – 30 µM into the skin. Thinking about the composition of the epidermis, most cells found in this layer of the skin are keratinocytes. The other cell type often mentioned are Langerhans cells, an APC that was long time thought to be a sub-type of DC but is recently more and more being labeled as a sub-type of macrophage (Doebel, Voisin, and Nagao 2017). Langerhans cells are taking up antigens in the skin; however, their role in the development of the ACD and CHS is controversial. While some studies show no role for Langerhans cells in CHS (Honda et al. 2010; Noordegraaf et al. 2010) others paint a picture of the CHS-suppressing Langerhans cell (Igyarto et al. 2009). Besides Langerhans cells, CD8+ T cells can also be found in the epidermis (Nestle et al. 2009). However, these cells need activation by APCs and therefore play no role in the first phase of ACD development. In addition, γδ T cells can be found in the epidermis (Cruz et al. 2018). These cells have been shown to play a role in CHS due to their production of IL-17 and other cytokines that is partially dependent on NKG2D ligands (Nielsen et al. 2014, 2015) that can be expressed by stressed keratinocytes (Komori et al. 2012) and might therefore contribute to the pro-inflammatory micromilieu.

As it has been shown that HaCaT keratinocytes can increase the sensitizer-induced activation of THP-1 DCs (Hennen and Blömeke 2017) the goal was to analyze the capability of HaCaT cells alone to activate THP-1 cells in the absence of the sensitizer. An initial comparison of different stimulation methods for THP-1 cells showed that the treatment of THP-1 cells in monoculture led to an increased expression of CD54 and CD86 (Figure 35). The same results for CD86 have been found for the stimulation using DNFB (Luís et al. 2014). However, the activation status was higher when the THP-1 cells were either stimulated in the presence of HaCaT cells (COCAT) (Hennen and Blömeke 2017) or when they were co-cultured with sensitizer-treated HaCaT cells after removing the sensitizer (COCAHS). Carrying on with the COCAHS experiment, the use of UPR inhibitors before the stimulation of the HaCaT cells was again able to show the involvement of the UPR in the keratinocyte-mediated activation of DCs. While the inhibitors had no effect on the HaCaT-induced CD54 expression, CD86 levels were downregulated after the pre-treatment of the HaCaT cells with the inhibitors (Figure 36, Gendrisch et al. submitted). These results show that activated keratinocytes alone are able to activate DCs even in the absence of an antigen. In addition, this process seems to be highly

dependent on a functional UPR as the use of specific inhibitors was able to reduce the CD86 expression. The lack of downregulating CD54 can be neglected in this case as CD86 is the one responsible for an efficient Th1 response (Lenschow et al. 1995) and inhibition of CD86 should therefore be enough to inhibit a T cell response after sensitizer treatment. The most obvious mechanism of the activation of the DCs by keratinocytes is the production of pro-inflammatory cytokines, in this case IL-6. This contactless mode of activation has also been seen in the co-culture setting by Hennen and colleagues (Jenny Hennen et al. 2011). A hypothesis about this kind of interaction was already proposed about 50 years ago.

Taken together, these results suggest a crucial role of the UPR in sensitizer-exposed keratinocytes in the ACD. In these cells, the UPR is initiated upon a potential ER stress induction by protein mis- or unfolding caused by sensitizers. The activated UPR then leads to an induction of the NF-κB pathway causing to the production of the pro-inflammatory cytokine IL-6. Using the COCAHS assay, keratinocytes have been shown to activate DCs even in the absence of sensitizers. This leads to the over-all idea, that keratinocytes in the development of the ACD are activated by sensitizers in the epidermis. The activated keratinocytes then produce cytokines leading to the full activation of DCs that sensitizers alone are not able to trigger (Esser and Martin 2017). This might also be the point where the unclear role of LCs in ACD is decided as the keratinocyte-derived cytokines might be required to switch these cells to a pro-inflammatory state. Together with dermal DCs that might get activated by antigens penetrating into the dermis in collaboration with keratinocyte-derived cytokines, these cells then migrate to the skin-draining lymph nodes.

9.5 Combinations of weak sensitizers mimic the effects of strong sensitizers

Up until here, the sensitizers that were used are counted among the group of strong sensitizers and are usually not found outside of laboratories. The most common sensitizers are ranked in lower potency classes (Loveless et al. 2010). Patients come into contact with these substances during their every-day life. The most common contact point is the use of cosmetics and cleaning products where in most cases a variety of different sensitizers is found. Out of fear of chemicals in their cosmetics product, many people turn to natural or organic cosmetics believing that they will be free of sensitizers which they often associate with industrial, synthetic chemicals.

This may be the case for some sensitizers like preservatives (Loeffel 1972). However, the truth is that many sensitizers will also be present in natural cosmetic products as for example most fragrances are found in a variety of plants and plant extracts (Avonto et al. 2016). Therefore, the contact to the same sensitizer may happen both in the form of the isolated substance in a cheaper cosmetics product as well as in organic natural cosmetics due to the use of essential oils containing the fragrance. In contrast to strong sensitizers, the use of these known weak sensitizers in every-day products is not prohibited as they pose a lower risk of sensitization. However, in products containing many different weak sensitizers, the possibility to be sensitized is increased. Different studies have found that combinations of different weak sensitizers lead to a synergistic effect in the development of the ACD (Johansen et al. 1998; Bonefeld et al. 2011) allowing an easier sensitization.

The goal of the next experiments was to find out where this synergistic effect originates from. In an initial experiment, a variety of weak sensitizers were tested for their ability to activate *Xbp-1* splicing in PAM212 keratinocytes. Different concentrations for each sensitizer were used, but none of the tested conditions led to any significant change of *Xbp-1* splicing (Figure 37). To follow up on the studies describing the synergistic effect of weak sensitizers in combination, a combination of two weak sensitizers was analyzed for its activity to induce *Xbp-1* splicing. In this setting, weak sensitizers alone were again not able to induce any increase of splicing. Interestingly, the combination of two weak sensitizers did achieve just that, fitting right into the previously found combinatorial effect (Figure 38). The increase of UPR activation was also not due to an increase of cytotoxicity as seen in Figure 39. When analyzing the mode of action of stronger sensitizers, an activation of the NF-kB signaling pathway was seen in treated keratinocytes. Therefore, the same analysis was performed on the combinations of weak sensitizers. Interestingly, the weak sensitizers alone did not lead to an increased nuclear translocation of p65 (Figure 40). However, an effect is seen when combining two of the weak sensitizers. This fits into the findings, that combining sensitizers leads to an increased potency (Bonefeld et al. 2011) as the combination of two weak sensitizers had a similar effect on the p65 translocation as the stronger sensitizers used before. It is a little surprising that the combinations containing eugenol are more effective in increasing the nuclear p65 levels than the combination of cinnamaldehyde and resorcinol. There was no higher effect of eugenol on the *Xbp-1* splicing and the viability seemed to be higher than in

untreated cells. In addition, the antioxidant and anti-inflammatory effects of eugenol have been widely described (Yogalakshmi, Viswanathan, and Anuradha 2010; Huang et al. 2015) leading to the expectation that eugenol should rather limit the nuclear translocation of p65. However, the increase of viability measured by the increased metabolism in the MTT assay after eugenol treatment hints towards increased proliferation of PAM212 cells after eugenol treatment. This fits to the increased p65 translocation of six percentage points in eugenol-treated cells as the NF-kB pathway has been shown to control proliferation of epithelial cells (Brantley et al. 2001).

9.6 Weak sensitizers in combination with SDS act like strong sensitizers

In addition to the combinations of different weak sensitizers one has to also consider the combination of weak sensitizers with irritants. Irritants, just like sensitizers, are found in many every-day products (Walker et al. 1997) owing to their variety of useful properties. One of the most known sensitizers is SDS. SDS can be synthesized but also extracted from natural oils like coconut or palm oil in the form of sodium coco sulfate. It is used as a detergent in cleaning products and also found in shampoos, body washes and tooth paste due to its foam-creating abilities. Different concentrations of SDS were tested in combination with a variety of weak sensitizers (Figure 42). Looking at the cytotoxicity results, 200 µM of SDS was chosen for further use. Again, the first step in evaluation of weak sensitizer/SDS combinations was the splicing of *Xbp-1* mRNA in PAM212 cells. In addition, TNCB was included into this set of experiments as former work showed that despite being a strong sensitizer TNCB showed much weaker responses in the UPR and pro-inflammatory pathways than expected from a strong sensitizer. The weak sensitizers alone had no significant effect on the splicing of *Xbp-1* (Figure 43). SDS used alone also showed an increase that was not significantly different from untreated cells. Theoretical results of an additive effect were included into the graph as a point of reference. Interestingly, the actual experimental results exceeded the additive effect and led to a splicing of *Xbp-1* beyond this level. Looking at the splicing induced by strong sensitizers, the SDS/weak sensitizer combinations are well within the same area. Going one step further, the p65 nuclear translocation was again used to test for the activation of NF-κB (Figure 44). In this experiment all tested substances had either no or a very minor

effect not even close to being significantly different in comparison to the untreated control when used alone. Therefore, an additive effect would have no effect on the nuclear translocation as well. However, this was not the case. Combining the weak sensitizers with SDS led to an increase of cells with nuclear p65 translocation in the same range that was seen with the strong sensitizers (Figure 45). These results are in line with findings of other studies. It was shown that adding SDS can increase the potency of a single sensitizer leading to a sensitization not seen when the sensitizer is used alone (Watanabe et al. 2008). In addition, a synergistic effect of the combination of SDS with nickel was found when challenging already sensitized patients (Agner et al. 2002). These are also important findings when thinking of the cosmetics industry. The usage of weak sensitizers in cosmetics or cleaning products is not prohibited but limited when it comes to the amount of sensitizer that is allowed to be used (Boss et al. 2015). However, these limits must consider the combinatorial effects the have been shown many studies including this thesis. As mentioned earlier, an idea was to use the activation of the UPR and the subsequent inflammatory response as a potential *in vitro* assay for the assessment of sensitizers. Generally speaking, weak sensitizers were not able to induce increased *Xbp-1* splicing and the nuclear translocation of p65, therefore offering potential for assay development. However, results have not been able to show a consistent pattern in activating the UPR and pro-inflammatory pathways for weak and strong sensitizers. TNCB, a sensitizer classified as strong, underperforms at activating the p65 nuclear translocation while eugenol was the strongest of all tested sensitizers in this respect. In addition, SDS as an irritant showed a similar reaction. Therefore, in a blinded test SDS would not be distinguishable from sensitizers using the UPR activation and p65 translocation as assays.

9.7 *C. elegans* as a reporter system for potential sensitizers

Testing of sensitizers for their UPR-activating abilities is a time and material-consuming process. Cells have to be cultured by regularly passaging them and renew the culture medium. Afterwards, cells have to be treated with the chemicals followed by the time-consuming isolation of the RNA in the case of *Xbp-1* splicing. cDNA has to be synthesized and the PCR with *Xbp-1*-specific primers has to be performed. This is followed by the separation of the PCR products on an agarose gel

and analyzing the results. The PERK branch is analyzed either by qPCR taking up nearly the same time as seen with the IRE-1 branch. Another possibility is the immunocytochemical staining of pPERK also taking up a lot of time. However, the analysis is very important as the many effects of the UPR have shown. As an alternative, a *C. elegans* reporter strain was used to analyze sensitizer-induced UPR activation. The used strain is called hsp-4::GFP and is characterized by an induction of GFP expression when the protein hsp-4, the homolog of the mammalian BiP, is expressed. The advantage of this method is that the whole process consists of culturing the animals, treatment and evaluation under the microscope. This leaves room for other experiments and is an easy readout without the need for further processes like PCR.

To test the animals, they were treated with different concentrations of a variety of sensitizers and SDS as an irritant. After 48 h the animals were evaluated under the microscope and pictures were taken for additional analysis (Figure 46). Just like with the analysis of the cells, there was no clear result concerning the potency of the used sensitizers (Figure 47). While strong to extreme sensitizers led to no or only minor increased GFP expression, weaker sensitizers like nickel (II) sulfate led to a greater expression.

However, this was just an initial experiment and further evaluation has to show if *C. elegans* reporters can be used as quick screening model for research of the UPR as it has already proven its high value in toxicity assessment (Hunt 2017; Xiong, Pears, and Woollard 2017). The process can be stepped up even more when using a variant of FACS called live animal FACS (laFACS) that allows for a high-throughput analysis of over 100000 animals per hour (Fernandez et al. 2010). This also allows for the use of the many different reporter animals that are commercially available to analyze the role of each UPR branch separately as the analysis is sped up a lot. The optimal solution would be the use of animals with different reporter constructs leading to the expression of different fluorescent proteins for each branch of the UPR to evaluate the expression within one animal. In addition, there are other animal reporter models that would be of potential use for the analysis of the UPR. ERAI mice expressing GFP upon the activation of the IRE-1 branch of the UPR (Iwawaki et al. 2004) enable the analysis of the UPR in the mammalian setting. As the reporter is present in all cells, the effect of the UPR can be analyzed in different tissues and organs using modern methods like FACS with focus on different diseases or processes of interest.

Another method that would allow for an easy read-out of the UPR activity would be the generation of an enzyme-based reporter system. For example, cells expressing horseradish peroxidase (HRP) under the promotor of a certain UPR gene could be used to quantify the UPR activity in a similar reaction as used for ELISA showing the differences in a change of color (Porstmann et al. 1985). However, all these methods using different species could be used equally to answer the general question of the UPR activation as the UPR is evolutionary highly conserved with homologs of the same proteins being found in mammals as well as in the nematode C. elegans (Hollien 2013). This allows for comparisons and transfer of knowledge of the UPR itself while downstream pathways have to be evaluated separately as they might differ in different species.

9.8 Interaction of a sensitizer-triggered UPR and autophagy

Up until here, a clear role for the UPR in the development of CHS and ACD was established. Another stress response of cells that has gained more attention recently is autophagy. The Nobel prize awarded to Yoshinori Ohsumi in 2016 for his work on autophagy brought attention to this important process used for the recycling of cellular components after stress induction (He and Klionsky 2009). In addition, a variety of functions in the immune system were discovered including its role in humoral immune responses (Arnold et al. 2016) as well as inflammation (Lapaquette et al. 2015). As there is also a tight connection between the UPR and autophagy (Deegan et al. 2015; Vidal and Hetz 2012), a potential role during CHS or ACD development is not far-fetched.

The initial experiment was therefore to look for modulated autophagy gene expression after sensitizer treatment of keratinocytes. There was no clear pattern visible as some genes were induced in contrast to others being inhibited after 6 h of treatment (Figure 48). The use of UPR inhibitors to analyze the potential involvement of the UPR in autophagy gene regulation was not successful as it gave inconclusive results. A test with a longer treatment period gave another inconclusive result (Figure 49). Therefore, further analysis of optimal time points and treatment doses was necessary and this part of the project was carried on by Max Sauerland for his bachelor thesis under my supervision and Theo Metzger for his master thesis. However, both could not find any significant changes of autophagy gene expression after the treatment of different skin cells with sensitizers or a role of the UPR in their

experiments including extensive dose titrations and time kinetics with the exception of tunicamycin. This is also the most used chemical in studies looking for the connection between the UPR and autophagy. For example, a study by Deegan and colleagues (Deegan et al. 2015) showed the increase of *Nbr1* expression after tunicamycin treatment. As we have seen an activation of the UPR by oxazolone in a similar strength as tunicamycin there remain open questions about the exact mode of action by which the UPR is activated possibly leading to a different effect on autophagy. Looking for LC3 levels was the next step in analyzing autophagy. LC3 is a key molecule in autophagy as a part of the formation of the autophagosome (Tanida, Ueno, and Kominami 2008). However, results of the experiment were not able to show a clear involvement of the sensitizer-induced UPR in autophagy (Figure 50). Finally, the autophagy was to be analyzed using MDC to stain autophagosomes (Munafó and Colombo 2001). The autophagosomes should then appear as bright spots under the microscope and can be used as an indicator for the activation of autophagy (Figure 51). The results were very inconclusive as only oxazolone caused a UPR-dependent increase of autophagosomes in comparison to the control.

All these results stand in contrast to many studies showing a clear regulation of autophagy by the UPR (Vidal and Hetz 2012; Senft and Ronai 2015b; Høyer-Hansen and Jäättelä 2007). In addition, a role of autophagy in allergic disease has been shown (J.-N. Liu et al. 2016). One reason for the non-matching results might be that autophagy is also tightly linked to the activation of the inflammasome (Saitoh and Akira 2016) , especially in the setting of environmental stressors like metal ions (R.-J. Chen et al. 2016). A role of the inflammasome in CHS has been shown by different studies (Sutterwala et al. 2006; Weber et al. 2010) but always linked to innate immune cells. As the keratinocytes used for most of the experiments in this work lacked an activation of the inflammasome as visualized by the lack of IL-1β production, it might be that the autophagy was examined in the wrong cell type. But the immune system is not only dependent on the inflammasome. For example, autophagy is also able to induce the release of IL-6 (Harris et al. 2011), another pro-inflammatory cytokine. As the results of this work could show an increased autophagy after 24 h visualized by the increased gene expression (Figure 49) and LC3 levels (Figure 50), a potential role in the increased release of IL-6 by HaCaT cells (Figure 34) is conceivable. Another important function of autophagy is the regulation of cell death. This might also play an important role during the sensitization

phase of the ACD. The creation of a pro-inflammatory micromilieu in the skin has been shown to be of importance for the development of the ACD as a full activation of the innate immune system needs further stimuli besides the contact sensitizer alone. Immunogenic types of cell death have been linked to autophagy (Michaud et al. 2011; Ko et al. 2014) and the release of DAMPs caused by these autophagy-mediated processes might contribute to the formation of this micromilieu in addition to the cytokines released by keratinocytes. This could also be a point to analyze for differences concerning weak and strong allergens. Weak sensitizers might not be able to induce autophagy leading to a lack of the pro-inflammatory micromilieu partially created by the autophagy.

9.9 Summary and conclusion

Taken together, all results of this work point towards an important role of the UPR in CHS. Keratinocytes, as the first cells to come into contact with the penetrating sensitizer, show an active inflammatory response as characterized by the nuclear translocation of the p65 subunit of NF-κB and the release of IL-6. This process is linked to the induction of the UPR as the use of specific UPR inhibitors was able to reduce the activation of the NF-κB pathway and the release of IL-6. This IL-6 might be one of the key players in the process of keratinocyte-mediated DC activation even in the absence of an antigen. This was shown by the decreased activation of DCs when keratinocytes were pre-treated with UPR inhibitors. In addition, combinations of weak sensitizers with either other weak sensitizers or an irritant show similar effects as strong sensitizers. They show a high induction of *Xbp-1* splicing and p65 nuclear translocation. This might be the mode of action by which patients are sensitized to allergens used in suboptimal doses in cosmetics and cleaning products. In addition, these results have implications for risk assessment. Up to now, only single substances are tested. However, our studies underline the importance of assessing the sensitizing potential of mixtures and formulations as used by consumers daily. The fact that using specific UPR inhibitors could interfere with the adverse effects of these weak sensitizers like they did with strong sensitizers makes the UPR an attractive potential target for treatment.

9.10 Outlook

One of the ideas behind this project was to deepen the knowledge on the mechanisms of the ACD for the development of an *in vitro* assay for the potency assessment of new chemicals. As this does not seem to work in the current setting of experiments, further work might still contribute to this endeavor. As mentioned, looking at the UPR in keratinocytes might be the wrong point in the process of ACD. Maybe the activation of APCs like DCs poses a better option for the discrimination between different potencies of sensitizers. However, deepening the knowledge on the role of the UPR in CHS and ACD opens the possibility to use topically applied UPR inhibitors as a treatment option. This was explored in further work of our group by using so-called ERAI reporter mice (Iwawaki et al. 2004). These mice start to express GFP when the IRE-1 branch of the UPR is activated. Using these mice, we could show that an epicutaneously applied small molecule inhibitor of IRE-1 was able to reduce the oxazolone-induced UPR in the ears of treated mice (Gendrisch et al. submitted) offering potential for the development of ointments containing such inhibitors. A further step would be to test different formulas which enable the inhibitors to penetrate the skin and offer an environment to keep the inhibitors stable in the formulation for a certain storage time. In addition, UPR inhibitors are not limited to the already known small molecule inhibitors. Natural inhibitors of the UPR are getting more and more attention (H. Liu et al. 2016) and could be used in a plant-based natural product for patients refusing classical medicine. Besides, many patients might unknowingly be already self-medicating their ACD. Antidepressant drugs have been shown to reduce the CHS response to DNFB (Curzytek et al. 2013). As depression has been linked to the UPR (Timberlake and Dwivedi 2018), a potential inhibitory effect of antidepressants on the UPR was tested in an initial experiment. And indeed, the use of opipramol, an often-prescribed antidepressant, was able to reduce the tunicamycin-induced splicing of *Xbp-1* in keratinocytes as seen in Figure 52. However, one has to consider the amount used in the culture medium and if this concentration is able to be reached in the body.

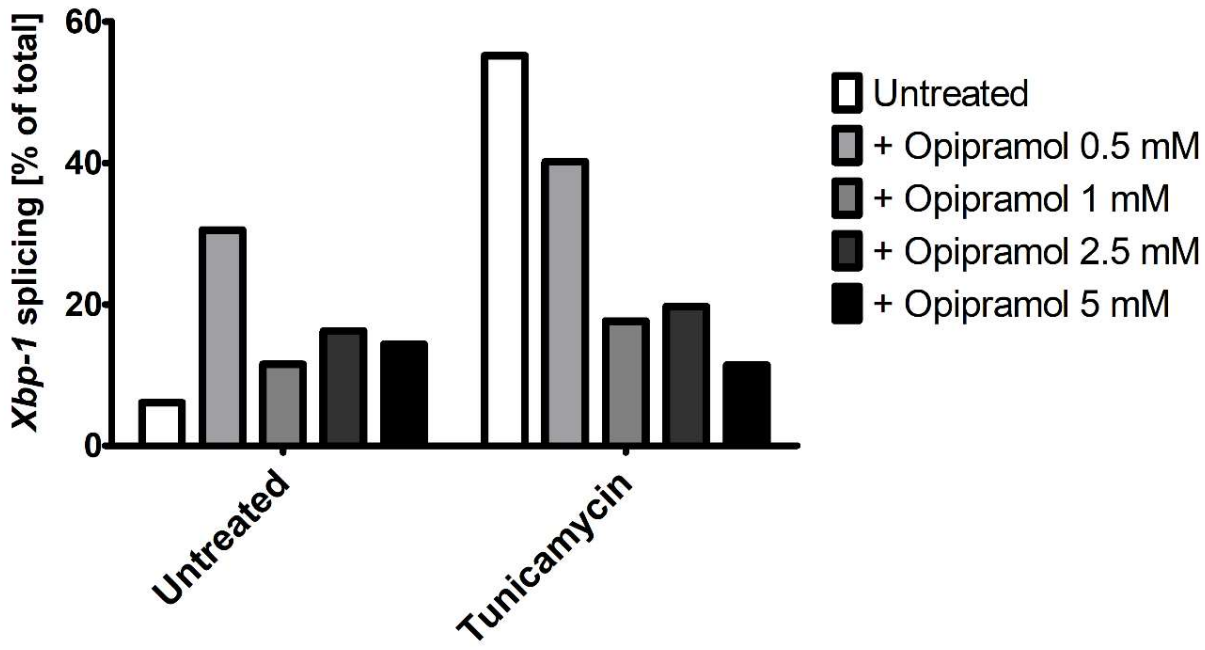

Figure 52: Opipramol treatment inhibits tunicamycin-induced *Xbp-1* splicing. PAM212 cells were pretreated with opipramol for 1 h followed by 6 h stimulation with 10 µg/ml tunicamycin. The activation status of the UPR was assessed by analyzing the splicing of *Xbp-1* using PCR. Result of one test experiment is shown.

Another potential UPR inhibitor many people come into contact with is caffeine. It acts as a chemical chaperone an has been shown to reduce ER stress-induced UPR activation (Hosoi et al. 2014). Again, the problem might be the high concentration used in cell culture and the availability of caffeine in the body.

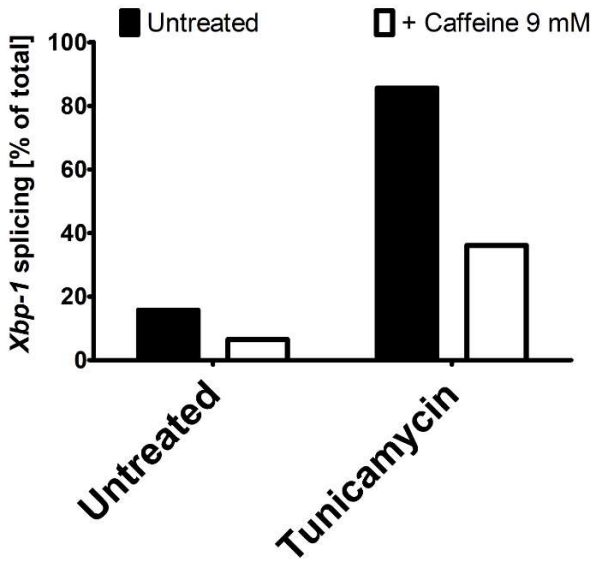

Figure 53: Caffeine inhibits tunicamycin-induced *Xbp-1* splicing. PAM212 cells were stimulated with tunicamycin for 6 h following 1 h pretreatment with 9 mM of caffeine. Induction of *Xbp-1* splicing was assessed by a PCR specific for *Xbp-1*. Result of one test experiment is shown.

However, as many people regularly consume caffeine in either coffee or tea and are prescribed antidepressants, a questionnaire asking patients about their caffeine consumption and the prescription of anti-depressants might offer an insight in the effects of these substances in the occurrence and severity of ACD as a long-term use might lead to a build-up of a certain active component level in the body leading to effects on the disease.

10 List of figures

11 List of tables

12 Bibliography

A. J. Swallow. 1960. *Radiation Chemistry of Organic Compounds*. 1st Edition. Pergamon. https://www.elsevier.com/books/radiation-chemistry-of-organic-compounds/swallow/978-0-08-009297-3.

Acosta-Alvear, Diego, Yiming Zhou, Alexandre Blais, Mary Tsikitis, Nathan H. Lents, Carolina Arias, Christen J. Lennon, Yuval Kluger, and Brian David Dynlacht. 2007. "XBP1 Controls Diverse Cell Type- and Condition-Specific Transcriptional Regulatory Networks." *Molecular Cell* 27 (1): 53–66. https://doi.org/10.1016/j.molcel.2007.06.011.

Adolph, Timon E., Michal F. Tomczak, Lukas Niederreiter, Hyun-Jeong Ko, Janne Böck, Eduardo Martinez-Naves, Jonathan N. Glickman, et al. 2013. "Paneth Cells as a Site of Origin for Intestinal Inflammation." *Nature* 503 (7475): 272–76. https://doi.org/10.1038/nature12599.

Agner, Tove, Jeanne Duus Johansen, Lene Overgaard, Aage Vølund, David Basketter, and Torkil Menné. 2002. "Combined Effects of Irritants and Allergens." *Contact Dermatitis* 47 (1): 21–26.

Akira, Shizuo, Satoshi Uematsu, and Osamu Takeuchi. 2006. "Pathogen Recognition and Innate Immunity." *Cell* 124 (4): 783–801. https://doi.org/10.1016/j.cell.2006.02.015.

Alberts, Bruce, Alexander Johnson, Julian Lewis, Martin Raff, Keith Roberts, and Peter Walter. 2002. "Lymphocytes and the Cellular Basis of Adaptive Immunity." https://www.ncbi.nlm.nih.gov/books/NBK26921/.

Aleksic, Maja, Camilla K. Pease, David A. Basketter, Maria Panico, Howard R. Morris, and Anne Dell. 2007. "Investigating Protein Haptenation Mechanisms of Skin Sensitisers Using Human Serum Albumin as a Model Protein." *Toxicology in Vitro* 21 (4): 723–33. https://doi.org/10.1016/j.tiv.2007.01.008.

Álvarez, Karen, and Gloria Vasquez. 2017. "Damage-Associated Molecular Patterns and Their Role as Initiators of Inflammatory and Auto-Immune Signals in Systemic Lupus Erythematosus." *International Reviews of Immunology* 36 (5): 259–70. https://doi.org/10.1080/08830185.2017.1365146.

Anding, Allyson L., and Eric H. Baehrecke. 2017. "Cleaning House: Selective Autophagy of Organelles." *Developmental Cell* 41 (1): 10–22. https://doi.org/10.1016/j.devcel.2017.02.016.

Aptula, Aynur O., Grace Patlewicz, and David W. Roberts. 2005. "Skin Sensitization: Reaction Mechanistic Applicability Domains for Structure−Activity Relationships." *Chemical Research in Toxicology* 18 (9): 1420–26. https://doi.org/10.1021/tx050075m.

Araki, Kazutaka, and Kazuhiro Nagata. 2011. "Protein Folding and Quality Control in the ER." *Cold Spring Harbor Perspectives in Biology* 3 (11): a007526. https://doi.org/10.1101/cshperspect.a007526.

Arango Duque, Guillermo, and Albert Descoteaux. 2014. "Macrophage Cytokines: Involvement in Immunity and Infectious Diseases." *Frontiers in Immunology* 5 (October). https://doi.org/10.3389/fimmu.2014.00491.

Arnold, J, D Murera, F Arbogast, J-D Fauny, S Muller, and F Gros. 2016. "Autophagy Is Dispensable for B-Cell Development but Essential for Humoral Autoimmune Responses." *Cell Death and Differentiation* 23 (5): 853–64. https://doi.org/10.1038/cdd.2015.149.

Avonto, Cristina, Amar G. Chittiboyina, Mei Wang, Yelkaira Vasquez, Diego Rua, and Ikhlas A. Khan. 2016. "In Chemico Evaluation of Tea Tree Essential Oils as

Skin Sensitizers: Impact of the Chemical Composition on Aging and Generation of Reactive Species." *Chemical Research in Toxicology* 29 (7): 1108–17. https://doi.org/10.1021/acs.chemrestox.5b00530.

Bartůňková, Jiřina, Jana Kayserová, and Yehuda Shoenfeld. 2009. "Allergy and Autoimmunity: Parallels and Dissimilarity: The Yin and Yang of Immunopathology." *Autoimmunity Reviews* 8 (4): 302–8. https://doi.org/10.1016/j.autrev.2008.09.004.

Bennett, Clare L., Erwin van Rijn, Steffen Jung, Kayo Inaba, Ralph M. Steinman, Martien L. Kapsenberg, and Björn E. Clausen. 2005. "Inducible Ablation of Mouse Langerhans Cells Diminishes but Fails to Abrogate Contact Hypersensitivity." *The Journal of Cell Biology* 169 (4): 569–76. https://doi.org/10.1083/jcb.200501071.

Berges, Carsten, Cord Naujokat, Sarah Tinapp, Hubert Wieczorek, Alexandra Höh, Mahmoud Sadeghi, Gerhard Opelz, and Volker Daniel. 2005. "A Cell Line Model for the Differentiation of Human Dendritic Cells." *Biochemical and Biophysical Research Communications* 333 (3): 896–907. https://doi.org/10.1016/j.bbrc.2005.05.171.

Bergmann, Karl-Christian, Joachim Heinrich, and Hildegard Niemann. 2016. "Current Status of Allergy Prevalence in Germany." *Allergo Journal International* 25: 6–10. https://doi.org/10.1007/s40629-016-0092-6.

Bertolotti, Anne, Yuhong Zhang, Linda M. Hendershot, Heather P. Harding, and David Ron. 2000. "Dynamic Interaction of BiP and ER Stress Transducers in the Unfolded-Protein Response." *Nature Cell Biology* 2 (6): 326–32. https://doi.org/10.1038/35014014.

Biederbick, A., H. F. Kern, and H. P. Elsässer. 1995. "Monodansylcadaverine (MDC) Is a Specific in Vivo Marker for Autophagic Vacuoles." *European Journal of Cell Biology* 66 (1): 3–14.

Blum, Janice S., Pamela A. Wearsch, and Peter Cresswell. 2013. "Pathways of Antigen Processing." *Annual Review of Immunology* 31: 443–73. https://doi.org/10.1146/annurev-immunol-032712-095910.

Bocchietto, E., C. Paolucci, D. Breda, E. Sabbioni, and S. E. Burastero. 2007. "Human Monocytoid THP-1 Cell Line versus Monocyte-Derived Human Immature Dendritic Cells as in Vitro Models for Predicting the Sensitising Potential of Chemicals." *International Journal of Immunopathology and Pharmacology* 20 (2): 259–65. https://doi.org/10.1177/039463200702000206.

Bonefeld, Charlotte Menné, Morten Milek Nielsen, Ingrid Maria Cecilia Rubin, Marie Torp Vennegaard, Sally Dabelsteen, Elena Gimenéz-Arnau, Jean-Pierre Lepoittevin, Carsten Geisler, and Jeanne Duus Johansen. 2011. "Enhanced Sensitization and Elicitation Responses Caused by Mixtures of Common Fragrance Allergens." *Contact Dermatitis* 65 (6): 336–42. https://doi.org/10.1111/j.1600-0536.2011.01945.x.

Boss, Martha J., Brad Boss, Cybil Boss, and Dennis W. Day. 2015. *Handbook of Chemical Regulations: Benchmarking, Implementation, and Engineering Concepts*. CRC Press.

Boukamp, P., R. T. Petrussevska, D. Breitkreutz, J. Hornung, A. Markham, and N. E. Fusenig. 1988. "Normal Keratinization in a Spontaneously Immortalized Aneuploid Human Keratinocyte Cell Line." *The Journal of Cell Biology* 106 (3): 761–71. https://doi.org/10.1083/jcb.106.3.761.

Brantley, Dana M., Chih-Li Chen, Rebecca S. Muraoka, Paul B. Bushdid, Jonathan L. Bradberry, Frances Kittrell, Daniel Medina, Lynn M. Matrisian, Lawrence D. Kerr, and Fiona E. Yull. 2001. "Nuclear Factor-KB (NF-KB) Regulates

Proliferation and Branching in Mouse Mammary Epithelium." *Molecular Biology of the Cell* 12 (5): 1445–55.

Charles A Janeway, Jr, Paul Travers, Mark Walport, and Mark J. Shlomchik. 2001. "Principles of Innate and Adaptive Immunity." https://www.ncbi.nlm.nih.gov/books/NBK27090/.

Chen, Rong-Jane, Yu-Hsuan Lee, Ya-Ling Yeh, Ying-Jan Wang, and Bour-Jr Wang. 2016. "The Roles of Autophagy and the Inflammasome during Environmental Stress-Triggered Skin Inflammation." *International Journal of Molecular Sciences* 17 (12): 2063. https://doi.org/10.3390/ijms17122063.

Chen, Yani, and Federica Brandizzi. 2013. "IRE1: ER Stress Sensor and Cell Fate Executor." *Trends in Cell Biology* 23 (11): 547–55. https://doi.org/10.1016/j.tcb.2013.06.005.

Cheng, Judy, and Kathryn A. Zug. 2014. "Fragrance Allergic Contact Dermatitis." *Dermatitis* 25 (5): 232–45. https://doi.org/10.1097/DER.0000000000000067.

Cho, Jin A., Ann-Hwee Lee, Barbara Platzer, Benedict C. S. Cross, Brooke M. Gardner, Heidi De Luca, Phi Luong, et al. 2013. "The Unfolded Protein Response Element IRE1α Senses Bacterial Proteins Invading the ER to Activate RIG-I and Innate Immune Signaling." *Cell Host & Microbe* 13 (5): 558–69. https://doi.org/10.1016/j.chom.2013.03.011.

Choovichian, Vorada, Lapakorn Chatapat, and Watcharapong Piyaphanee. 2015. "A Bubble Turtle: Bullous Contact Dermatitis after a Black Henna Tattoo in a Backpacker in Thailand." *Journal of Travel Medicine* 22 (4): 287–88. https://doi.org/10.1111/jtm.12202.

Cobb, Hana K., Michi M. Shinohara, Jason T. Huss, Marshall P. Welch, and Jennifer M. Gardner. 2017. "Systemic Contact Dermatitis to a Surgical Implant Presenting as Red Decorative Tattoo Reaction." *JAAD Case Reports* 3 (4): 348–50. https://doi.org/10.1016/j.jdcr.2017.05.003.

Corthay, A. 2009. "How Do Regulatory T Cells Work?" *Scandinavian Journal of Immunology* 70 (4): 326–36. https://doi.org/10.1111/j.1365-3083.2009.02308.x.

Cruz, Michelle S., Alani Diamond, Astrid Russell, and Julie Marie Jameson. 2018. "Human Aβ and Γδ T Cells in Skin Immunity and Disease." *Frontiers in Immunology* 9 (June). https://doi.org/10.3389/fimmu.2018.01304.

Cuervo, Ana Maria, and Esther Wong. 2014. "Chaperone-Mediated Autophagy: Roles in Disease and Aging." *Cell Research* 24 (1): 92–104. https://doi.org/10.1038/cr.2013.153.

Curzytek, Katarzyna, Marta Kubera, Monika Majewska-Szczepanik, Marian Szczepanik, Katarzyna Marcińska, W\lodzimierz Ptak, Weronika Duda, et al. 2013. "Inhibition of 2, 4-Dinitrofluorobenzene-Induced Contact Hypersensitivity Reaction by Antidepressant Drugs." *Pharmacological Reports* 65 (5): 1237–1246.

Dajee, Maya, Tony Muchamuel, Brian Schryver, Aung Oo, Jennifer Alleman-Sposeto, Christopher G. De Vry, Srinivasa Prasad, et al. 2006. "Blockade of Experimental Atopic Dermatitis via Topical NF-KB Decoy Oligonucleotide." *Journal of Investigative Dermatology* 126 (8): 1792–1803. https://doi.org/10.1038/sj.jid.5700307.

De Benedetto, Anna, Akiharu Kubo, and Lisa A. Beck. 2012. "Skin Barrier Disruption - A Requirement for Allergen Sensitization?" *The Journal of Investigative Dermatology* 132 (3 0 2): 949–63. https://doi.org/10.1038/jid.2011.435.

Deegan, Shane, Izabela Koryga, Sharon A. Glynn, Sanjeev Gupta, Adrienne M. Gorman, and Afshin Samali. 2015. "A Close Connection between the PERK

and IRE Arms of the UPR and the Transcriptional Regulation of Autophagy." *Biochemical and Biophysical Research Communications* 456 (1): 305–11. https://doi.org/10.1016/j.bbrc.2014.11.076.

Deza, Gustavo, and Ana M. Giménez-arnau. 2017. "Allergic Contact Dermatitis in Preservatives: Current Standing and Future Options." *Current Opinion in Allergy and Clinical Immunology* 17 (4): 263–68. https://doi.org/10.1097/ACI.0000000000000373.

Diepgen, T. L., R. F. Ofenloch, M. Bruze, P. Bertuccio, S. Cazzaniga, P.-J. Coenraads, P. Elsner, M. Goncalo, Å Svensson, and L. Naldi. 2016. "Prevalence of Contact Allergy in the General Population in Different European Regions." *British Journal of Dermatology* 174 (2): 319–29. https://doi.org/10.1111/bjd.14167.

Diepgen, Thomas L. 2003. "Occupational Skin-Disease Data in Europe." *International Archives of Occupational and Environmental Health* 76 (5): 331–38. https://doi.org/10.1007/s00420-002-0418-1.

Diepgen, Thomas L., Luigi Naldi, Magnus Bruze, Simone Cazzaniga, Marie-Louise Schuttelaar, Peter Elsner, Margarida Goncalo, Robert Ofenloch, and Åke Svensson. 2016. "Prevalence of Contact Allergy to P-Phenylenediamine in the European General Population." *The Journal of Investigative Dermatology* 136 (2): 409–15. https://doi.org/10.1016/j.jid.2015.10.064.

Divkovic, Maja, Camilla K. Pease, G. Frank Gerberick, and David A. Basketter. 2005. "Hapten–protein Binding: From Theory to Practical Application in the in Vitro Prediction of Skin Sensitization." *Contact Dermatitis* 53 (4): 189–200. https://doi.org/10.1111/j.0105-1873.2005.00683.x.

Doebel, Thomas, Benjamin Voisin, and Keisuke Nagao. 2017. "Langerhans Cells – The Macrophage in Dendritic Cell Clothing." *Trends in Immunology*, July. https://doi.org/10.1016/j.it.2017.06.008.

El Ali, Z., C. Gerbeix, P. Hemon, P. R. Esser, S. F. Martin, M. Pallardy, and S. Kerdine-Romer. 2013. "Allergic Skin Inflammation Induced by Chemical Sensitizers Is Controlled by the Transcription Factor Nrf2." *Toxicological Sciences* 134 (1): 39–48. https://doi.org/10.1093/toxsci/kft084.

Engin, F., and G. S. Hotamisligil. 2010. "Restoring Endoplasmic Reticulum Function by Chemical Chaperones: An Emerging Therapeutic Approach for Metabolic Diseases." *Diabetes, Obesity and Metabolism* 12 (October): 108–15. https://doi.org/10.1111/j.1463-1326.2010.01282.x.

England, Hazel, Holly R. Summersgill, Michelle E. Edye, Nancy J. Rothwell, and David Brough. 2014. "Release of Interleukin-1α or Interleukin-1β Depends on Mechanism of Cell Death." *The Journal of Biological Chemistry* 289 (23): 15942–50. https://doi.org/10.1074/jbc.M114.557561.

Esser, Philipp R., and Stefan F. Martin. 2017. "Pathomechanisms of Contact Sensitization." *Current Allergy and Asthma Reports* 17 (12): 83. https://doi.org/10.1007/s11882-017-0752-8.

Esser, Philipp R., Ute Wölfle, Christoph Dürr, Friederike D. von Loewenich, Christoph M. Schempp, Marina A. Freudenberg, Thilo Jakob, and Stefan F. Martin. 2012. "Contact Sensitizers Induce Skin Inflammation via ROS Production and Hyaluronic Acid Degradation." Edited by Nikos K. Karamanos. *PLoS ONE* 7 (7): e41340. https://doi.org/10.1371/journal.pone.0041340.

Fan, Ping, Amit K. Tyagi, Fadeke A. Agboke, Rohit Mathur, Niranjana Pokharel, and V. Craig Jordan. 2018. "Modulation of Nuclear Factor-Kappa B Activation by the Endoplasmic Reticulum Stress Sensor PERK to Mediate Estrogen-Induced

Apoptosis in Breast Cancer Cells." *Cell Death Discovery* 4 (1): 15. https://doi.org/10.1038/s41420-017-0012-7.

Fernandez, Anita G., Emily K. Mis, Bastiaan O.R. Bargmann, Kenneth D. Birnbaum, and Fabio Piano. 2010. "Automated Sorting of Live C. Elegans Using LaFACS." *Nature Methods* 7 (6): 417–18. https://doi.org/10.1038/nmeth.f.304.

Fitzpatrick, Jeremy M., David W. Roberts, and Grace Patlewicz. 2017. "What Determines Skin Sensitization Potency: Myths, Maybes and Realities. The 500 Molecular Weight Cut-off: An Updated Analysis." *Journal of Applied Toxicology: JAT* 37 (1): 105–16. https://doi.org/10.1002/jat.3348.

Flannagan, Ronald S., Gabriela Cosío, and Sergio Grinstein. 2009. "Antimicrobial Mechanisms of Phagocytes and Bacterial Evasion Strategies." *Nature Reviews Microbiology* 7 (5): 355. https://doi.org/10.1038/nrmicro2128.

Fleming, Alexander. 1922. "On a Remarkable Bacteriolytic Element Found in Tissues and Secretions." *Proceedings of the Royal Society of London. Series B, Containing Papers of a Biological Character* 93 (653): 306–17. https://doi.org/10.1098/rspb.1922.0023.

Galdiero, Maria R., Cecilia Garlanda, Sébastien Jaillon, Gianni Marone, and Alberto Mantovani. 2013. "Tumor Associated Macrophages and Neutrophils in Tumor Progression." *Journal of Cellular Physiology* 228 (7): 1404–12. https://doi.org/10.1002/jcp.24260.

Gallucci, Stefania, Martijn Lolkema, and Polly Matzinger. 1999. "Natural Adjuvants: Endogenous Activators of Dendritic Cells." *Nature Medicine* 5 (11): 1249–55. https://doi.org/10.1038/15200.

Gardner, Brooke M., and Peter Walter. 2011. "Unfolded Proteins Are Ire1-Activating Ligands That Directly Induce the Unfolded Protein Response." *Science* 333 (6051): 1891–94. https://doi.org/10.1126/science.1209126.

Gendrisch, Fabian. 2012. "Mechanismen Der Kontaktallergie - Die Rolle Der Allergen-Induzierten Unfolded Protein Response."

———. 2015. "The Role of the Unfolded Protein Response in Allergic Contact Dermatitis."

Goldsmith, Lowell A. 2014. "Reply to Sontheimer." *The Journal of Investigative Dermatology* 134 (2): 582. https://doi.org/10.1038/jid.2013.336.

Gomez de Agüero, Mercedes, Marc Vocanson, Fériel Hacini-Rachinel, Morgan Taillardet, Tim Sparwasser, Adrien Kissenpfennig, Bernard Malissen, Dominique Kaiserlian, and Bertrand Dubois. 2012. "Langerhans Cells Protect from Allergic Contact Dermatitis in Mice by Tolerizing CD8+ T Cells and Activating Foxp3+ Regulatory T Cells." *The Journal of Clinical Investigation* 122 (5): 1700–1711. https://doi.org/10.1172/JCI59725.

Görlach, Agnes, Katharina Bertram, Sona Hudecova, and Olga Krizanova. 2015. "Calcium and ROS: A Mutual Interplay." *Redox Biology* 6 (December): 260–71. https://doi.org/10.1016/j.redox.2015.08.010.

Groban, Eli S., Arjun Narayanan, and Matthew P. Jacobson. 2006. "Conformational Changes in Protein Loops and Helices Induced by Post-Translational Phosphorylation." *PLOS Computational Biology* 2 (4): e32. https://doi.org/10.1371/journal.pcbi.0020032.

Grootjans, Joep, Arthur Kaser, Randal J. Kaufman, and Richard S. Blumberg. 2016. "The Unfolded Protein Response in Immunity and Inflammation." *Nature Reviews Immunology* 16 (8): 469–84. https://doi.org/10.1038/nri.2016.62.

Guzman, Javier Rivera, Ja Seol Koo, Jason R. Goldsmith, Marcus Mühlbauer, Acharan Narula, and Christian Jobin. 2013. "Oxymatrine Prevents NF-KB

Nuclear Translocation And Ameliorates Acute Intestinal Inflammation." *Scientific Reports* 3 (1). https://doi.org/10.1038/srep01629.

Hagvall, Lina, Ann-Therese Karlberg, and Johanna Bråred Christensson. 2012. "Contact Allergy to Air-Exposed Geraniol: Clinical Observations and Report of 14 Cases." *Contact Dermatitis* 67 (1): 20–27. https://doi.org/10.1111/j.1600-0536.2012.02079.x.

Hammad, Hamida, and Bart N. Lambrecht. 2008. "Dendritic Cells and Epithelial Cells: Linking Innate and Adaptive Immunity in Asthma." *Nature Reviews Immunology* 8 (3): 193–204. https://doi.org/10.1038/nri2275.

Harding, Heather P, Isabel Novoa, Yuhong Zhang, Huiqing Zeng, Ron Wek, Matthieu Schapira, and David Ron. 2000. "Regulated Translation Initiation Controls Stress-Induced Gene Expression in Mammalian Cells." *Molecular Cell* 6 (5): 1099–1108. https://doi.org/10.1016/S1097-2765(00)00108-8.

Harding, Heather P., Yuhong Zhang, Huiquing Zeng, Isabel Novoa, Phoebe D. Lu, Marcella Calfon, Navid Sadri, et al. 2003. "An Integrated Stress Response Regulates Amino Acid Metabolism and Resistance to Oxidative Stress." *Molecular Cell* 11 (3): 619–33. https://doi.org/10.1016/S1097-2765(03)00105-9.

Harris, James, Michelle Hartman, Caitrionna Roche, Shijuan G. Zeng, Amy O'Shea, Fiona A. Sharp, Eimear M. Lambe, et al. 2011. "Autophagy Controls IL-1β Secretion by Targeting Pro-IL-1β for Degradation." *Journal of Biological Chemistry* 286 (11): 9587–97. https://doi.org/10.1074/jbc.M110.202911.

Hartmann, B., F. Staedtler, N. Hartmann, J. Meingassner, and H. Firat. 2006. "Gene Expression Profiling of Skin and Draining Lymph Nodes of Rats Affected with Cutaneous Contact Hypersensitivity." *Inflammation Research* 55 (8): 322–34. https://doi.org/10.1007/s00011-006-5141-z.

Haze, Kyosuke, Hiderou Yoshida, Hideki Yanagi, Takashi Yura, and Kazutoshi Mori. 1999. "Mammalian Transcription Factor ATF6 Is Synthesized as a Transmembrane Protein and Activated by Proteolysis in Response to Endoplasmic Reticulum Stress." *Molecular Biology of the Cell* 10 (11): 3787–99. https://doi.org/10.1091/mbc.10.11.3787.

He, Congcong, and Daniel J. Klionsky. 2009. "Regulation Mechanisms and Signaling Pathways of Autophagy." *Annual Review of Genetics* 43: 67–93. https://doi.org/10.1146/annurev-genet-102808-114910.

Hennen, and Blömeke. 2017. "Keratinocytes Improve Prediction of Sensitization Potential and Potency of Chemicals with THP-1 Cells." *ALTEX* 34 (2): 279–88. https://doi.org/10.14573/altex.1606171.

Hennen, Jenny, Pierre Aeby, Carsten Goebel, Thomas Schettgen, Aurelia Oberli, Michaela Kalmes, and Brunhilde Blömeke. 2011. "Cross Talk between Keratinocytes and Dendritic Cells: Impact on the Prediction of Sensitization." *Toxicological Sciences* 123 (2): 501–10. https://doi.org/10.1093/toxsci/kfr174.

Hetz, Claudio, Eric Chevet, and Heather P. Harding. 2013. "Targeting the Unfolded Protein Response in Disease." *Nature Reviews Drug Discovery* 12 (9): 703–19. https://doi.org/10.1038/nrd3976.

Hetz, Claudio, and Feroz R. Papa. 2017. "The Unfolded Protein Response and Cell Fate Control." *Molecular Cell*, November. https://doi.org/10.1016/j.molcel.2017.06.017.

Hogquist, K. A., M. A. Nett, E. R. Unanue, and D. D. Chaplin. 1991. "Interleukin 1 Is Processed and Released during Apoptosis." *Proceedings of the National Academy of Sciences* 88 (19): 8485–89. https://doi.org/10.1073/pnas.88.19.8485.

Hollien, Julie. 2013. “Evolution of the Unfolded Protein Response.” *Biochimica et Biophysica Acta (BBA) - Molecular Cell Research*, Functional and structural diversity of the endoplasmic reticulum, 1833 (11): 2458–63. https://doi.org/10.1016/j.bbamcr.2013.01.016.

Hollien, Julie, and Jonathan S. Weissman. 2006. “Decay of Endoplasmic Reticulum-Localized MRNAs During the Unfolded Protein Response.” *Science* 313 (5783): 104–7. https://doi.org/10.1126/science.1129631.

Honda, Tetsuya, Saeko Nakajima, Gyohei Egawa, Kouetsu Ogasawara, Bernard Malissen, Yoshiki Miyachi, and Kenji Kabashima. 2010. “Compensatory Role of Langerhans Cells and Langerin-Positive Dermal Dendritic Cells in the Sensitization Phase of Murine Contact Hypersensitivity.” *Journal of Allergy and Clinical Immunology* 125 (5): 1154–1156.e2. https://doi.org/10.1016/j.jaci.2009.12.005.

Hosoi, Toru, Keisuke Toyoda, Kanako Nakatsu, and Koichiro Ozawa. 2014. “Caffeine Attenuated ER Stress-Induced Leptin Resistance in Neurons.” *Neuroscience Letters* 569 (May): 23–26. https://doi.org/10.1016/j.neulet.2014.03.053.

Høyer-Hansen, M., and M. Jäättelä. 2007. “Connecting Endoplasmic Reticulum Stress to Autophagy by Unfolded Protein Response and Calcium.” *Cell Death & Differentiation* 14 (9): 1576–1582.

Hu, Ping, Zhang Han, Anthony D. Couvillon, Randal J. Kaufman, and John H. Exton. 2006. “Autocrine Tumor Necrosis Factor Alpha Links Endoplasmic Reticulum Stress to the Membrane Death Receptor Pathway through IRE1α-Mediated NF-KB Activation and Down-Regulation of TRAF2 Expression.” *Molecular and Cellular Biology* 26 (8): 3071–84. https://doi.org/10.1128/MCB.26.8.3071-3084.2006.

Hua, Zhaolin, and Baidong Hou. 2013. “TLR Signaling in B-Cell Development and Activation.” *Cellular & Molecular Immunology* 10 (2): 103–6. https://doi.org/10.1038/cmi.2012.61.

Huang, Xianfeng, Yuanyuan Liu, Yingxun Lu, and Chunhua Ma. 2015. “Anti-Inflammatory Effects of Eugenol on Lipopolysaccharide-Induced Inflammatory Reaction in Acute Lung Injury via Regulating Inflammation and Redox Status.” *International Immunopharmacology* 26 (1): 265–71. https://doi.org/10.1016/j.intimp.2015.03.026.

Hunt, Piper Reid. 2017. “The C. Elegans Model in Toxicity Testing.” *Journal of Applied Toxicology* 37 (1): 50–59. https://doi.org/10.1002/jat.3357.

Hurley, James H., and Lindsey N. Young. 2017. “Mechanisms of Autophagy Initiation.” *Annual Review of Biochemistry* 86: 225–44. https://doi.org/10.1146/annurev-biochem-061516-044820.

Igyarto, Botond Z., Matthew C. Jenison, Jan C. Dudda, Axel Roers, Werner Müller, Pandelakis A. Koni, Daniel J. Campbell, Mark J. Shlomchik, and Daniel H. Kaplan. 2009. “Langerhans Cells Suppress Contact Hypersensitivity Responses Via Cognate CD4 Interaction and Langerhans Cell-Derived IL-10.” *The Journal of Immunology* 183 (8): 5085–93. https://doi.org/10.4049/jimmunol.0901884.

Itano, Andrea A, Stephen J McSorley, R. Lee Reinhardt, Benjamin D Ehst, Elizabeth Ingulli, Alexander Y Rudensky, and Marc K Jenkins. 2003. “Distinct Dendritic Cell Populations Sequentially Present Antigen to CD4 T Cells and Stimulate Different Aspects of Cell-Mediated Immunity.” *Immunity* 19 (1): 47–57. https://doi.org/10.1016/S1074-7613(03)00175-4.

Iwakoshi, N. N., M. Pypaert, and L. H. Glimcher. 2007. “The Transcription Factor XBP-1 Is Essential for the Development and Survival of Dendritic Cells.”

Journal of Experimental Medicine 204 (10): 2267–75. https://doi.org/10.1084/jem.20070525.

Iwakoshi, Neal N., Ann-Hwee Lee, Prasanth Vallabhajosyula, Kevin L. Otipoby, Klaus Rajewsky, and Laurie H. Glimcher. 2003. "Plasma Cell Differentiation and the Unfolded Protein Response Intersect at the Transcription Factor XBP-1." *Nature Immunology* 4 (4): 321–29. https://doi.org/10.1038/ni907.

Iwawaki, Takao, Ryoko Akai, Kenji Kohno, and Masayuki Miura. 2004. "A Transgenic Mouse Model for Monitoring Endoplasmic Reticulum Stress." *Nature Medicine* 10 (1): 98–102. https://doi.org/10.1038/nm970.

Jackson, Katherine J. L., Marie J. Kidd, Yan Wang, and Andrew M. Collins. 2013. "The Shape of the Lymphocyte Receptor Repertoire: Lessons from the B Cell Receptor." *Frontiers in Immunology* 4 (September). https://doi.org/10.3389/fimmu.2013.00263.

Janssens, Sophie, Bali Pulendran, and Bart N. Lambrecht. 2014. "Emerging Functions of the Unfolded Protein Response in Immunity." *Nature Immunology* 15 (10): 910–19. https://doi.org/10.1038/ni.2991.

Jenkinson, Claire, Rosalind E. Jenkins, Maja Aleksic, Munir Pirmohamed, Dean J. Naisbitt, and B. Kevin Park. 2010. "Characterization of P-Phenylenediamine-Albumin Binding Sites and T-Cell Responses to Hapten-Modified Protein." *The Journal of Investigative Dermatology* 130 (3): 732–42. https://doi.org/10.1038/jid.2009.271.

Jiang, Hao-Yuan, Sheree A. Wek, Barbara C. McGrath, Donalyn Scheuner, Randal J. Kaufman, Douglas R. Cavener, and Ronald C. Wek. 2003. "Phosphorylation of the Alpha Subunit of Eukaryotic Initiation Factor 2 Is Required for Activation of NF-KB in Response to Diverse Cellular Stresses." *Molecular and Cellular Biology* 23 (16): 5651–63. https://doi.org/10.1128/MCB.23.16.5651-5663.2003.

Johansen, J. D., L. Skov, A. Volund, K. Andersen, and T. Menné. 1998. "Allergens in Combination Have a Synergistic Effect on the Elicitation Response: A Study of Fragrance-Sensitized Individuals." *The British Journal of Dermatology* 139 (2): 264–70.

Kabat, Agnieszka M., Johanna Pott, and Kevin J. Maloy. 2016. "The Mucosal Immune System and Its Regulation by Autophagy." *Frontiers in Immunology* 7 (June). https://doi.org/10.3389/fimmu.2016.00240.

Kadivar, Salmon, and Donald V. Belsito. 2015. "Occupational Dermatitis in Health Care Workers Evaluated for Suspected Allergic Contact Dermatitis." *Dermatitis* 26 (4): 177–83. https://doi.org/10.1097/DER.0000000000000124.

Kamsteeg, M., P.a.m. Jansen, I.m.j.j. Van Vlijmen-Willems, P.e.j. Van Erp, D. Rodijk-Olthuis, P.g. Van Der Valk, T. Feuth, P.l.j.m. Zeeuwen, and J. Schalkwijk. 2010. "Molecular Diagnostics of Psoriasis, Atopic Dermatitis, Allergic Contact Dermatitis and Irritant Contact Dermatitis." *British Journal of Dermatology* 162 (3): 568–78. https://doi.org/10.1111/j.1365-2133.2009.09547.x.

Kaplan, Daniel H. 2017. "Ontogeny and Function of Murine Epidermal Langerhans Cells." *Nature Immunology* 18 (10): 1068–75. https://doi.org/10.1038/ni.3815.

Kaplan, Daniel H., Botond Z. Igyártó, and Anthony A. Gaspari. 2012. "Early Immune Events in the Induction of Allergic Contact Dermatitis." *Nature Reviews Immunology*, January. https://doi.org/10.1038/nri3150.

Karagöz, G. Elif, Diego Acosta-Alvear, Hieu T. Nguyen, Crystal P. Lee, Feixia Chu, and Peter Walter. 2017. "An Unfolded Protein-Induced Conformational Switch Activates Mammalian IRE1." *ELife* 6.

Kaur, Jasvinder, and Jayanta Debnath. 2015. “Autophagy at the Crossroads of Catabolism and Anabolism.” *Nature Reviews Molecular Cell Biology* 16 (8): 461–72. https://doi.org/10.1038/nrm4024.

Keestra-Gounder, A. Marijke, Mariana X. Byndloss, Núbia Seyffert, Briana M. Young, Alfredo Chávez-Arroyo, April Y. Tsai, Stephanie A. Cevallos, et al. 2016. “NOD1 and NOD2 Signalling Links ER Stress with Inflammation.” *Nature* 532 (7599): 394–97. https://doi.org/10.1038/nature17631.

Kim, Busun, Youngmin Lee, Eunsom Kim, Areum Kwak, Soyoon Ryoo, Seung Hyeon Bae, Tania Azam, Soohyun Kim, and Charles A. Dinarello. 2013. “The Interleukin-1α Precursor Is Biologically Active and Is Likely a Key Alarmin in the IL-1 Family of Cytokines.” *Frontiers in Immunology* 4 (November). https://doi.org/10.3389/fimmu.2013.00391.

Kim, Donghye, Noo Ri Lee, Sang-Yeon Park, Myungsoo Jun, Kyohoon Lee, Sunki Kim, Chang Seo Park, Kwang-Hyeon Liu, and Eung Ho Choi. 2017. “As in Atopic Dermatitis, Nonlesional Skin in Allergic Contact Dermatitis Displays Abnormalities in Barrier Function and Ceramide Content.” *Journal of Investigative Dermatology* 137 (3): 748–50. https://doi.org/10.1016/j.jid.2016.10.034.

Kimata, Yukio, and Kenji Kohno. 2011. “Endoplasmic Reticulum Stress-Sensing Mechanisms in Yeast and Mammalian Cells.” *Current Opinion in Cell Biology*, Cell regulation, 23 (2): 135–42. https://doi.org/10.1016/j.ceb.2010.10.008.

Kitamura, Masanori. 2011. “Control of NF-KB and Inflammation by the Unfolded Protein Response.” *International Reviews of Immunology* 30 (1): 4–15. https://doi.org/10.3109/08830185.2010.522281.

Klebanoff, S. J. 1999. “Myeloperoxidase.” *Proceedings of the Association of American Physicians* 111 (5): 383–89.

Klionsky, Daniel J, Eeva-Liisa Eskelinen, and Vojo Deretic. 2014. “Autophagosomes, Phagosomes, Autolysosomes, Phagolysosomes, Autophagolysosomes… Wait, I’m Confused.” *Autophagy* 10 (4): 549–51. https://doi.org/10.4161/auto.28448.

Ko, A., A. Kanehisa, I. Martins, L. Senovilla, C. Chargari, D. Dugue, G. Mariño, et al. 2014. “Autophagy Inhibition Radiosensitizes in Vitro, yet Reduces Radioresponses in Vivo Due to Deficient Immunogenic Signalling.” *Cell Death and Differentiation* 21 (1): 92–99. https://doi.org/10.1038/cdd.2013.124.

Komori, H. Kiyomi, Deborah A. Witherden, Ryan Kelly, Kevin Sendaydiego, Julie M. Jameson, Luc Teyton, and Wendy L. Havran. 2012. “Cutting Edge: Dendritic Epidermal Γδ T Cell Ligands Are Rapidly and Locally Expressed by Keratinocytes Following Cutaneous Wounding.” *Journal of Immunology (Baltimore, Md.: 1950)* 188 (7): 2972–76. https://doi.org/10.4049/jimmunol.1100887.

Kupsco, Allison, and Daniel Schlenk. 2015. “Oxidative Stress, Unfolded Protein Response, and Apoptosis in Developmental Toxicity.” *International Review of Cell and Molecular Biology* 317: 1. https://doi.org/10.1016/bs.ircmb.2015.02.002.

Lapaquette, Pierre, Jean Guzzo, Lionel Bretillon, and Marie-Agnès Bringer. 2015. “Cellular and Molecular Connections between Autophagy and Inflammation.” *Mediators of Inflammation* 2015: 1–13. https://doi.org/10.1155/2015/398483.

Lee, Ann-Hwee, Neal N. Iwakoshi, and Laurie H. Glimcher. 2003. “XBP-1 Regulates a Subset of Endoplasmic Reticulum Resident Chaperone Genes in the Unfolded Protein Response.” *Molecular and Cellular Biology* 23 (21): 7448–59. https://doi.org/10.1128/MCB.23.21.7448-7459.2003.

Lee, Ying-Ray, Huan-Yao Lei, Ming-Tao Liu, Jen-Ren Wang, Shun-Hua Chen, Ya-Fen Jiang-Shieh, Yee-Shin Lin, Trai-Ming Yeh, Ching-Chuan Liu, and Hsiao-Sheng Liu. 2008. “Autophagic Machinery Activated by Dengue Virus Enhances Virus Replication.” *Virology* 374 (2): 240–48. https://doi.org/10.1016/j.virol.2008.02.016.

Lenschow, D. J., S. C. Ho, H. Sattar, L. Rhee, G. Gray, N. Nabavi, K. C. Herold, and J. A. Bluestone. 1995. “Differential Effects of Anti-B7-1 and Anti-B7-2 Monoclonal Antibody Treatment on the Development of Diabetes in the Nonobese Diabetic Mouse.” *The Journal of Experimental Medicine* 181 (3): 1145–55.

Lerner, Alana G., John-Paul Upton, P. V. K. Praveen, Rajarshi Ghosh, Yoshimi Nakagawa, Aeid Igbaria, Sarah Shen, et al. 2012. “IRE1α Induces Thioredoxin-Interacting Protein to Activate the NLRP3 Inflammasome and Promote Programmed Cell Death under Irremediable ER Stress.” *Cell Metabolism* 16 (2): 250–64. https://doi.org/10.1016/j.cmet.2012.07.007.

Liang, X. H., L. K. Kleeman, H. H. Jiang, G. Gordon, J. E. Goldman, G. Berry, B. Herman, and B. Levine. 1998. “Protection against Fatal Sindbis Virus Encephalitis by Beclin, a Novel Bcl-2-Interacting Protein.” *Journal of Virology* 72 (11): 8586–96.

Lin, J. H., H. Li, D. Yasumura, H. R. Cohen, C. Zhang, B. Panning, K. M. Shokat, M. M. LaVail, and P. Walter. 2007. “IRE1 Signaling Affects Cell Fate During the Unfolded Protein Response.” *Science* 318 (5852): 944–49. https://doi.org/10.1126/science.1146361.

Linard, Christine, Christel Marquette, Jacques Mathieu, André Pennequin, Didier Clarençon, and Denis Mathé. 2004. “Acute Induction of Inflammatory Cytokine Expression after γ-Irradiation in the Rat: Effect of an NF-KB Inhibitor.” *International Journal of Radiation Oncology • Biology • Physics* 58 (2): 427–34. https://doi.org/10.1016/j.ijrobp.2003.09.039.

Lind, Marie-Louise, Stina Johnsson, Carola Lidén, Birgitta Meding, and Anders Boman. 2017. “Hairdressers’ Skin Exposure to Hair Dyes during Different Hair Dyeing Tasks.” *Contact Dermatitis* 77 (5): 303–10. https://doi.org/10.1111/cod.12833.

Liu, Hai, Jianqiong Yang, Linfu Li, Weimei Shi, Xiaoliang Yuan, and Longhuo Wu. 2016. “The Natural Occurring Compounds Targeting Endoplasmic Reticulum Stress.” *Evidence-Based Complementary and Alternative Medicine : ECAM* 2016. https://doi.org/10.1155/2016/7831282.

Liu, Jing-Nan, Dong-Hyeon Suh, Hoang Kim Tu Trinh, Yong-Joon Chwae, Hae-Sim Park, and Yoo Seob Shin. 2016. “The Role of Autophagy in Allergic Inflammation: A New Target for Severe Asthma.” *Experimental & Molecular Medicine* 48 (7): e243. https://doi.org/10.1038/emm.2016.38.

Loeffel, E. Dorinda. 1972. “Preservatives as Sensitizers.” *California Medicine* 116 (6): 50.

Loveless, S. E., A. -M. Api, R. W. R. Crevel, E. Debruyne, A. Gamer, I. R. Jowsey, P. Kern, et al. 2010. “Potency Values from the Local Lymph Node Assay: Application to Classification, Labelling and Risk Assessment.” *Regulatory Toxicology and Pharmacology* 56 (1): 54–66. https://doi.org/10.1016/j.yrtph.2009.08.016.

Luís, Andreia, João Demétrio Martins, Ana Silva, Isabel Ferreira, Maria Teresa Cruz, and Bruno Miguel Neves. 2014. “Oxidative Stress-Dependent Activation of the EIF2α–ATFr Unfolded Protein Response Branch by Skin Sensitizer 1-Fluoro-2,4-Dinitrobenzene Modulates Dendritic-like Cell Maturation and Inflammatory

Status in a Biphasic Manner." *Free Radical Biology and Medicine* 77 (December): 217–29. https://doi.org/10.1016/j.freeradbiomed.2014.09.008.
Mahler, Vera, Johannes Geier, and Axel Schnuch. 2014. "Neue Entwicklungen zum Thema Epikutantest – aktuelle Daten aus der Deutschen Kontaktallergie-Gruppe (DKG) und Informationsverbund Dermatologischer Kliniken (IVDK)." *JDDG: Journal der Deutschen Dermatologischen Gesellschaft* 12 (7): 583–93. https://doi.org/10.1111/ddg.12371_suppl.
Majumder, Mithu, Charlie Huang, Martin D. Snider, Anton A. Komar, Junichi Tanaka, Randal J. Kaufman, Dawid Krokowski, and Maria Hatzoglou. 2012. "A Novel Feedback Loop Regulates the Response to Endoplasmic Reticulum Stress via the Cooperation of Cytoplasmic Splicing and MRNA Translation." *Molecular and Cellular Biology* 32 (5): 992–1003. https://doi.org/10.1128/MCB.06665-11.
Malhotra, Jyoti D., and Randal J. Kaufman. 2007. "Endoplasmic Reticulum Stress and Oxidative Stress: A Vicious Cycle or a Double-Edged Sword?" *Antioxidants & Redox Signaling* 9 (12): 2277–94. https://doi.org/10.1089/ars.2007.1782.
Malmberg, Per, Thomas Guttenberg, Marica B. Ericson, and Lina Hagvall. 2017. "Imaging Mass Spectrometry for Novel Insights into Contact Allergy – a Proof-of-Concept Study on Nickel." *Contact Dermatitis*, n/a-n/a. https://doi.org/10.1111/cod.12911.
Marsh, Elizabeth K., and Robin C. May. 2012. "Caenorhabditis Elegans, a Model Organism for Investigating Immunity." *Applied and Environmental Microbiology* 78 (7): 2075–81. https://doi.org/10.1128/AEM.07486-11.
Martin, S. F., J. C. Dudda, E. Bachtanian, A. Lembo, S. Liller, C. Durr, M. M. Heimesaat, et al. 2008. "Toll-like Receptor and IL-12 Signaling Control Susceptibility to Contact Hypersensitivity." *Journal of Experimental Medicine* 205 (9): 2151–62. https://doi.org/10.1084/jem.20070509.
Martin, S. F., P. R. Esser, F. C. Weber, T. Jakob, M. A. Freudenberg, M. Schmidt, and M. Goebeler. 2011. "Mechanisms of Chemical-Induced Innate Immunity in Allergic Contact Dermatitis: Contact Allergen-Induced Innate Immunity." *Allergy* 66 (9): 1152–63. https://doi.org/10.1111/j.1398-9995.2011.02652.x.
Martin, Stefan F. 2012. "Contact Dermatitis: From Pathomechanisms to Immunotoxicology: Contact Dermatitis - an Update." *Experimental Dermatology* 21 (5): 382–89. https://doi.org/10.1111/j.1600-0625.2012.01471.x.
Martin, Stefan, Michael B. Lappin, Jochen Kohler, Virginie Delattre, Cornelia Leicht, Tobias Preckel, Jan C. Simon, and Hans Ulrich Weltzien. 2000. "Peptide Immunization Indicates That CD8+ T Cells Are the Dominant Effector Cells in Trinitrophenyl-Specific Contact Hypersensitivity." *Journal of Investigative Dermatology* 115 (2): 260–66. https://doi.org/10.1046/j.1523-1747.2000.00038.x.
Martinon, Fabio, Xi Chen, Ann-Hwee Lee, and Laurie H Glimcher. 2010. "TLR Activation of the Transcription Factor XBP1 Regulates Innate Immune Responses in Macrophages." *Nature Immunology* 11 (5): 411–18. https://doi.org/10.1038/ni.1857.
Matejuk, Agata. 2018. "Skin Immunity." *Archivum Immunologiae et Therapiae Experimentalis* 66 (1): 45–54. https://doi.org/10.1007/s00005-017-0477-3.
Matsue, Hiroyuki, Ponciano D Cruz, Paul R Bergstresser, and Akira Takashima. 1992. "Cytokine Expression by Epidermal Cell Subpopulations." *Journal of Investigative Dermatology* 99 (5, Supplement): S42–45. https://doi.org/10.1111/1523-1747.ep12668619.

Maurel, M., E. Chevet, J. Tavernier, and S. Gerlo. 2014. “Getting RIDD of RNA: IRE1 in Cell Fate Regulation.” *Trends in Biochemical Sciences* 39 (5): 245–54. https://doi.org/10.1016/j.tibs.2014.02.008.

McFadden, J. P., and D. A. Basketter. 2000. “Contact Allergy, Irritancy and ‘Danger.’” *Contact Dermatitis* 42 (3): 123–27. https://doi.org/10.1034/j.1600-0536.2000.042003123.x.

Mee, John B., Christos Antonopoulos, Stephen Poole, Thomas S. Kupper, and Richard W. Groves. 2005. “Counter-Regulation of Interleukin-1α (IL-1α) and IL-1 Receptor Antagonist in Murine Keratinocytes.” *Journal of Investigative Dermatology* 124 (6): 1267–1274.

Merenyi. 2014. “REACH: Regulation (EC) No 1907/2006.”

Michaud, Mickaël, Isabelle Martins, Abdul Qader Sukkurwala, Sandy Adjemian, Yuting Ma, Patrizia Pellegatti, Shensi Shen, et al. 2011. “Autophagy-Dependent Anticancer Immune Responses Induced by Chemotherapeutic Agents in Mice.” *Science (New York, N.Y.)* 334 (6062): 1573–77. https://doi.org/10.1126/science.1208347.

Migdal, Camille, Lucie Foggia, Magalie Tailhardat, Pascal Courtellemont, Marek Haftek, and Mireille Serres. 2010. “Sensitization Effect of Thimerosal Is Mediated in Vitro via Reactive Oxygen Species and Calcium Signaling.” *Toxicology* 274 (1): 1–9. https://doi.org/10.1016/j.tox.2010.04.016.

Mizushima, Noboru, Yoshinori Ohsumi, and Tamotsu Yoshimori. 2002. “Autophagosome Formation in Mammalian Cells.” *Cell Structure and Function* 27 (6): 421–29.

Morl, Kazutoshi, Wenzhen Ma, Mary-Jane Gething, and Joseph Sambrook. 1993. “A Transmembrane Protein with a Cdc2+CDC28-Related Kinase Activity Is Required for Signaling from the ER to the Nucleus.” *Cell* 74 (4): 743–56. https://doi.org/10.1016/0092-8674(93)90521-Q.

Mosley, B., D. L. Urdal, K. S. Prickett, A. Larsen, D. Cosman, P. J. Conlon, S. Gillis, and S. K. Dower. 1987. “The Interleukin-1 Receptor Binds the Human Interleukin-1 Alpha Precursor but Not the Interleukin-1 Beta Precursor.” *The Journal of Biological Chemistry* 262 (7): 2941–44.

Munafó, Daniela B., and María I. Colombo. 2001. “A Novel Assay to Study Autophagy: Regulation of Autophagosome Vacuole Size by Amino Acid Deprivation.” *Journal of Cell Science* 114 (20): 3619–3629.

Murthy, Aditya, Yun Li, Ivan Peng, Mike Reichelt, Anand Kumar Katakam, Rajkumar Noubade, Merone Roose-Girma, et al. 2014. “A Crohn’s Disease Variant in Atg16l1 Enhances Its Degradation by Caspase 3.” *Nature* 506 (7489): 456–62. https://doi.org/10.1038/nature13044.

Naik, Edwina, and Vishva M. Dixit. 2011. “Mitochondrial Reactive Oxygen Species Drive Proinflammatory Cytokine Production.” *The Journal of Experimental Medicine* 208 (3): 417–20. https://doi.org/10.1084/jem.20110367.

Nakagawa, Ichiro, Atsuo Amano, Noboru Mizushima, Akitsugu Yamamoto, Hitomi Yamaguchi, Takahiro Kamimoto, Atsuki Nara, et al. 2004. “Autophagy Defends Cells Against Invading Group A Streptococcus.” *Science* 306 (5698): 1037–40. https://doi.org/10.1126/science.1103966.

Nedjic, Jelena, Martin Aichinger, Jan Emmerich, Noboru Mizushima, and Ludger Klein. 2008. “Autophagy in Thymic Epithelium Shapes the T-Cell Repertoire and Is Essential for Tolerance.” *Nature* 455 (7211): 396–400. https://doi.org/10.1038/nature07208.

Nestle, Frank O., Paola Di Meglio, Jian-Zhong Qin, and Brian J. Nickoloff. 2009. “Skin Immune Sentinels in Health and Disease.” *Nature Reviews Immunology*, September. https://doi.org/10.1038/nri2622.

Newby, Craig S., Robert M. Barr, Malcolm W. Greaves, and Anthony I. Mallet. 2000. “Cytokine Release and Cytotoxicity in Human Keratinocytes and Fibroblasts Induced by Phenols and Sodium Dodecyl Sulfate.” *Journal of Investigative Dermatology* 115 (2): 292–98. https://doi.org/10.1046/j.1523-1747.2000.00056.x.

Nielsen, Beatrice Dyring-Andersen, Jonas D. Schmidt, Deborah Witherden, Paola Lovato, Anders Woetmann, Niels Ødum, et al. 2015. “NKG2D-Dependent Activation of Dendritic Epidermal T Cells in Contact Hypersensitivity.” *The Journal of Investigative Dermatology* 135 (5): 1311–19. https://doi.org/10.1038/jid.2015.23.

Nielsen, P. Lovato, A. S. MacLeod, D. A. Witherden, L. Skov, B. Dyring-Andersen, S. Dabelsteen, et al. 2014. “IL-1 -Dependent Activation of Dendritic Epidermal T Cells in Contact Hypersensitivity.” *The Journal of Immunology* 192 (7): 2975–83. https://doi.org/10.4049/jimmunol.1301689.

Nijholt, D. a. T., T. R. de Graaf, E. S. van Haastert, A. Osório Oliveira, C. R. Berkers, R. Zwart, H. Ovaa, F. Baas, J. J. M. Hoozemans, and W. Scheper. 2011. “Endoplasmic Reticulum Stress Activates Autophagy but Not the Proteasome in Neuronal Cells: Implications for Alzheimer’s Disease.” *Cell Death & Differentiation* 18 (6): 1071–81. https://doi.org/10.1038/cdd.2010.176.

Nishitoh, Hideki, Atsushi Matsuzawa, Kei Tobiume, Kaoru Saegusa, Kohsuke Takeda, Kiyoshi Inoue, Seiji Hori, Akira Kakizuka, and Hidenori Ichijo. 2002. “ASK1 Is Essential for Endoplasmic Reticulum Stress-Induced Neuronal Cell Death Triggered by Expanded Polyglutamine Repeats.” *Genes & Development* 16 (11): 1345–55. https://doi.org/10.1101/gad.992302.

Noordegraaf, Madelon, Vincent Flacher, Patrizia Stoitzner, and Björn E. Clausen. 2010. “Functional Redundancy of Langerhans Cells and Langerin+ Dermal Dendritic Cells in Contact Hypersensitivity.” *Journal of Investigative Dermatology* 130 (12): 2752–2759.

Nouri-Aria, K. T., F. O’brien, W. Noble, M. R. Jabcobson, K. Rajakulasingam, and S. R. Durham. 2000. “Cytokine Expression during Allergen-Induced Late Nasal Responses: IL-4 and IL-5 MRNA Is Expressed Early (at 6 h) Predominantly by Eosinophils.” *Clinical & Experimental Allergy* 30 (12): 1709–16. https://doi.org/10.1046/j.1365-2222.2000.00998.x.

O’Connor, Tracy, Katherine R. Sadleir, Erika Maus, Rodney A. Velliquette, Jie Zhao, Sarah L. Cole, William A. Eimer, et al. 2008. “Phosphorylation of the Translation Initiation Factor EIF2α Increases BACE1 Levels and Promotes Amyloidogenesis.” *Neuron* 60 (6): 988–1009. https://doi.org/10.1016/j.neuron.2008.10.047.

Oikawa, Daisuke, Yukio Kimata, Kenji Kohno, and Takao Iwawaki. 2009. “Activation of Mammalian IRE1α upon ER Stress Depends on Dissociation of BiP Rather than on Direct Interaction with Unfolded Proteins.” *Experimental Cell Research* 315 (15): 2496–2504. https://doi.org/10.1016/j.yexcr.2009.06.009.

Pahl, Heike L. 1999. “Activators and Target Genes of Rel/NF-KB Transcription Factors.” *Oncogene* 18 (49): 6853–66. https://doi.org/10.1038/sj.onc.1203239.

Paquet, P., and G. E. Piérard. 1996. “Interleukin-6 and the Skin.” *International Archives of Allergy and Immunology* 109 (4): 308–17. https://doi.org/10.1159/000237257.

Parish, Lawrence. 2010. “Test Concentrations and Vehicles for 4350 Chemicals, 3rd Ed., DeGroot AC Acdegroot Publishing, Wapserveen, The Netherlands (2008), 455 Pp; List Price: €129.95.” *Clinics in Dermatology - CLIN DERMATOL* 28 (June): 355–355. https://doi.org/10.1016/j.clindermatol.2009.12.017.

Parker, Darien, Paul V. Long, and John L. Turk. 1983. “A Comparison of the Conjugation of DNTB and Other Dinitrobenzenes with Free Protein Radicals and Their Ability to Sensitize or Tolerize.” *Journal of Investigative Dermatology* 81 (3): 198–201. https://doi.org/10.1111/1523-1747.ep12517692.

Parkinson, Erika, Pete Boyd, Maja Aleksic, Richard Cubberley, David O’Connor, and Paul Skipp. 2014. “Stable Isotope Labeling Method for the Investigation of Protein Haptenation by Electrophilic Skin Sensitizers.” *Toxicological Sciences* 142 (1): 239–49. https://doi.org/10.1093/toxsci/kfu168.

Peiser, M., T. Tralau, J. Heidler, A. M. Api, J. H. E. Arts, D. A. Basketter, J. English, et al. 2012. “Allergic Contact Dermatitis: Epidemiology, Molecular Mechanisms, in Vitro Methods and Regulatory Aspects: Current Knowledge Assembled at an International Workshop at BfR, Germany.” *Cellular and Molecular Life Sciences* 69 (5): 763–81. https://doi.org/10.1007/s00018-011-0846-8.

Poltorak, A. 1998. “Defective LPS Signaling in C3H/HeJ and C57BL/10ScCr Mice: Mutations in Tlr4 Gene.” *Science* 282 (5396): 2085–88. https://doi.org/10.1126/science.282.5396.2085.

Porstmann, B., T. Porstmann, E. Nugel, and U. Evers. 1985. “Which of the Commonly Used Marker Enzymes Gives the Best Results in Colorimetric and Fluorimetric Enzyme Immunoassays: Horseradish Peroxidase, Alkaline Phosphatase or Beta-Galactosidase?” *Journal of Immunological Methods* 79 (1): 27–37.

Pua, Heather H., Ivan Dzhagalov, Mariana Chuck, Noboru Mizushima, and You-Wen He. 2007. “A Critical Role for the Autophagy Gene Atg5 in T Cell Survival and Proliferation.” *The Journal of Experimental Medicine* 204 (1): 25–31. https://doi.org/10.1084/jem.20061303.

Purath, Ulrich, Rouba Ibrahim, Jana Zeitvogel, Harald Renz, Frank Runkel, Thomas Schmidts, Dorota Dobler, Thomas Werfel, Anke Müller, and Holger Garn. 2016. “Efficacy of T-Cell Transcription Factor–specific DNAzymes in Murine Skin Inflammation Models.” *Journal of Allergy and Clinical Immunology* 137 (2): 644–647.e8. https://doi.org/10.1016/j.jaci.2015.09.022.

Qin, Rosie, and Heather P. Lampel. 2015. “Review of Occupational Contact Dermatitis—Top Allergens, Best Avoidance Measures.” *Current Treatment Options in Allergy* 2 (4): 349–64. https://doi.org/10.1007/s40521-015-0063-z.

Rachmawati, Dessy, Hetty J. Bontkes, Marleen I. Verstege, Joris Muris, B. Mary E. von Blomberg, Rik J. Scheper, and Ingrid M. W. van Hoogstraten. 2013. “Transition Metal Sensing by Toll-like Receptor-4: Next to Nickel, Cobalt and Palladium Are Potent Human Dendritic Cell Stimulators.” *Contact Dermatitis* 68 (6): 331–38. https://doi.org/10.1111/cod.12042.

Raghavan, Badrinarayanan, Stefan F Martin, Philipp R Esser, Matthias Goebeler, and Marc Schmidt. 2012. “Metal Allergens Nickel and Cobalt Facilitate TLR4 Homodimerization Independently of MD2.” *EMBO Reports* 13 (12): 1109–15. https://doi.org/10.1038/embor.2012.155.

Reggiori, Fulvio, Masaaki Komatsu, Kim Finley, and Anne Simonsen. 2012. “Autophagy: More Than a Nonselective Pathway.” Research article. International Journal of Cell Biology. 2012. https://doi.org/10.1155/2012/219625.

Riemann, Helge, Karin Loser, Stefan Beissert, Mayumi Fujita, Agatha Schwarz, Thomas Schwarz, and Stephan Grabbe. 2005. “IL-12 Breaks Dinitrothiocyanobenzene (DNTB)-Mediated Tolerance and Converts the Tolerogen DNTB into an Immunogen.” *The Journal of Immunology* 175 (9): 5866–74. https://doi.org/10.4049/jimmunol.175.9.5866.

Rock, Kenneth L., Arron Hearn, Chun-Jen Chen, and Yan Shi. 2005. “Natural Endogenous Adjuvants.” *Springer Seminars in Immunopathology* 26 (3): 231–46. https://doi.org/10.1007/s00281-004-0173-3.

Ross-Hansen, K., A. Linneberg, J.d. Johansen, L.-G. Hersoug, C. Brasch-Andersen, T. Menné, and J.p. Thyssen. 2013. “The Role of Glutathione S-Transferase and Claudin-1 Gene Polymorphisms in Contact Sensitization: A Cross-Sectional Study.” *British Journal of Dermatology* 168 (4): 762–70. https://doi.org/10.1111/bjd.12126.

Saitoh, Tatsuya, and Shizuo Akira. 2016. “Regulation of Inflammasomes by Autophagy.” *Journal of Allergy and Clinical Immunology* 138 (1): 28–36. https://doi.org/10.1016/j.jaci.2016.05.009.

Samuelsson, Kristin, Moa Andresen Bergström, Charlotte A Jonsson, Gunnar Westman, and Ann-Therese Karlberg. 2011. “Diphenylthiourea, a Common Rubber Chemical, Is Bioactivated to Potent Skin Sensitizers.” *Chemical Research in Toxicology* 24 (1): 35–44. https://doi.org/10.1021/tx100241z.

Scheper, Gert C., Marjo S. van der Knaap, and Christopher G. Proud. 2007. “Translation Matters: Protein Synthesis Defects in Inherited Disease.” *Nature Reviews. Genetics* 8 (9): 711–23. https://doi.org/10.1038/nrg2142.

Schichl, Yvonne M., Ulrike Resch, Renate Hofer-Warbinek, and Rainer de Martin. 2009. “Tristetraprolin Impairs NF-KB/P65 Nuclear Translocation.” *Journal of Biological Chemistry* 284 (43): 29571–81. https://doi.org/10.1074/jbc.M109.031237.

Schmidt, Marc, Badrinarayanan Raghavan, Verena Müller, Thomas Vogl, György Fejer, Sandrine Tchaptchet, Simone Keck, et al. 2010. “Crucial Role for Human Toll-like Receptor 4 in the Development of Contact Allergy to Nickel.” *Nature Immunology* 11 (9): 814–19. https://doi.org/10.1038/ni.1919.

Schmittgen, Thomas D, and Kenneth J Livak. 2008. “Analyzing Real-Time PCR Data by the Comparative CT Method.” *Nature Protocols* 3 (6): 1101–8. https://doi.org/10.1038/nprot.2008.73.

Schmitz, M. Lienhard, M. Samer Shaban, B. Vincent Albert, Anke Gökçen, and Michael Kracht. 2018. “The Crosstalk of Endoplasmic Reticulum (ER) Stress Pathways with NF-KB: Complex Mechanisms Relevant for Cancer, Inflammation and Infection.” *Biomedicines* 6 (2). https://doi.org/10.3390/biomedicines6020058.

Senft, Daniela, and Ze’ev A. Ronai. 2015a. “UPR, Autophagy, and Mitochondria Crosstalk Underlies the ER Stress Response.” *Trends in Biochemical Sciences* 40 (3): 141–48. https://doi.org/10.1016/j.tibs.2015.01.002.

———. 2015b. “UPR, Autophagy and Mitochondria Crosstalk Underlies the ER Stress Response.” *Trends in Biochemical Sciences* 40 (3): 141–48. https://doi.org/10.1016/j.tibs.2015.01.002.

Sengupta, Piali, and Aravinthan D.T. Samuel. 2009. “C. Elegans: A Model System for Systems Neuroscience.” *Current Opinion in Neurobiology* 19 (6): 637–43. https://doi.org/10.1016/j.conb.2009.09.009.

Sha, W. C., H. C. Liou, E. I. Tuomanen, and D. Baltimore. 1995. “Targeted Disruption of the P50 Subunit of NF-Kappa B Leads to Multifocal Defects in Immune Responses.” *Cell* 80 (2): 321–30.

Shen, Jingshi, Xi Chen, Linda Hendershot, and Ron Prywes. 2002. “ER Stress Regulation of ATF6 Localization by Dissociation of BiP/GRP78 Binding and Unmasking of Golgi Localization Signals.” *Developmental Cell* 3 (1): 99–111. https://doi.org/10.1016/S1534-5807(02)00203-4.

Shibutani, Shusaku T, Tatsuya Saitoh, Heike Nowag, Christian Münz, and Tamotsu Yoshimori. 2015. “Autophagy and Autophagy-Related Proteins in the Immune System.” *Nature Immunology* 16 (10): 1014–24. https://doi.org/10.1038/ni.3273.

Shih, Vincent Feng-Sheng, Rachel Tsui, Andrew Caldwell, and Alexander Hoffmann. 2011. “A Single NFκB System for Both Canonical and Non-Canonical Signaling.” *Cell Research* 21 (1): 86–102. https://doi.org/10.1038/cr.2010.161.

Shore, Gordon C., Feroz R. Papa, and Scott A. Oakes. 2011. “Signaling Cell Death from the Endoplasmic Reticulum Stress Response.” *Current Opinion in Cell Biology* 23 (2): 143–49. https://doi.org/10.1016/j.ceb.2010.11.003.

Shoulders, Matthew D., Lisa M. Ryno, Joseph C. Genereux, James J. Moresco, Patricia G. Tu, Chunlei Wu, John R. Yates III, Andrew I. Su, Jeffery W. Kelly, and R. Luke Wiseman. 2013. “Stress-Independent Activation of XBP1s and/or ATF6 Reveals Three Functionally Diverse ER Proteostasis Environments.” *Cell Reports* 3 (4): 1279–92. https://doi.org/10.1016/j.celrep.2013.03.024.

Smith, Judith A. 2018. “Regulation of Cytokine Production by the Unfolded Protein Response; Implications for Infection and Autoimmunity.” *Frontiers in Immunology* 9 (March). https://doi.org/10.3389/fimmu.2018.00422.

Smith, Melanie H., Hidde L. Ploegh, and Jonathan S. Weissman. 2011. “Road to Ruin: Targeting Proteins for Degradation in the Endoplasmic Reticulum.” *Science* 334 (6059): 1086–90. https://doi.org/10.1126/science.1209235.

Stefan, Loic, Franck Denat, and David Monchaud. 2012. “Insights into How Nucleotide Supplements Enhance the Peroxidase-Mimicking DNAzyme Activity of the G-Quadruplex/Hemin System.” *Nucleic Acids Research* 40 (17): 8759–72. https://doi.org/10.1093/nar/gks581.

Stefani, Massimo. 2004. “Protein Misfolding and Aggregation: New Examples in Medicine and Biology of the Dark Side of the Protein World.” *Biochimica et Biophysica Acta (BBA) - Molecular Basis of Disease* 1739 (1): 5–25. https://doi.org/10.1016/j.bbadis.2004.08.004.

Sugita, K, K Kabashima, K Atarashi, T Shimauchi, M Kobayashi, and Y Tokura. 2007. “Innate Immunity Mediated by Epidermal Keratinocytes Promotes Acquired Immunity Involving Langerhans Cells and T Cells in the Skin.” *Clinical and Experimental Immunology* 147 (1): 176–83. https://doi.org/10.1111/j.1365-2249.2006.03258.x.

Sutterwala, Fayyaz S., Yasunori Ogura, Marian Szczepanik, Maria Lara-Tejero, G. Scott Lichtenberger, Ethan P. Grant, John Bertin, et al. 2006. “Critical Role for NALP3/CIAS1/Cryopyrin in Innate and Adaptive Immunity through Its Regulation of Caspase-1.” *Immunity* 24 (3): 317–27. https://doi.org/10.1016/j.immuni.2006.02.004.

Sykes, Erin, Swetlana Mactier, and Richard Christopherson. 2016. “Melanoma and the Unfolded Protein Response.” *Cancers* 8 (3): 30. https://doi.org/10.3390/cancers8030030.

Tanida, Isei, Takashi Ueno, and Eiki Kominami. 2008. “LC3 and Autophagy.” *Methods in Molecular Biology (Clifton, N.J.)* 445: 77–88. https://doi.org/10.1007/978-1-59745-157-4_4.

Theillet, Francois-Xavier, Caroline Smet-Nocca, Stamatios Liokatis, Rossukon Thongwichian, Jonas Kosten, Mi-Kyung Yoon, Richard W. Kriwacki, Isabelle

Landrieu, Guy Lippens, and Philipp Selenko. 2012. “Cell Signaling, Post-Translational Protein Modifications and NMR Spectroscopy.” *Journal of Biomolecular NMR* 54 (3): 217–36. https://doi.org/10.1007/s10858-012-9674-x.

Thorbecke, G. Jeanette, Inga Silberberg-Sinakin, and Thomas J. Flotte. 1980. “Langerhans Cells as Macrophages in Skin and Lymhphoid Organs.” *Journal of Investigative Dermatology* 75 (1): 32–43. https://doi.org/10.1111/1523-1747.ep12521083.

Thyssen, Jacob P., Allan Linneberg, Katrine Ross-Hansen, Berit C. Carlsen, Michael Meldgaard, Pal B. Szecsi, Steen Stender, Torkil Menné, and Jeanne D. Johansen. 2013. “Filaggrin Mutations Are Strongly Associated with Contact Sensitization in Individuals with Dermatitis.” *Contact Dermatitis* 68 (5): 273–76. https://doi.org/10.1111/cod.12021.

Timberlake, Matthew II, and Yogesh Dwivedi. 2018. “Linking Unfolded Protein Response to Inflammation and Depression: Potential Pathologic and Therapeutic Implications.” *Molecular Psychiatry*, September, 1. https://doi.org/10.1038/s41380-018-0241-z.

Tinari, Antonella, Anna Maria Giammarioli, Valeria Manganelli, Laura Ciarlo, and Walter Malorni. 2008. “Chapter One Analyzing Morphological and Ultrastructural Features in Cell Death.” In *Methods in Enzymology*, 442:1–26. Programmed Cell Death,General Principles ForStudying Cell Death, Part A. Academic Press. https://doi.org/10.1016/S0076-6879(08)01401-8.

Tsuchiya, S., M. Yamabe, Y. Yamaguchi, Y. Kobayashi, T. Konno, and K. Tada. 1980. “Establishment and Characterization of a Human Acute Monocytic Leukemia Cell Line (THP-1).” *International Journal of Cancer* 26 (2): 171–76.

Upton, John-Paul, Likun Wang, Dan Han, Eric S. Wang, Noelle E. Huskey, Lionel Lim, Morgan Truitt, et al. 2012. “IRE1α Cleaves Select MicroRNAs During ER Stress to Derepress Translation of Proapoptotic Caspase-2.” *Science (New York, N.Y.)* 338 (6108): 818–22. https://doi.org/10.1126/science.1226191.

Urano, F., X. Wang, A. Bertolotti, Y. Zhang, P. Chung, H. P. Harding, and D. Ron. 2000. “Coupling of Stress in the ER to Activation of JNK Protein Kinases by Transmembrane Protein Kinase IRE1.” *Science (New York, N.Y.)* 287 (5453): 664–66.

Vidal, René L., and Claudio Hetz. 2012. “Crosstalk between the UPR and Autophagy Pathway Contributes to Handling Cellular Stress in Neurodegenerative Disease.” *Autophagy* 8 (6): 970–72. https://doi.org/10.4161/auto.20139.

Vogel, Christine, and Edward M. Marcotte. 2012. “Insights into the Regulation of Protein Abundance from Proteomic and Transcriptomic Analyses.” *Nature Reviews Genetics* 13 (4): 227–32. https://doi.org/10.1038/nrg3185.

Walker, A. P., D. A. Basketter, M. Baverel, W. Diembeck, W. Matthies, D. Mougin, R. RÖthlisberger, and M. Coroama. 1997. “Test Guidelines for the Assessment of Skin Tolerance of Potentially Irritant Cosmetic Ingredients in Man.” *Food and Chemical Toxicology* 35 (10): 1099–1106. https://doi.org/10.1016/S0278-6915(97)00106-3.

Walter, F., J. Schmid, H. Düssmann, C. G. Concannon, and J. H. M. Prehn. 2015. “Imaging of Single Cell Responses to ER Stress Indicates That the Relative Dynamics of IRE1/XBP1 and PERK/ATF4 Signalling Rather than a Switch between Signalling Branches Determine Cell Survival.” *Cell Death and Differentiation* 22 (9): 1502. https://doi.org/10.1038/cdd.2014.241.

Walter, P., and D. Ron. 2011. “The Unfolded Protein Response: From Stress Pathway to Homeostatic Regulation.” *Science* 334 (6059): 1081–86. https://doi.org/10.1126/science.1209038.

Wang, Lifeng, Fu-Sheng Wang, and M. Eric Gershwin. 2015. “Human Autoimmune Diseases: A Comprehensive Update.” *Journal of Internal Medicine* 278 (4): 369–95. https://doi.org/10.1111/joim.12395.

Wang, Xingqi, Chunhui Hu, Xingxin Wu, Shiyu Wang, Aihua Zhang, Wei Chen, Yan Shen, et al. 2016. “Roseotoxin B Improves Allergic Contact Dermatitis through a Unique Anti-Inflammatory Mechanism Involving Excessive Activation of Autophagy in Activated T Lymphocytes.” *The Journal of Investigative Dermatology* 136 (8): 1636–46. https://doi.org/10.1016/j.jid.2016.04.017.

Wareing, Britta, Daniel Urbisch, Susanne Noreen Kolle, Naveed Honarvar, Ursula G. Sauer, Annette Mehling, and Robert Landsiedel. 2017. “Prediction of Skin Sensitization Potency Sub-Categories Using Peptide Reactivity Data.” *Toxicology in Vitro* 45 (December): 134–45. https://doi.org/10.1016/j.tiv.2017.08.015.

Watanabe, Hideki, Samuel Gehrke, Emmanuel Contassot, Stéphanie Roques, Jürg Tschopp, Peter S. Friedmann, Lars E. French, and Olivier Gaide. 2008. “Danger Signaling through the Inflammasome Acts as a Master Switch between Tolerance and Sensitization.” *The Journal of Immunology* 180 (9): 5826–32. https://doi.org/10.4049/jimmunol.180.9.5826.

Weber, F. C., P. R. Esser, T. Muller, J. Ganesan, P. Pellegatti, M. M. Simon, R. Zeiser, M. Idzko, T. Jakob, and S. F. Martin. 2010. “Lack of the Purinergic Receptor P2X7 Results in Resistance to Contact Hypersensitivity.” *Journal of Experimental Medicine* 207 (12): 2609–19. https://doi.org/10.1084/jem.20092489.

Xin, Fuxiao, and Predrag Radivojac. 2012. “Post-Translational Modifications Induce Significant yet Not Extreme Changes to Protein Structure.” *Bioinformatics* 28 (22): 2905–13. https://doi.org/10.1093/bioinformatics/bts541.

Xiong, Huajiang, Catherine Pears, and Alison Woollard. 2017. “An Enhanced C. Elegans Based Platform for Toxicity Assessment.” *Scientific Reports* 7 (August). https://doi.org/10.1038/s41598-017-10454-3.

Yamamoto, Keisuke, Takashi Sato, Toshie Matsui, Masanori Sato, Tetsuya Okada, Hiderou Yoshida, Akihiro Harada, and Kazutoshi Mori. 2007. “Transcriptional Induction of Mammalian ER Quality Control Proteins Is Mediated by Single or Combined Action of ATF6α and XBP1.” *Developmental Cell* 13 (3): 365–76. https://doi.org/10.1016/j.devcel.2007.07.018.

Yamazaki, Hiroaki, Nobuhiko Hiramatsu, Kunihiro Hayakawa, Yasuhiro Tagawa, Maro Okamura, Ryouji Ogata, Tao Huang, et al. 2009. “Activation of the Akt-NF-KB Pathway by Subtilase Cytotoxin through the ATF6 Branch of the Unfolded Protein Response.” *The Journal of Immunology* 183 (2): 1480–87. https://doi.org/10.4049/jimmunol.0900017.

Yogalakshmi, Baskaran, Periyasamy Viswanathan, and Carani Venkatraman Anuradha. 2010. “Investigation of Antioxidant, Anti-Inflammatory and DNA-Protective Properties of Eugenol in Thioacetamide-Induced Liver Injury in Rats.” *Toxicology*, This issue includes a Special Issue Section on: Highlights of the 2009 Annual Congress of The British Toxicology Society, 268 (3): 204–12. https://doi.org/10.1016/j.tox.2009.12.018.

Yoshida, Hiderou, Toshie Matsui, Akira Yamamoto, Tetsuya Okada, and Kazutoshi Mori. 2001. “XBP1 MRNA Is Induced by ATF6 and Spliced by IRE1 in

Response to ER Stress to Produce a Highly Active Transcription Factor." *Cell* 107 (7): 881–891.

Yu, Xiaocong, Tshidi Tsibane, Patricia A. McGraw, Frances S. House, Christopher J. Keefer, Mark D. Hicar, Terrence M. Tumpey, et al. 2008. "Neutralizing Antibodies Derived from the B Cells of 1918 Influenza Pandemic Survivors." *Nature* 455 (7212): nature07231. https://doi.org/10.1038/nature07231.

Yun, Wang, and Chunfeng Li. 2010. "JNK Pathway Is Required for TNCB-Induced IL-18 Expression in Murine Keratinocytes." *Toxicology in Vitro* 24 (4): 1064–69. https://doi.org/10.1016/j.tiv.2010.04.001.

Yuspa, Stuart H., Pamela Hawley-Nelson, Barbara Koehler, and John R. Stanley. 1980. "A Survey of Transformation Markers in Differentiating Epidermal Cell Lines in Culture." *Cancer Research* 40 (12): 4694–4703.

Zhang, Peichuan, Barbara McGrath, Sheng'ai Li, Ami Frank, Frank Zambito, Jamie Reinert, Maureen Gannon, Kun Ma, Kelly McNaughton, and Douglas R. Cavener. 2002. "The PERK Eukaryotic Initiation Factor 2? Kinase Is Required for the Development of the Skeletal System, Postnatal Growth, and the Function and Viability of the Pancreas." *Molecular and Cellular Biology* 22 (11): 3864–74. https://doi.org/10.1128/MCB.22.11.3864-3874.2002.

Zhou, Rongbin, Amir S. Yazdi, Philippe Menu, and Jürg Tschopp. 2011. "A Role for Mitochondria in NLRP3 Inflammasome Activation." *Nature* 469 (7329): 221–25. https://doi.org/10.1038/nature09663.

Zhu, Jinfang, and William E. Paul. 2008. "CD4 T Cells: Fates, Functions, and Faults." *Blood* 112 (5): 1557–69. https://doi.org/10.1182/blood-2008-05-078154.

Acknowledgements

First, I would like to thank Prof. Dr. Leena Bruckner-Tuderman, Prof. Dr. Stefan F. Martin and Dr. Philipp R. Esser for giving me the opportunity to conduct my dissertation in the Allergy Research Group in the Department of Dermatology and Venereology of the University Medical Center Freiburg.

I want to express my great gratitude to Prof. Dr. Stefan F. Martin and Dr. Philipp R. Esser for the supervision of my dissertation. Once again, I was able to benefit from your passion for science, your knowledge, your helpfulness in any situation and the contents of your huge paper stacks. I was fortunate to be allowed to get glimpses into the real-life scientist world by traveling through Germany and different European countries to attend different meetings and of course taste different cuisines together.

I especially want to thank Philipp for putting up with me for the third time. I was lucky enough to be allowed into your office six and a half years ago and could not imagine a better place to start what would lead me to this point of my scientific life. Besides being an excellent supervisor, you showed me to see the fun side of science leading to many strange actions like plucking our eyebrows for experiments. And I want to apologize for the excessive talks on Star Wars and the rice wafer smell you had to endure.

Of course, I want to thank all current and former members of the Allergy Research Group and our lab partners of skinitial for making the lab a great place to work. Your support in all situations from small things like looking for chemicals to saving the lab from burning down was as indispensable as the fun times outside the lab.

I also want to thank my friends and members of the world’s best WhatsApp group for putting up with my whining and distracting me from the lab life.

Finally, I want to thank my family and especially my parents for their ongoing support through the years that allowed me to focus on finishing this dissertation.

Declaration

1. I herewith declare that I have prepared the present work without any unallowed help from third parties and without the use of any aids beyond those given. All data and concepts taken either directly or indirectly from other sources are so indicated along with a notation of the source. In particular I have not made use of any paid assistance from exchange or consulting services (doctoral degree advisors or other persons). No one has received remuneration from me either directly or indirectly for work which is related to the content of the present dissertation.
2. The work has not been submitted in this country or abroad to any other examination board in this or similar form.
3. The provisions of the doctoral degree examination procedure of the Faculty of Biology of the University of Freiburg are known to me. In particular I am aware that before the awarding of the final doctoral degree I am not entitled to use the title of Dr.

Erklärung

1. Ich erkläre hiermit, dass ich die vorliegende Arbeit ohne unzulässige Hilfe Dritter und ohne Benutzung anderer als der angegebenen Hilfsmittel angefertigt habe. Die aus anderen Quellen direkt oder indirekt übernommenen Daten und Konzepte sind unter Angabe der Quellen gekennzeichnet. Insbesondere habe ich hierfür nicht die entgeltliche Hilfe von Vermittlungs- beziehungsweise Beratungsdiensten (Promotionsberater oder anderer Personen) in Anspruch genommen. Niemand hat von mir unmittelbar oder mittelbar geldwerte Leistungen für Arbeiten erhalten, die im Zusammenhang mit dem Inhalt der vorgelegten Dissertation stehen.
2. Die Arbeit wurde bisher weder im In- noch im Ausland in gleicher oder ähnlicher Form einer anderen Prüfungsbehörde vorgelegt.
3. Die Bestimmungen der Promotionsordnung der Fakultät für Biologie der Universität Freiburg sind mir bekannt, insbesondere weiß ich, dass ich vor Vollzug der Promotion zur Führung des Doktortitels nicht berechtigt bin.

Fabian Gendrisch